Monopole Elements with Disk Ground Planes on Flat Earth: Atlas of Directivity, Radiation Efficiency, Radiation Resistance, and Input Impedance

M. M. Weiner

MTR 92B0000089
June 1992

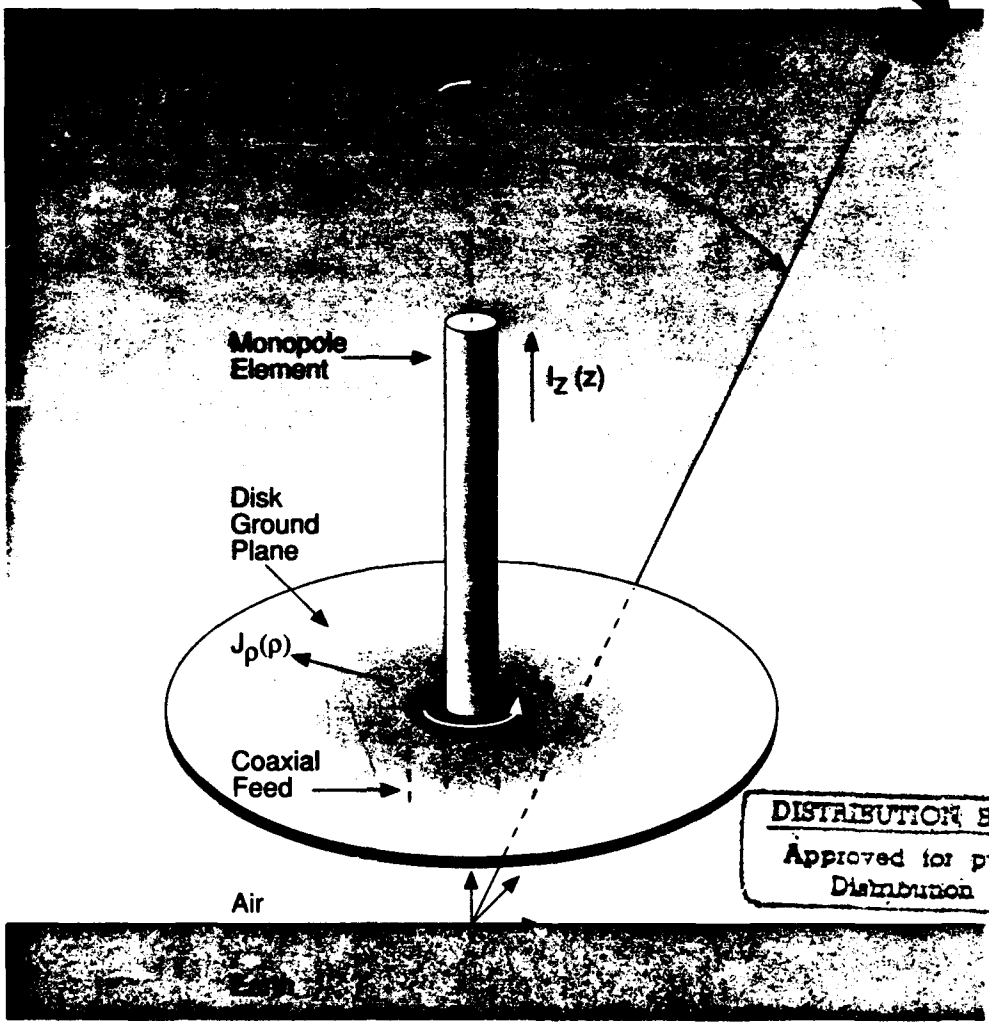

MITRE
Bedford, Massachusetts

REPORT DOCUMENTATION PAGE

Form Approved
OMB No. 0704-0188

1. AGENCY USE ONLY *(Leave blank)*	2. REPORT DATE	3. REPORT TYPE AND DATES COVERED
	June 1992	

4. TITLE AND SUBTITLE
Monopole Elements with Disk Ground Planes on Flat Earth: Atlas of Directivity, Radiation Efficiency, Radiation Resistance, and Input Impedance

5. FUNDING NUMBERS

6. AUTHOR(S)
M. M. Weiner

7. PERFORMING ORGANIZATION NAME(S) AND ADDRESS(ES)
The MITRE Corporation
202 Burlington Road
Bedford, MA 01730-1420

8. PERFORMING ORGANIZATION REPORT NUMBER
MTR 92B0000089

9. SPONSORING/MONITORING AGENCY NAME(S) AND ADDRESS(ES)

10. SPONSORING/MONITORING AGENCY REPORT NUMBER

11. SUPPLEMENTARY NOTES

12a. DISTRIBUTION/AVAILABILITY STATEMENT
Approved for public release; distribution unlimited.

12b. DISTRIBUTION CODE

13. ABSTRACT *(Maximum 200 words)*

Richmond's moment-method programs IRCHMOND3 and RICHMOND4 for monopole elements with disk ground planes above flat Earth are used to obtain computer plots of directivity, radiation efficiency, radiation resistance, and input impedance at 15 MHz. Results, in the form of an atlas, are presented as a function of Earth classification for thin, quarter-wave monopole elements whose ground planes or radii 0 to 8 wavenumbers rest on Earth.

Results are compared with those for a perfect ground plane (of infinite extent and coductivity) and ground plane in free-space. Sea-water enhancement of radiation efficiency and low-angle directivity by comparing results for sea water with those for medium dry ground.

14. SUBJECT TERMS	15. NUMBER OF PAGES
monopole elements, disk ground planes, radiation resistance, input impedance	16. PRICE CODE

17. SECURITY CLASSIFICATION OF REPORT	18. SECURITY CLASSIFICATION OF THIS PAGE	19. SECURITY CLASSIFICATION OF ABSTRACT	20. LIMITATION OF ABSTRACT
Unclassified	Unclassified	Unclassified	

Monopole Elements with Disk Ground Planes on Flat Earth: Atlas of Directivity, Radiation Efficiency, Radiation Resistance, and Input Impedance

MTR 92B0000089
June 1992

M. M. Weiner

Contract Sponsor MSR
Contract No. N/A
Project No. 91260
Dept. D085

MITRE
Bedford, Massachusetts

Department Approval: _____
Nicholas M. Tomljanovich

MITRE Project Approval: _____
Melvin M. Weiner

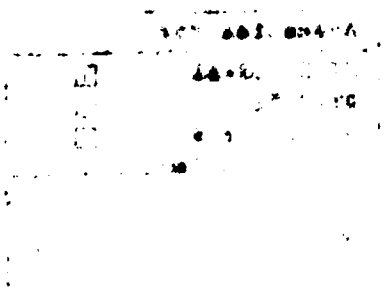

ABSTRACT

Richmond's moment-method programs RICHMOND3 and RICHMOND4 for monopole elements with disk ground planes above flat Earth are used to obtain computer plots of directivity, radiation efficiency, radiation resistance, and input impedance at 15 MHz. Results, in the form of an atlas, are presented as a function of Earth classification for thin, quarter-wave monopole elements whose ground planes of radii 0 to 8 wavenumbers rest on Earth.

Results are compared with those for a perfect ground plane (of infinite extent and conductivity) and ground plane in free-space. Sea-water enhancement of radiation efficiency and low-angle directivity is illustrated by comparing results for sea water with those for medium dry ground.

ACKNOWLEDGMENTS

Computer programs RICHMOND3 and RICHMOND4 were written by Jack H. Richmond (deceased) of Ohio State University. The latter program was written when he was a member of the technical advisor group to the MITRE-sponsored research project 91260 "High-Frequency Antenna Element Modeling," Melvin M. Weiner, Principal Investigator. Christopher Sharpe, Laurie Giandomenico, and Enis Vlashi performed the computer runs and obtained the computer plots.

TABLE OF CONTENTS

LIST OF FIGURES

LIST OF TABLES

SECTION 1

INTRODUCTION

The modeling of monopole elements with circular ground planes in proximity to Earth has been greatly enhanced in recent years by method-of-moments programs developed by Richmond for disk ground planes [1,2] and by Burke, et al. for radial-wire ground planes [3,4,5].

Method-of-moments models, unlike models based on Sommerfeld's attenuation function [6] or variational models based on Monteath's compensation theorem [7,8,9,10], determine the directivity and radiation efficiency as separate entities rather than lumping them together as a product to yield the antenna gain. Other advantages of the method-of-moments models include the following: more exact determination of current distributions; applicability to electrically small ground planes; direct determination of ground-plane edge diffraction; and avoidance of analytical restrictions on evaluating Sommerfeld's integral (such as requiring that the Earth's complex relative permittivity have a modulus much greater than unity).

A disadvantage of method-of-moments models is that they are restricted to relatively small ground-plane radii. This restriction is required so that ground-plane segmentation of unknown current variables does not exceed the computer's computational capacity and precision in solving for the unknown currents.

Richmond has presented a moment-method analysis for the current distributions and input impedance of a monopole element on disk ground planes in free space [1] and above flat Earth [2] with numerical evaluation by computer programs RICHMD1 and RICHMOND3, respectively. Weiner, et al. [11,12], have utilized the current distributions in reference 1 to develop a computer program, RICHMD2, for the far-zone field when the ground plane is in free space. Subsequently, Richmond used the current distributions in reference 2 to develop a computer program, RICHMOND4, for the far-zone field when the ground plane is above flat Earth. This latter effort has been reported by Weiner [13] who has also presented some numerical results and the validation of the numerical results. Listings of programs

RICHMD1 and RICHMD2 are given in reference 12. Listings of programs RICHMOND3 and RICHMOND4 are given in reference 13.

The present effort uses programs RICHMOND3 and RICHMOND4 to obtain computer plots of directivity (directive gain), radiation efficiency, radiation resistance, and input impedance for the International Radio Consultative Committee (CCIR) classifications of Earth [14]. Numerical results are presented in the form of an atlas of computer plots for thin, quarter-wave, monopole elements whose disk ground planes of radii 0 to 8 wavenumbers rest on Earth.

The antenna parameters are defined in section 2. Computer plots of numerical results are presented in section 3.

Examples of numerical results for only one type of Earth (medium dry Earth) are given in reference 13. The statement is made in reference 13 that *approximately* similar numerical results are obtained for other classifications of Earth with the exception of sea water. The present atlas provides numerical results to support such a statement and in particular to determine the quantitative differences in antenna performance for various classifications of Earth. The prior literature contains relatively little quantitative information on the performance of monopole elements with disk ground planes in close proximity to Earth. The intention of the present atlas is to address this deficiency for the benefit of the radar, communication, and broadcast communities.

SECTION 2

ANTENNA PARAMETERS

The antenna geometry consists of a vertical monopole element (length h and radius b) at the center of an infinitely thin disk ground plane of radius a (see figure 1). The ground plane is at a height z_o above flat Earth. The monopole element and disk are assumed to have infinite conductivity.

The Earth [with a dielectric constant ε_r and conductivity σ(S/m) for a waveform of time dependence $e^{j\omega t}$ at a radian frequency ω (rad/s) and free-space wavelength λ (m)] has a complex relative permittivity $\varepsilon^*/\varepsilon_o = \varepsilon_r(1 - j \tan\delta)$ where $\tan\delta$ = loss tangent = $\sigma/(\omega\varepsilon_r\varepsilon_o)$ $= (\lambda\sigma/2\pi\varepsilon_r)(\mu_o/\varepsilon_o)^{1/2} \approx 60\lambda\,\sigma/\varepsilon_r$; μ_o and ε_o are the free-space permeability and permittivity, respectively. The location of an arbitrary far-zone observation point P is designated by spherical coordinates (r, θ, ϕ).

The feed for the monopole antenna is a coaxial line with its inner conductor connected to the vertical monopole element through a hole of radius b_1 at the center of the ground plane. The coaxial-line outer conductor of diameter $2b_1$ is connected by means of a flange to the ground plane. The coaxial-line inner-conductor diameter is equal to the monopole element diameter $2b$. The current on the outside of the coaxial-line outer conductor is assumed to be zero because of attenuation by lossy ferrite toroids along the exterior of the coaxial-line feed (see section 2.4 of reference 12).

The Earth constants, loss tangents, and penetration depths are summarized in table 2-1 for CCIR 527-1 classifications of Earth [14] in the 3-MHz through 30-MHz high-frequency band. Cases (2) through (9) correspond to CCIR classifications of Earth. Cases (1) and (11) correspond to perfect ground planes (of infinite conductivity and extent) and ground planes in free space, respectively. Case (10) is arbitrarily defined as Average Land and corresponds to Earth constants $\varepsilon_r = 10.0$, $\sigma = 5 \times 10^{-3}$ S/m.

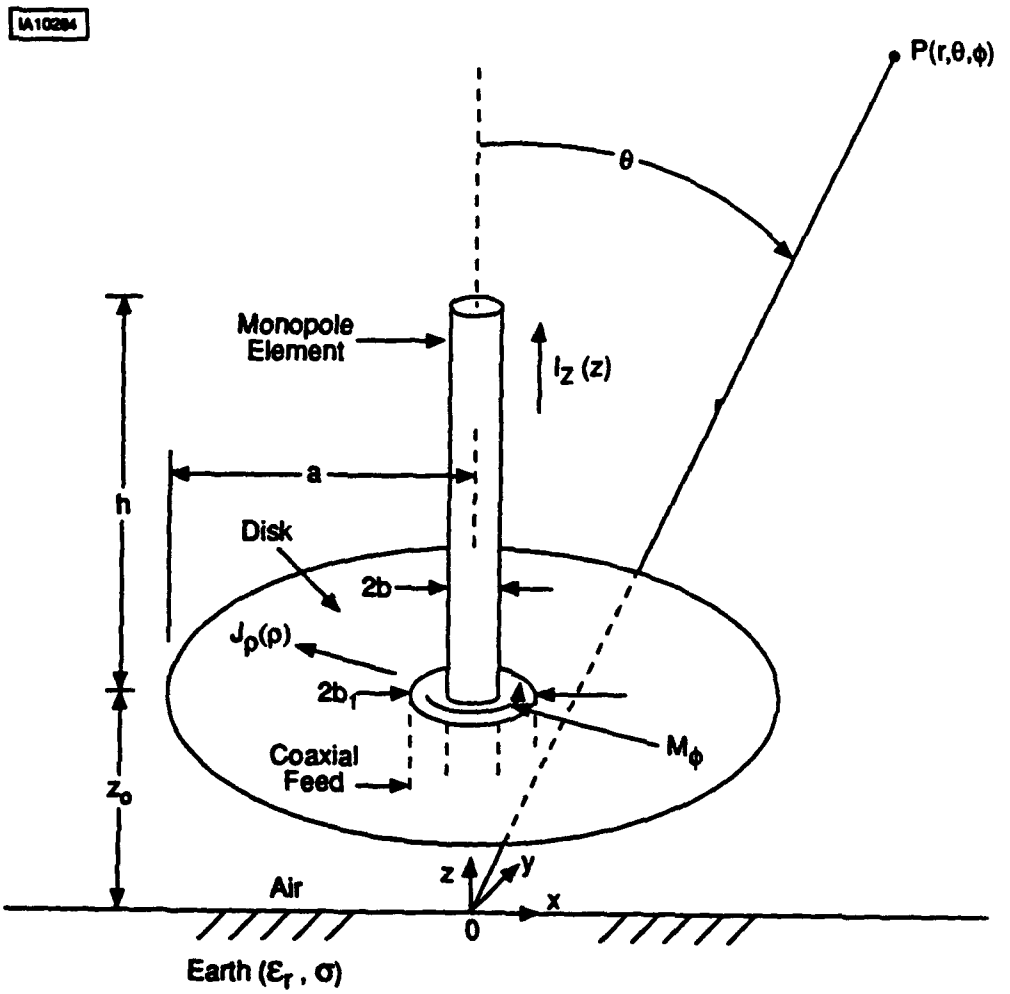

Figure 2-1. Monopole Element on Disk Ground Plane above Flat Earth

Table 2-1. Permittivity, Loss Tangent, and Penetration Depth of CCIR 527-1 Classifications of Earth

Cases	CONSTANTS		LOSS TANGENT			PENETRATION DEPTH		
	ε_r	σ (S/m)	$\sigma/(\omega\varepsilon_r\varepsilon_0) = (60\lambda)(\sigma/\varepsilon_r)$			δ (m)		
			Frequency (MHz) [Wavelength (m)]			Frequency (MHz) [Wavelength (m)]		
			3 [99.93]	15 [19.986]	30 [9.993]	3 [99.93]	15 [19.986]	30 [9.993]
(1) Perfect Ground	1.0	∞	∞	∞	∞	0	0	0
(2) Sea Water (average Salinity 20°C)	70.0	5.0	4.282×10^{2}	8.425×10^{1}	4.283×10^{1}	1.3×10^{-1}	5.8×10^{-2}	4.1×10^{-2}
(3) Fresh Water	80.0	3.0×10^{-2}	2.251×10^{0}	4.497×10^{-1}	2.248×10^{-1}	2.1×10^{0}	1.6×10^{0}	1.6×10^{0}
(4) Wet Ground	30.0	1.0×10^{-2}	1.999×10^{0}	3.997×10^{-1}	1.999×10^{-1}	3.7×10^{0}	3.0×10^{0}	2.9×10^{0}
(5) Medium Dry Ground	15.0	1.0×10^{-3}	3.997×10^{-1}	7.995×10^{-2}	3.997×10^{-2}	2.1×10^{1}	2.1×10^{1}	2.1×10^{1}
(6) Very Dry Ground	3.0	1.0×10^{-4}	1.999×10^{-1}	3.997×10^{-2}	1.999×10^{-2}	9.2×10^{1}	9.2×10^{1}	9.2×10^{1}
(7) Pure Water, 20°C	80.0	1.8×10^{-6} 5.0×10^{-4} 1.7×10^{-3}	1.350×10^{-4} - -	- 7.495×10^{-3} -	- - 1.274×10^{-2}	2.6×10^{4} - -	- 9.4×10^{2} -	- - 2.7×10^{1}
(8) Ice (fresh water, -1°C)	3.0	6.0×10^{-5} 9.0×10^{-5} 1.0×10^{-4}	1.199×10^{-1} - -	- 3.597×10^{-2} -	- - 1.999×10^{-2}	1.5×10^{2} - -	- 1.0×10^{2} -	- - 9.2×10^{1}
(9) Ice (fresh water, -10°C)	3.0	1.8×10^{-5} 2.7×10^{-5} 3.5×10^{-5}	3.597×10^{-2} - -	- 1.079×10^{-2} -	- - 6.995×10^{-3}	5.1×10^{2} - -	- 3.4×10^{2} -	- - 2.6×10^{2}
(10) Average Land	10.0	5.0×10^{-3}	2.998×10^{0}	5.996×10^{-1}	2.998×10^{-1}	4.8×10^{0}	1.6×10^{0}	3.4×10^{0}
(11) Free Space	1.0	0	0	0	0	∞	∞	∞

Numerical results are presented in section 3 for each Earth classification of table 2-1 and antenna parameters with the following numerical values: $h/\lambda = 0.25$, $b/\lambda = 10^{-6}$, $b_1/b = 3.5$, $2\pi a/\lambda = 0$ through 8, $z_o/\lambda = 0$, and $f = 15$ MHz ($\lambda = 20$ m).

The electrical characteristics that are evaluated are antenna directivity (also called "directive gain"), radiation efficiency, radiation resistance, and input impedance.

The total far-zone electric field $\vec{E}(r,\theta,\phi) = \hat{u}_\theta E_\theta(r,\theta,\phi)$ where $\hat{u}_\theta$ is the unit vector in the θ direction. The far-zone electric field is zero in the azimuthal direction because of the uniformity of the antenna geometry about the z axis. The total far-zone field amplitude $E_\theta(r,\theta,\phi)$ is the sum of the far-zone fields from the monopole element, the disk ground plane, and the equivalent magnetic current density (magnetic frill) M_ϕ of the coaxial-line feed excitation [13]. The total far-zone field is independent of the azimuthal coordinate ϕ because of the azimuthal symmetry of the antenna geometry in figure 2-1. Therefore, $E_\theta(r,\theta,\phi) = E_\theta(r,\theta)$.

Consider now the cases where the Earth medium either is lossy ($\sigma > 0$) or is free space ($\sigma = 0$, $\varepsilon_r = 1$). The total far-zone radiated power P_r is given by

$$P_r = \begin{cases} (\pi/\eta_o) \Big/ \int_0^{\pi/2} |E_\theta(r,\theta)|^2 r^2 \sin\theta \, d\theta, & \sigma > 0 \\ (\pi/\eta_o) \Big/ \int_0^{\pi} |E_\theta(r,\theta)|^2 r^2 \sin\theta \, d\theta; & \sigma = 0,\ \varepsilon_r = 1 \end{cases} \tag{2-1}$$

where $\eta_o = (\mu_o/\varepsilon_o)^{1/2}$ is the free-space wave impedance (ohms). For the case $\sigma > 0$ the integrand in equation 2-1 is integrated over only the hemisphere above the Earth because the field in lossy Earth, relative to that in free space, approaches zero at large radial distances r.

The antenna directivity $d(\theta)$ expressed as a dimensionless number is given by

$$d(\theta) = 2|E_\theta(r,\theta)|^2 / P_r . \tag{2-2}$$

The antenna directivity $D(\theta)$ expressed in decibels is given by

$$D(\theta) = 10 log_{10} d(\theta) \ (dB). \tag{2-3}$$

The time-averaged input power P_{in} to the monopole antenna is given by

$$P_{in} = (1/2) Re[V(0) I^*(0)] \tag{2-4}$$

where $V(0)$ = peak input voltage (volts). The input voltage $V(0)$ is usually set equal to 1 volt in the moment-method analysis.

$I^*(0)$ = conjugate of the peak input current $I(0)$ at the base of the monopole element. This current is solved for by the moment-method analysis in reference 2.

The input impedance Z_{in} is given by

$$Z_{in} = R_{in} + jX_{in} = V(0)/I(0) \tag{2-5}$$

where R_{in} and X_{in} are the input resistance and input reactance, respectively.

The antenna radiation resistance R_{rad} is defined as

$$R_{rad} = 2P_r / |I(0)|^2 . \tag{2-6}$$

The antenna radiation efficiency η is defined as

$$\eta = P_r / P_{in} = \left[1 + \left(R_{rad} / R_{in}\right)\right]^{-1}. \tag{2-7}$$

For the case of free-space $(\sigma = 0,\ \varepsilon_r = 1)$, the radiation efficiency is equal to unity because the monopole element and disk ground-plane conductivities are assumed to be infinite.

SECTION 3

COMPUTER PLOTS OF NUMERICAL RESULTS

Numerical results are presented in the form of an atlas of computer plots for thin, quarter-wave monopole elements whose disk ground planes of radii 0 to 8 wavenumbers rest on Earth. Computer plots are presented in sections 3.1 through 3.9 for each Earth classification of table 1 at a frequency of 15 MHz. In each computer plot, results are compared with those for perfect ground planes (of infinite extent and conductivity) and ground planes in free space. Section 3.10 compares results for sea water with those for medium dry ground.

In the presence of Earth, the directivity patterns are approximately independent of disk radius (for ground-plane radii of 0 to 8 wavenumbers). The peak directivity is within 0.5 dBi of that for a perfect ground plane. The Earth softens the edge of the ground plane and minimizes changes in peak directivity resulting from ground-plane edge diffraction. In the absence of Earth, large changes in directivity occur because ground-plane edge diffraction is more pronounced.

The direction of peak directivity is approximately 30 degrees above the horizon, except for sea water, in which case the direction of peak directivity is approximately 10 degrees above the horizon. Relatively small changes in ground plane radius for particular radii can cause large changes in the angle of peak directivity regardless whether the ground plane is in close proximity to Earth or not and despite the broad 3 dB beamwidth of the elevation radiation pattern. The jump in angle of peak directivity between $2\pi a/\lambda = 5.5$ and 5.75 wavenumbers corresponds to a change of only 0.5 dB in directivity and is due to a change in beam shape.

The radiation efficiency increases monotonically with increasing disk radius, except for sea water, in which case the increase is not monotonic but the radiation efficiency is enhanced over that for other classifications of Earth. The radiation efficiency is small for small ground planes because most of the antenna input energy is redirected into the Earth by a surface wave that is generated at the air-Earth interface.

Each of the following subsections contains computer plots of the following antenna performance characteristics:

a. Numeric directivity patterns for disk radii $2\pi a/\lambda = 0.025, 3.0, 4.0, 5.0, 6.5$ wavenumbers. The patterns in the elevation plane at any azimuthal angle are polar plots with the same numerical scale.
b. Peak numeric directivity
c. Angle of incidence of peak directivity
d. Radiation efficiency
e. Radiation resistance
f. Input resistance
g. Input reactance
h. Directivity in decibels for angles of incidence $\theta = 82, 84, 86, 88$, and 90 degrees.

3.1 SEA WATER (AVERAGE SALINITY, 20°C)

NUMERIC DIRECTIVE GAIN POLAR PLOT

Case 2, Sea Water (average salinity 20 deg C) at 15 MHz

$2\pi a/\lambda = 0.025$ (Wavenumbers)

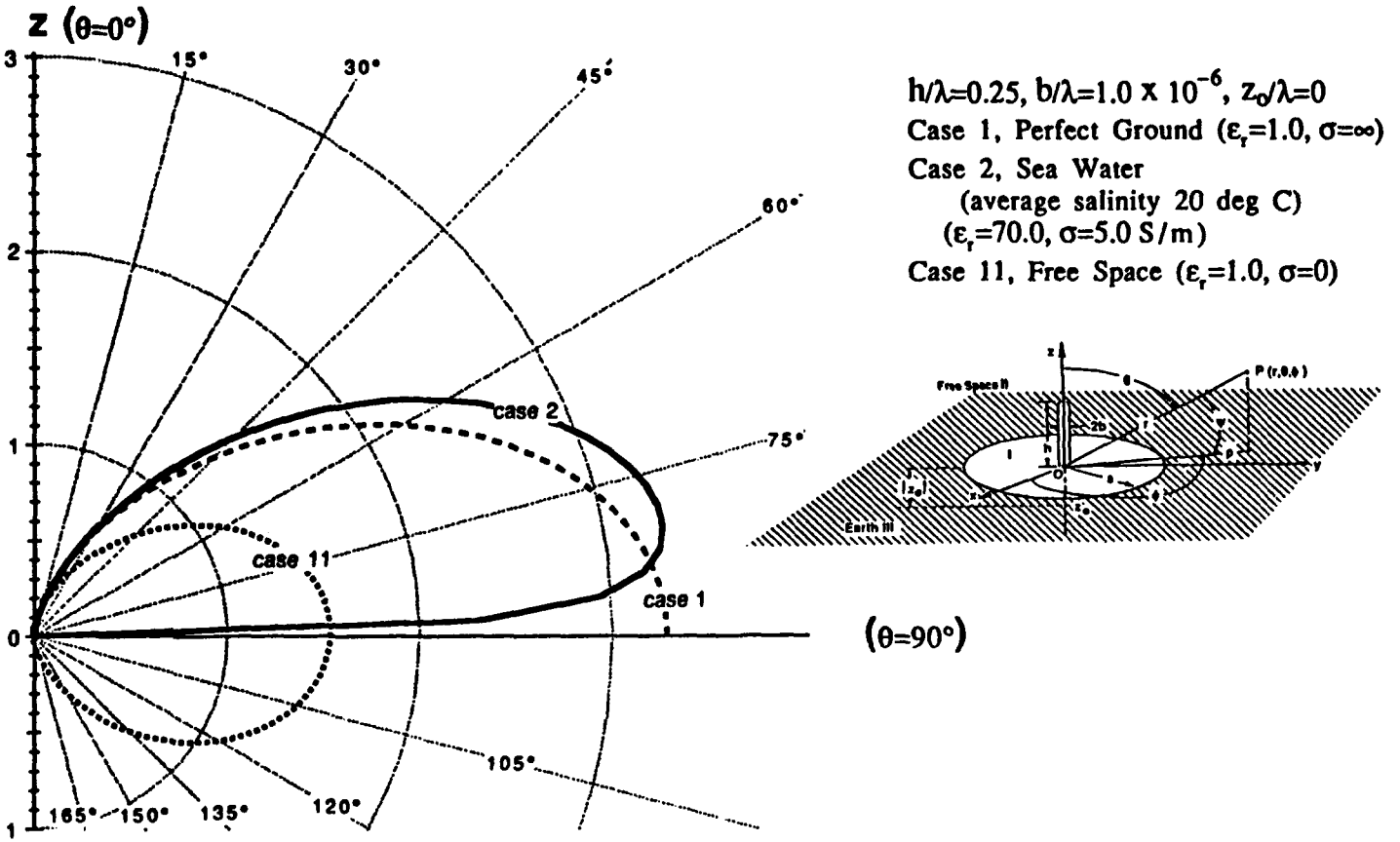

Figure 3-1. Directivity Pattern, $2\pi a/\lambda = 0.025$, Sea Water (Average Salinity, 20°C)

NUMERIC DIRECTIVE GAIN POLAR PLOT

Case 2, Sea Water (average salinity 20 deg C) at 15 MHz

$2\pi a/\lambda =$ 3.0 (Wavenumbers)

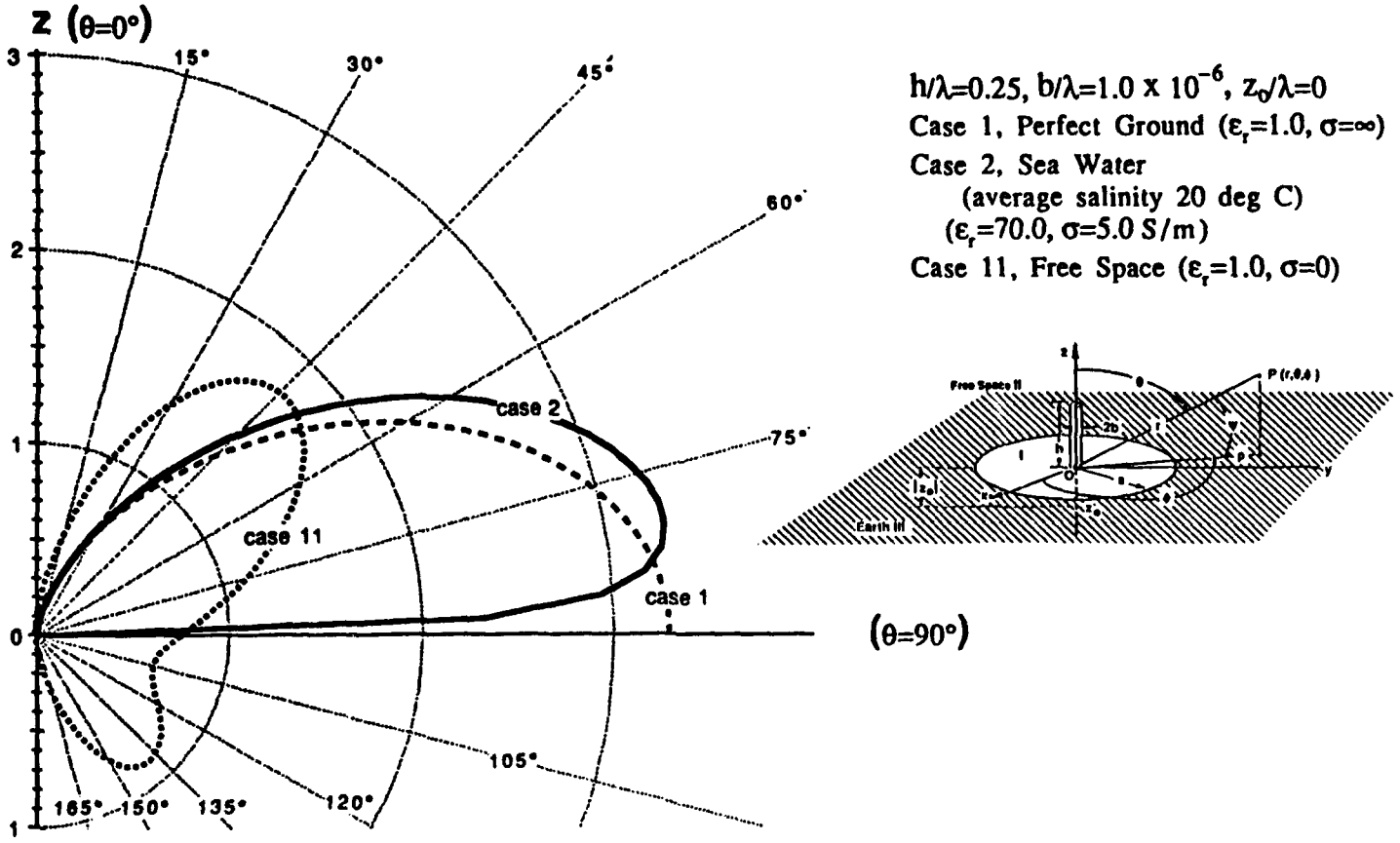

Figure 3-2. Directivity Pattern, $2\pi a/\lambda = 3.0$, Sea Water (Average Salinity, 20°C)

NUMERIC DIRECTIVE GAIN POLAR PLOT

Case 2, Sea Water (average salinity 20 deg C) at 15 MHz

$2\pi a/\lambda =$ **4.0 (Wavenumbers)**

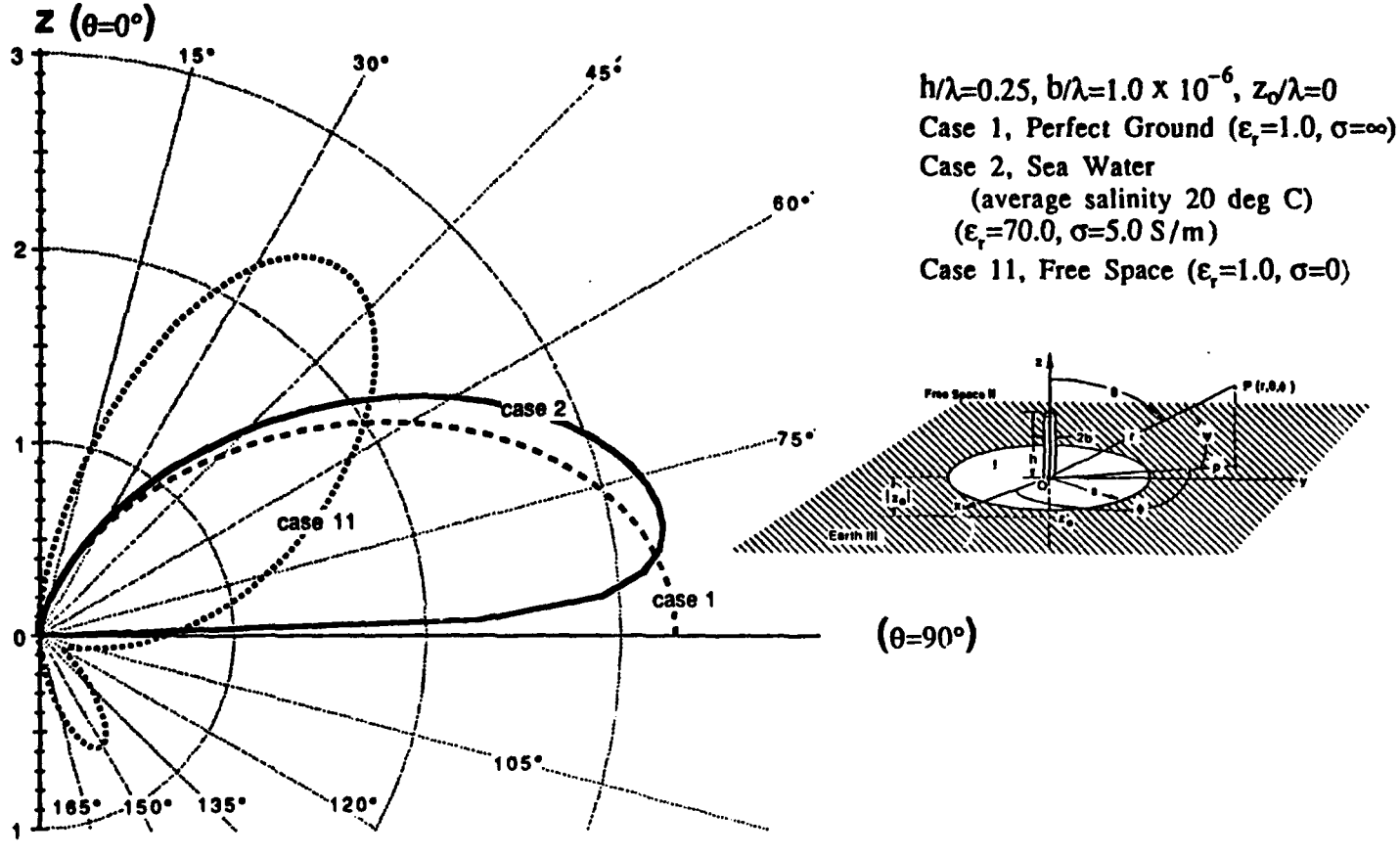

Figure 3-3. Directivity Pattern, $2\pi a/\lambda = 4.0$, Sea Water (Average Salinity, 20°C)

NUMERIC DIRECTIVE GAIN POLAR PLOT

Case 2, Sea Water (average salinity 20 deg C) at 15 MHz

$2\pi a/\lambda =$ 5.0 (Wavenumbers)

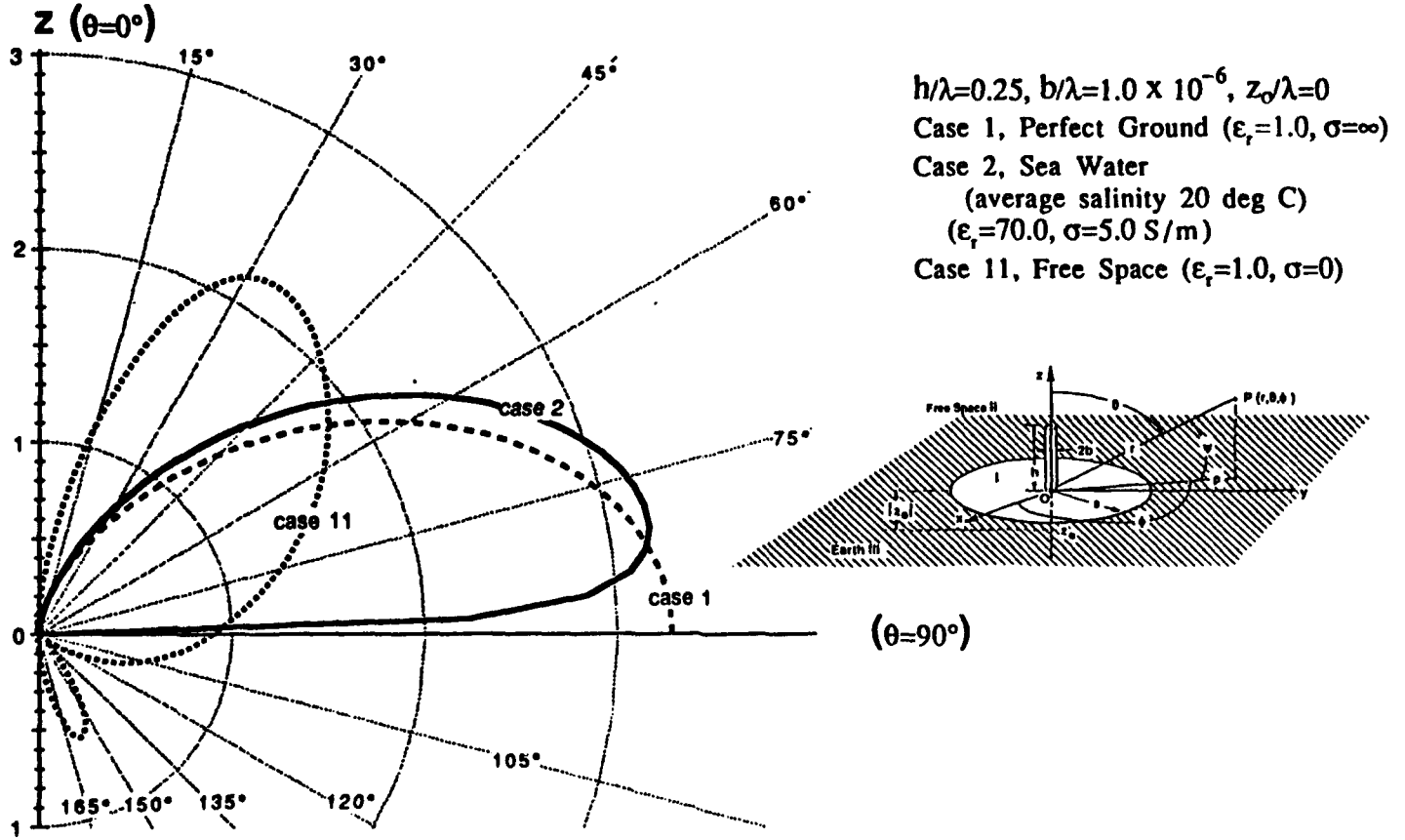

Figure 3-4. Directivity Pattern, $2\pi a/\lambda = 5.0$, Sea Water (Average Salinity, 20°C)

NUMERIC DIRECTIVE GAIN POLAR PLOT

Case 2, Sea Water (average salinity 20 deg C) at 15 MHz

$2\pi a/\lambda =$ **6.5 (Wavenumbers)**

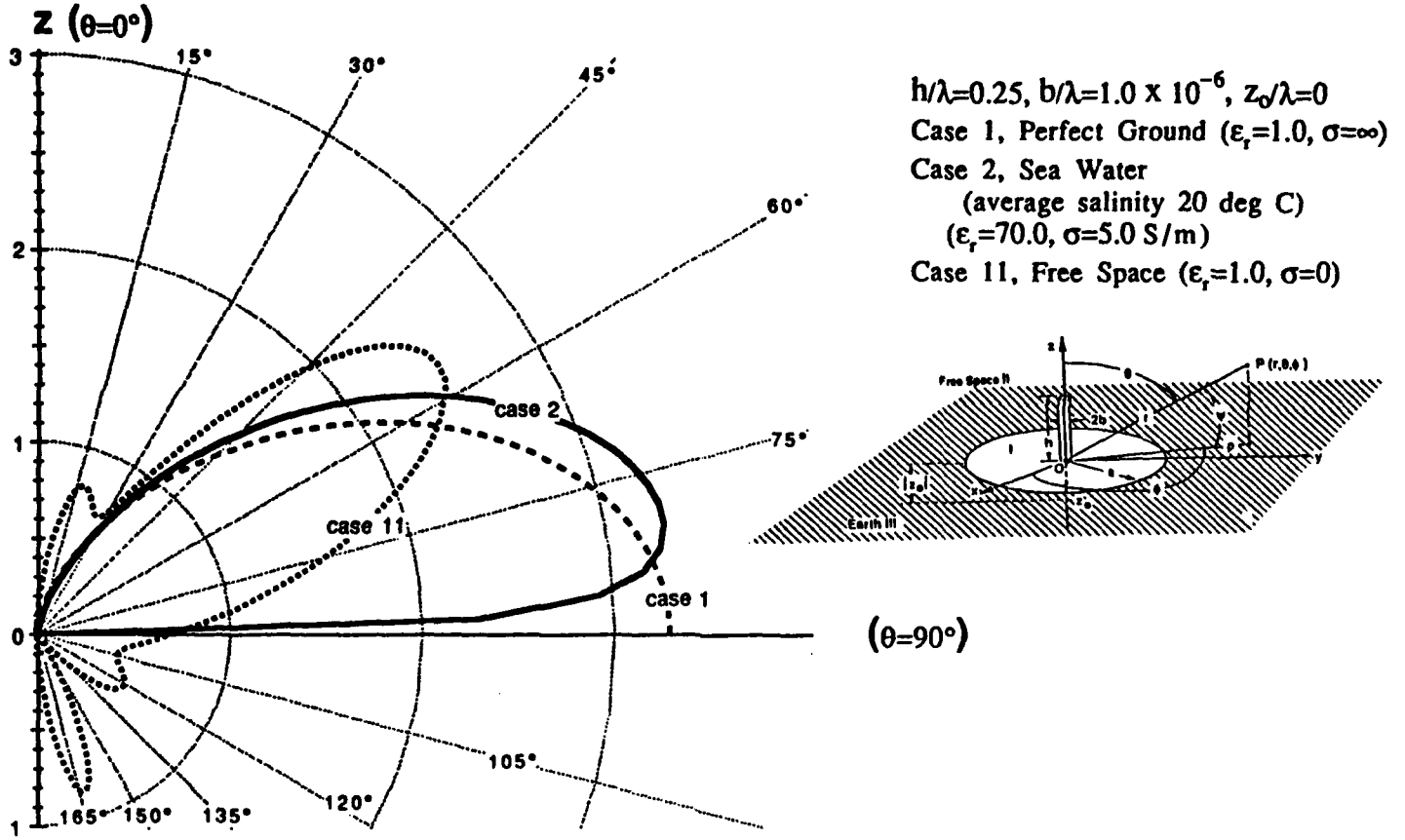

Figure 3-5. Directivity Pattern, $2\pi a/\lambda = 6.5$, Sea Water (Average Salinity, 20°C)

PEAK DIRECTIVITY

Case 2, Sea Water (average salinity 20 deg C) at 15 MHz

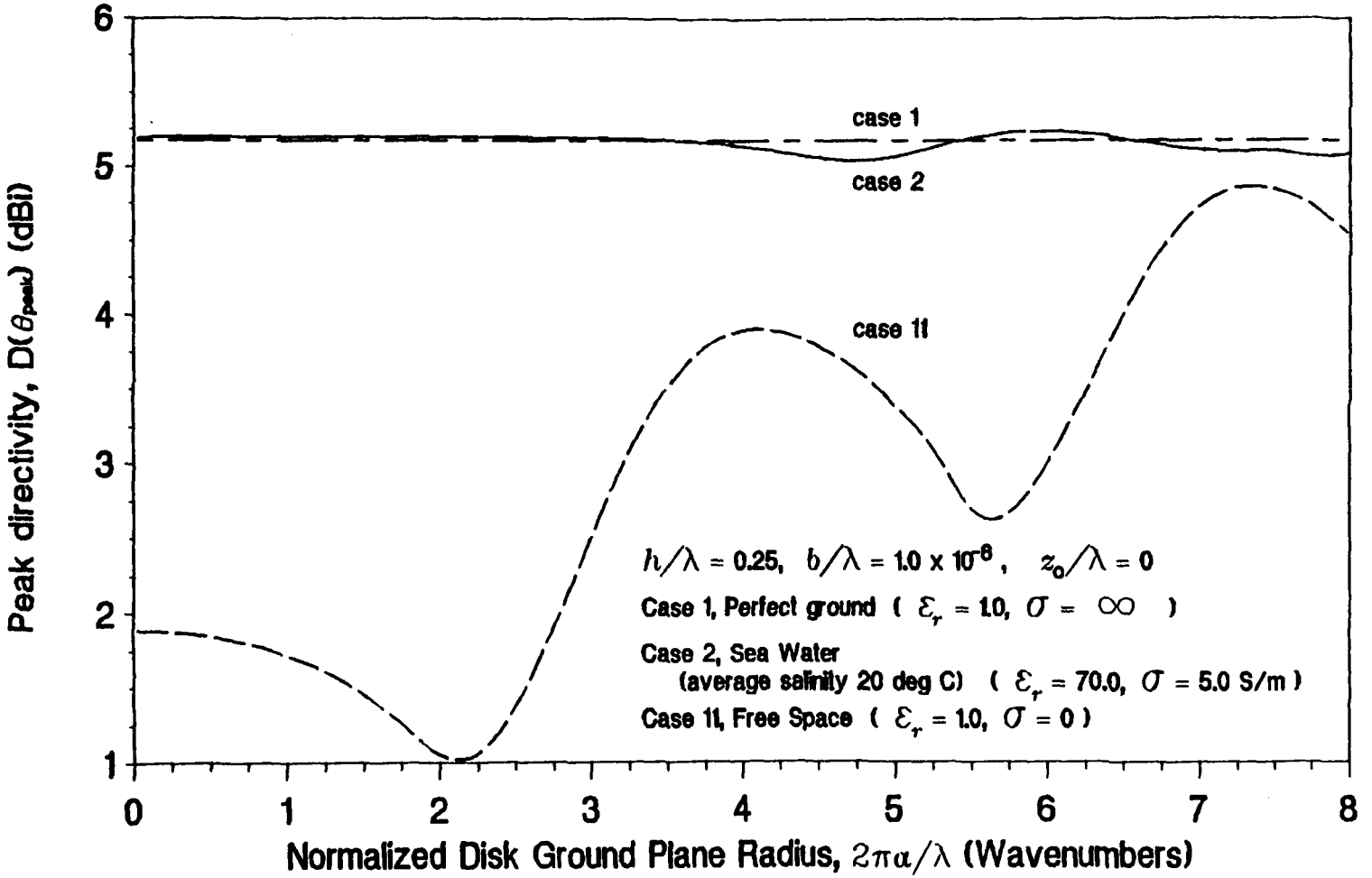

Figure 3-6. Peak Directivity, Sea Water (Average Salinity, 20°C)

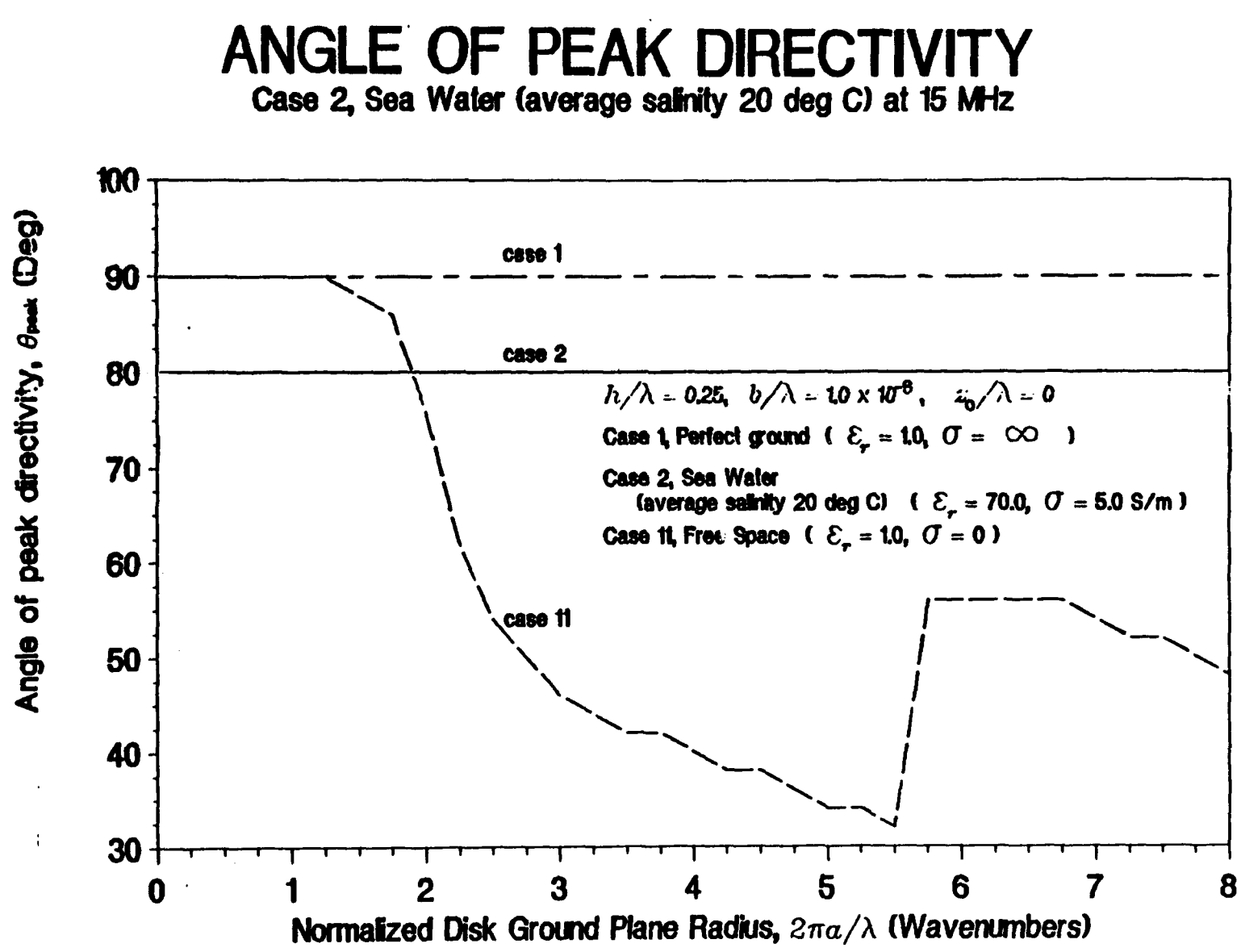

Figure 3-7. Angle of Incidence of Peak Directivity, Sea Water (Average Salinity, 20°C)

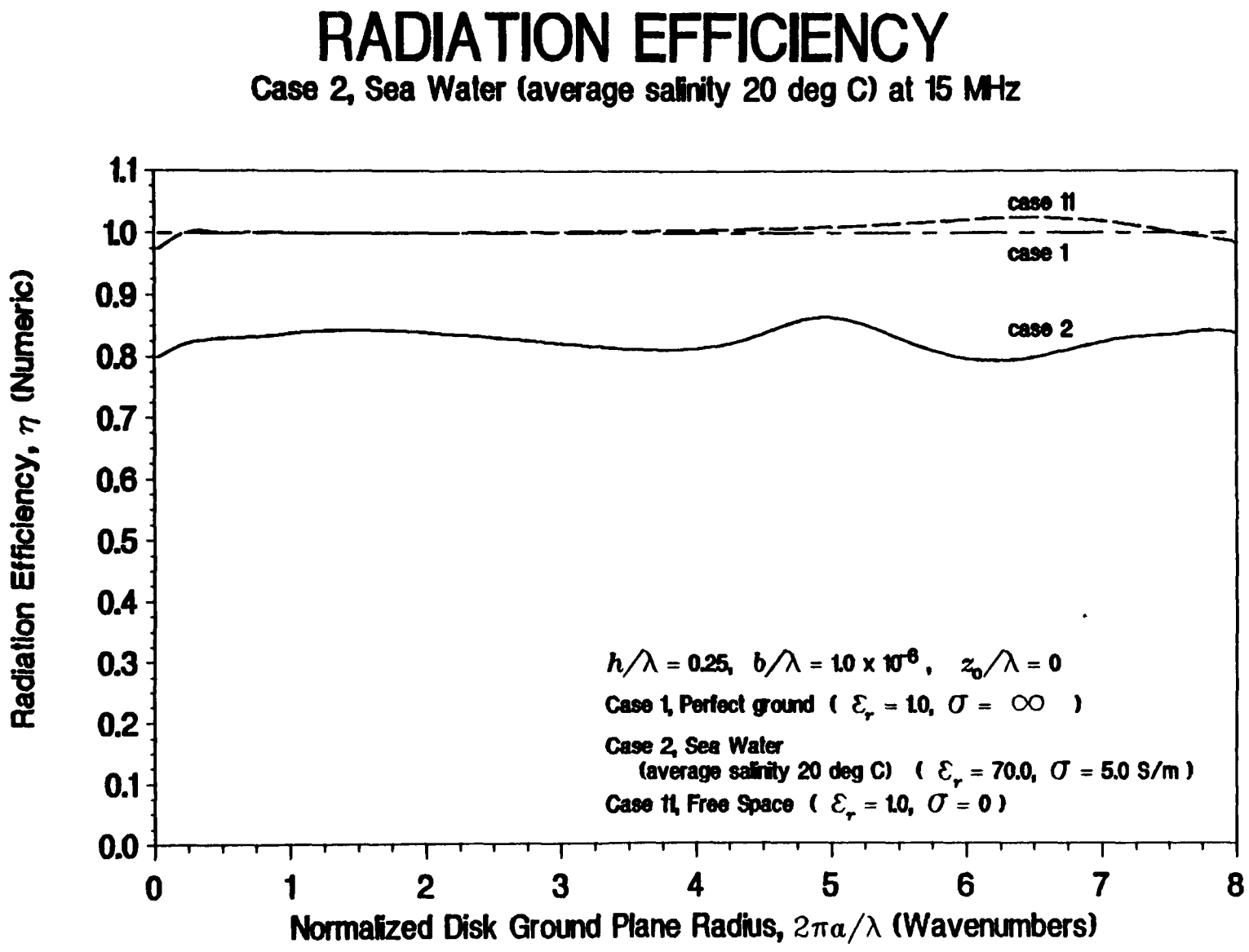

Figure 3-8. Radiation Efficiency, Sea Water (Average Salinity, 20°C)

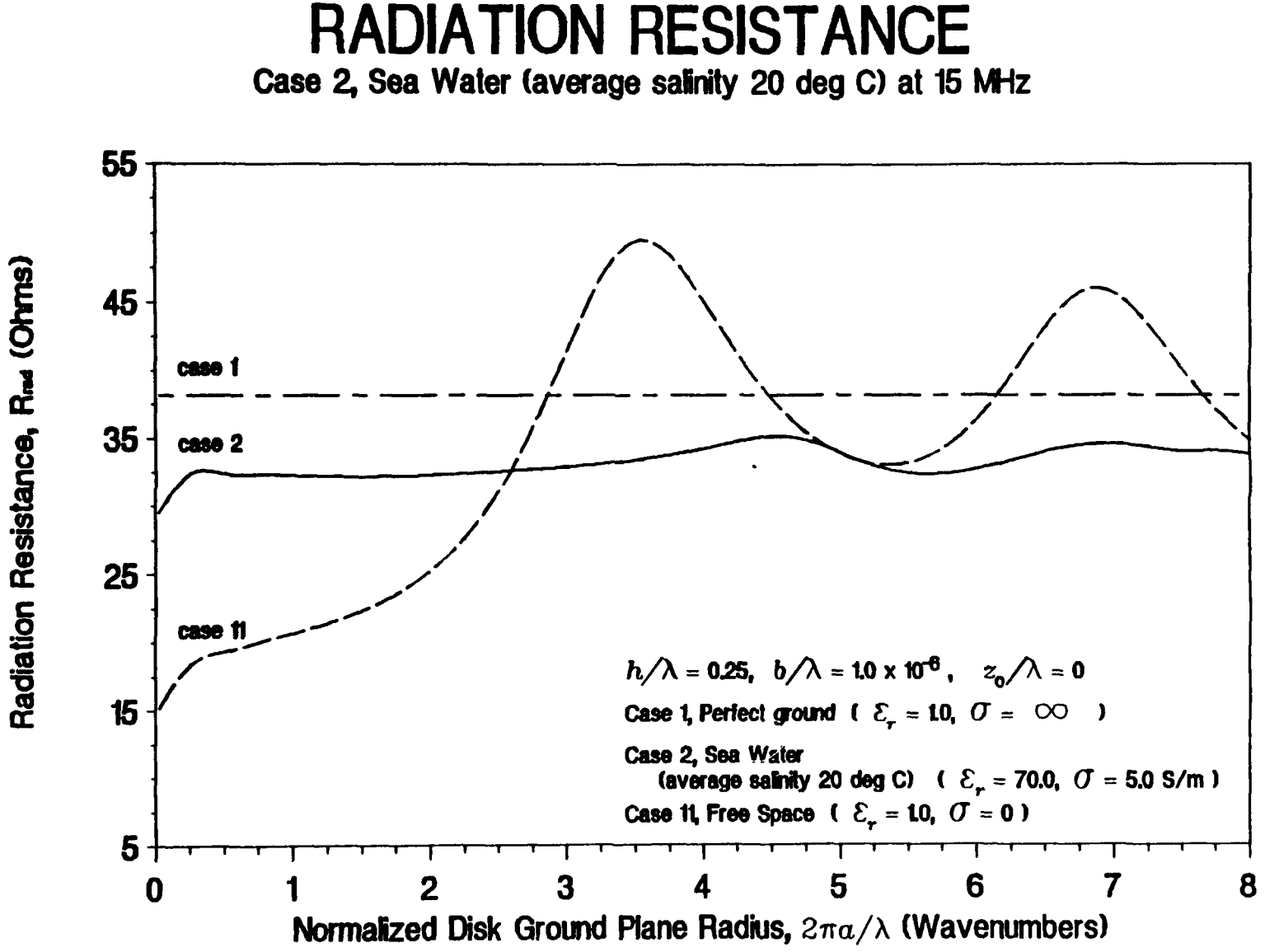

Figure 3-9. Radiation Resistance, Sea Water (Average Salinity, 20°C)

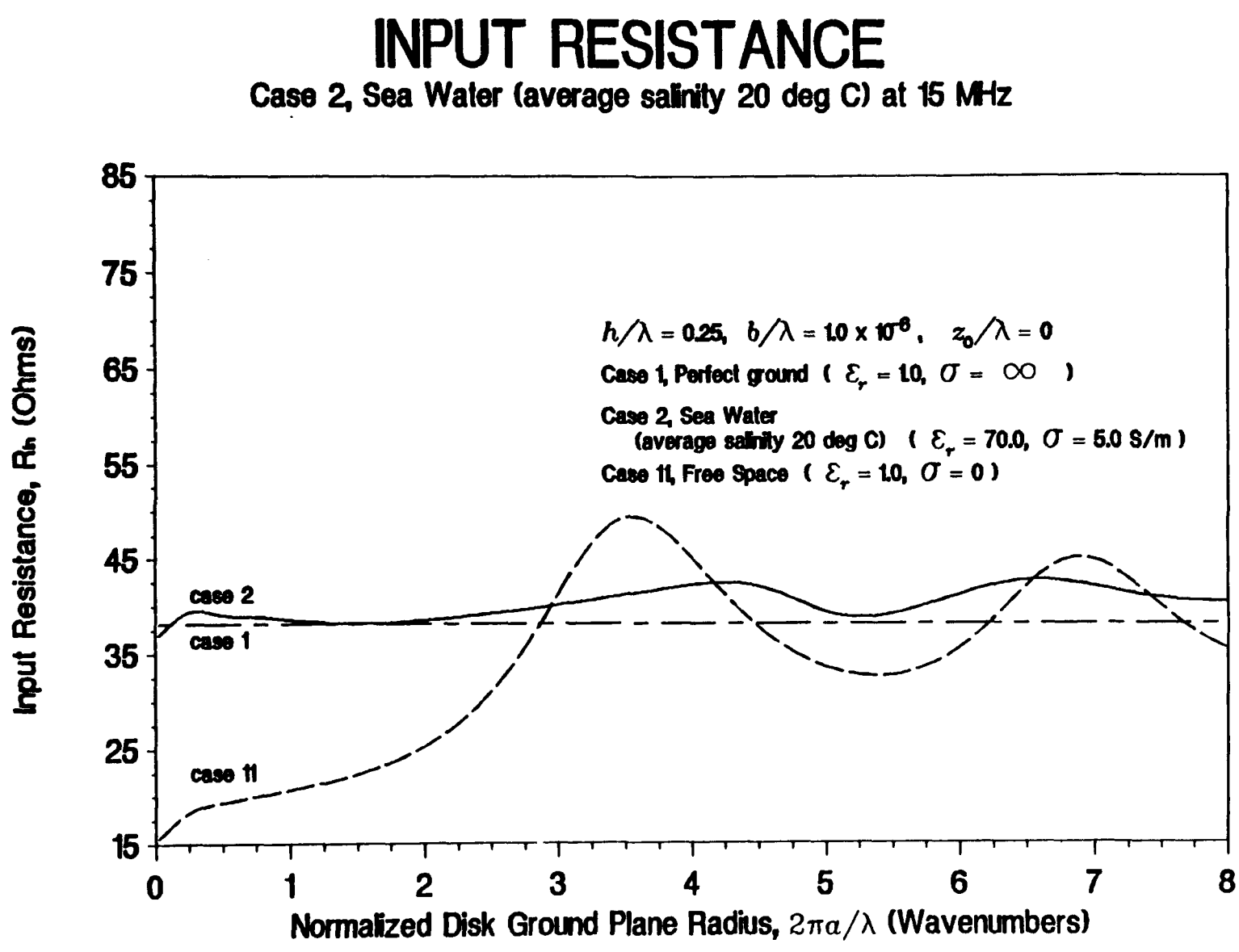

Figure 3-10. Input Resistance, Sea Water (Average Salinity, 20°C)

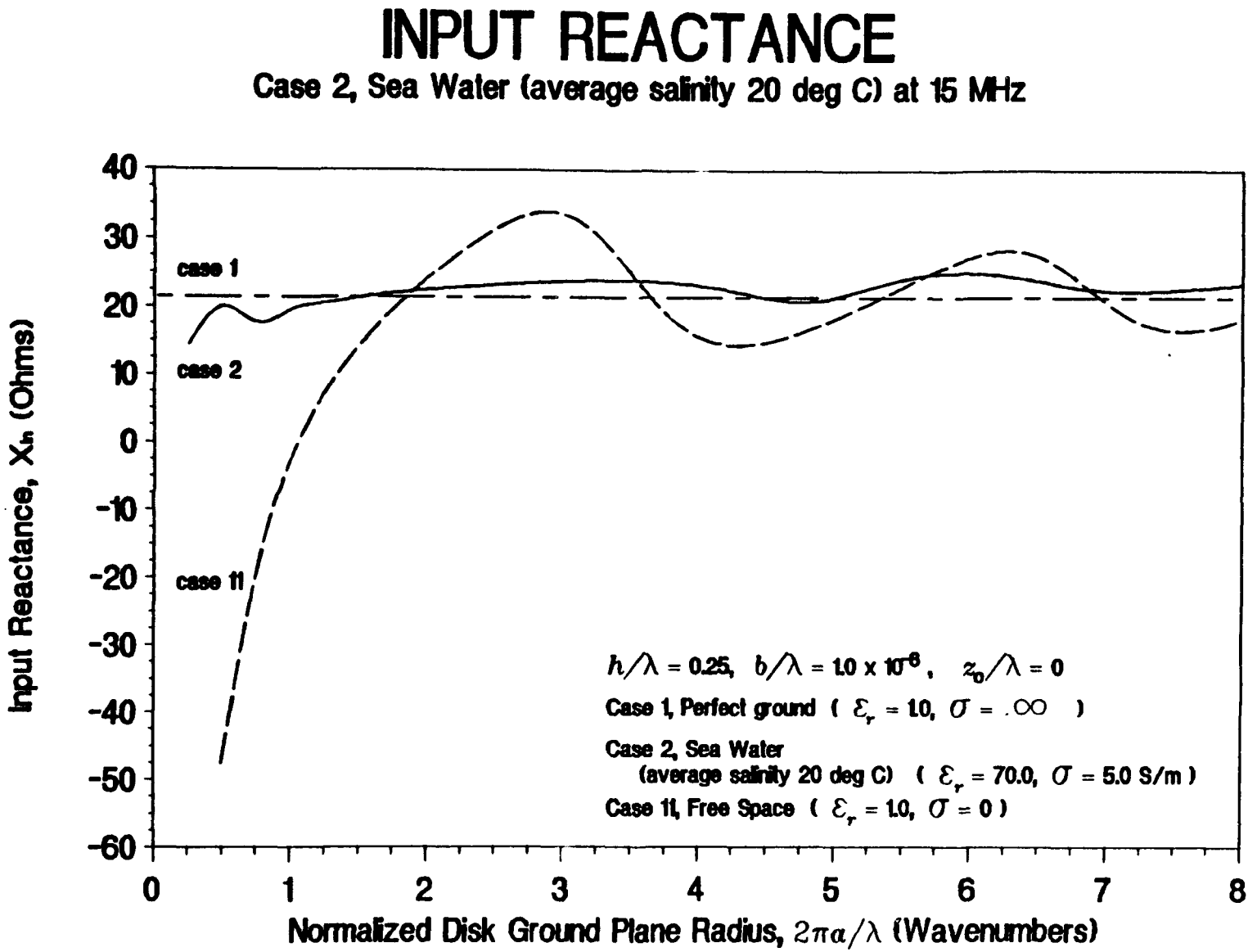

Figure 3-11. Input Reactance, Sea Water (Average Salinity, 20°C)

DIRECTIVE GAIN AT 82 DEG ELEVATION

Case 2, Sea Water (average salinity 20 deg C) at 15 MHz

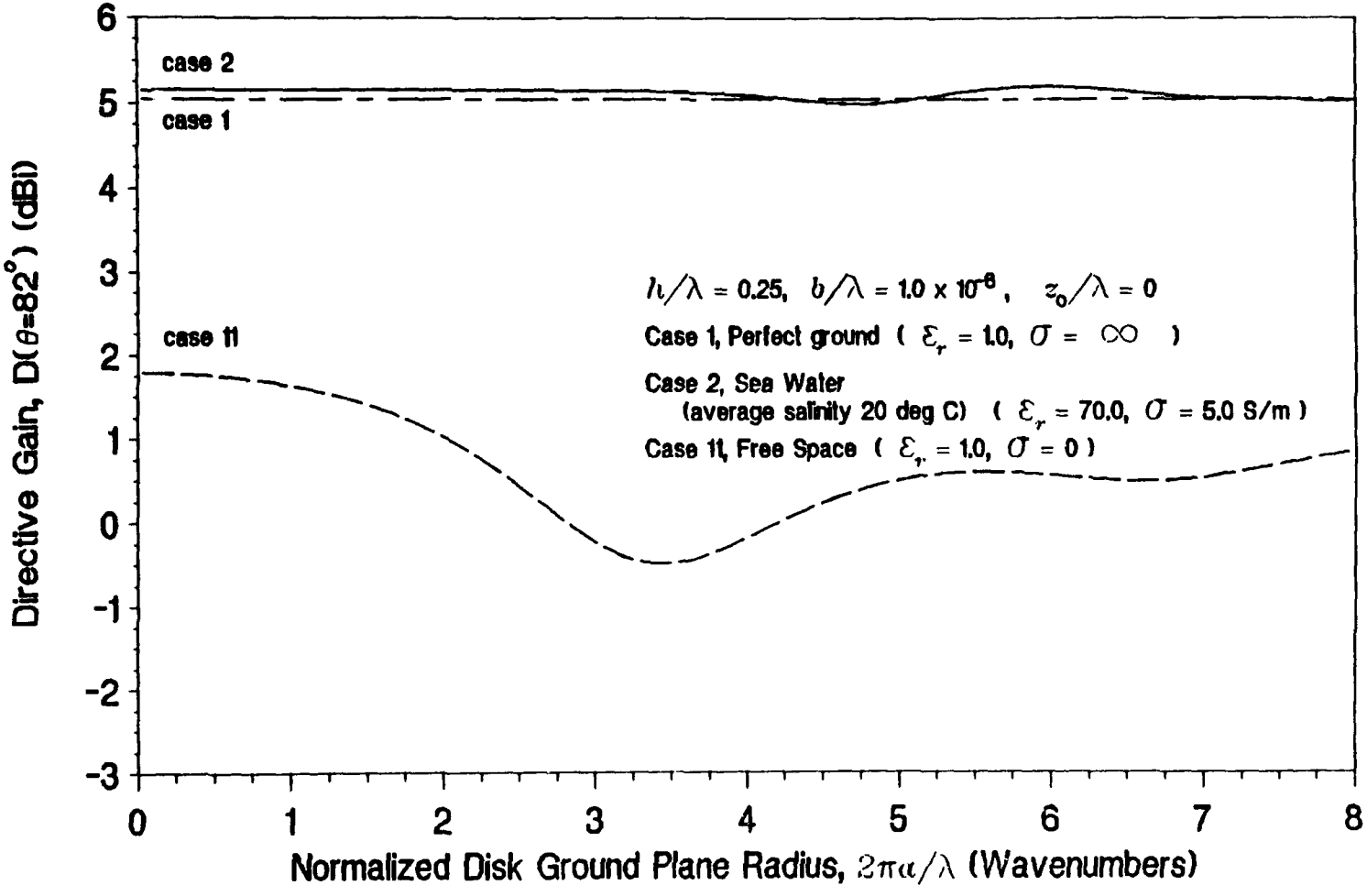

Figure 3-12. Directivity at 8 Degrees Above the Horizon, Sea Water (Average Salinity, 20°C)

DIRECTIVE GAIN AT 84 DEG ELEVATION

Case 2, Sea Water (average salinity 20 deg C) at 15 MHz

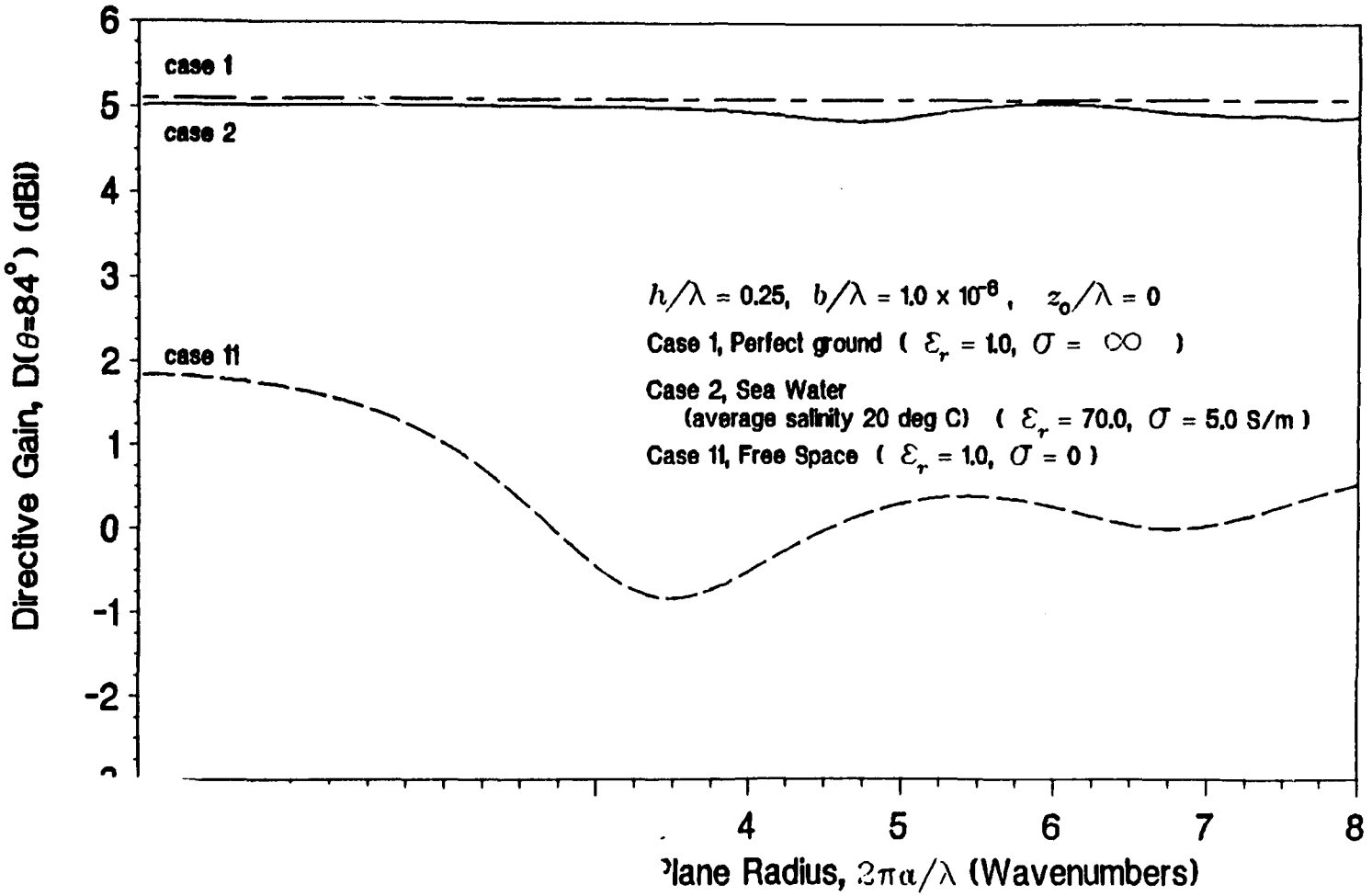

Figure 3-13. Directivity at 6 Degrees Above the Horizon, Sea Water (Average Salinity, 20°C)

DIRECTIVE GAIN AT 86 DEG ELEVATION

Case 2, Sea Water (average salinity 20 deg C) at 15 MHz

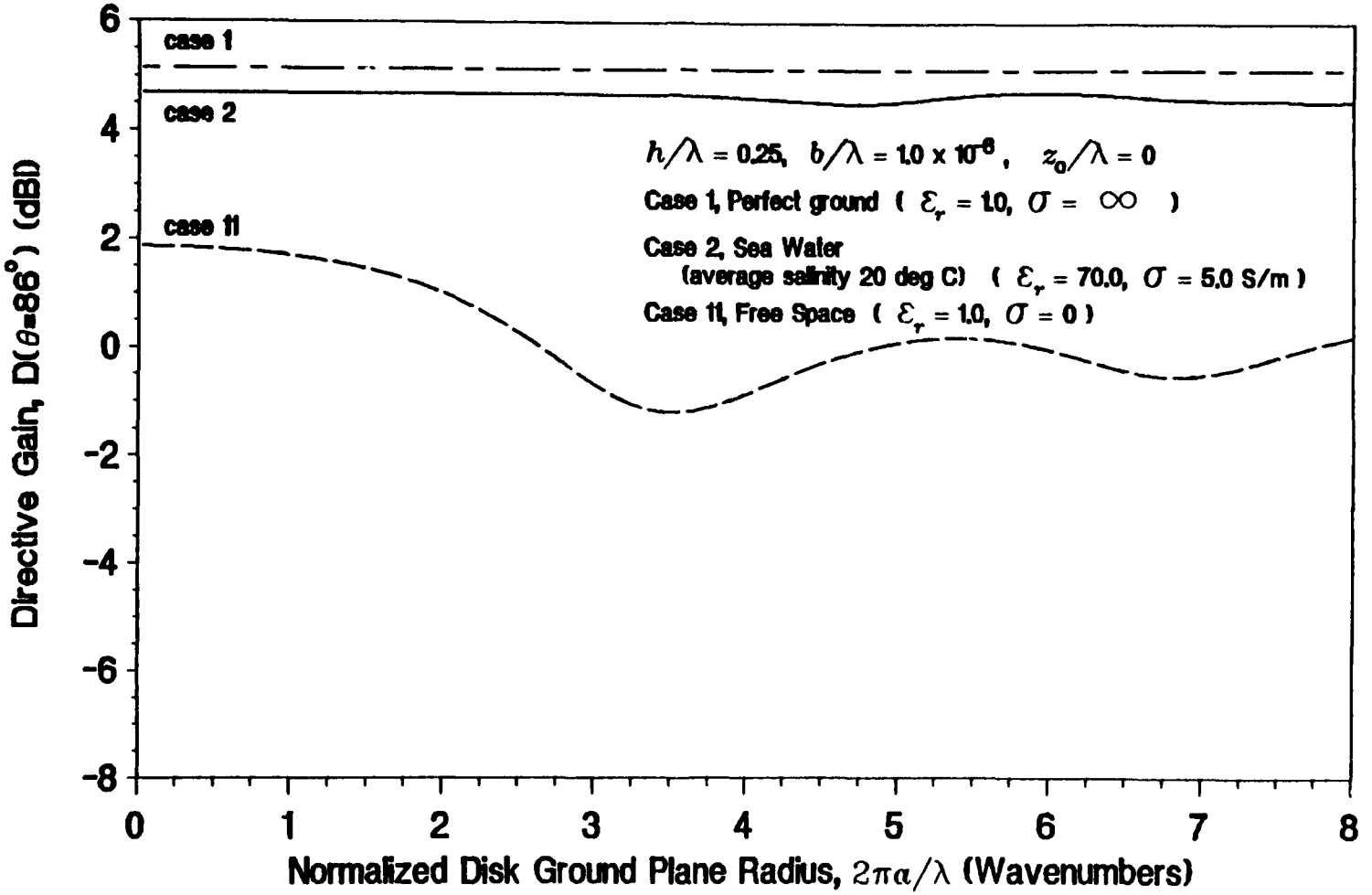

Figure 3-14. Directivity at 4 Degrees Above the Horizon, Sea Water (Average Salinity, 20°C)

DIRECTIVE GAIN AT 88 DEG ELEVATION

Case 2, Sea Water (average salinity 20 deg C) at 15 MHz

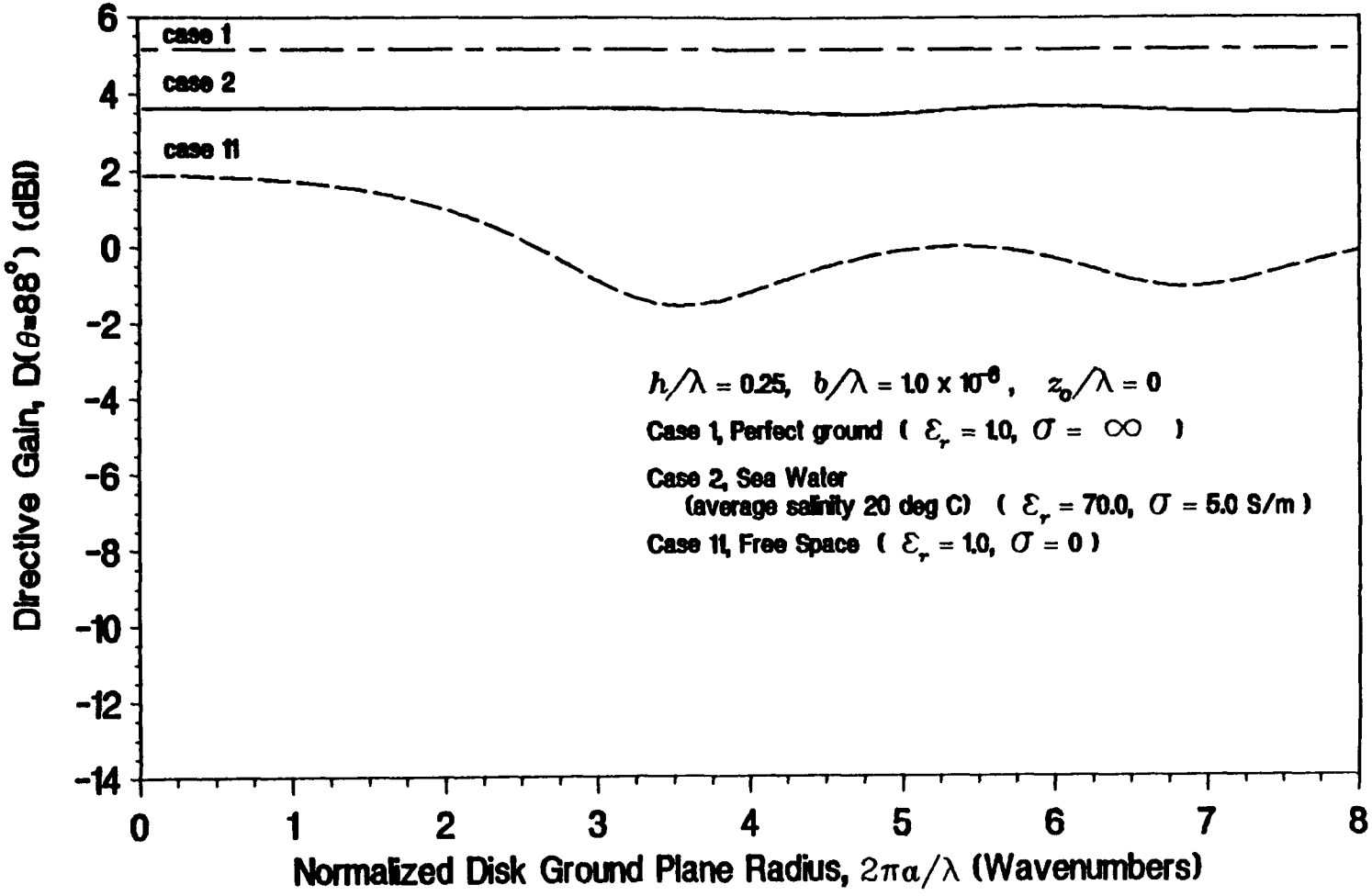

Figure 3-15. Directivity at 2 Degrees Above the Horizon, Sea Water (Average Salinity, 20°C)

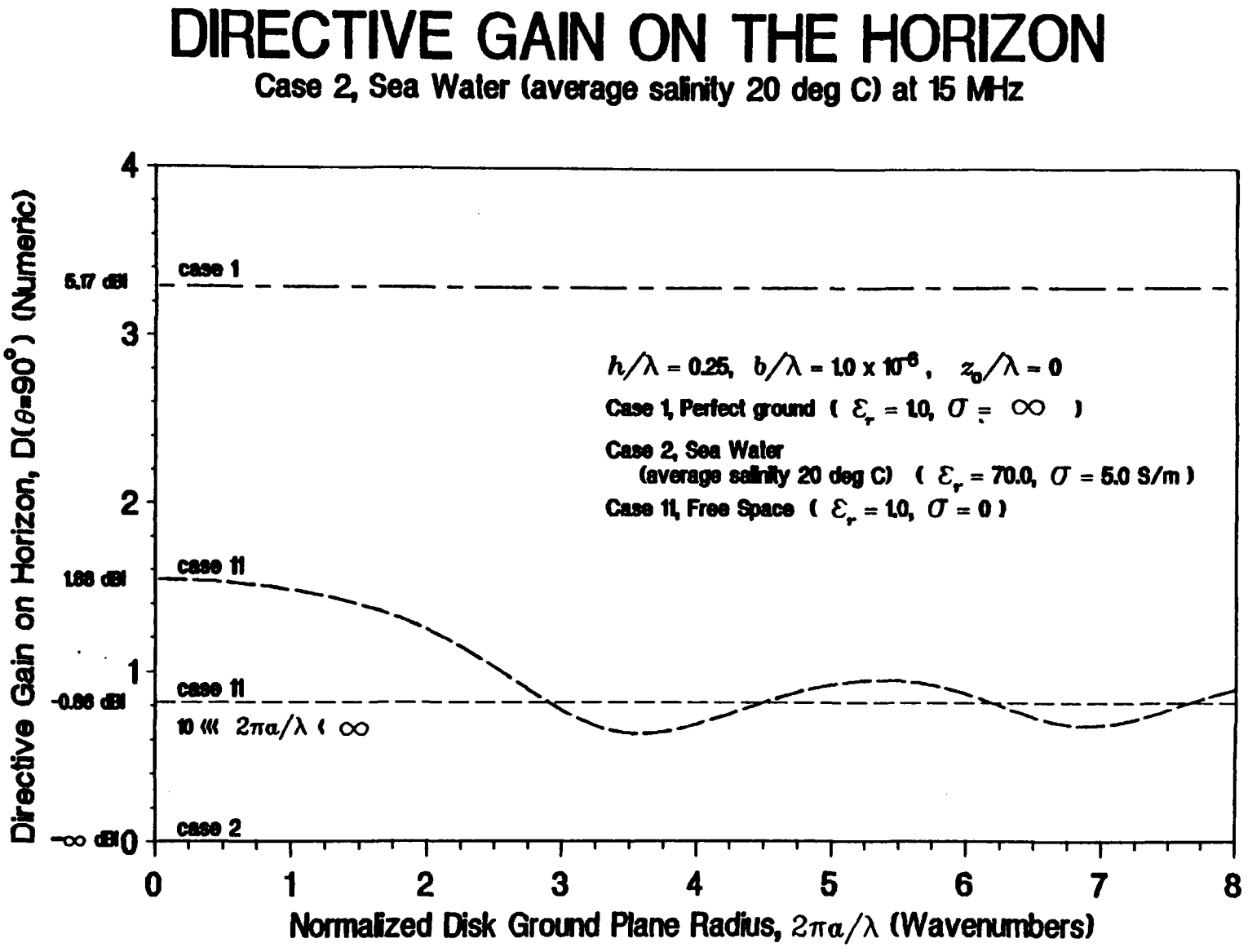

Figure 3-16. Directivity on the Horizon, Sea Water (Average Salinity, 20°C)

3.2 FRESH WATER

NUMERIC DIRECTIVE GAIN POLAR PLOT

Case 3, Fresh Water at 15 MHz

$2\pi a/\lambda = 0.025$ (Wavenumbers)

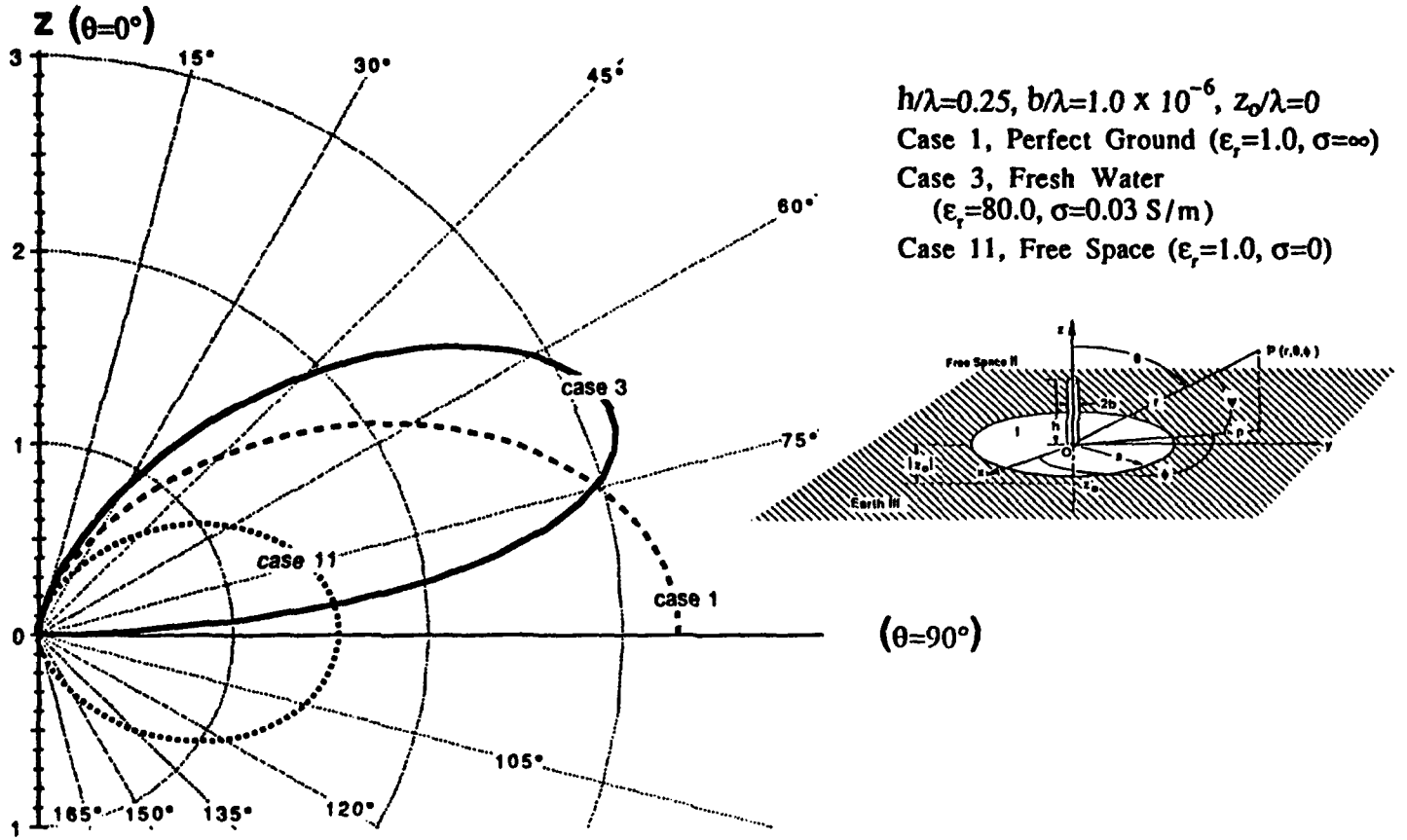

Figure 3-17. Directivity Pattern, $2\pi a/\lambda = 0.025$, Fresh Water

NUMERIC DIRECTIVE GAIN POLAR PLOT

Case 3, Fresh Water at 15 MHz

$2\pi a/\lambda =$ 3.0 (Wavenumbers)

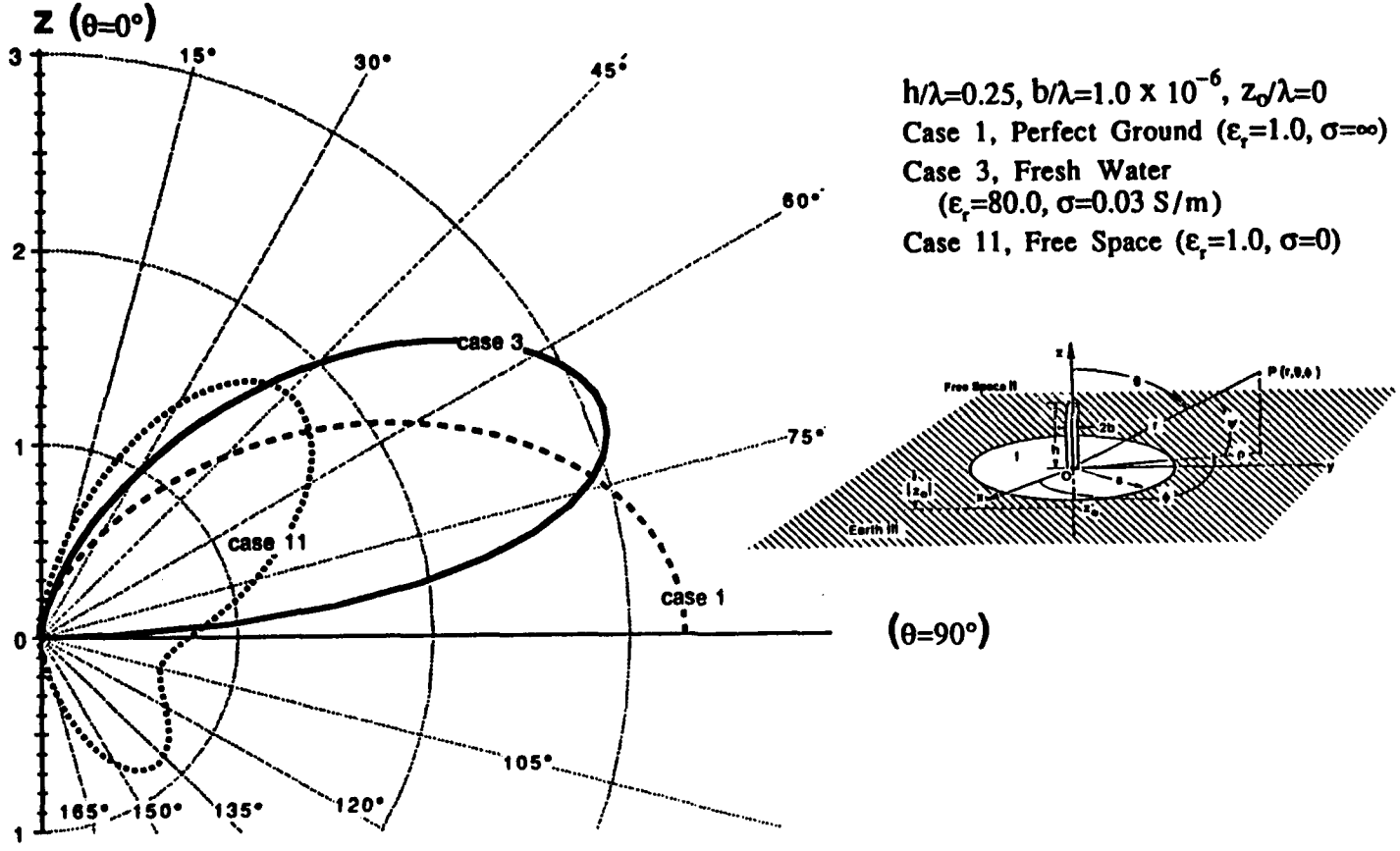

Figure 3-18. Directivity Pattern, $2\pi a/\lambda = 3.0$, Fresh Water

NUMERIC DIRECTIVE GAIN POLAR PLOT

Case 3, Fresh Water at 15 MHz

$2\pi a/\lambda =$ **4.0 (Wavenumbers)**

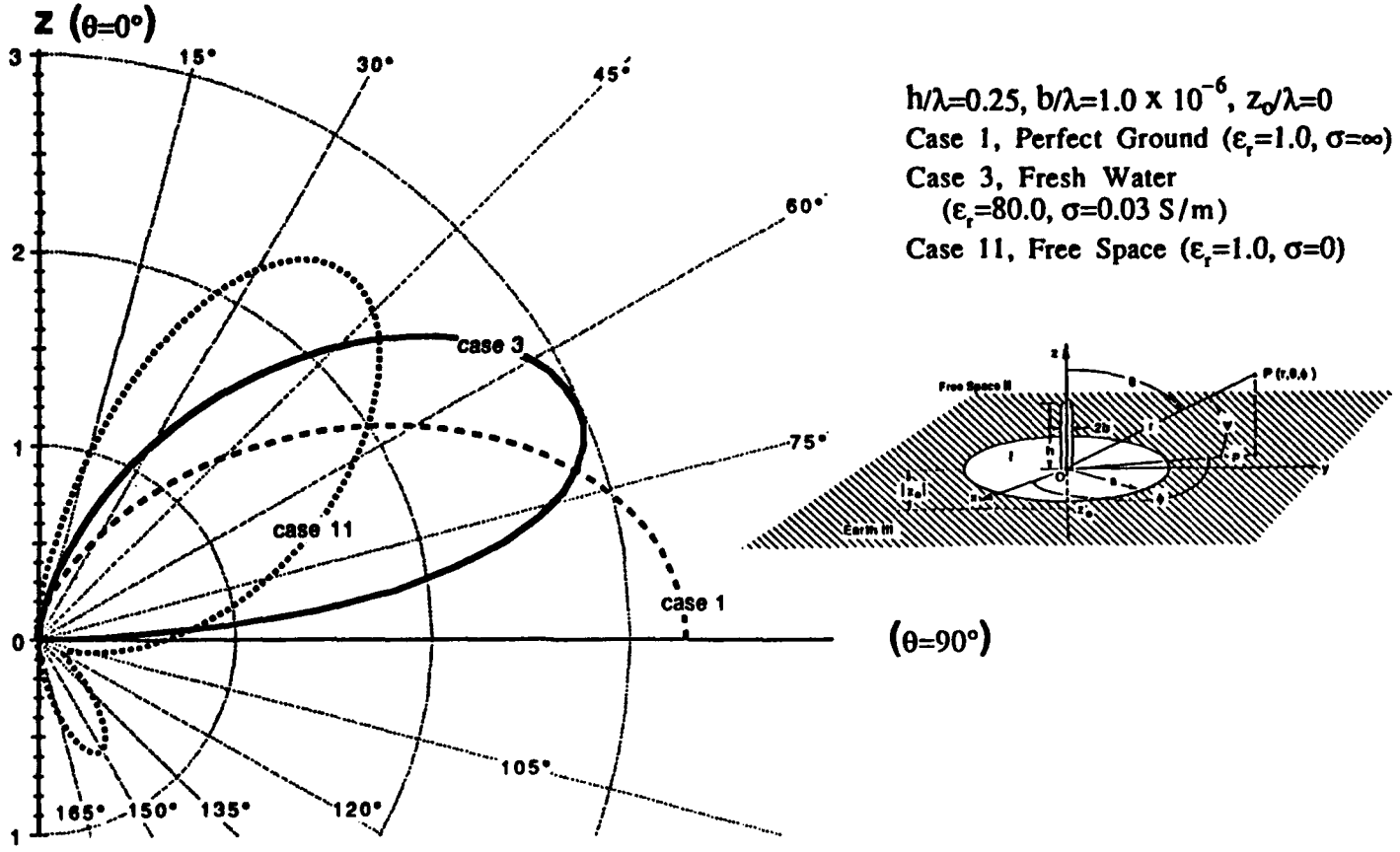

Figure 3-19. Directivity Pattern, $2\pi a/\lambda = 4.0$, Fresh Water

NUMERIC DIRECTIVE GAIN POLAR PLOT

Case 3, Fresh Water at 15 MHz

$2\pi a/\lambda =$ 5.0 (Wavenumbers)

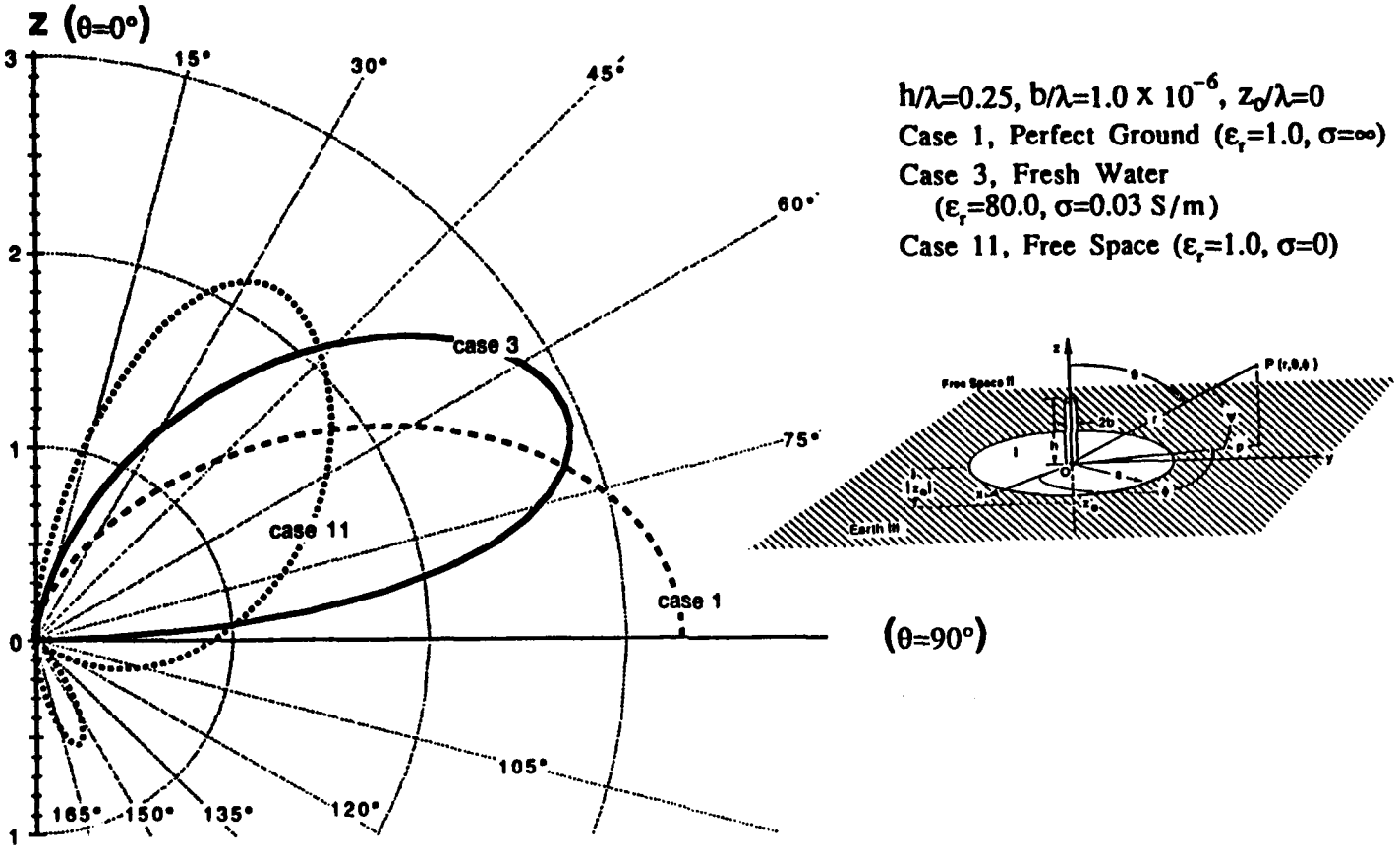

Figure 3-20. Directivity Pattern, $2\pi a/\lambda = 5.0$, Fresh Water

NUMERIC DIRECTIVE GAIN POLAR PLOT

Case 3, Fresh Water at 15 MHz

$2\pi a/\lambda =$ **6.5 (Wavenumbers)**

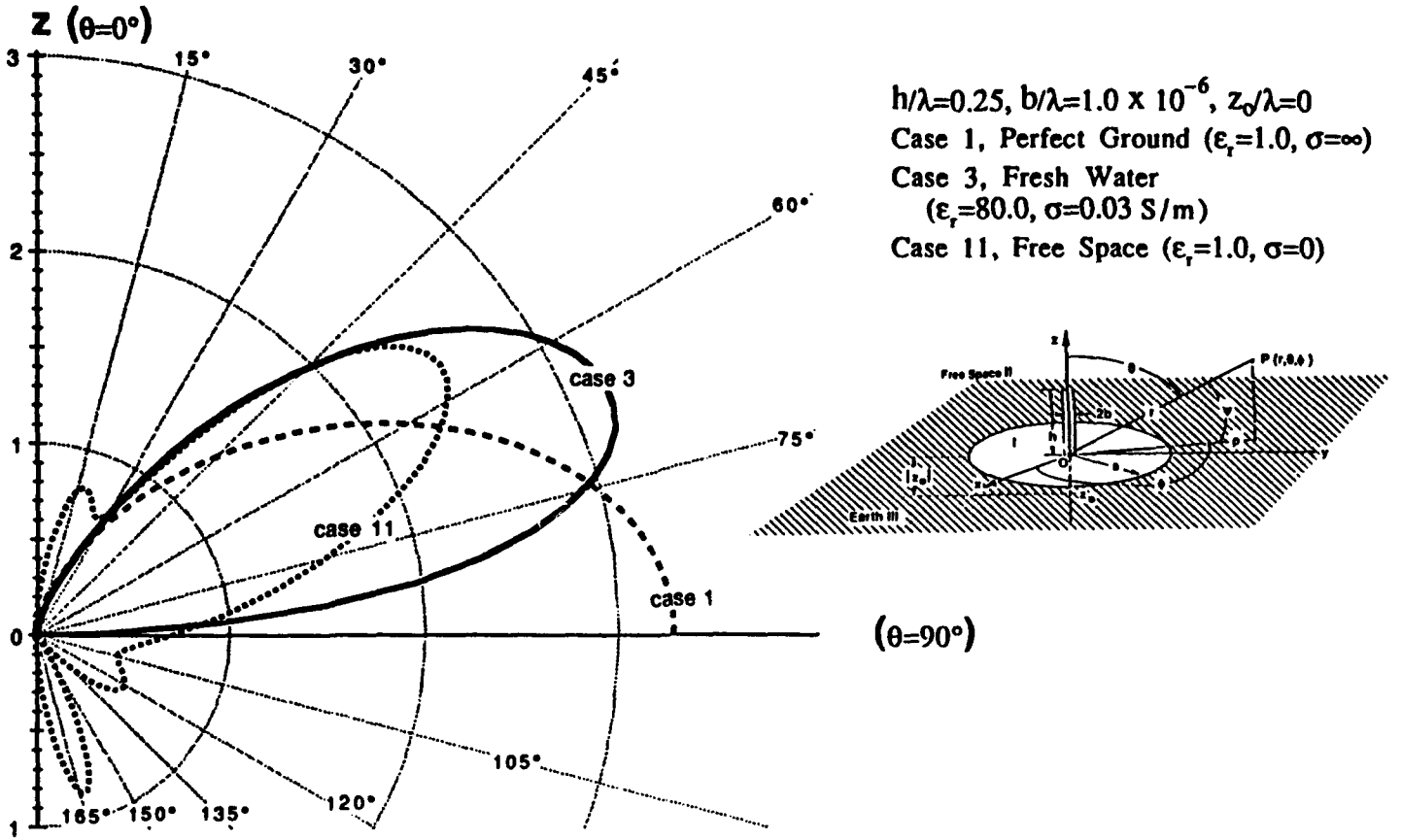

Figure 3-21. Directivity Pattern, $2\pi a/\lambda = 6.5$, Fresh Water

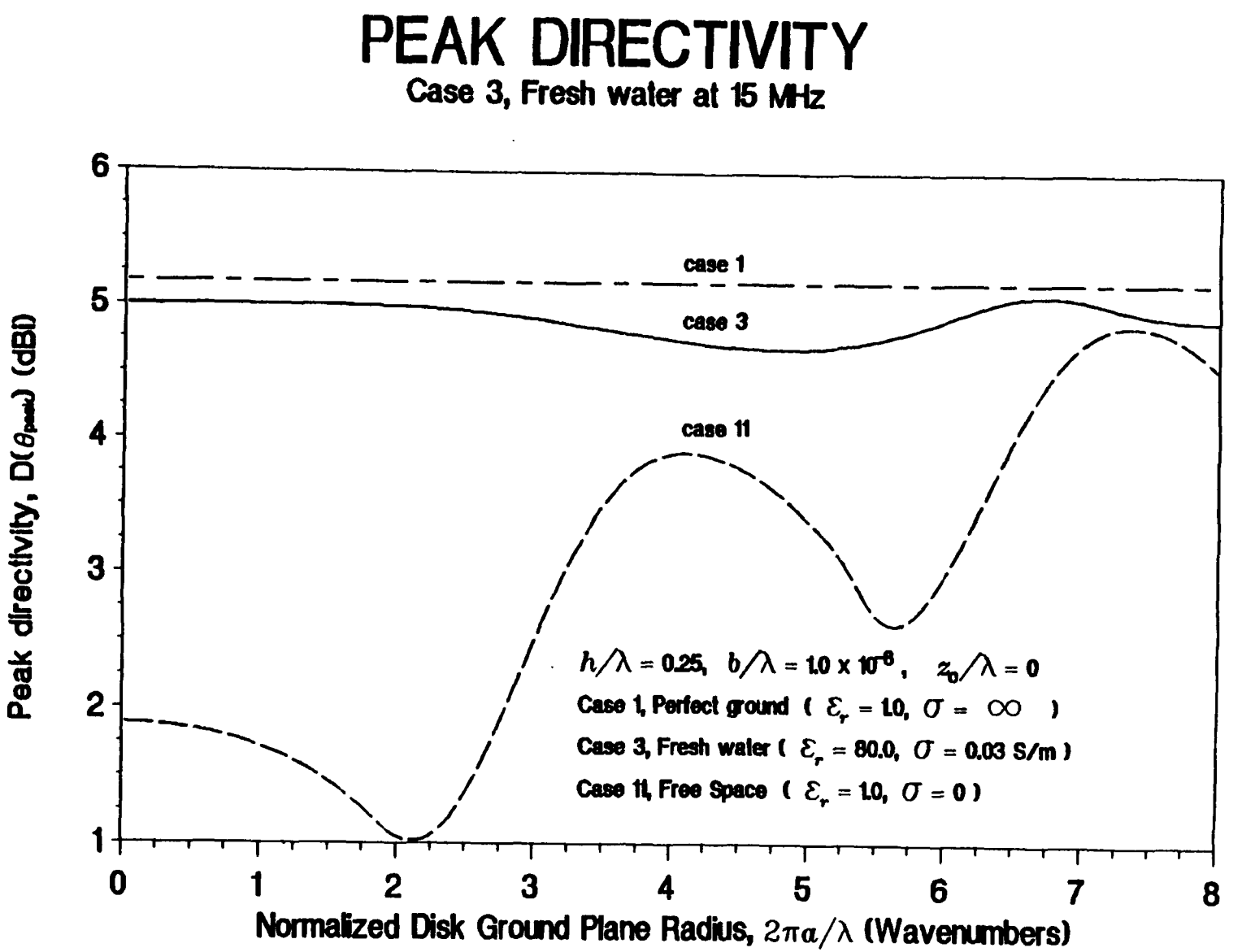

Figure 3-22. Peak Directivity, Fresh Water

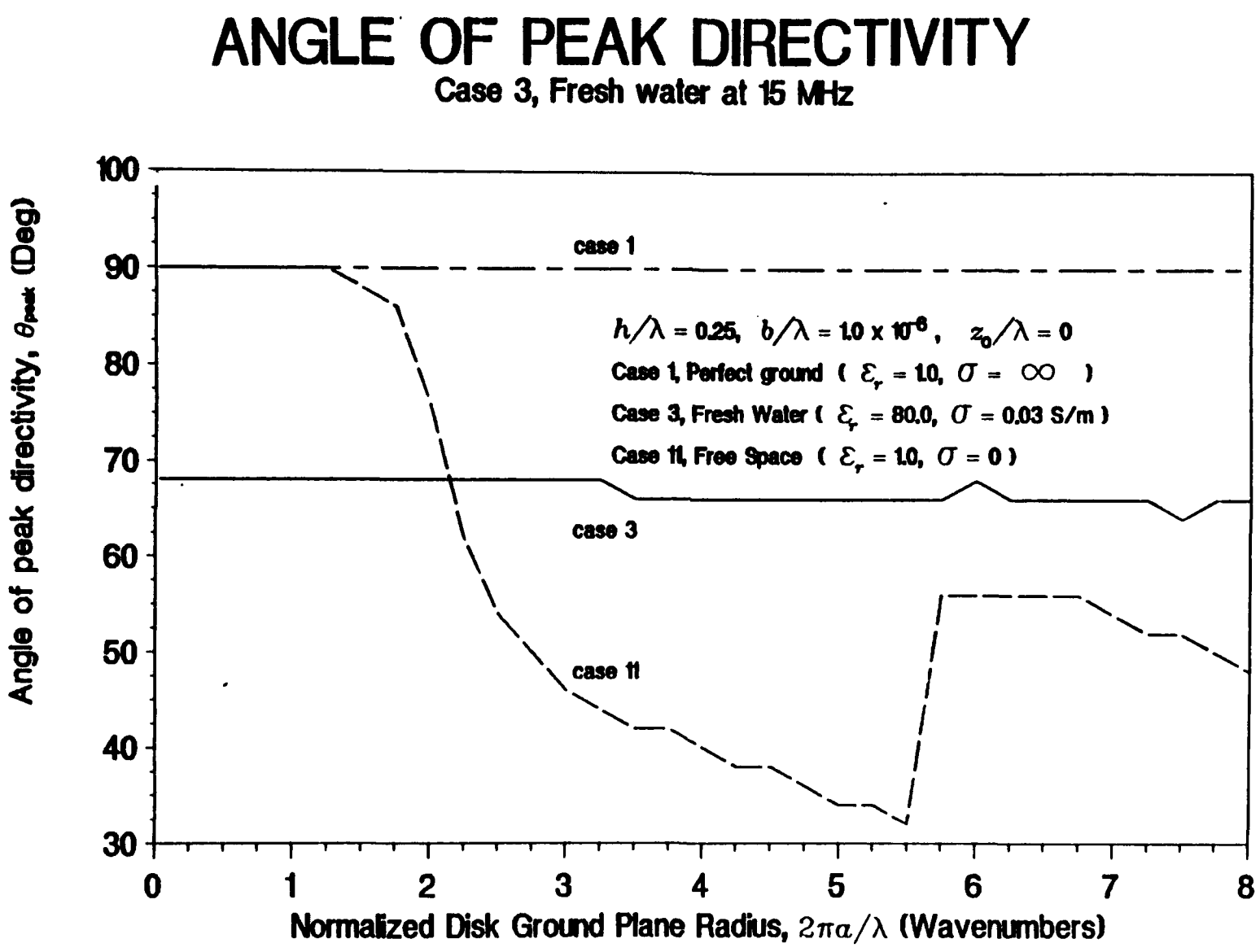

Figure 3-23. Angle of Incidence of Peak Directivity, Fresh Water

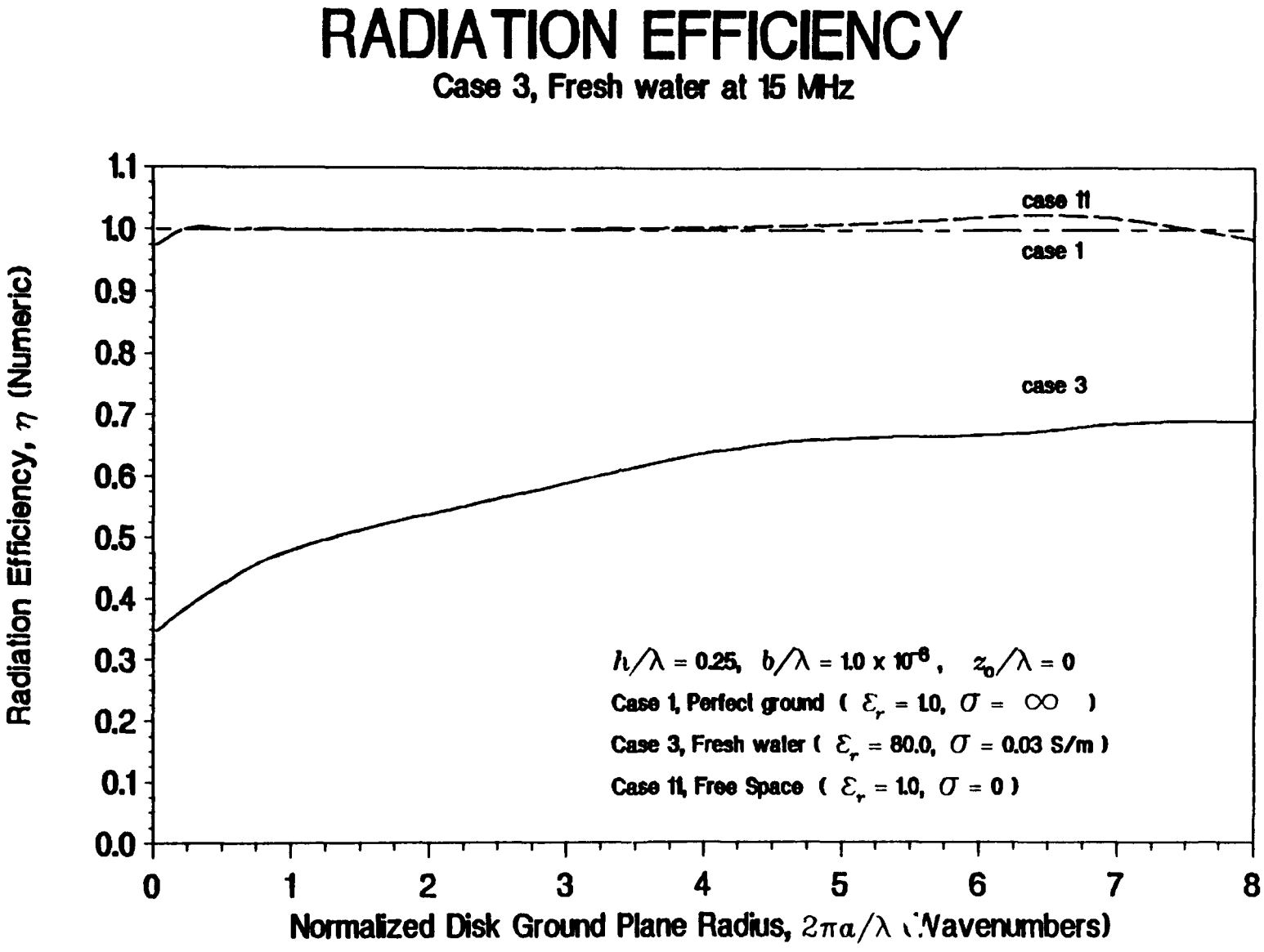

Figure 3-24. Radiation Efficiency, Fresh Water

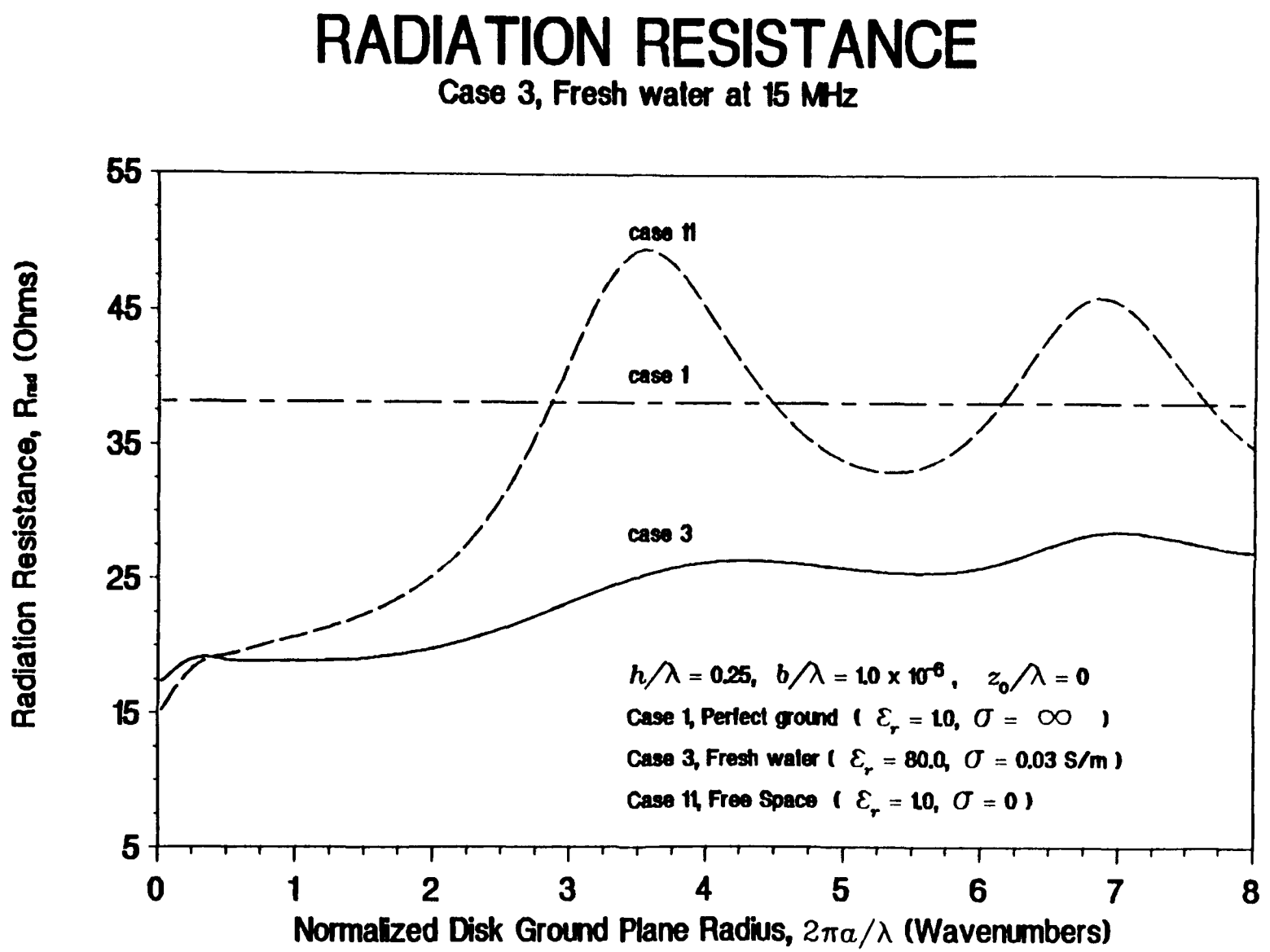

Figure 3-25. Radiation Resistance, Fresh Water

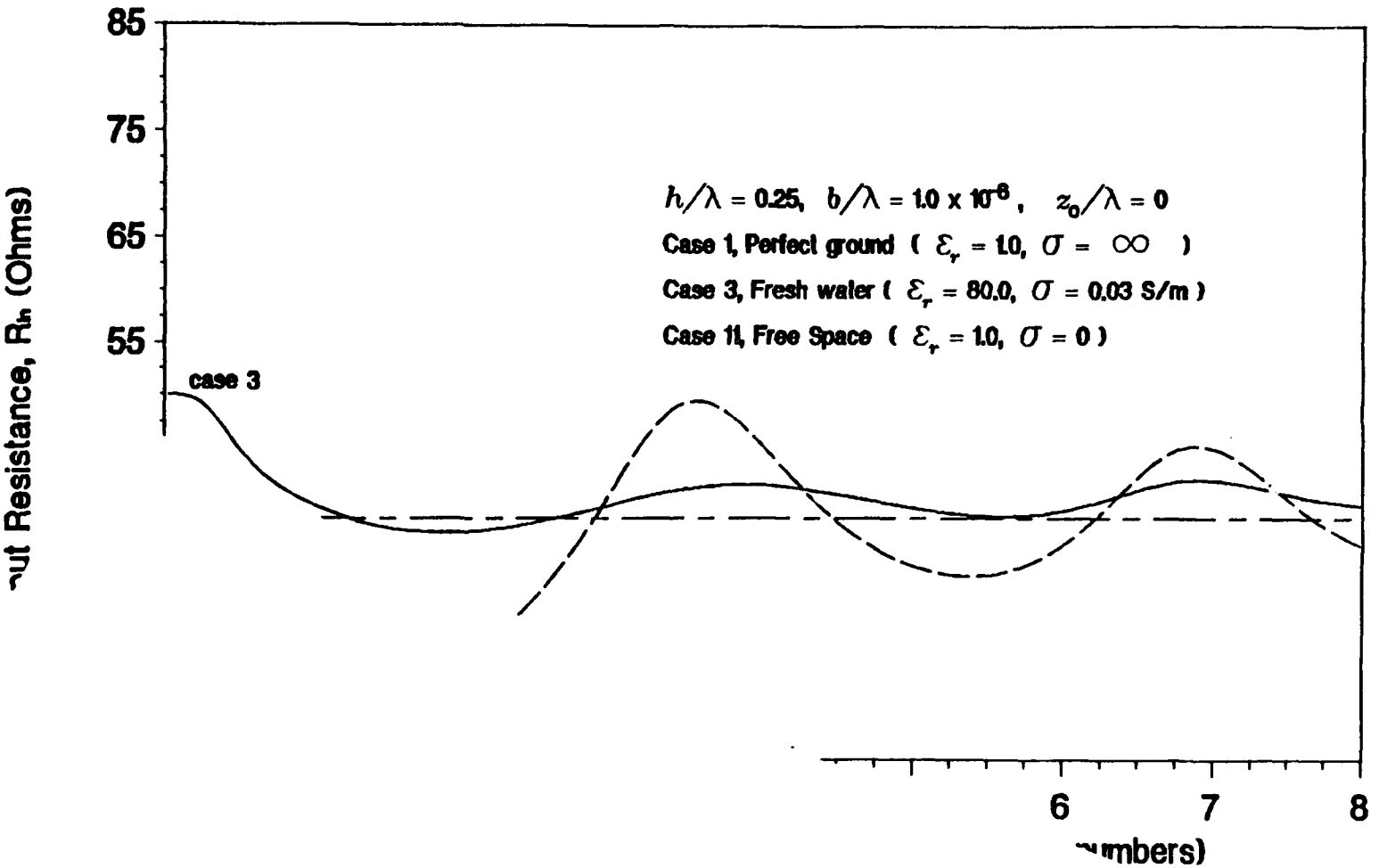

Figure 3-26. Input Resistance, Fresh Water

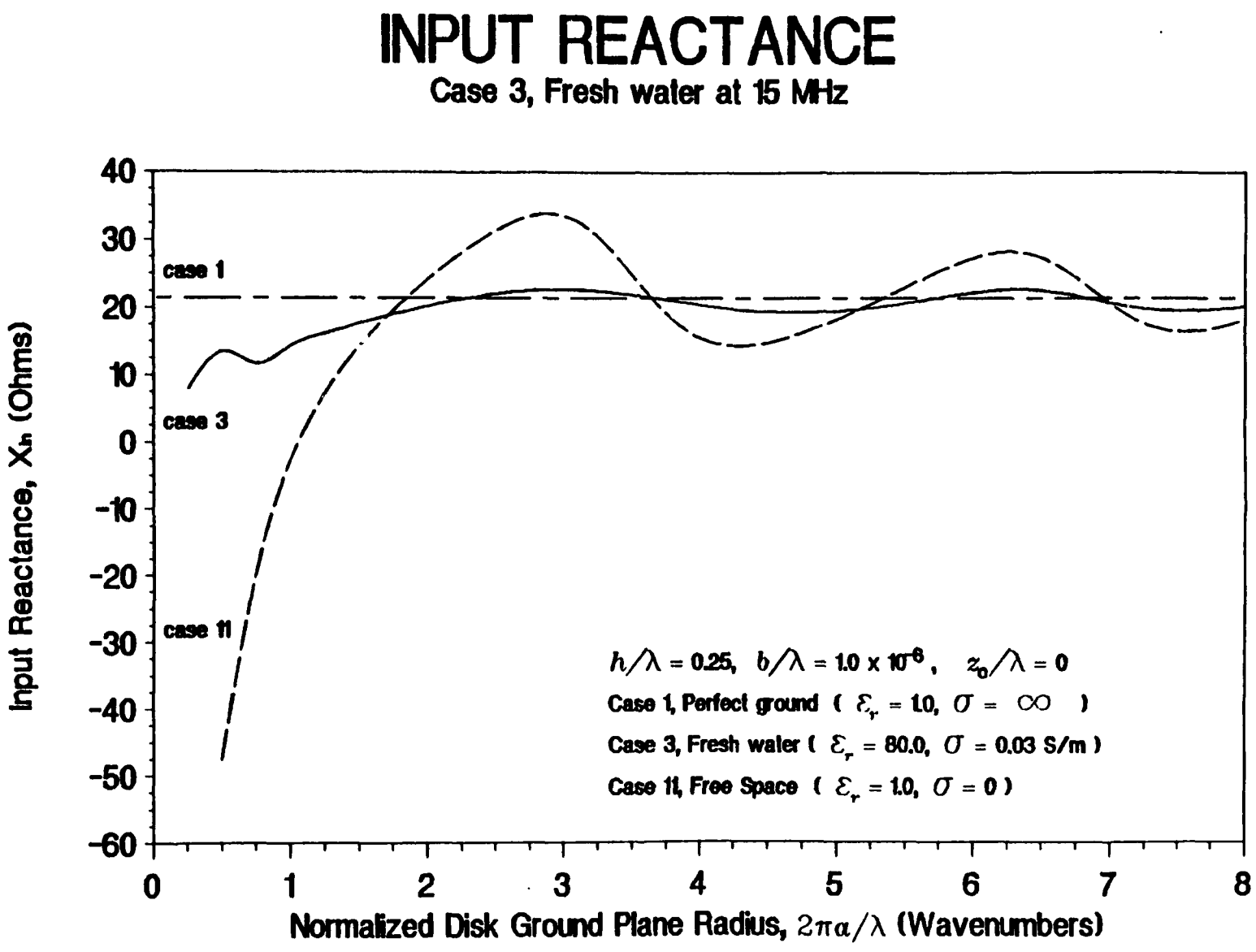

Figure 3-27. Input Reactance, Fresh Water

DIRECTIVE GAIN AT 88 DEG ELEVATION

Case 3, Fresh water at 15 MHz

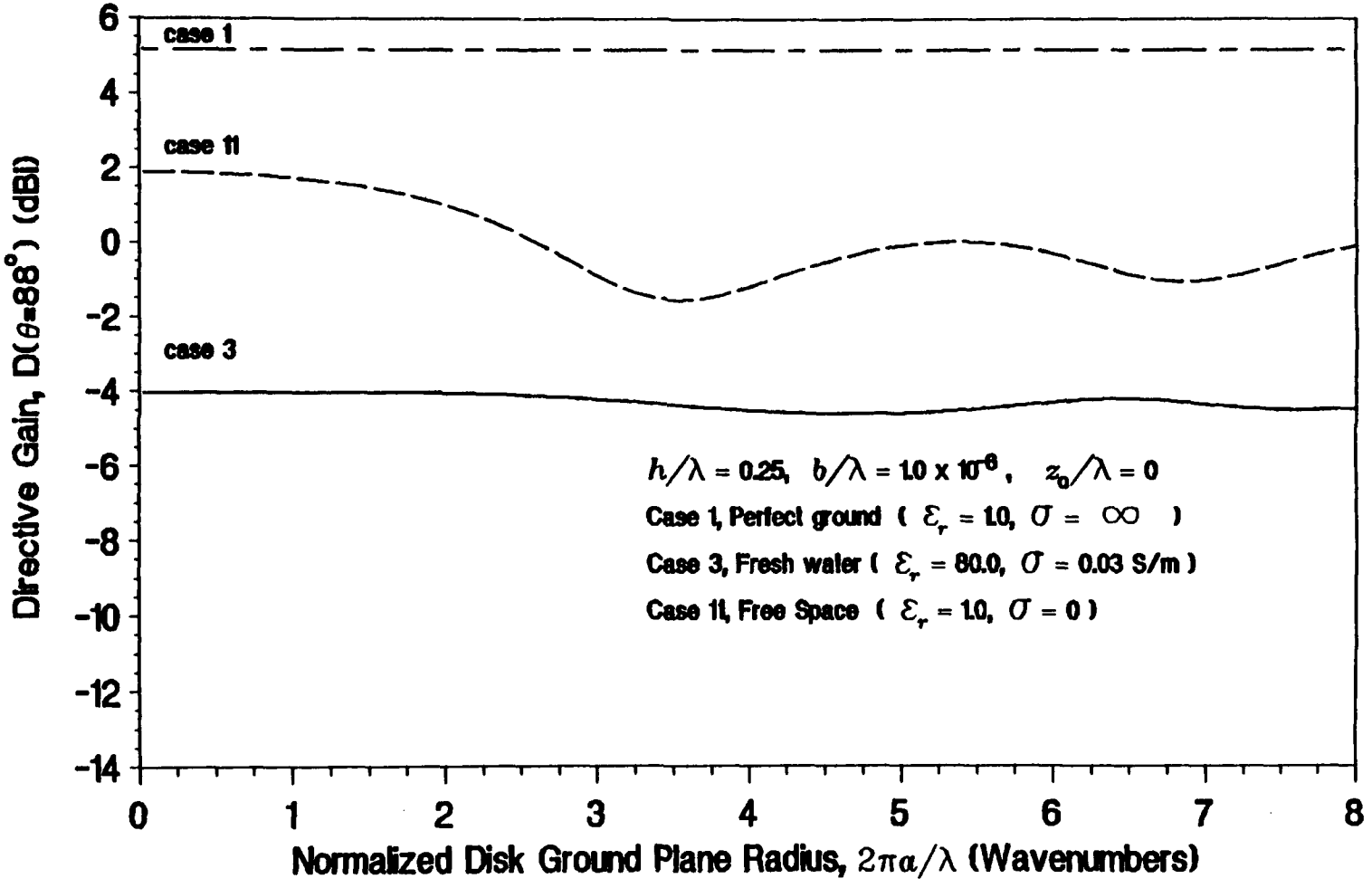

Figure 3-28. Directivity at 8 Degrees Above the Horizon, Fresh Water

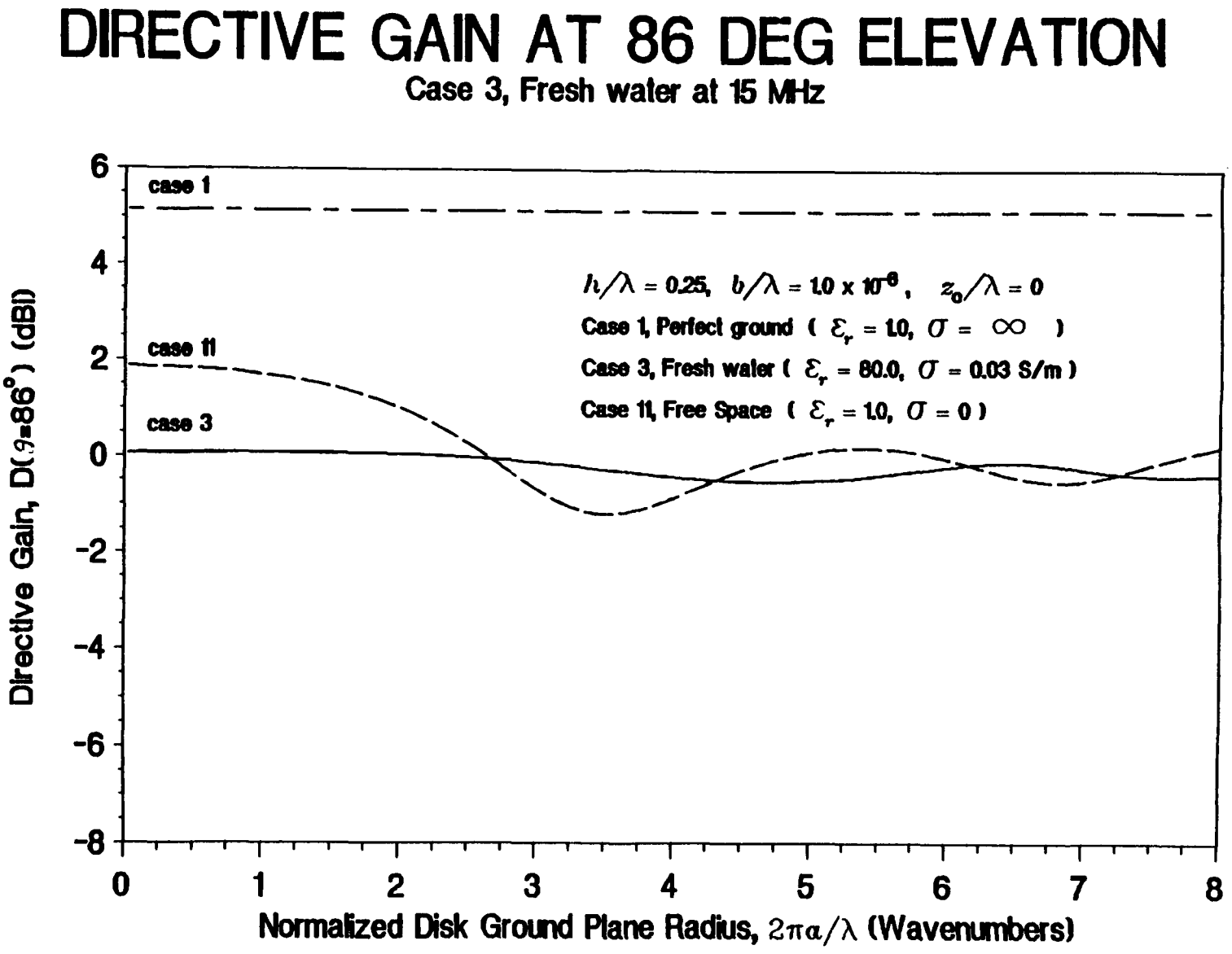

Figure 3-29. Directivity at 6 Degrees Above the Horizon, Fresh Water

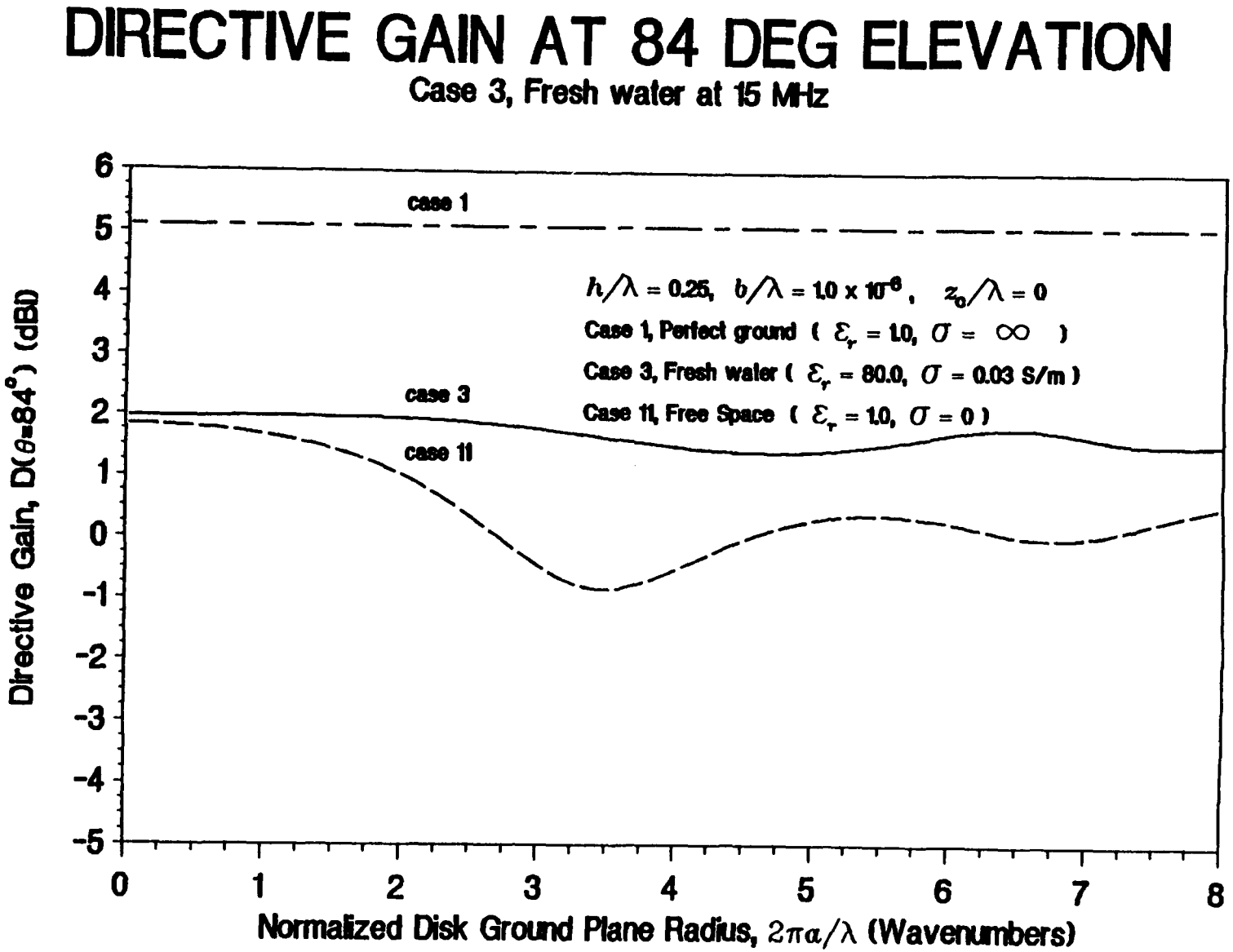

Figure 3-30. Directivity at 4 Degrees Above the Horizon, Fresh Water

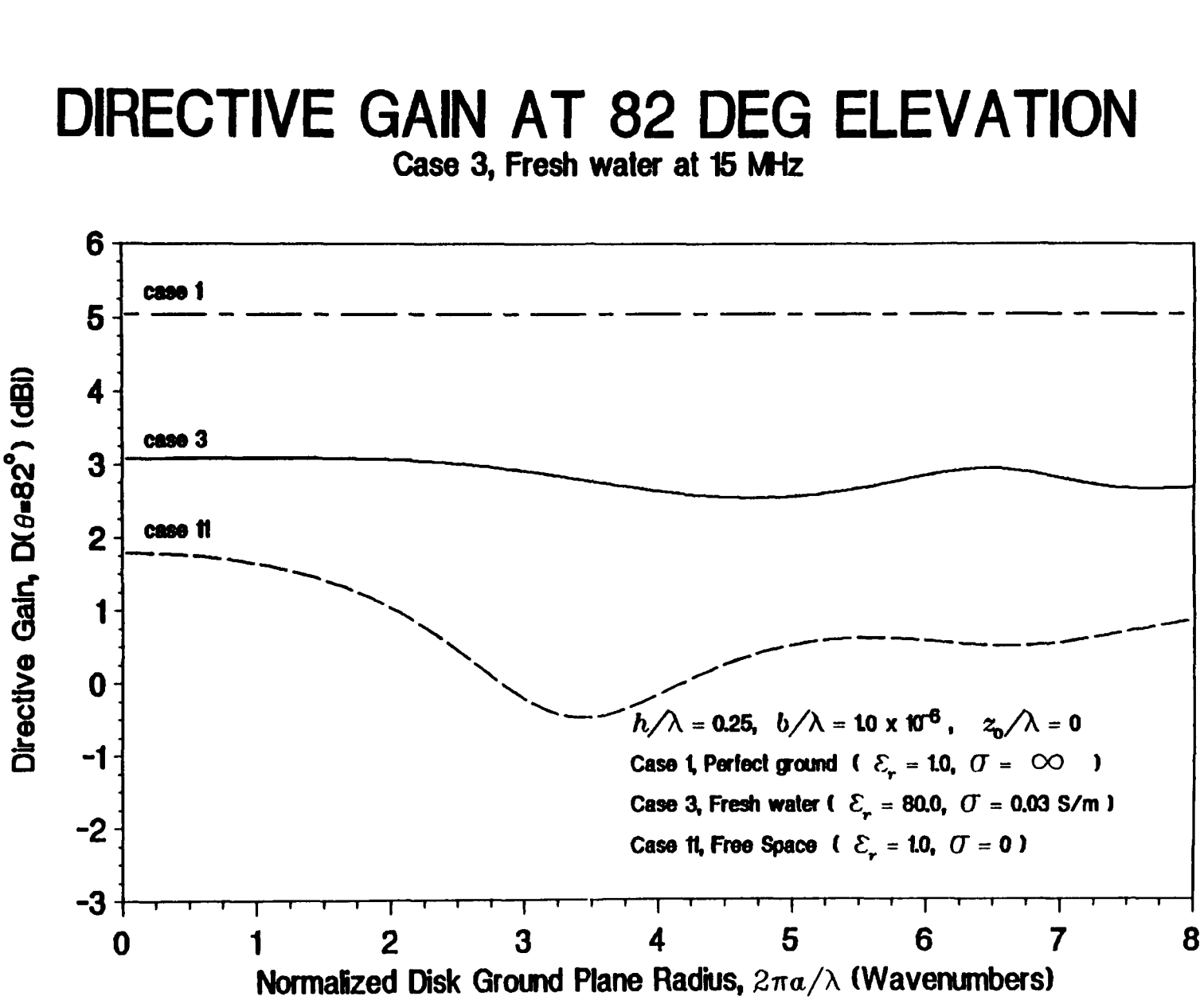

Figure 3-31. Directivity at 2 Degrees Above the Horizon, Fresh Water

DIRECTIVE GAIN ON THE HORIZON

Case 3, Fresh water at 15 MHz

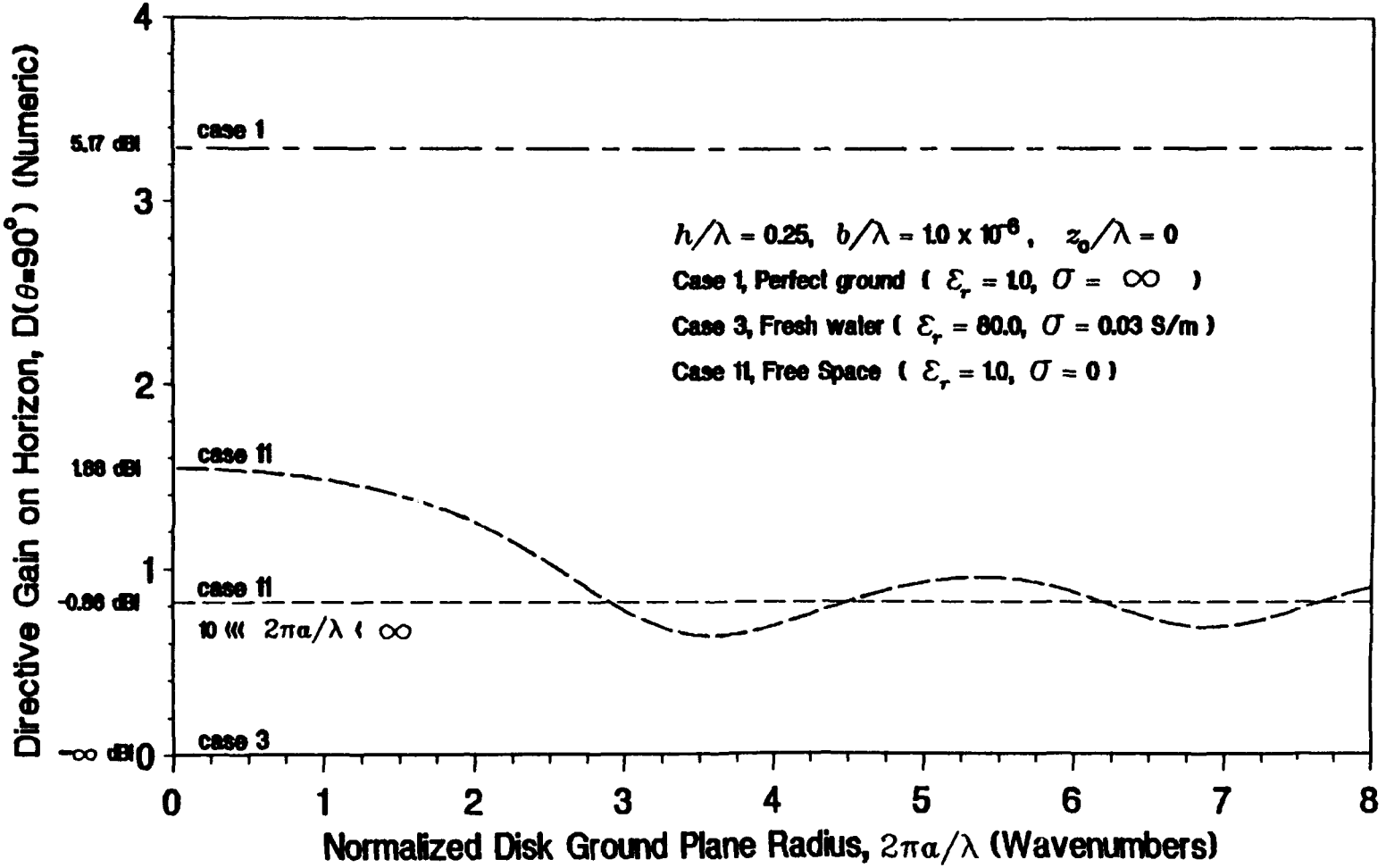

Figure 3-32. Directivity on the Horizon, Fresh Water

3.3 WET GROUND

NUMERIC DIRECTIVE GAIN POLAR PLOT

Case 4, Wet Ground at 15 MHz

$2\pi a/\lambda = 0.025$ (Wavenumbers)

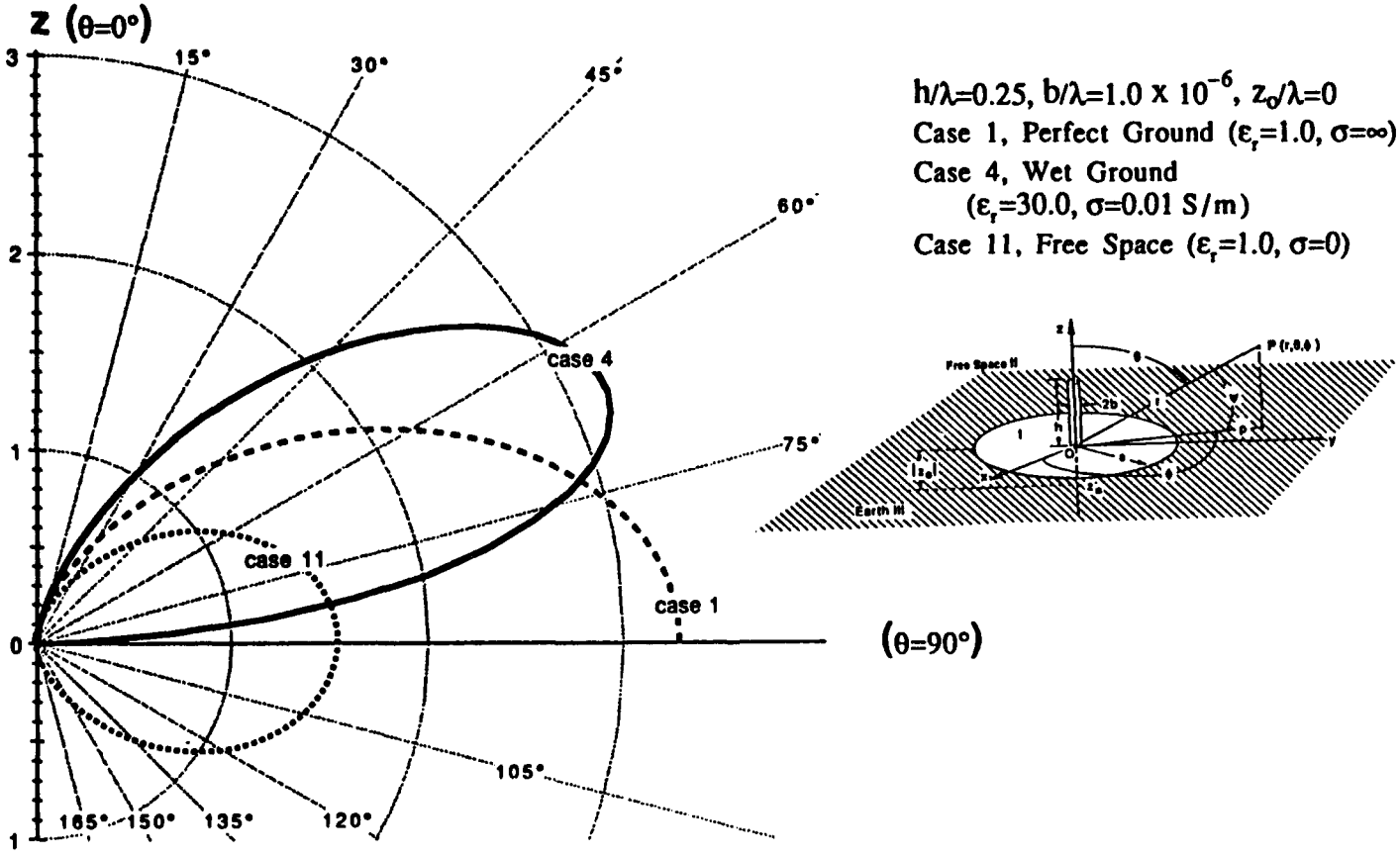

Figure 3-33. Directivity Pattern, $2\pi a/\lambda = 0.025$, Wet Ground

NUMERIC DIRECTIVE GAIN POLAR PLOT

Case 4, Wet Ground at 15 MHz

$2\pi a/\lambda =$ 3.0 (Wavenumbers)

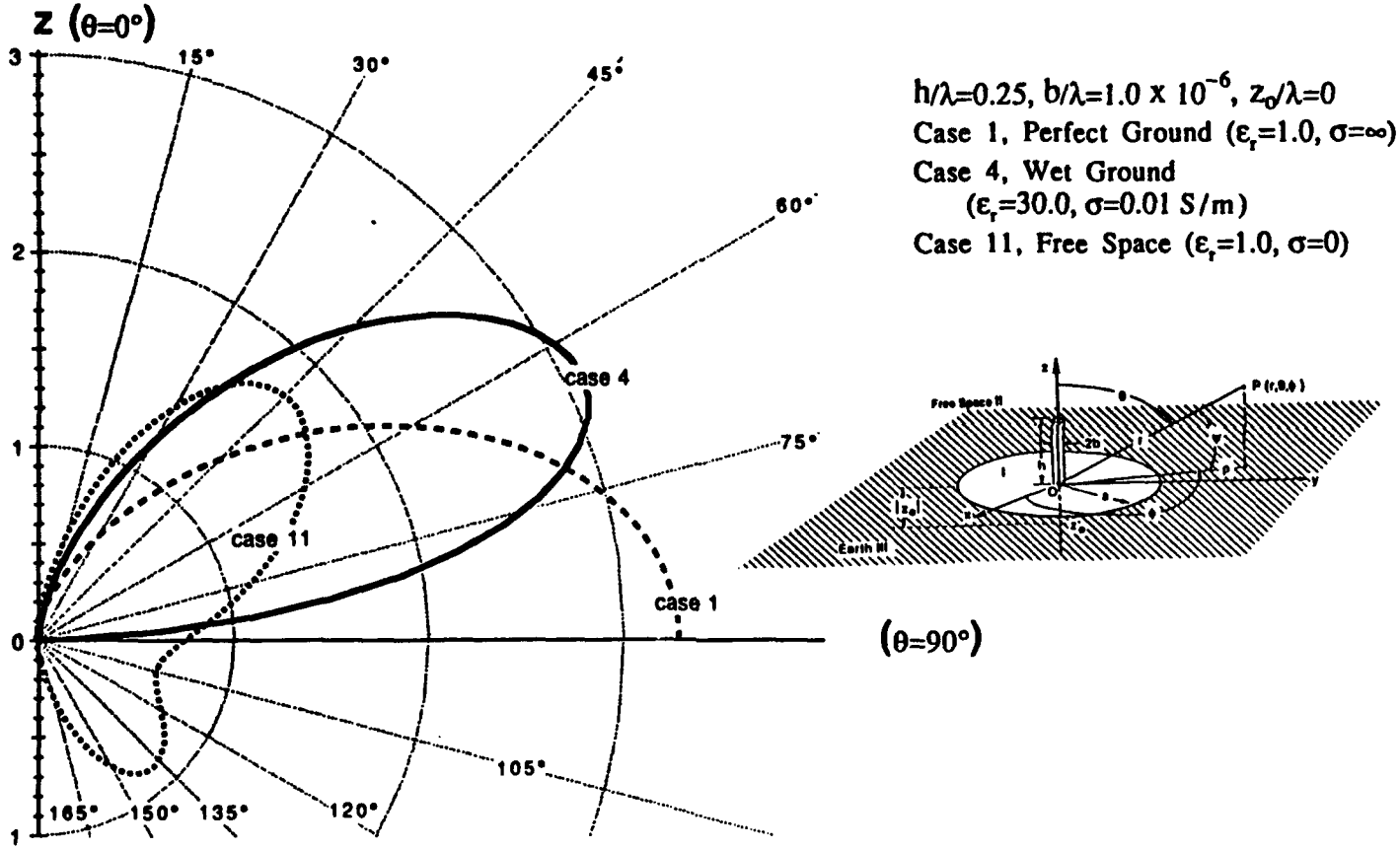

Figure 3-34. Directivity Pattern, $2\pi a/\lambda = 3.0$, Wet Ground

NUMERIC DIRECTIVE GAIN POLAR PLOT

Case 4, Wet Ground at 15 MHz

$2\pi a/\lambda =$ 4.0 (Wavenumbers)

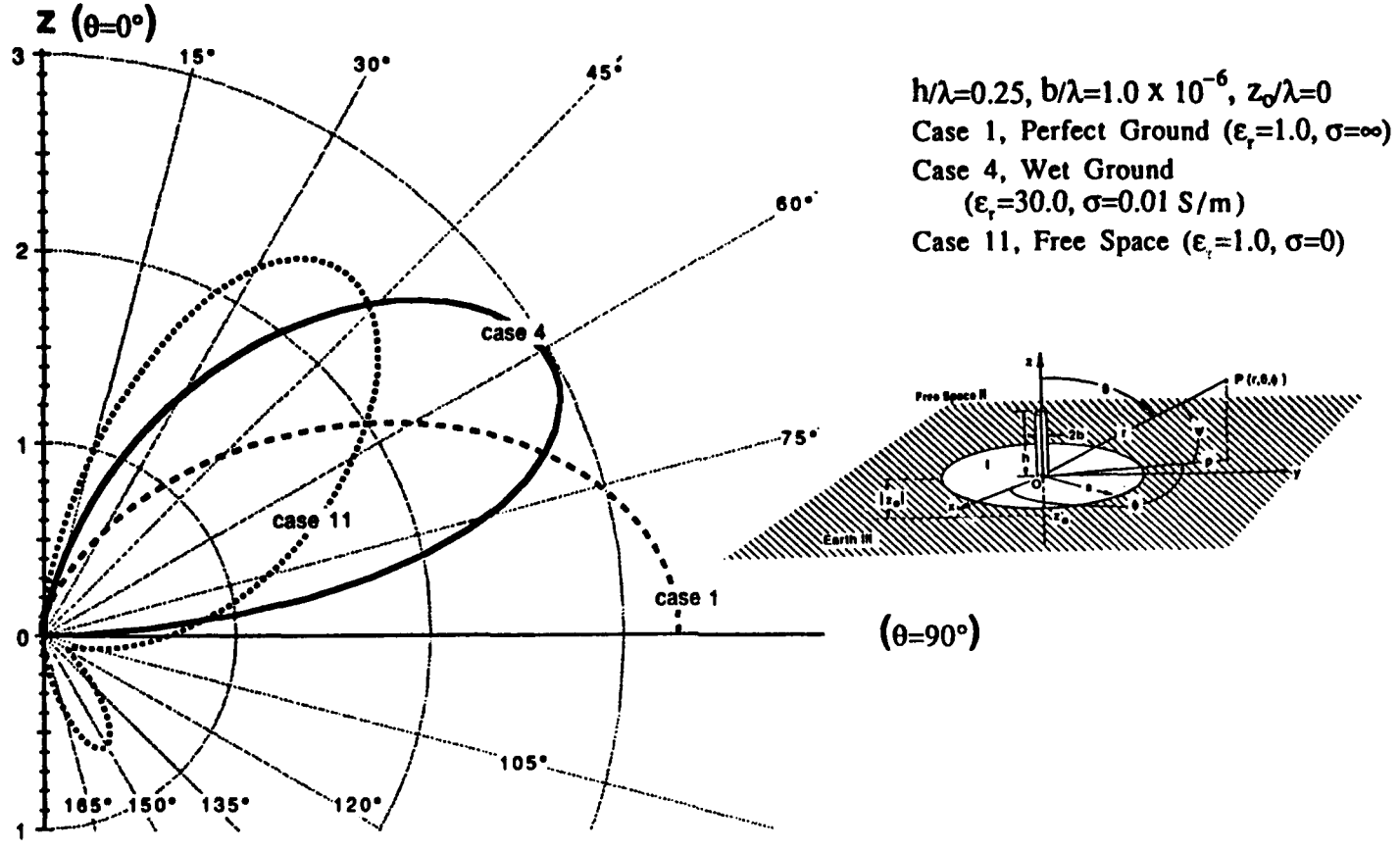

Figure 3-35. Directivity Pattern, $2\pi a/\lambda = 4.0$, Wet Ground

NUMERIC DIRECTIVE GAIN POLAR PLOT

Case 4, Wet Ground at 15 MHz

$2\pi a/\lambda =$ **5.0 (Wavenumbers)**

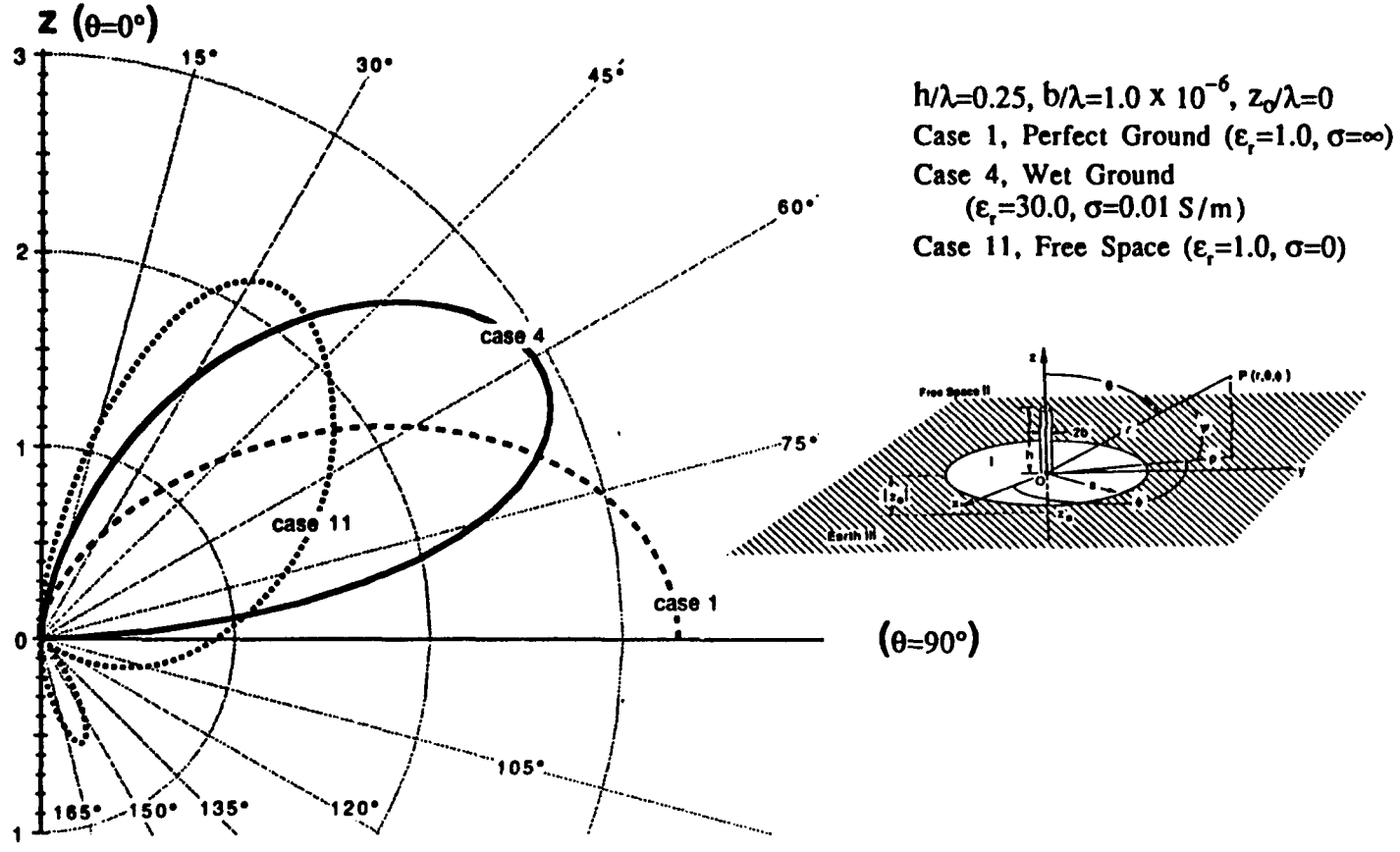

Figure 3-36. Directivity Pattern, $2\pi a/\lambda = 5.0$, Wet Ground

NUMERIC DIRECTIVE GAIN POLAR PLOT

Case 4, Wet Ground at 15 MHz

$2\pi a/\lambda =$ **6.5 (Wavenumbers)**

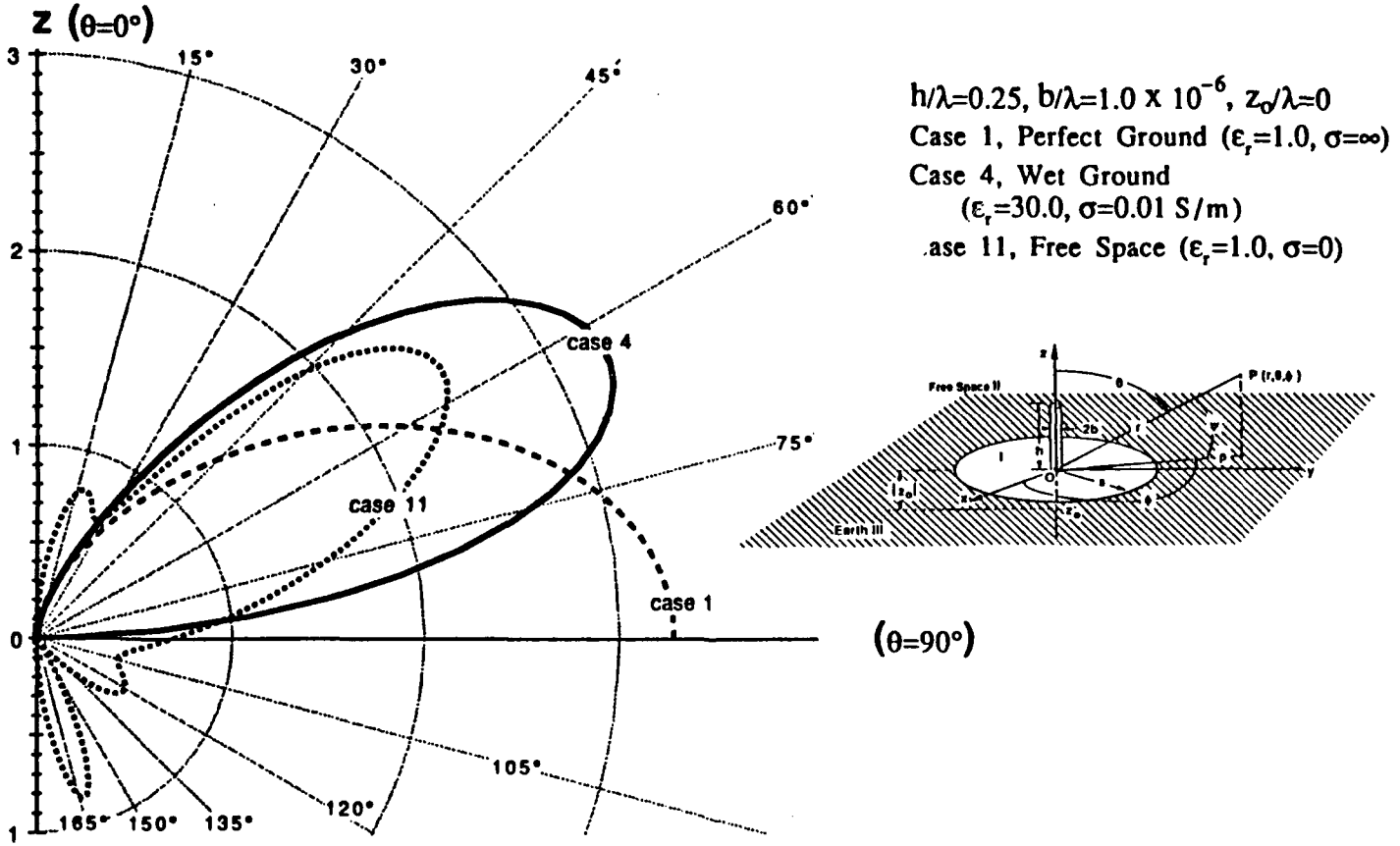

Figure 3-37. Directivity Pattern, $2\pi a/\lambda = 6.5$, Wet Ground

PEAK DIRECTIVITY

Case 4, Wet Ground at 15 MHz

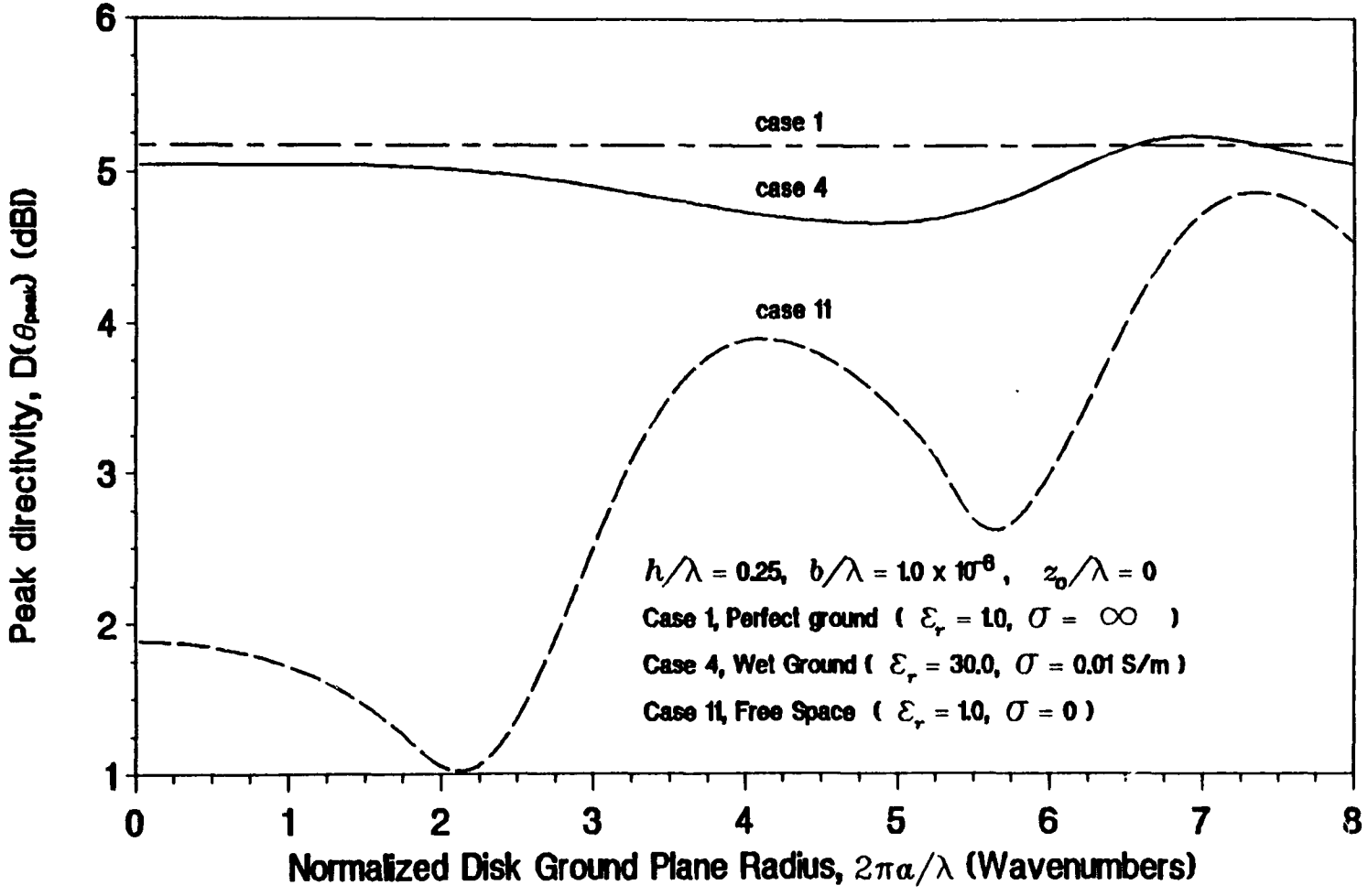

Figure 3-38. Peak Directivity, Wet Ground

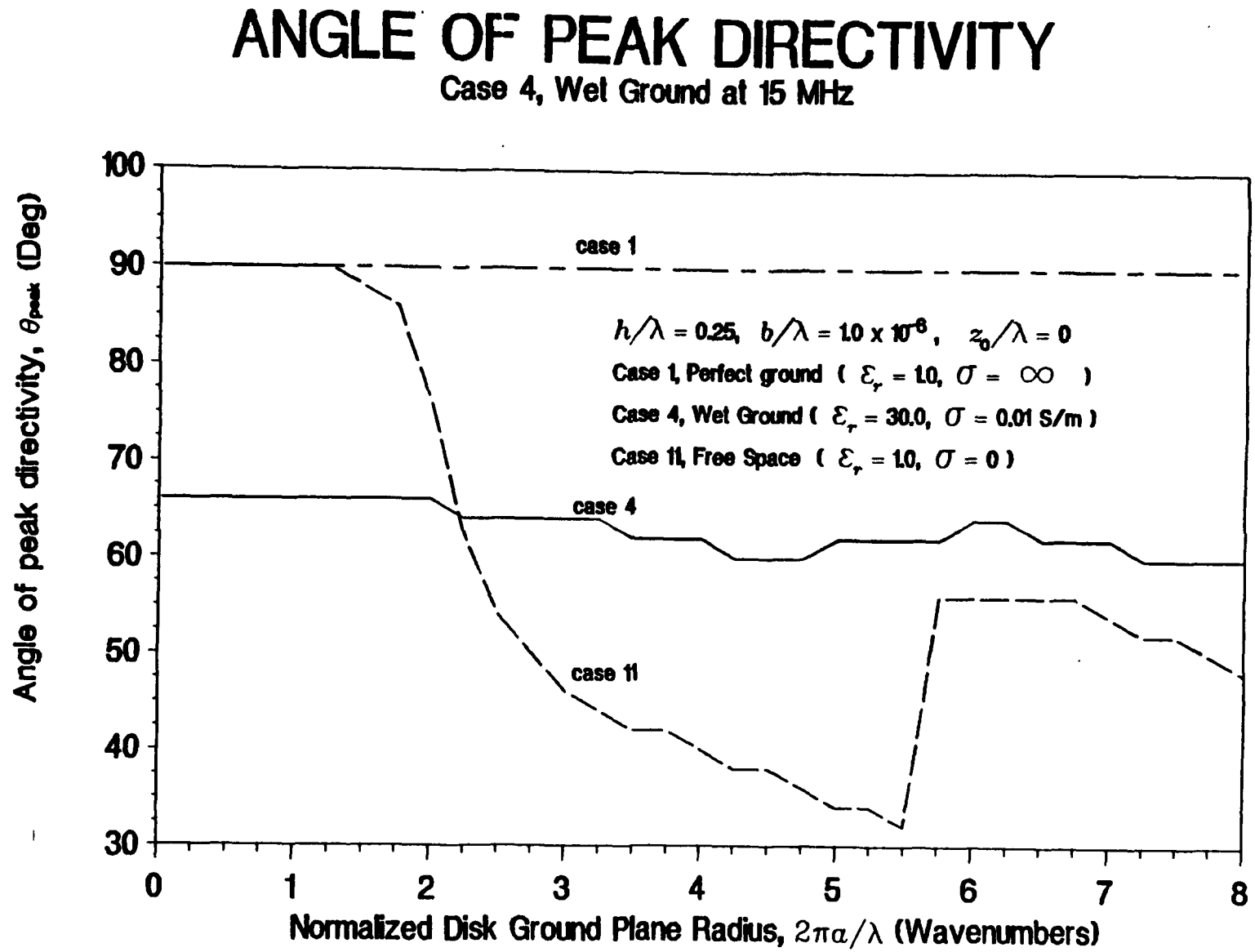

Figure 3-39. Angle of Incidence of Peak Directivity, Wet Ground

RADIATION EFFICIENCY

Case 4, Wet Ground at 15 MHz

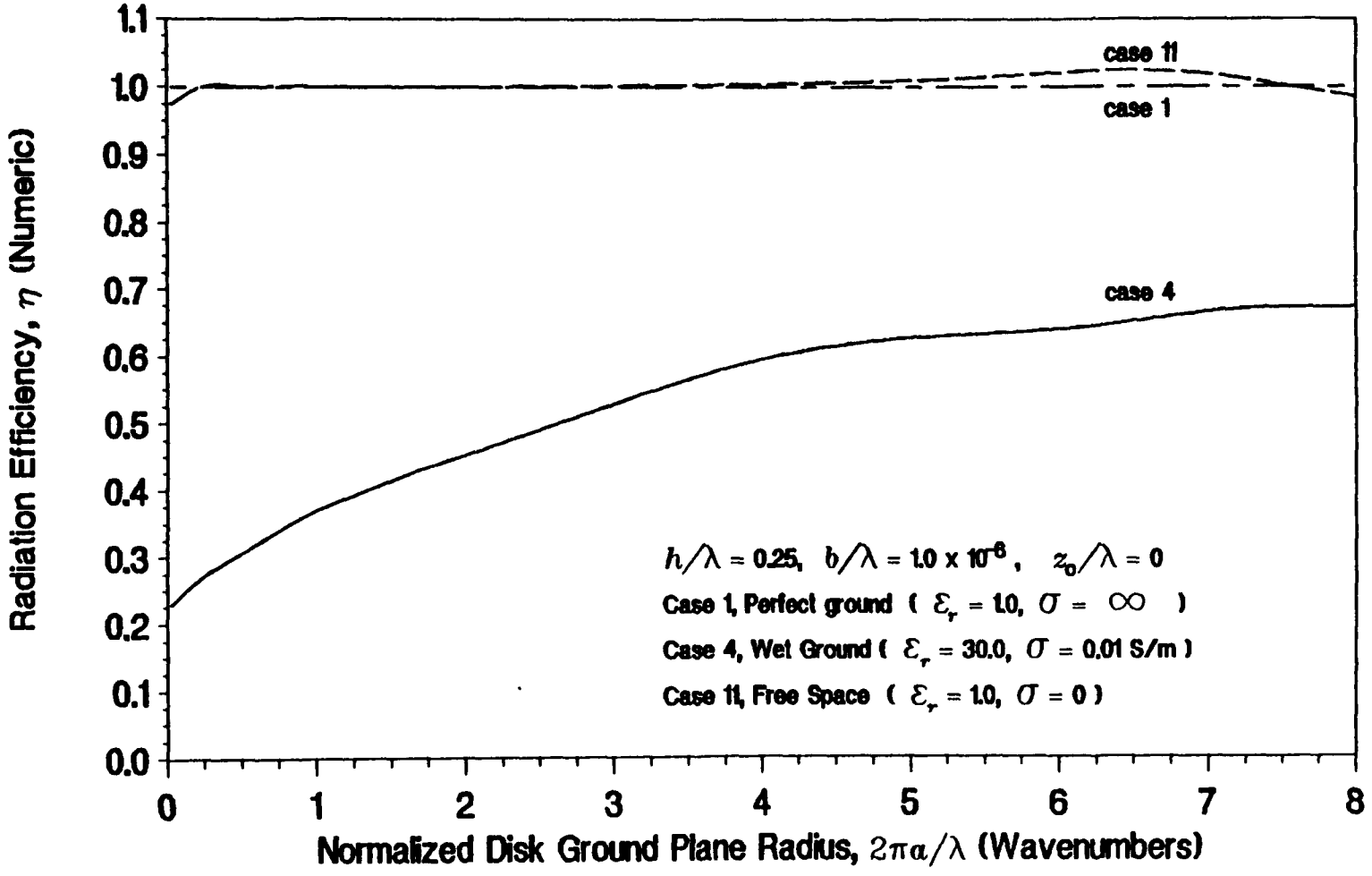

Figure 3-40. Radiation Efficiency, Wet Ground

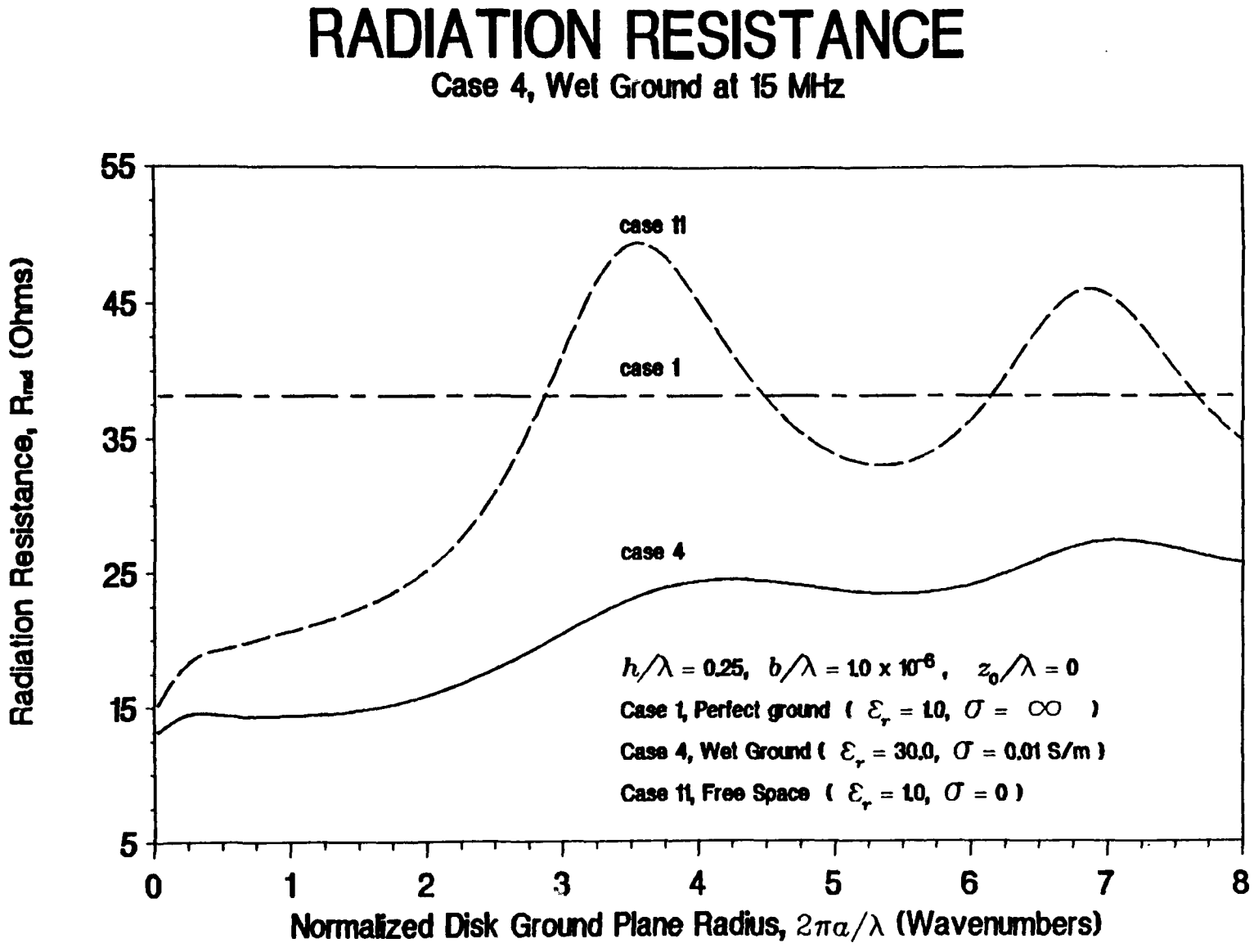

Figure 3-41. Radiation Resistance, Wet Ground

INPUT RESISTANCE

Case 4, Wet Ground at 15 MHz

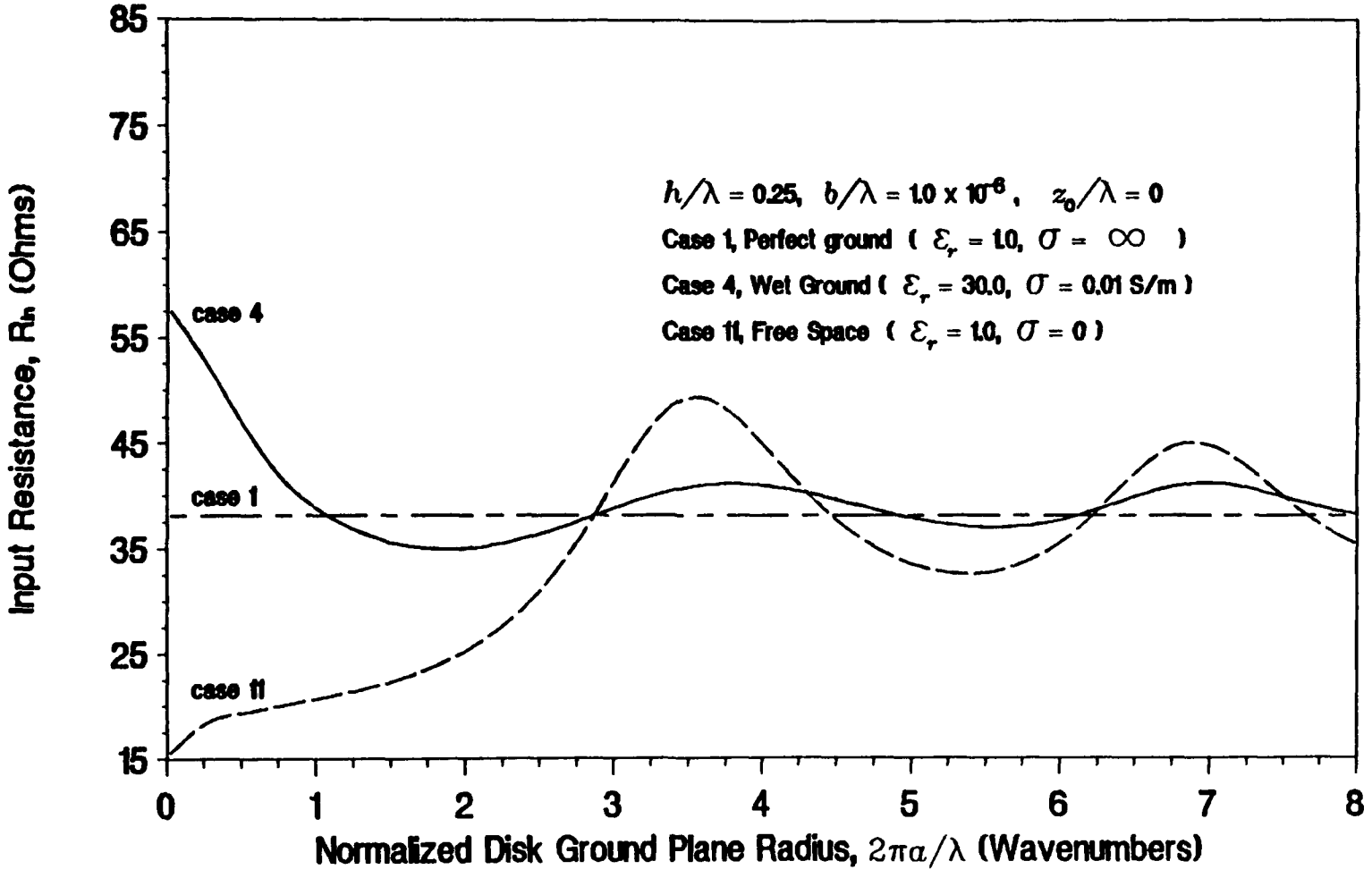

Figure 3-42. Input Resistance, Wet Ground

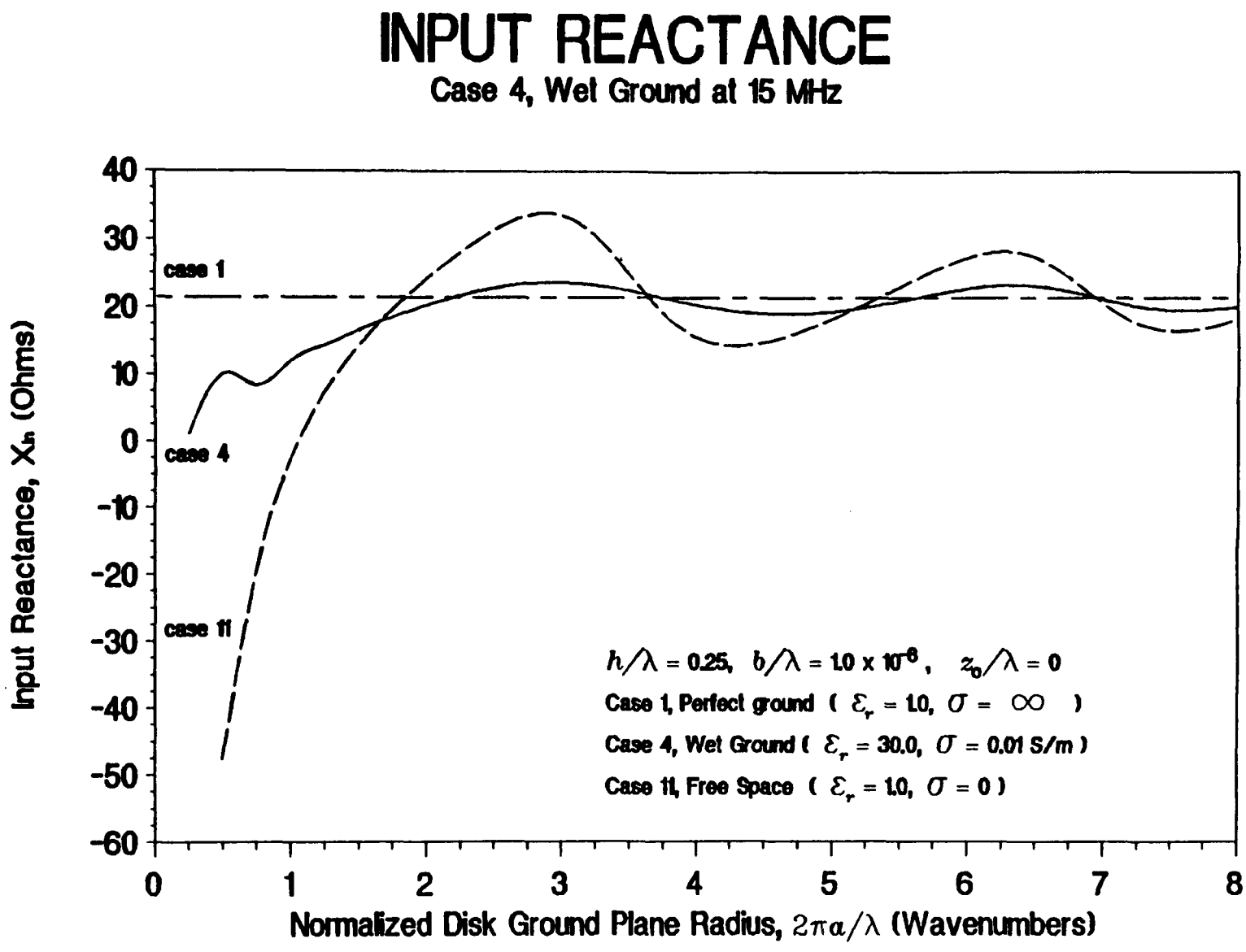

Figure 3-43. Input Reactance, Wet Ground

DIRECTIVE GAIN AT 82 DEG ELEVATION

Case 4, Wet Ground at 15 MHz

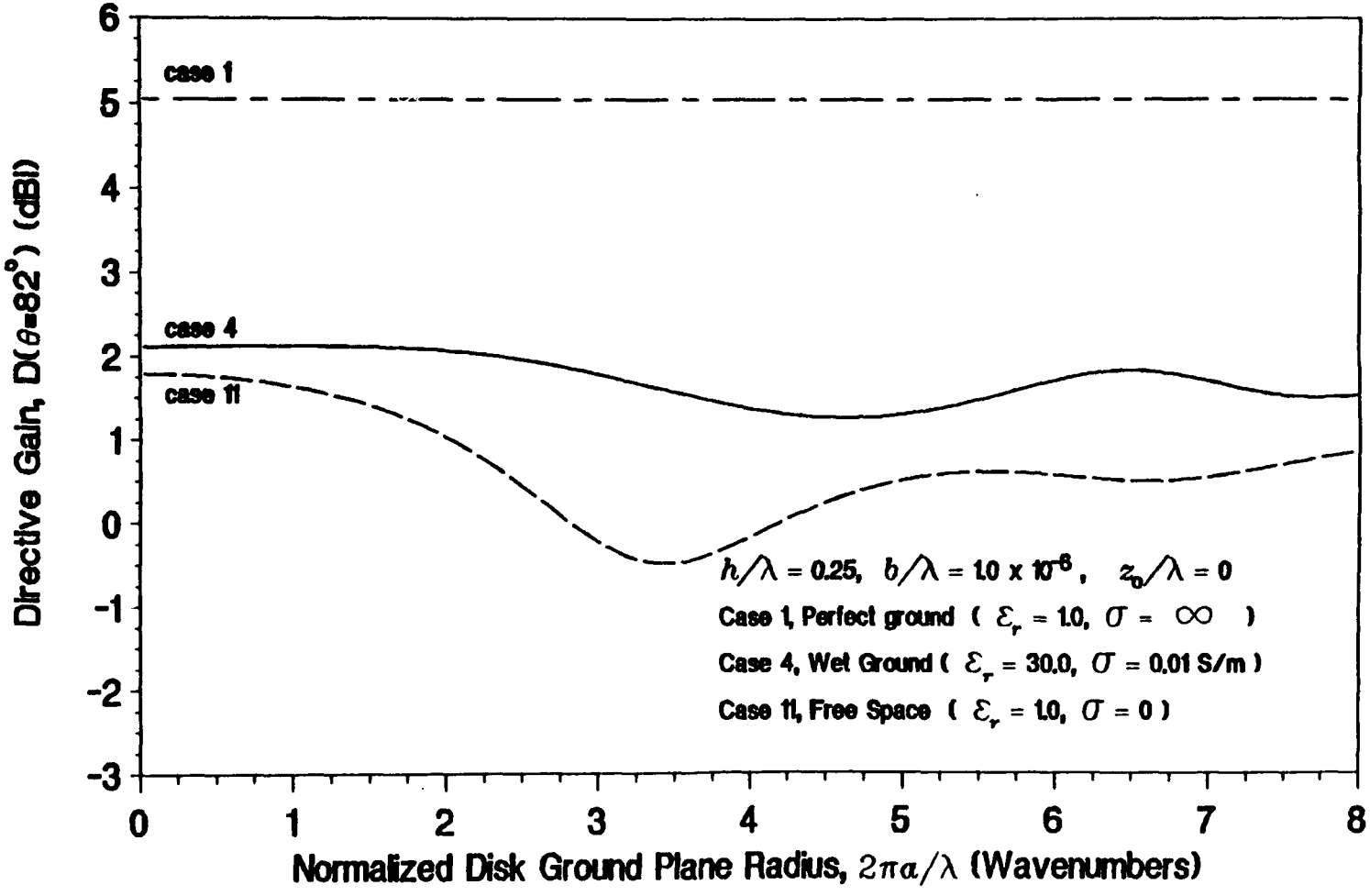

Figure 3-44. Directivity at 8 Degrees Above the Horizon, Wet Ground

DIRECTIVE GAIN AT 84 DEG ELEVATION

Case 4, Wet Ground at 15 MHz

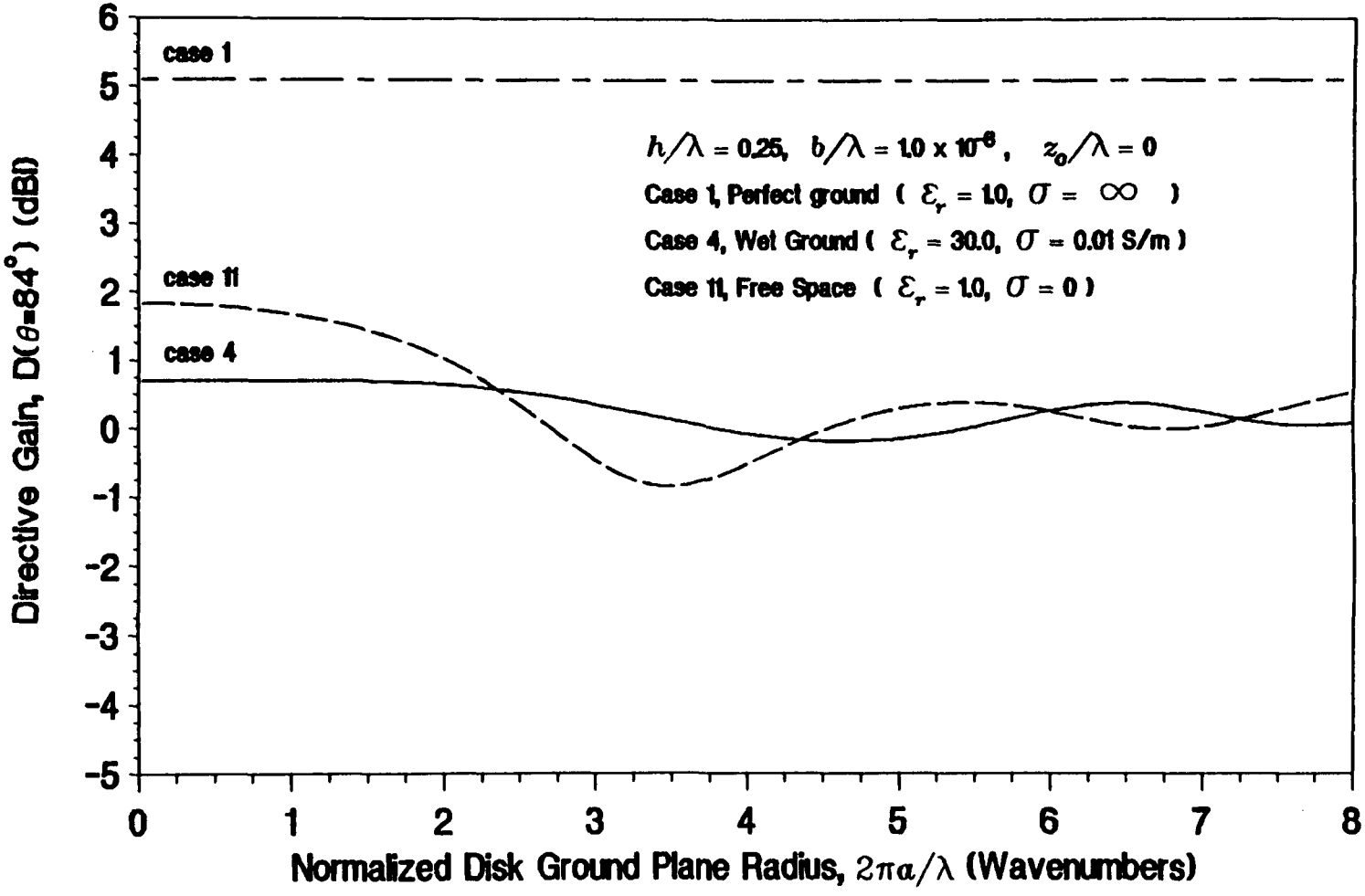

Figure 3-45. Directivity at 6 Degrees Above the Horizon, Wet Ground

DIRECTIVE GAIN AT 86 DEG ELEVATION

Case 4, Wet Ground at 15 MHz

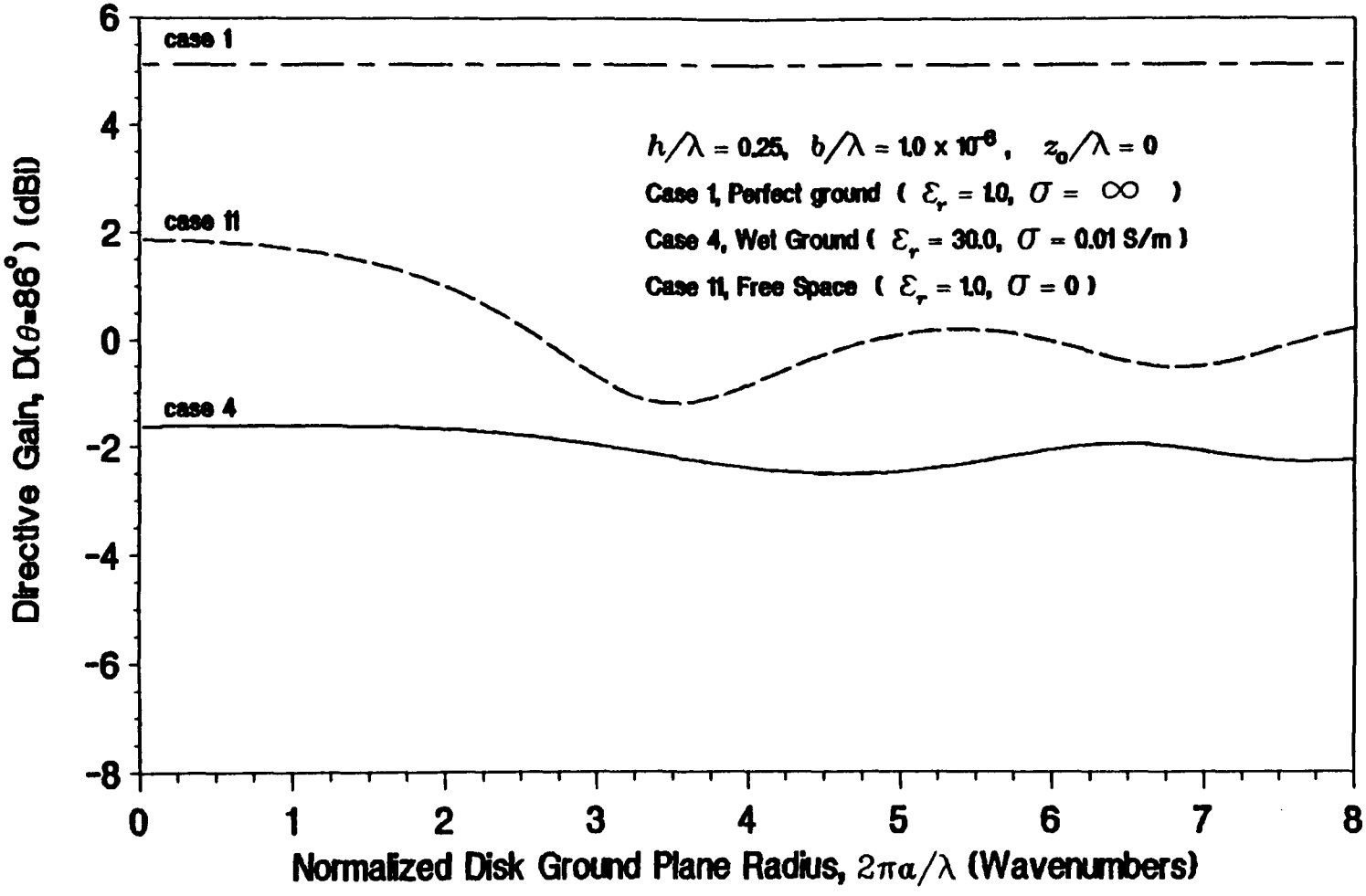

Figure 3-46. Directivity at 4 Degrees Above the Horizon, Wet Ground

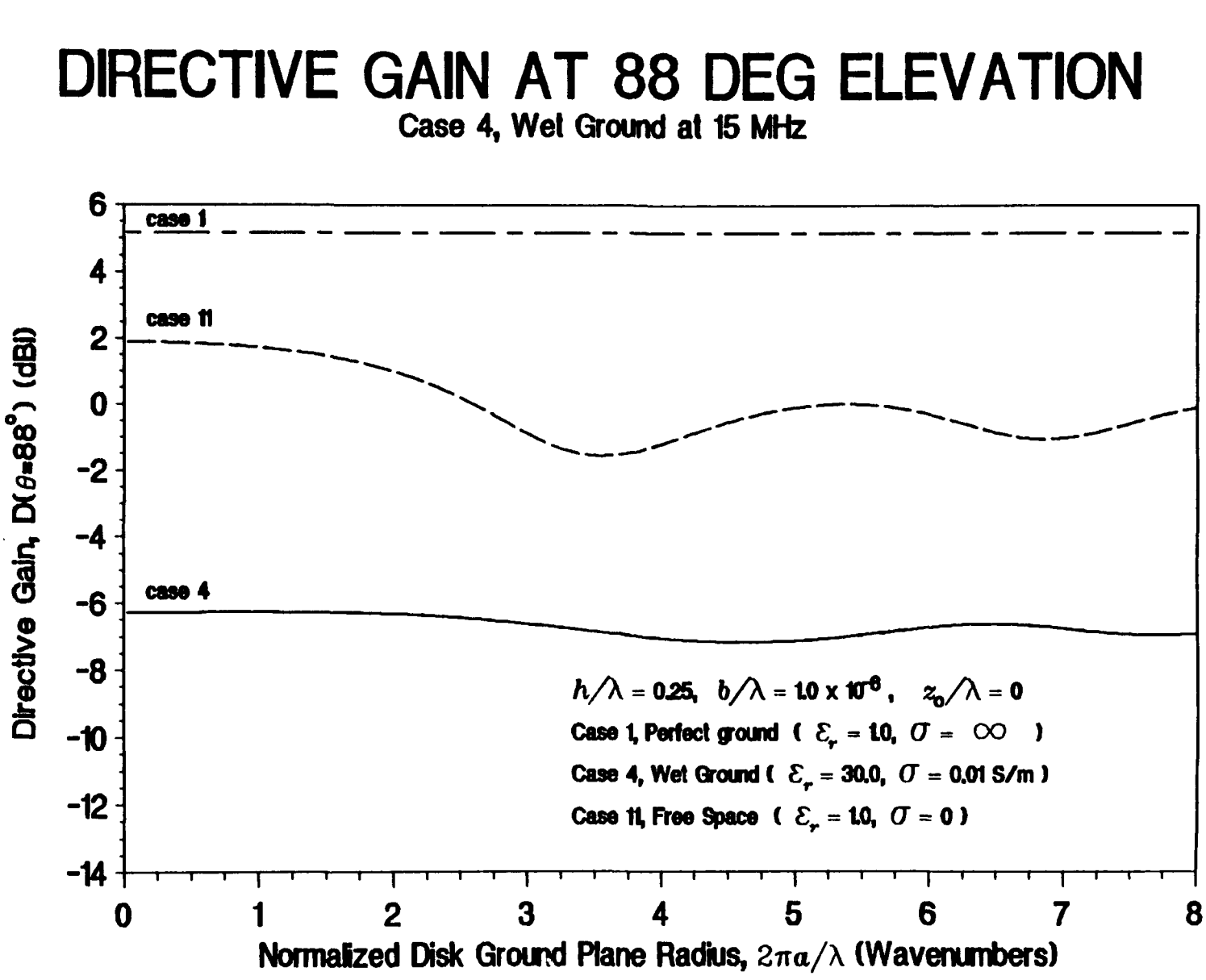

Figure 3-47. Directivity at 2 Degrees Above the Horizon, Wet Ground

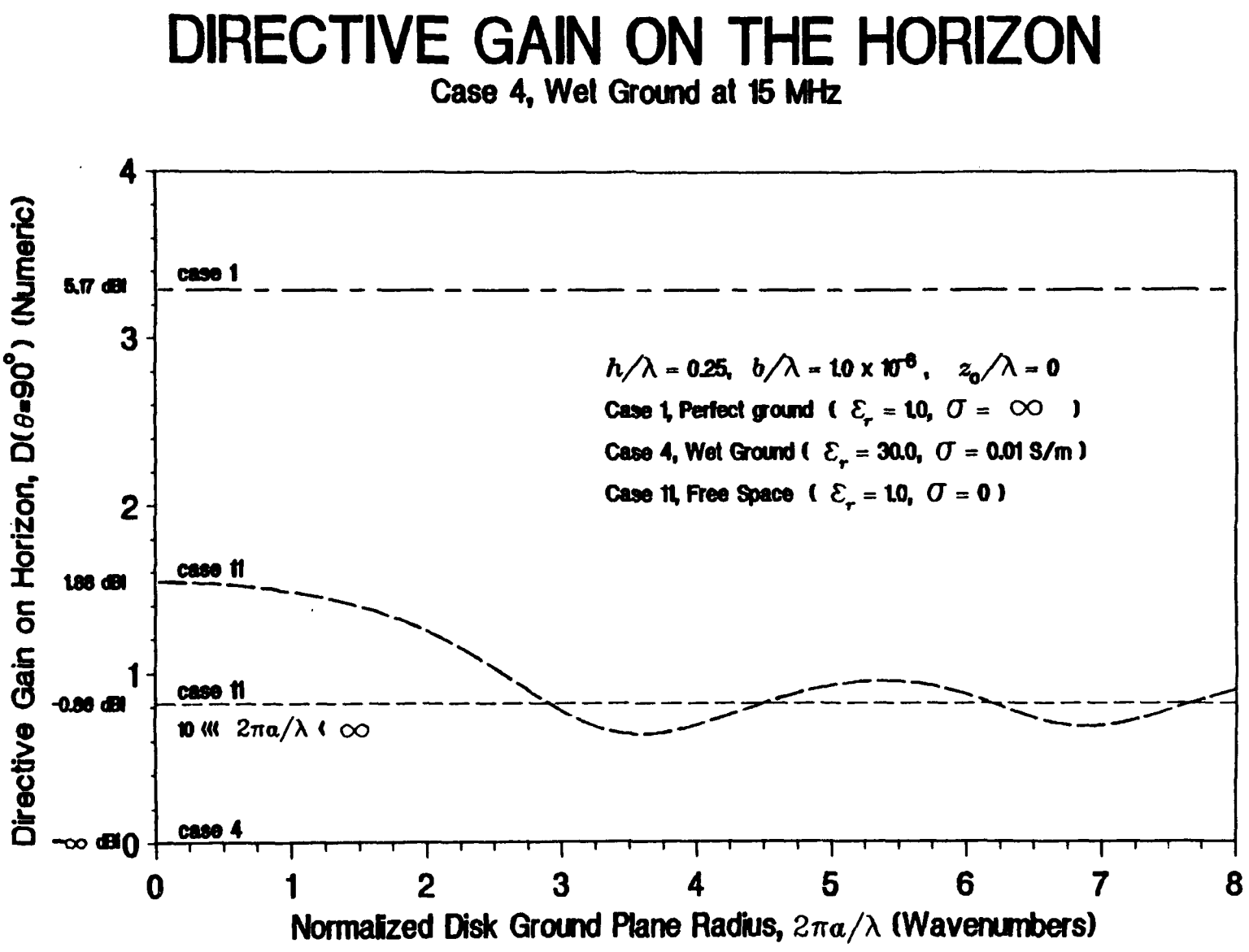

Figure 3-48. Directivity on the Horizon, Wet Ground

3.4 MEDIUM DRY GROUND

NUMERIC DIRECTIVE GAIN POLAR PLOT

Case 5, Medium Dry Ground at 15 MHz

$2\pi a/\lambda = 0.025$ (Wavenumbers)

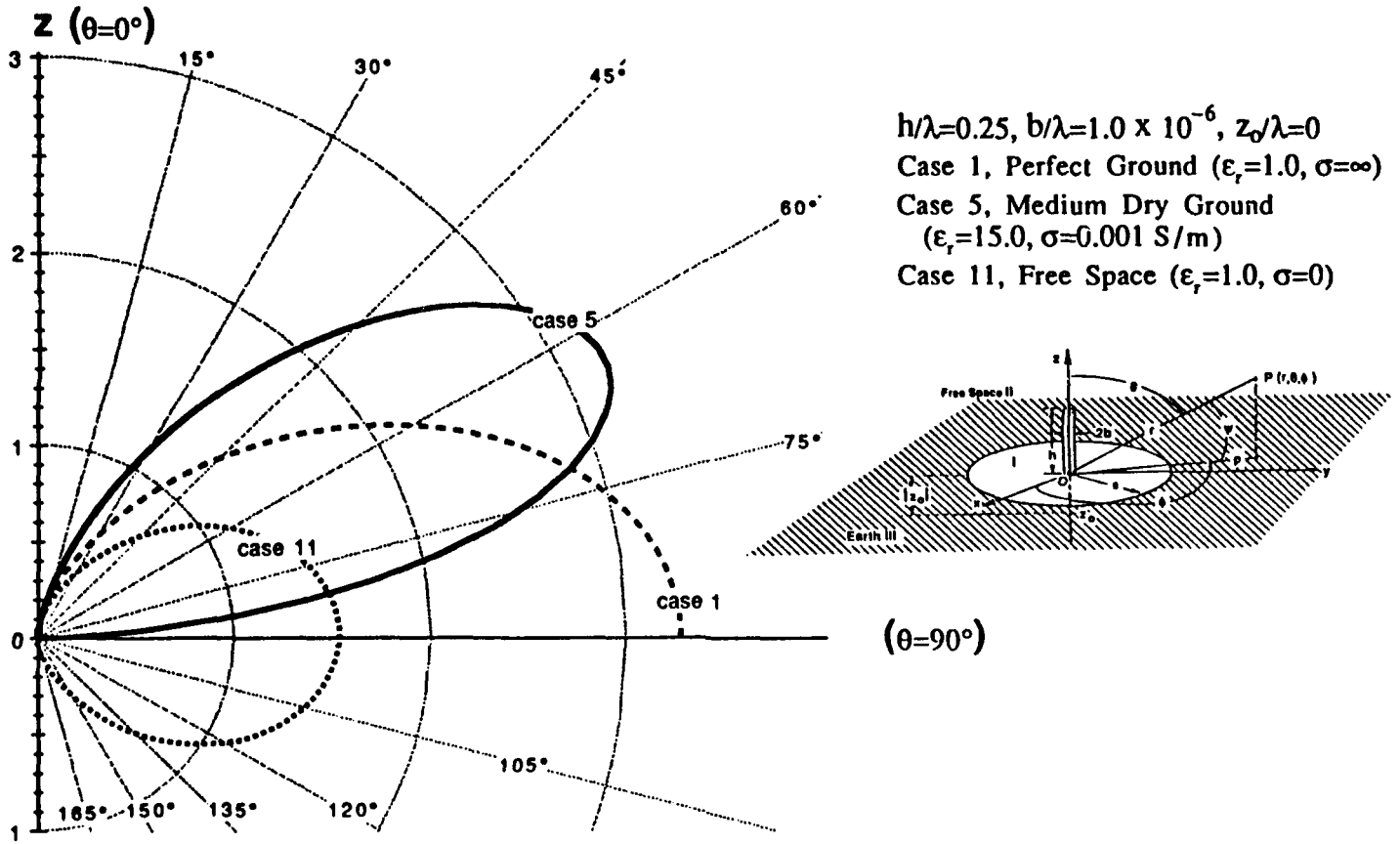

Figure 3-49. Directivity Pattern, $2\pi a/\lambda = 0.025$, Medium Dry Ground

NUMERIC DIRECTIVE GAIN POLAR PLOT

Case 5, Medium Dry Ground at 15 MHz

$2\pi a/\lambda =$ 3.0 (Wavenumbers)

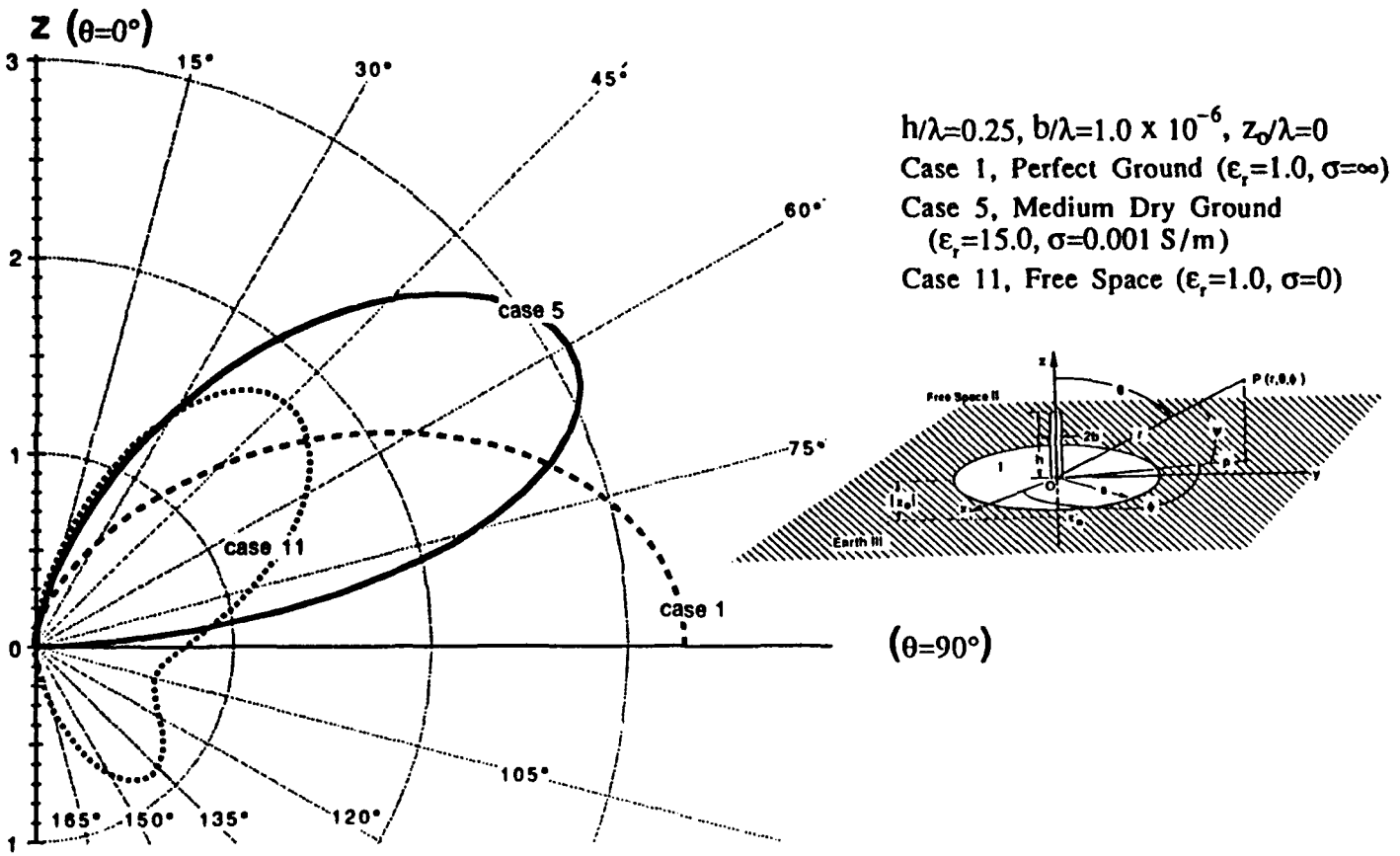

Figure 3-50. Directivity Pattern, $2\pi a/\lambda = 3.0$, Medium Dry Ground

NUMERIC DIRECTIVE GAIN POLAR PLOT

Case 5, Medium Dry Ground at 15 MHz

$2\pi a/\lambda =$ 4.0 (Wavenumbers)

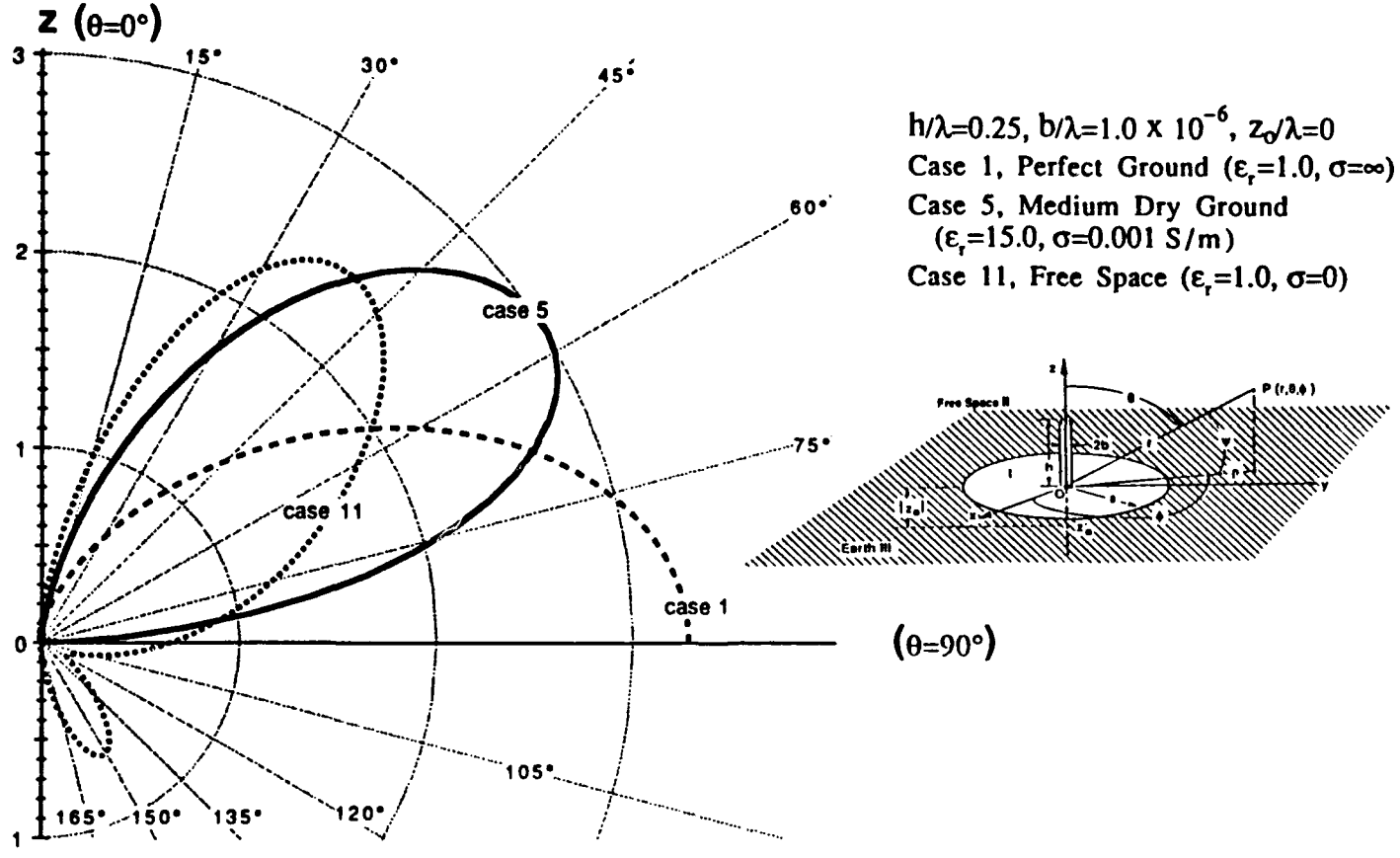

Figure 3-51. Directivity Pattern, $2\pi a/\lambda = 4.0$, Medium Dry Ground

NUMERIC DIRECTIVE GAIN POLAR PLOT

Case 5, Medium Dry Ground at 15 MHz

$2\pi a/\lambda =$ **5.0 (Wavenumbers)**

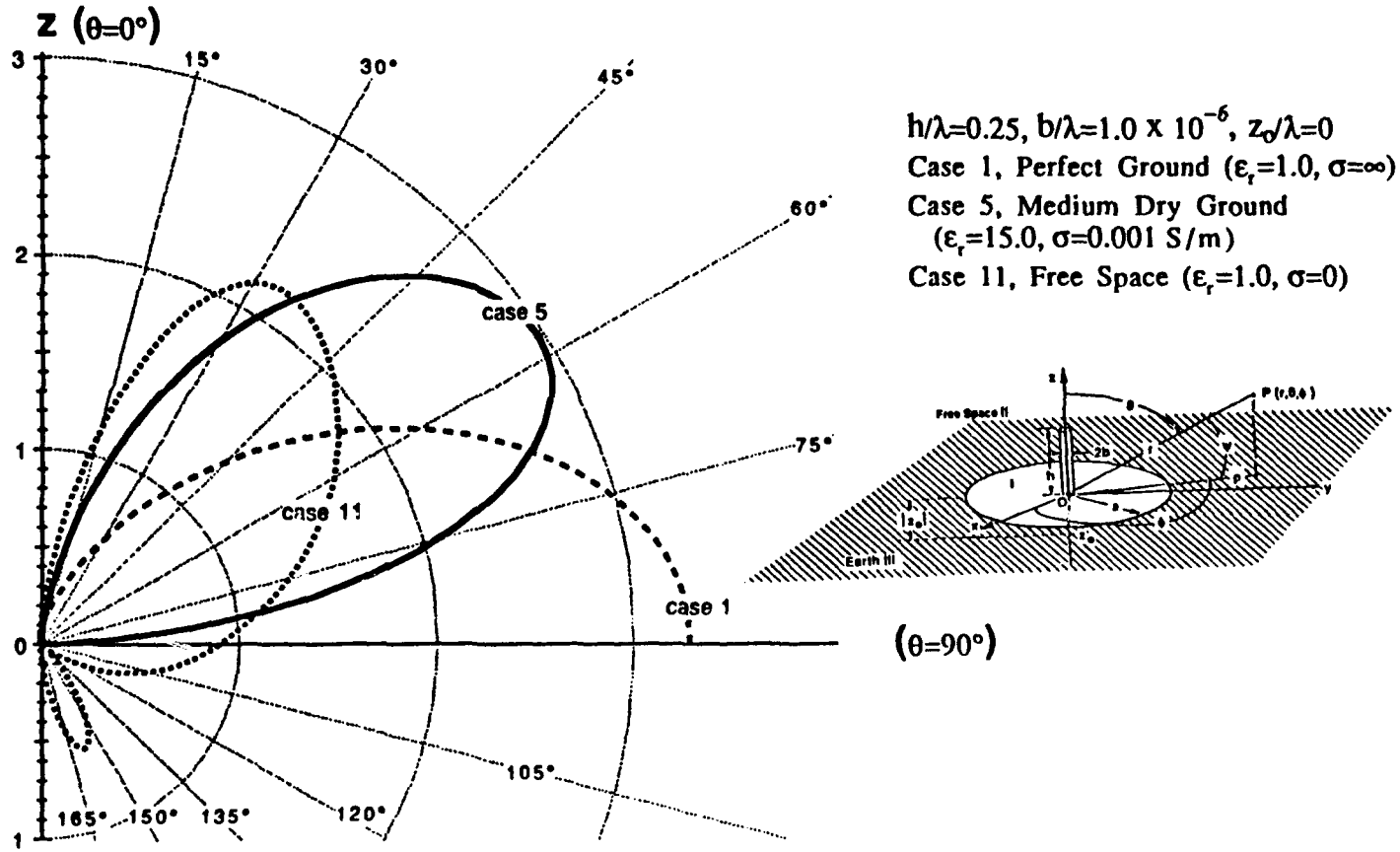

Figure 3-52. Directivity Pattern, $2\pi a/\lambda = 5.0$, Medium Dry Ground

NUMERIC DIRECTIVE GAIN POLAR PLOT

Case 5, Medium Dry Ground at 15 MHz

$2\pi a/\lambda =$ 6.5 (Wavenumbers)

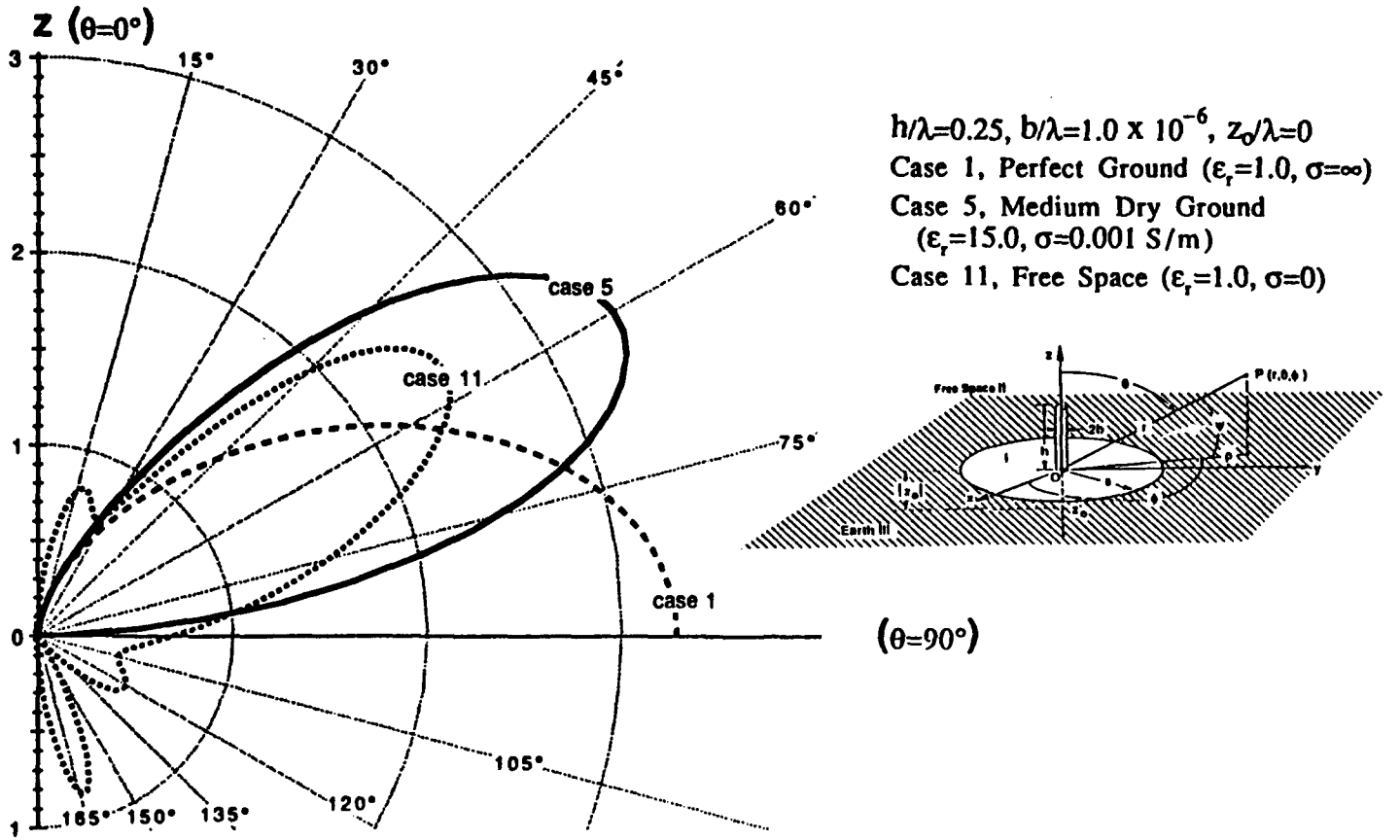

Figure 3-53. Directivity Pattern, $2\pi a/\lambda = 6.5$, Medium Dry Ground

PEAK DIRECTIVITY

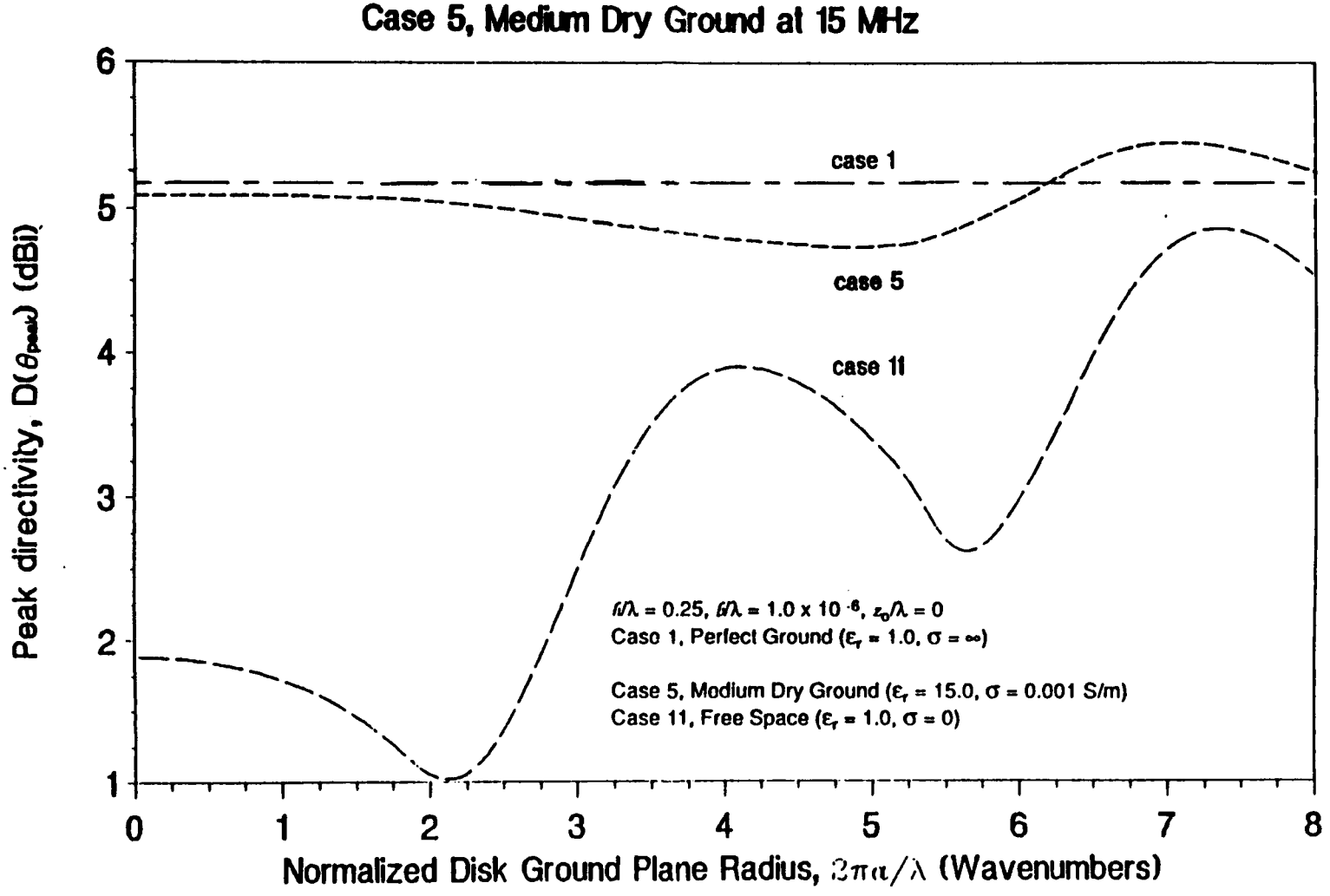

Figure 3-54. Peak Directivity, Medium Dry Ground

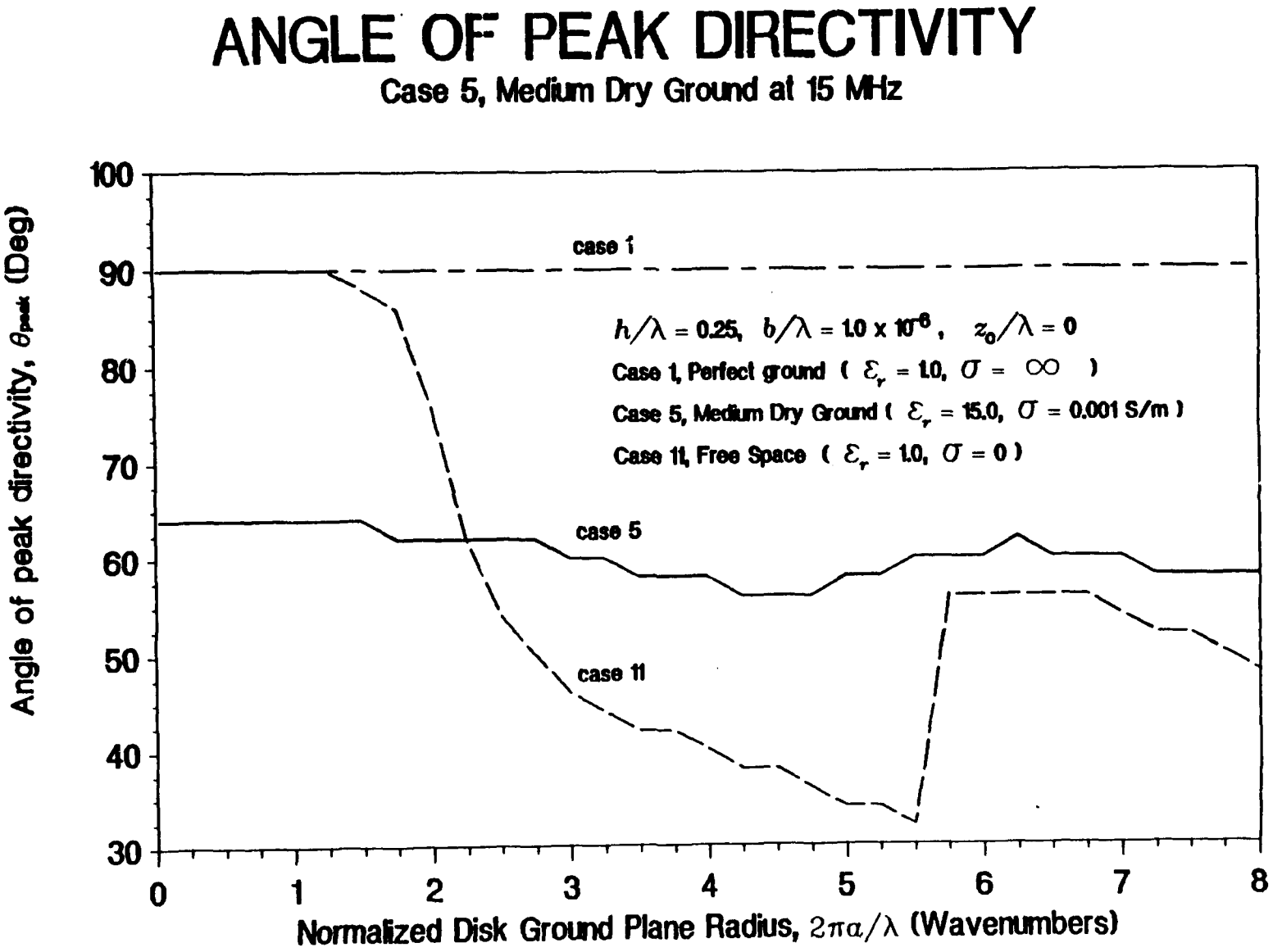

Figure 3-55. Angle of Incidence of Peak Directivity, Medium Dry Ground

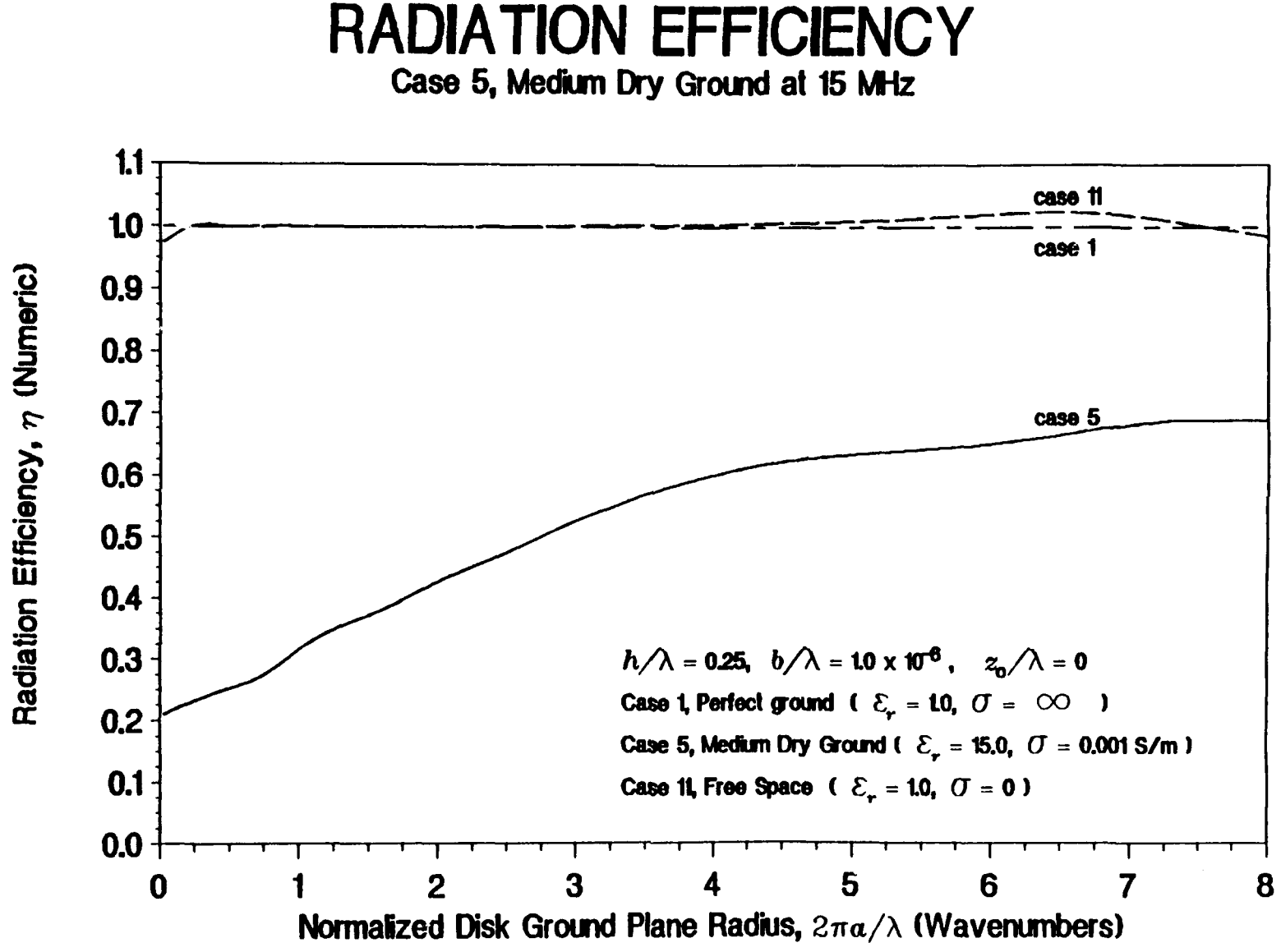

Figure 3-56. Radiation Efficiency, Medium Dry Ground

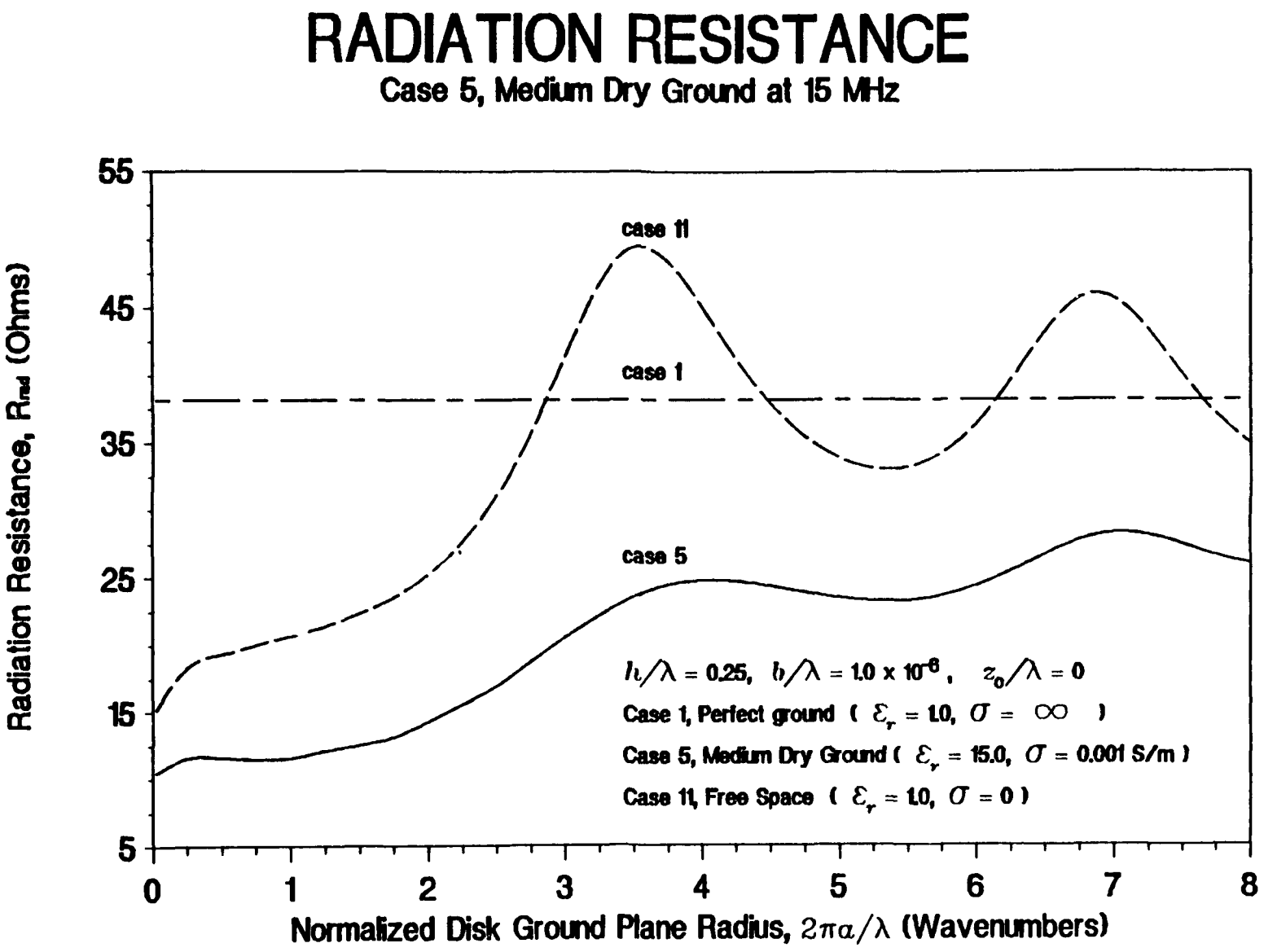

Figure 3-57. Radiation Resistance, Medium Dry Ground

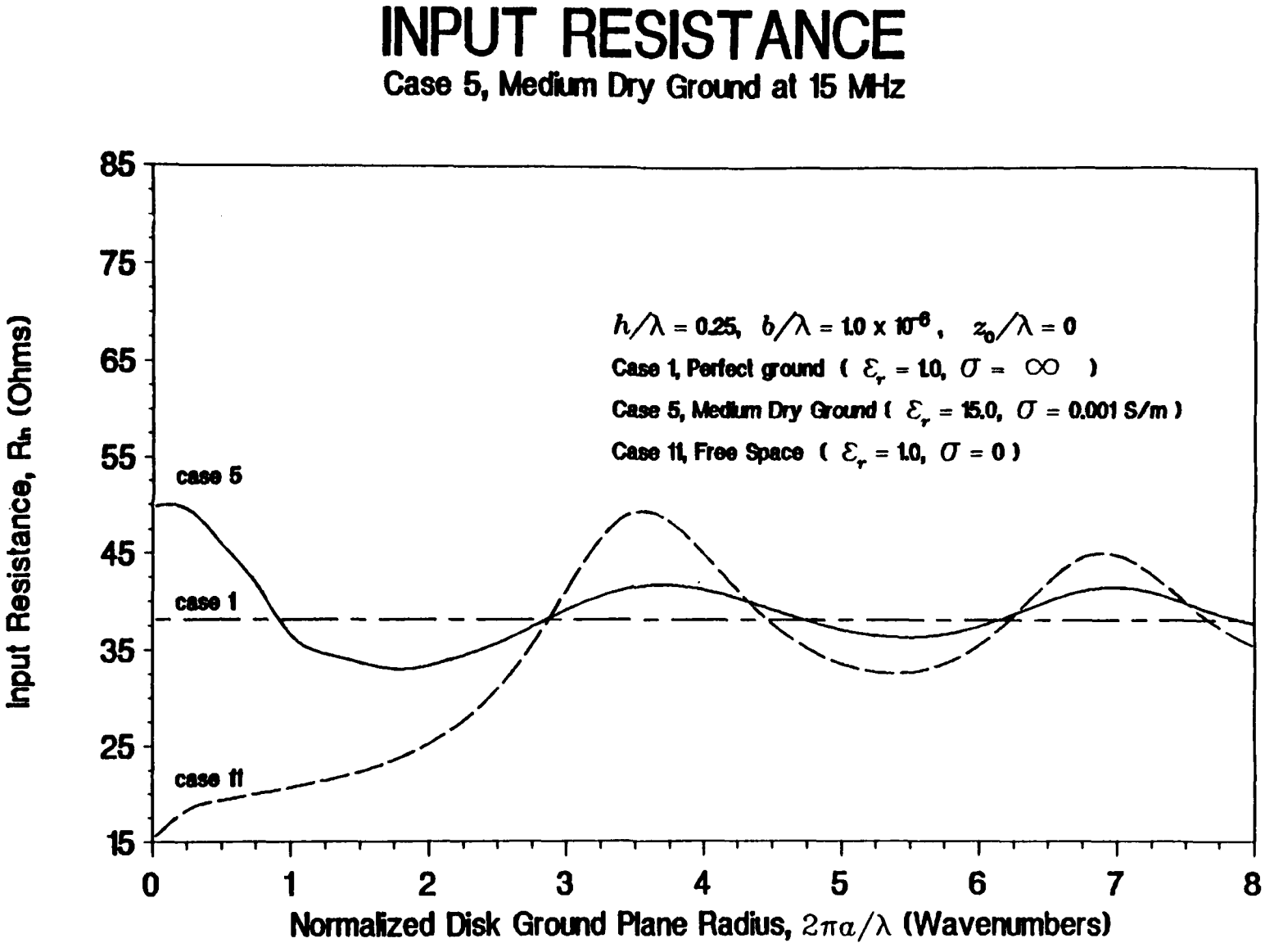

Figure 3-58. Input Resistance, Medium Dry Ground

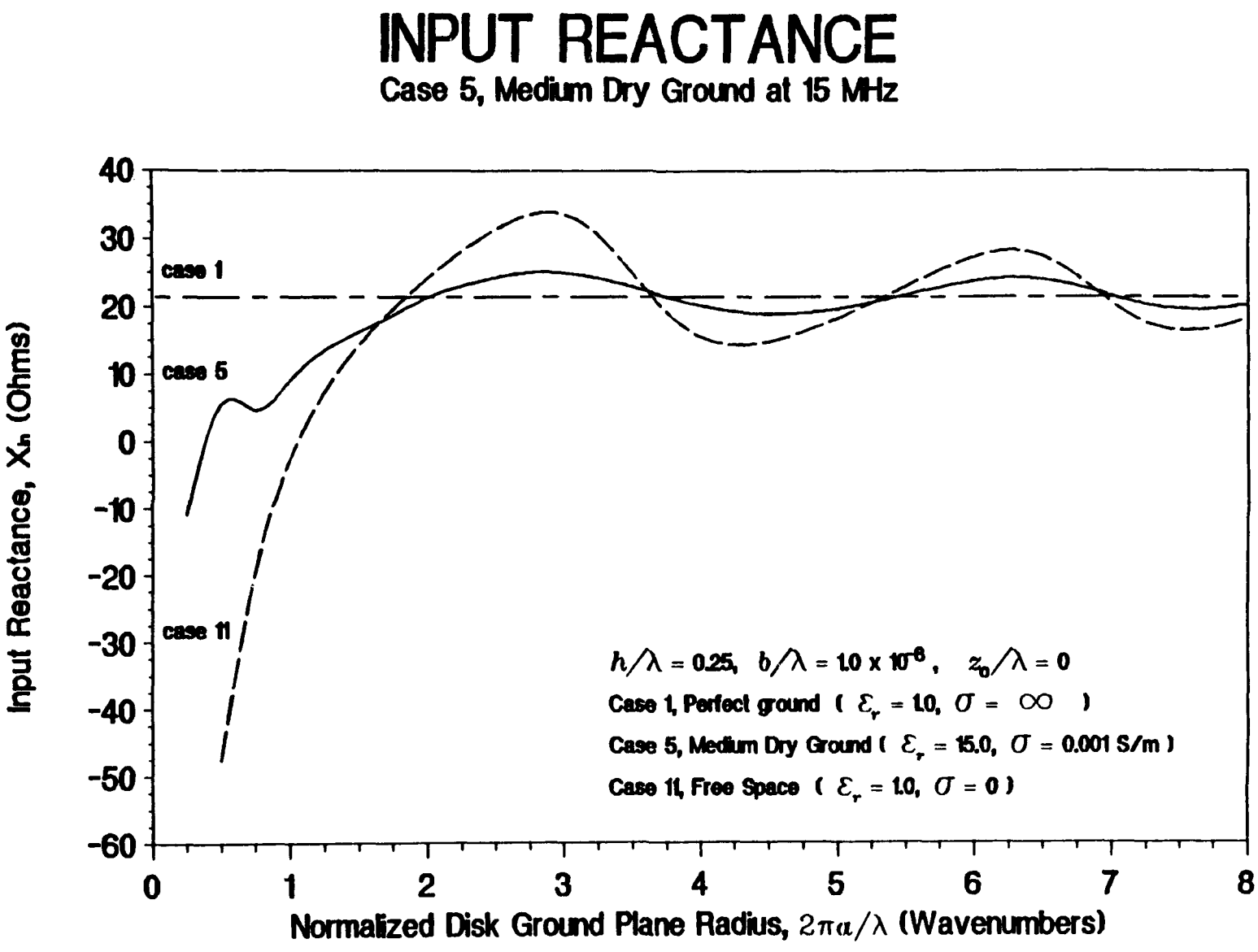

Figure 3-59. Input Reactance, Medium Dry Ground

DIRECTIVE GAIN AT 82 DEG ELEVATION

Case 5, Medium Dry Ground at 15 MHz

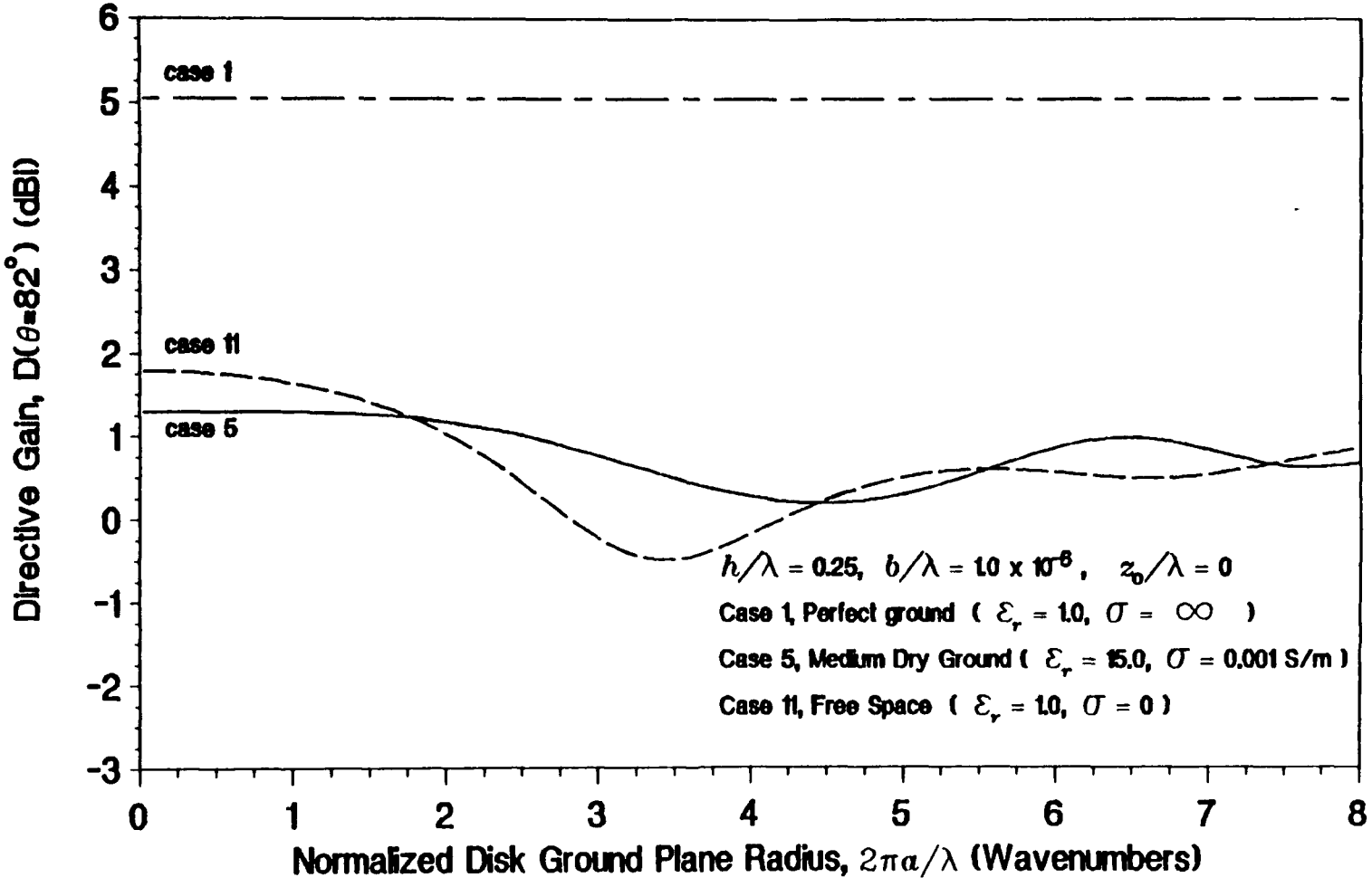

Figure 3-60. Directivity at 8 Degrees Above the Horizon, Medium Dry Ground

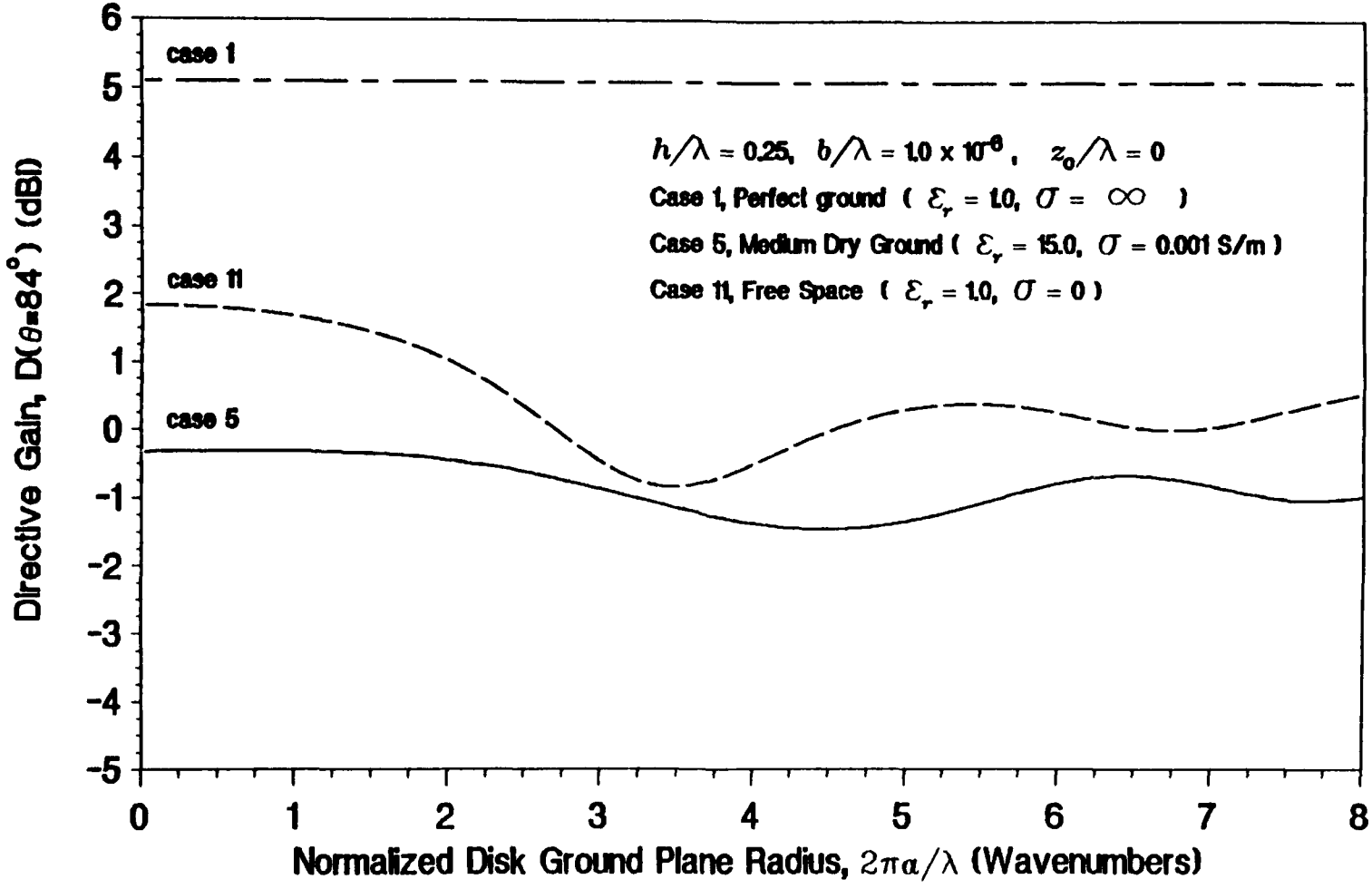

Figure 3-61. Directivity at 6 Degrees Above the Horizon, Medium Dry Ground

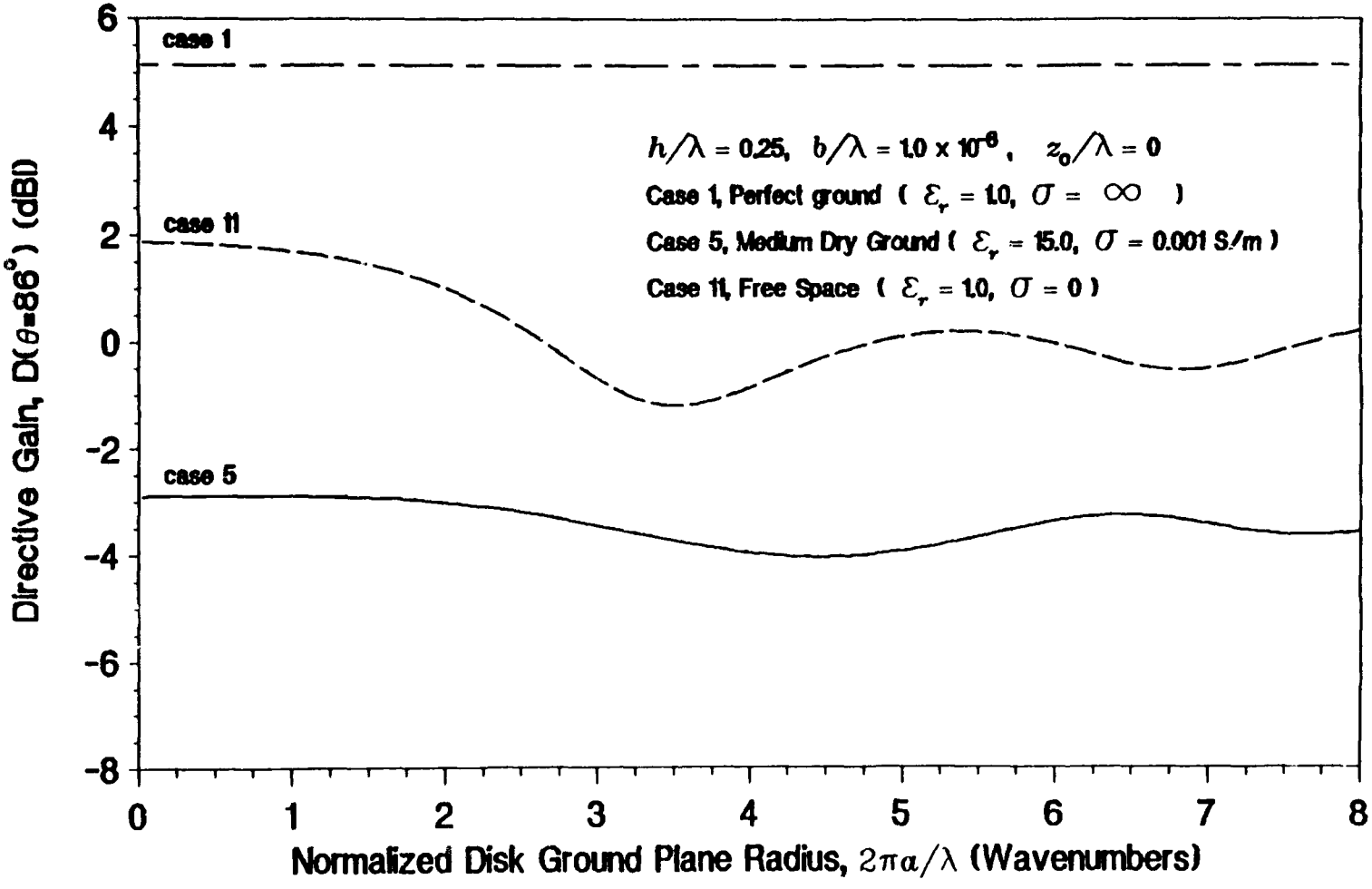

Figure 3-62. Directivity at 4 Degrees Above the Horizon, Medium Dry Ground

DIRECTIVE GAIN AT 88 DEG ELEVATION

Case 5, Medium Dry Ground at 15 MHz

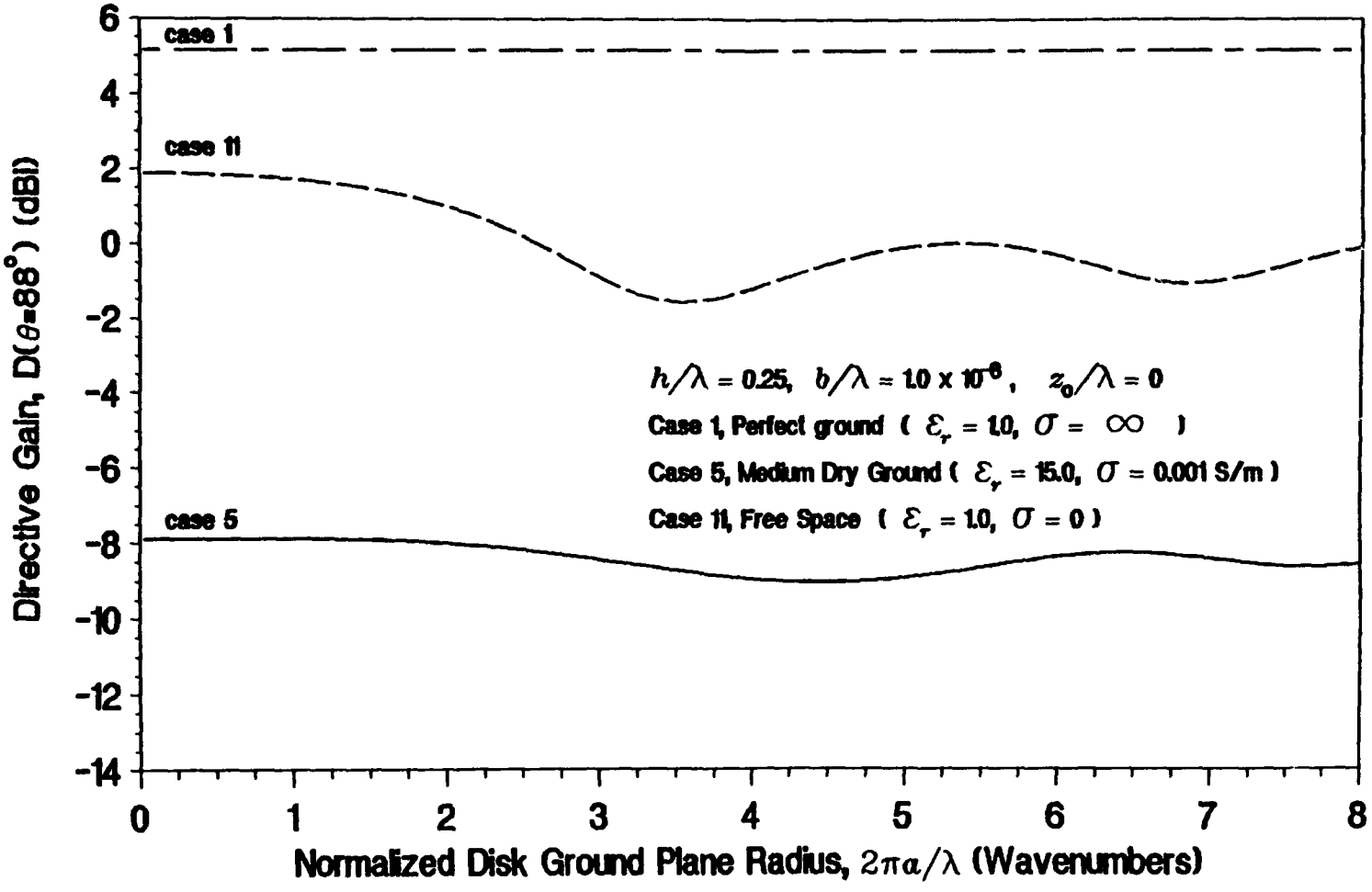

Figure 3-63. Directivity at 2 Degrees Above the Horizon, Medium Dry Ground

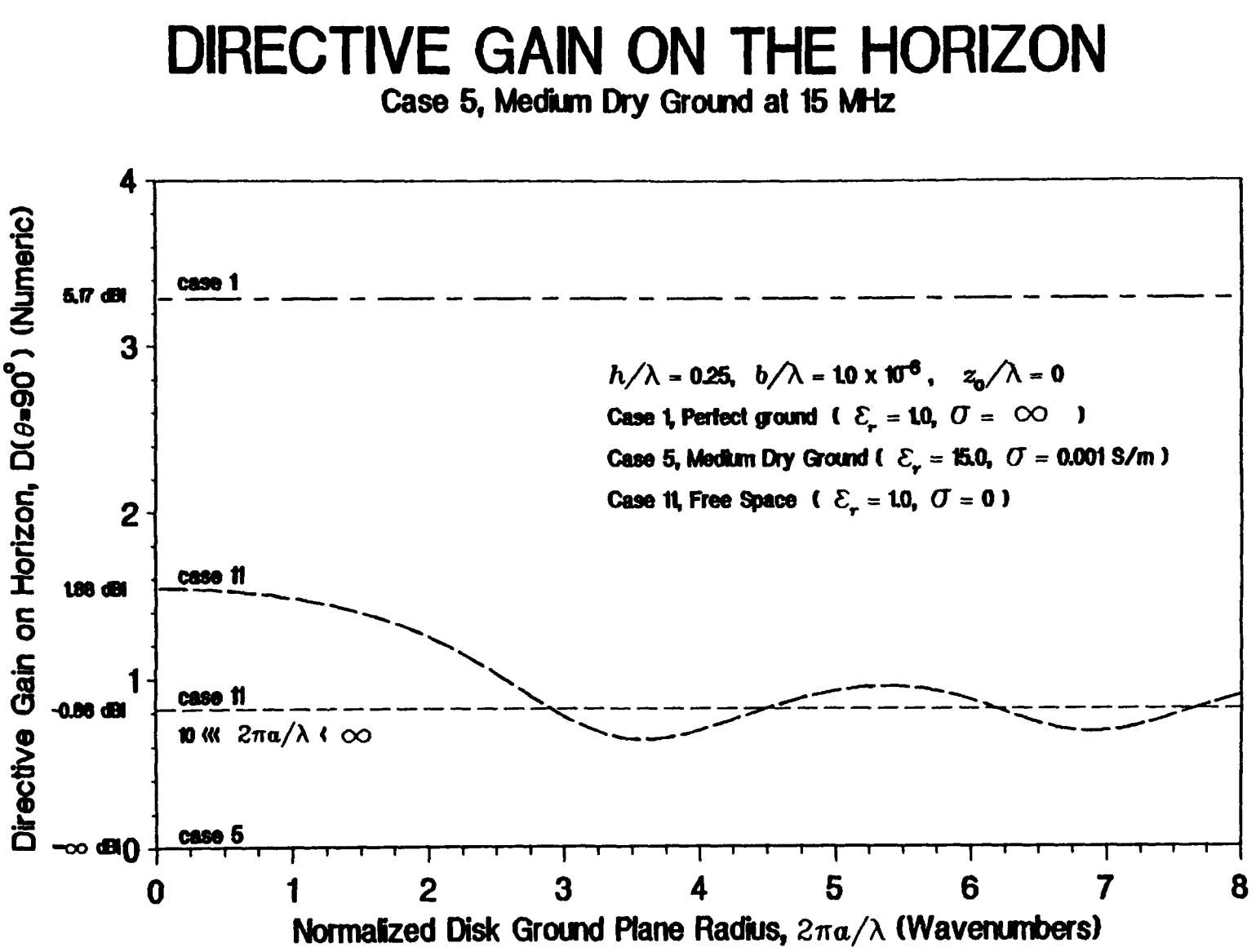

Figure 3-64. Directivity on the Horizon, Medium Dry Ground

3.5 VERY DRY GROUND

NUMERIC DIRECTIVE GAIN POLAR PLOT

Case 6, Very Dry Ground at 15 MHz

$2\pi a/\lambda = 0.025$ (Wavenumbers)

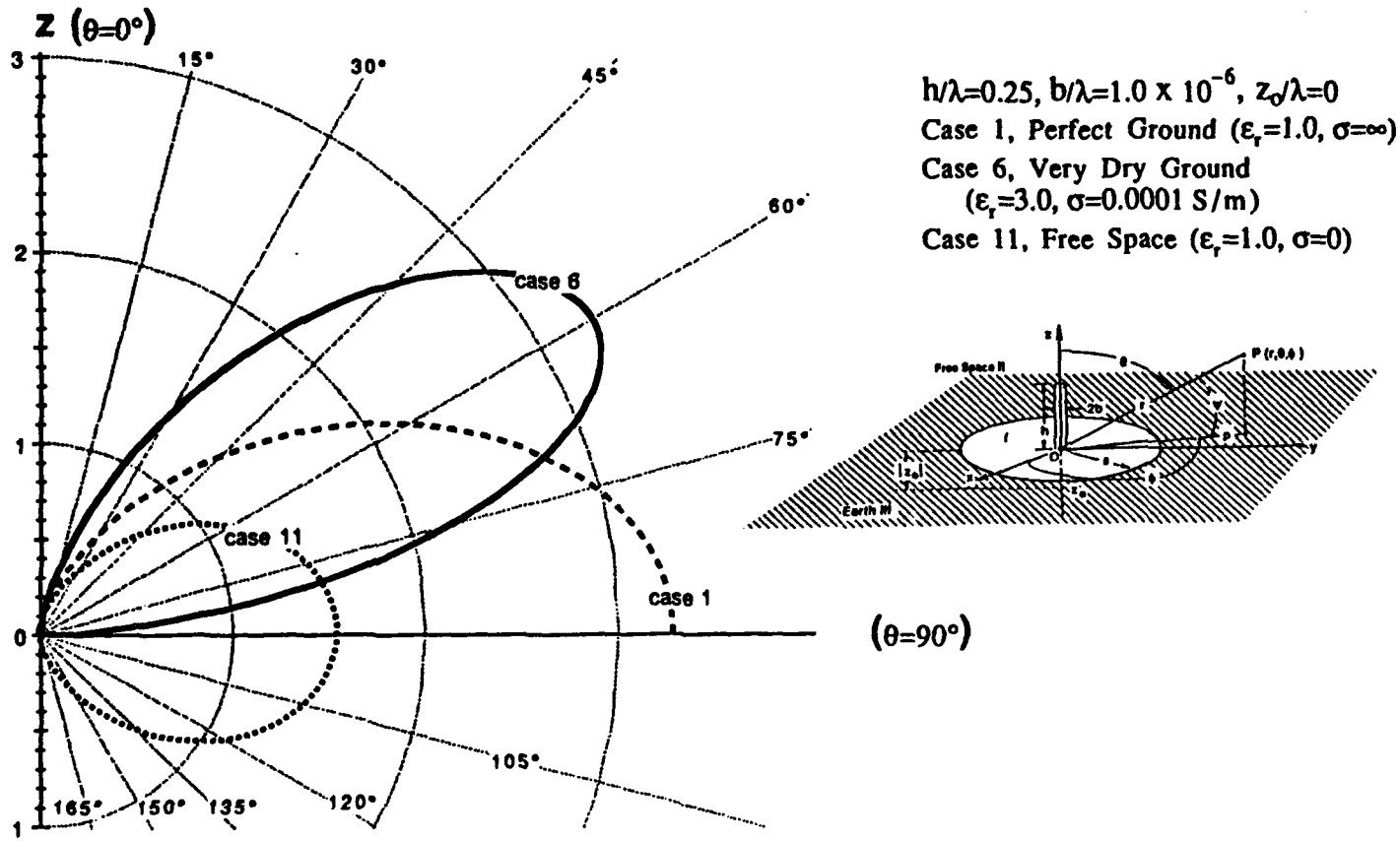

Figure 3-65. Directivity Pattern, $2\pi a/\lambda = 0.025$, Very Dry Ground

NUMERIC DIRECTIVE GAIN POLAR PLOT

Case 6, Very Dry Ground at 15 MHz

$2\pi a/\lambda =$ 3.0 (Wavenumbers)

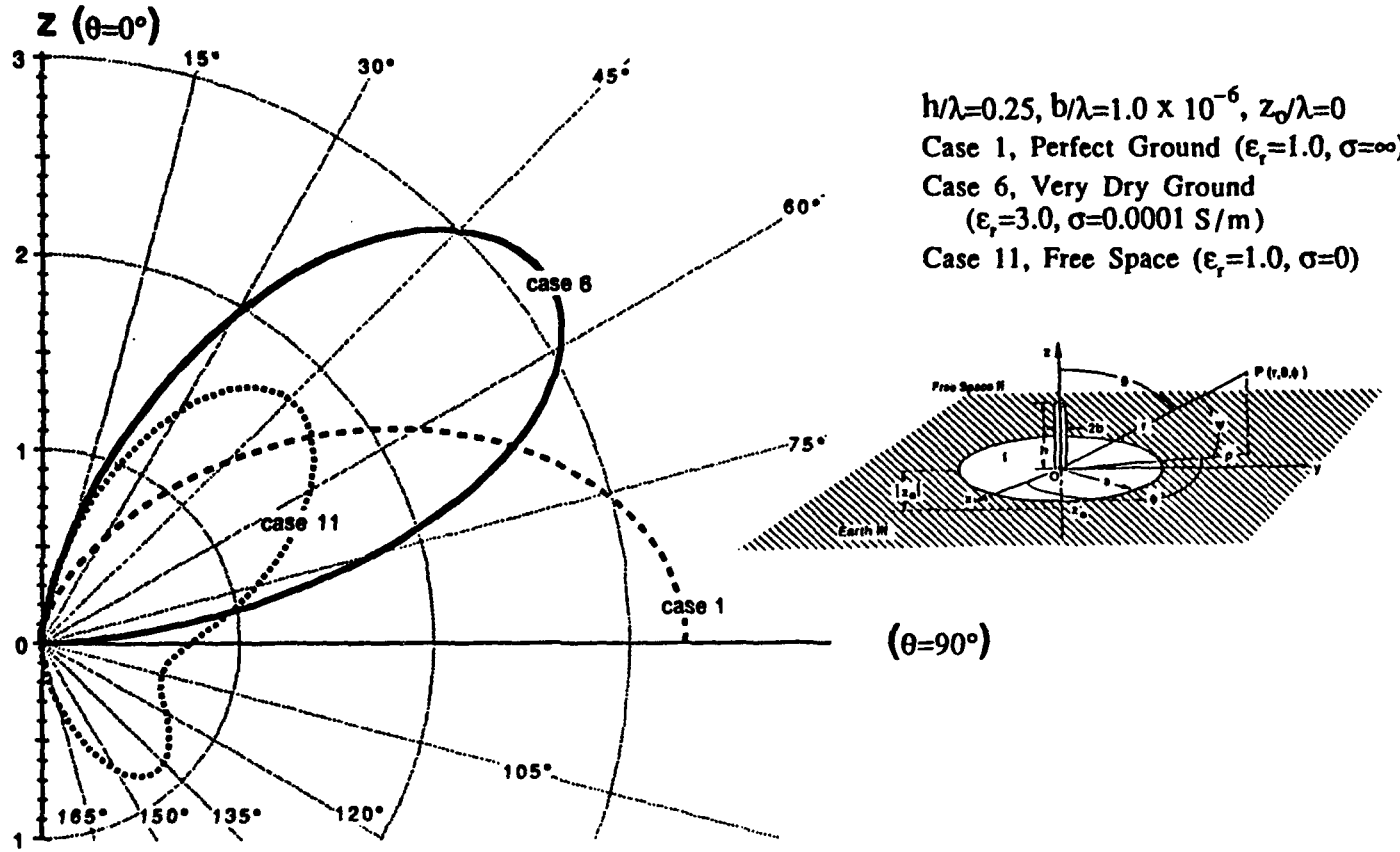

Figure 3-66. Directivity Pattern, $2\pi a/\lambda = 3.0$, Very Dry Ground

NUMERIC DIRECTIVE GAIN POLAR PLOT

Case 6, Very Dry Ground at 15 MHz

$2\pi a/\lambda =$ 4.0 (Wavenumbers)

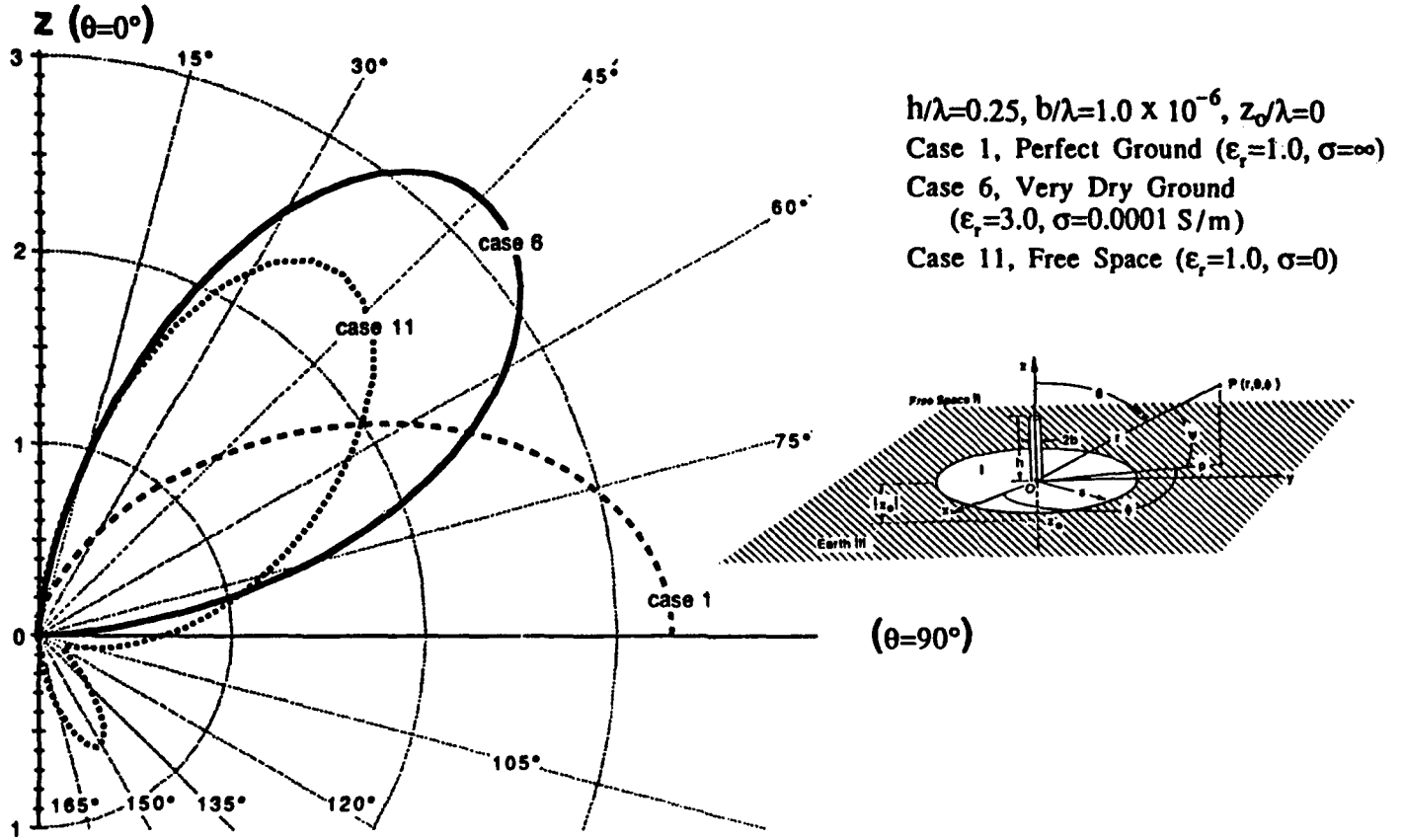

Figure 3-67. Directivity Pattern, $2\pi a/\lambda = 4.0$, Very Dry Ground

NUMERIC DIRECTIVE GAIN POLAR PLOT

Case 6, Very Dry Ground at 15 MHz

$2\pi a/\lambda =$ 5.0 (Wavenumbers)

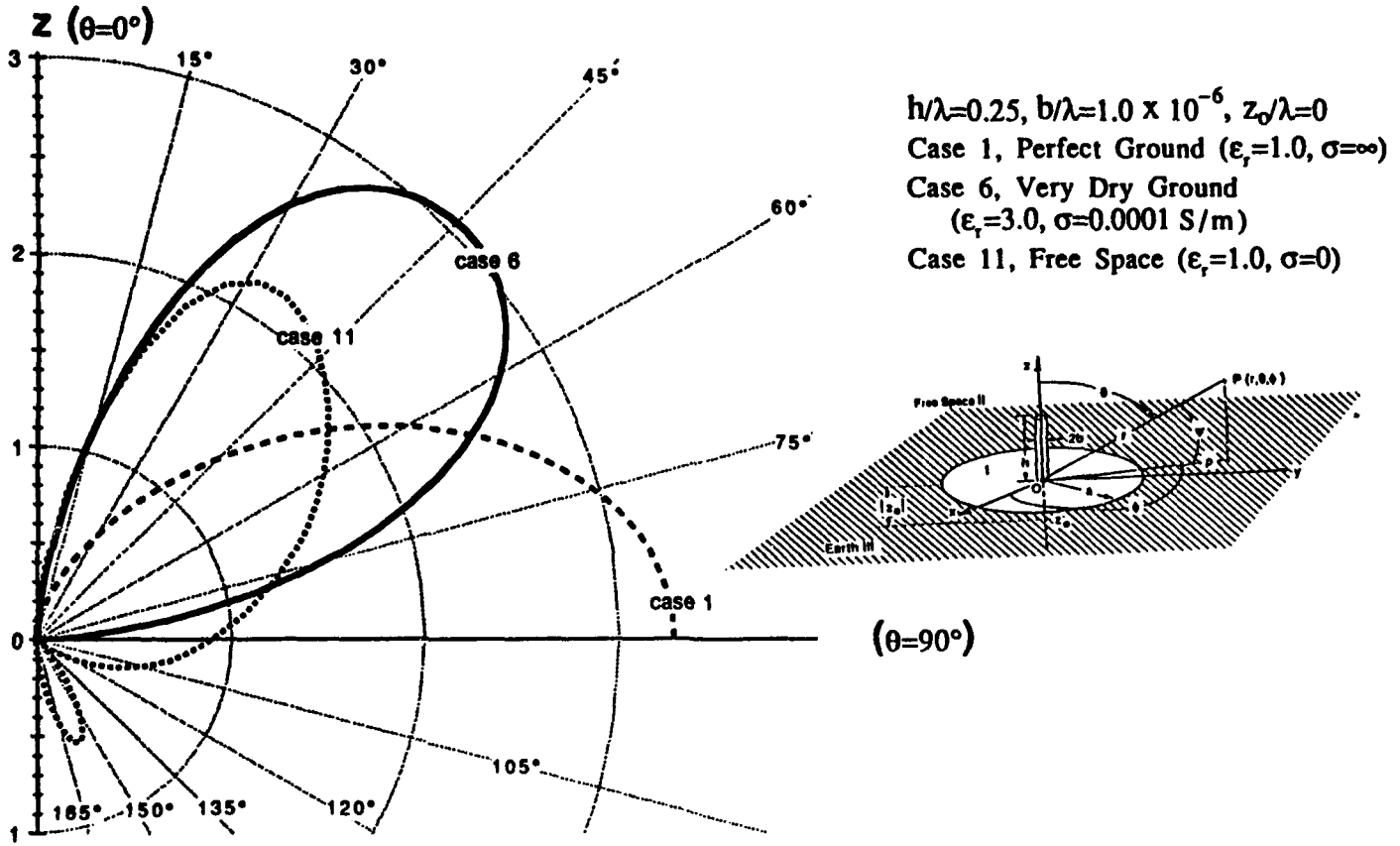

Figure 3-68. Directivity Pattern, $2\pi a/\lambda = 5.0$, Very Dry Ground

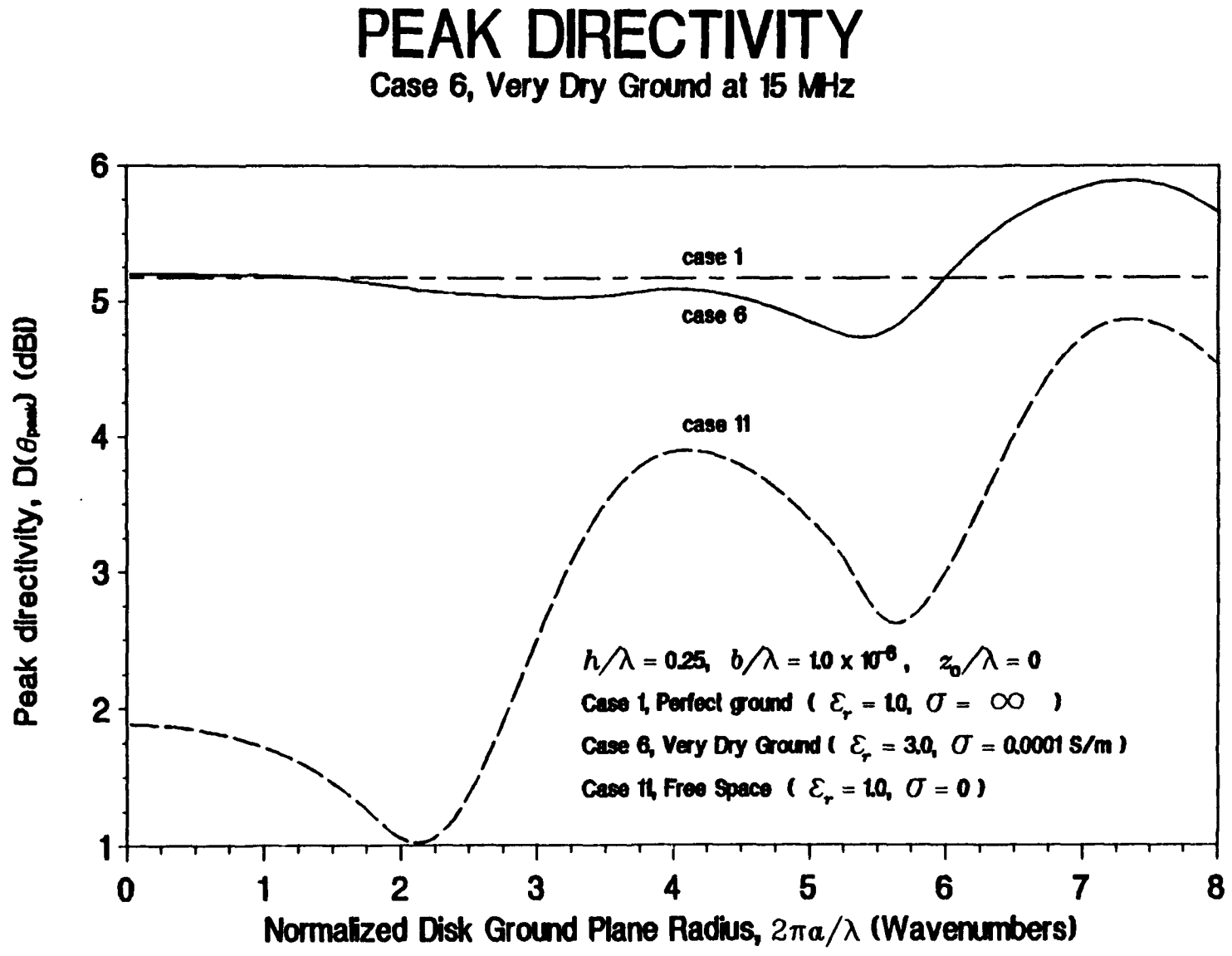

Figure 3-70. Directivity Pattern, Very Dry Ground

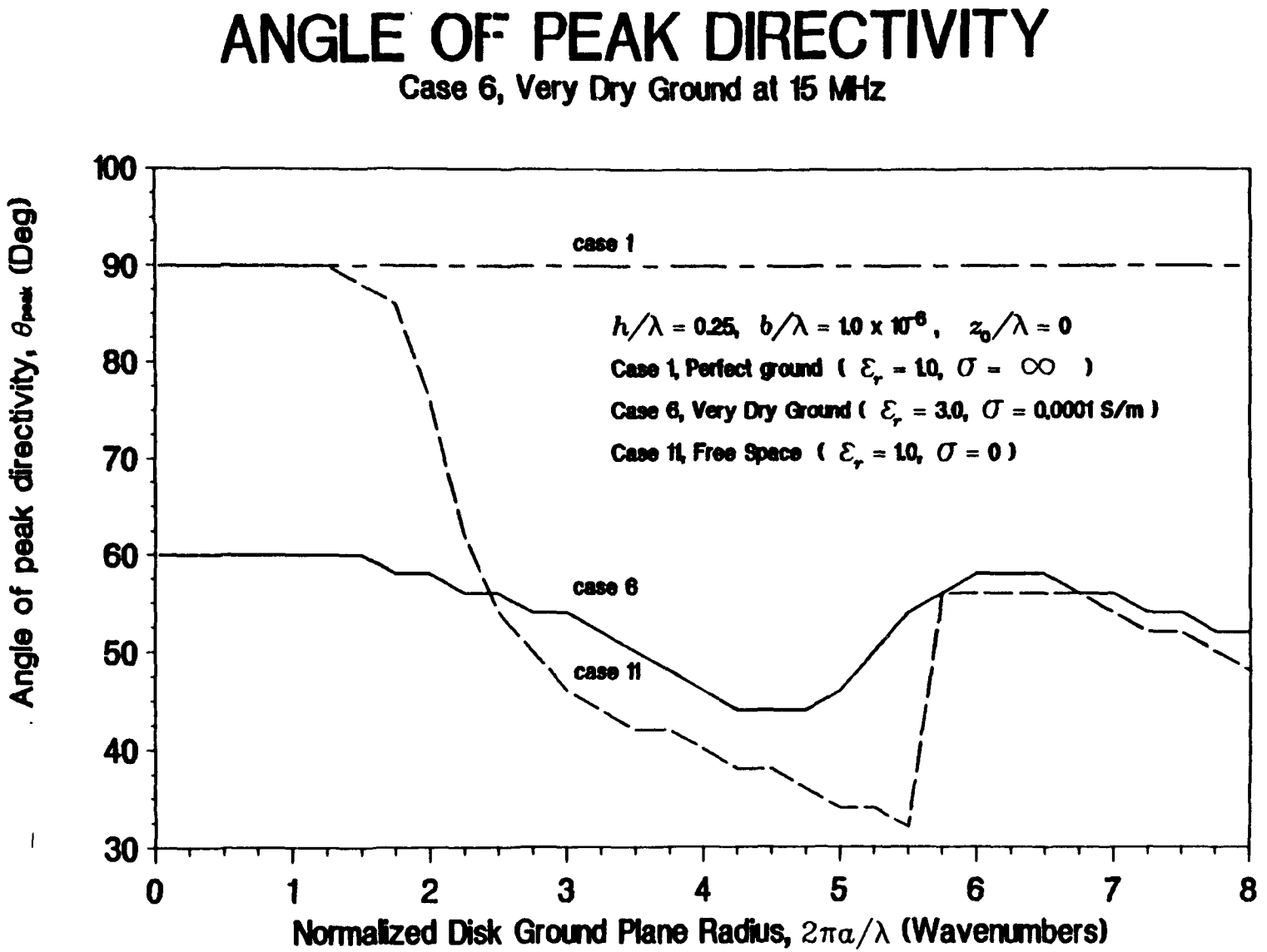

Figure 3-71. Angle of Incidence of Peak Directivity, Very Dry Ground

RADIATION EFFICIENCY

Case 6, Very Dry Ground at 15 MHz

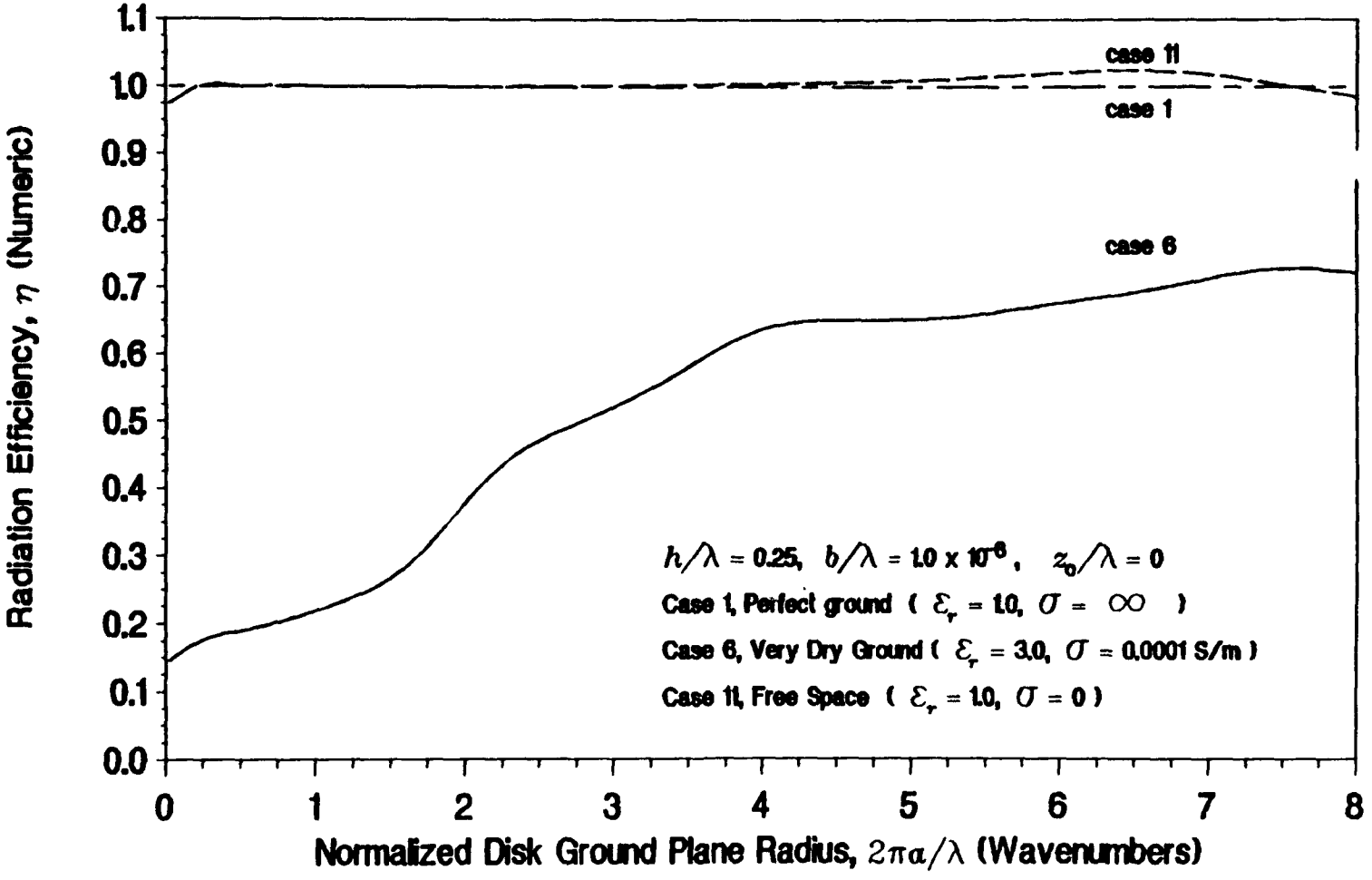

Figure 3-72. Radiation Efficiency, Very Dry Ground

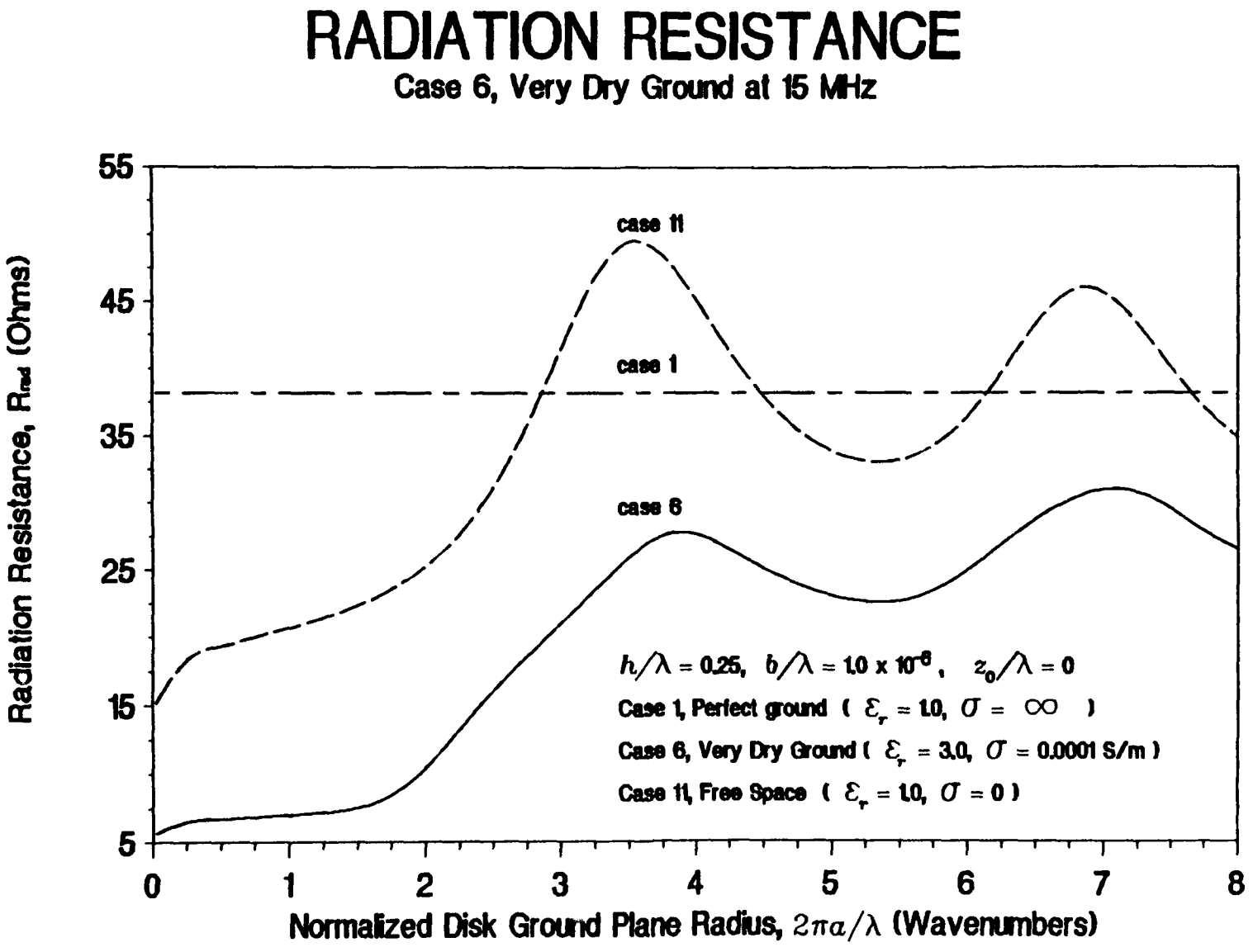

Figure 3-73. Radiation Resistance, Very Dry Ground

INPUT RESISTANCE

Case 6, Very Dry Ground at 15 MHz

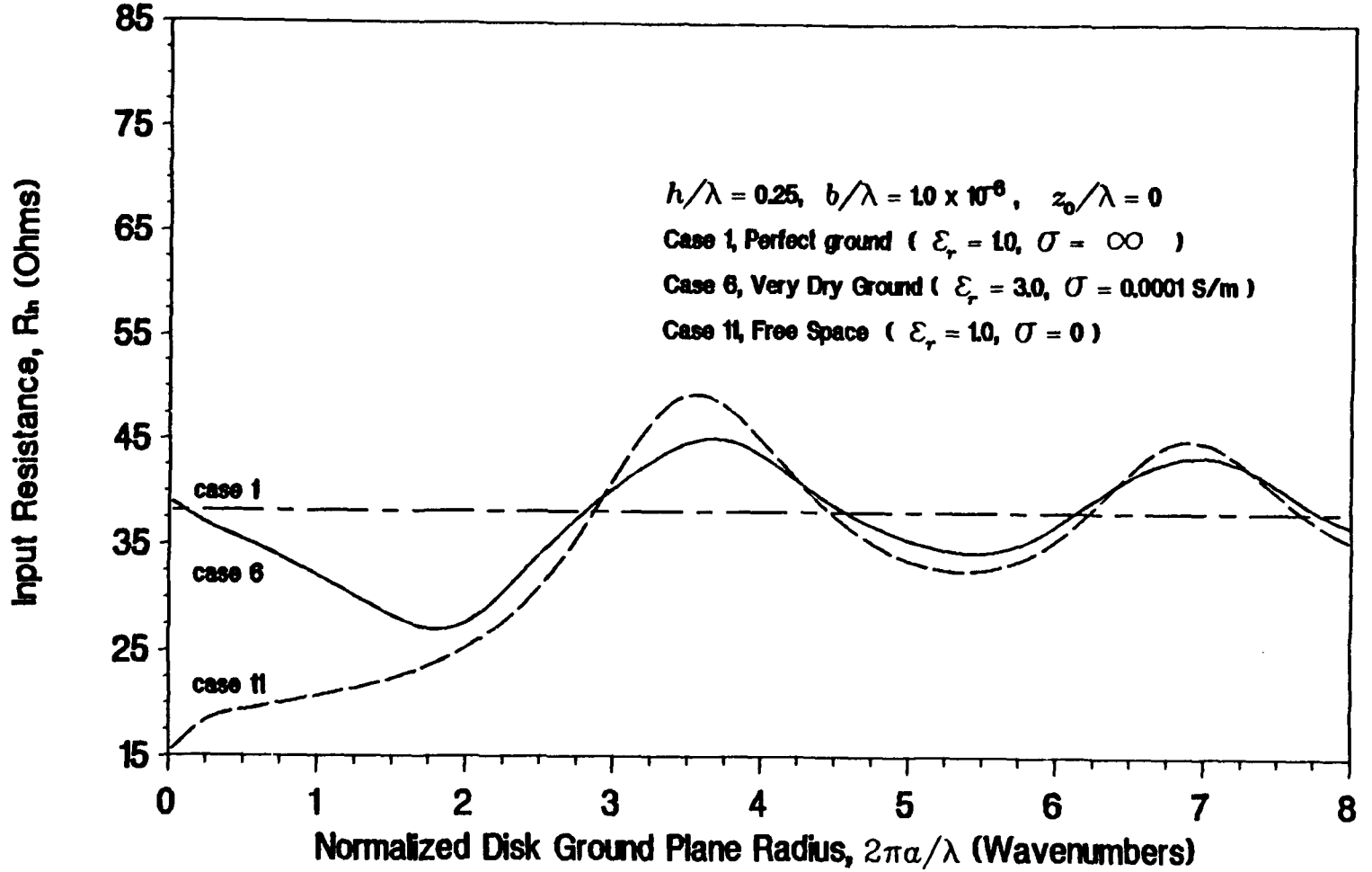

Figure 3-74. Input Resistance, Very Dry Ground

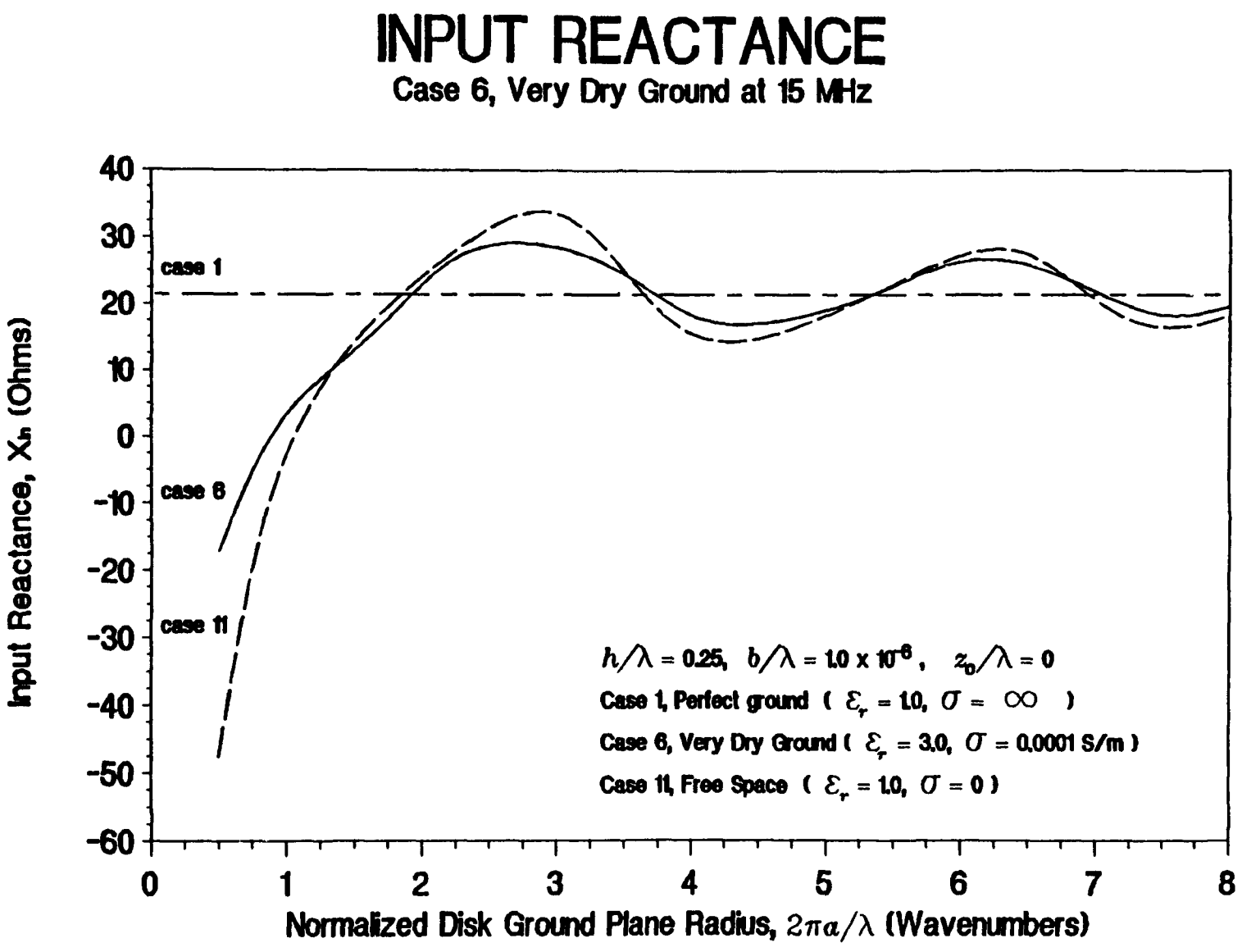

Figure 3-75. Input Reactance, Very Dry Ground

DIRECTIVE GAIN AT 82 DEG ELEVATION

Case 6, Very Dry Ground at 15 MHz

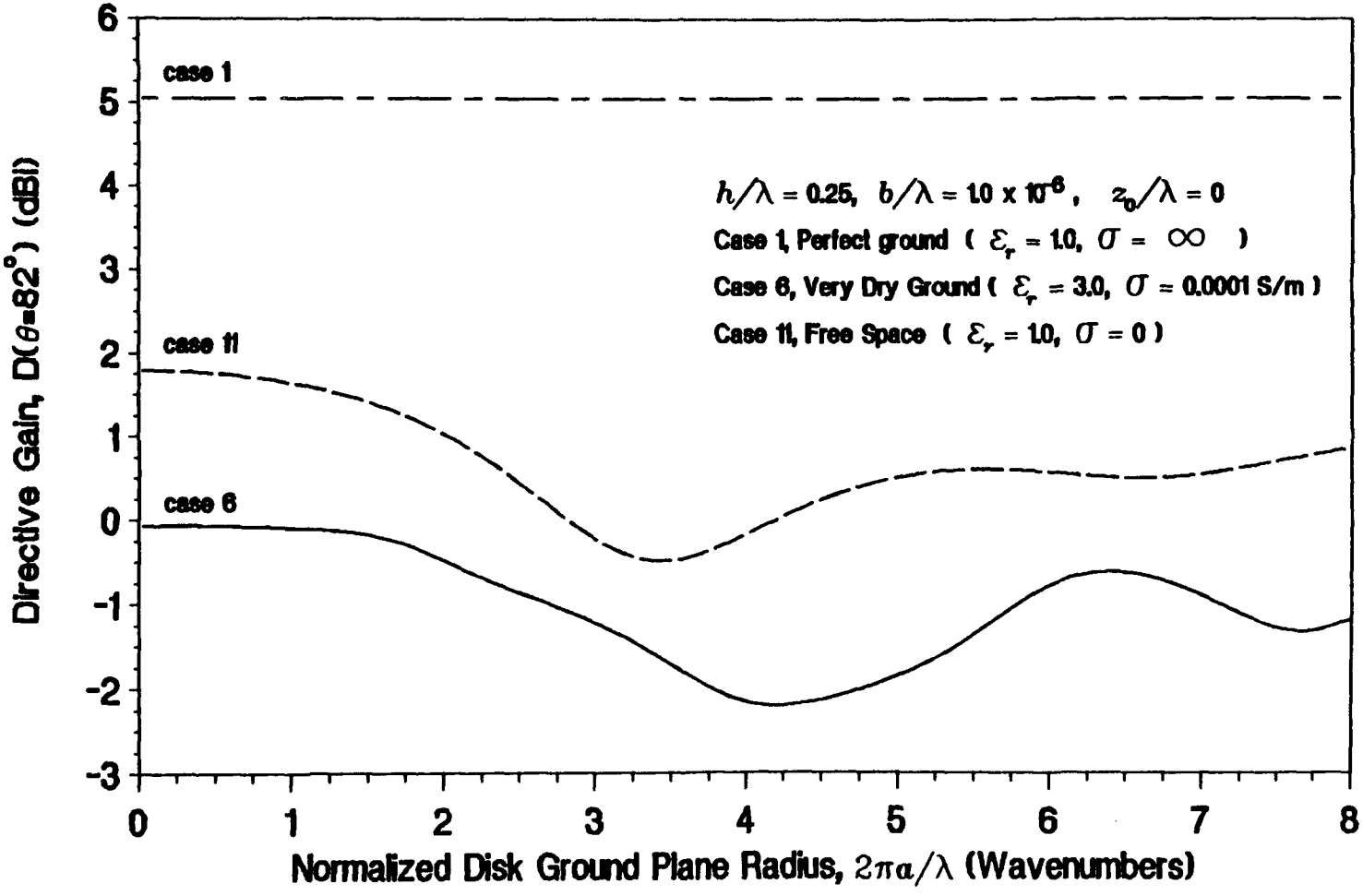

Figure 3-76. Directivity at 8 Degrees Above the Horizon, Very Dry Ground

DIRECTIVE GAIN AT 84 DEG ELEVATION

Case 6, Very Dry Ground at 15 MHz

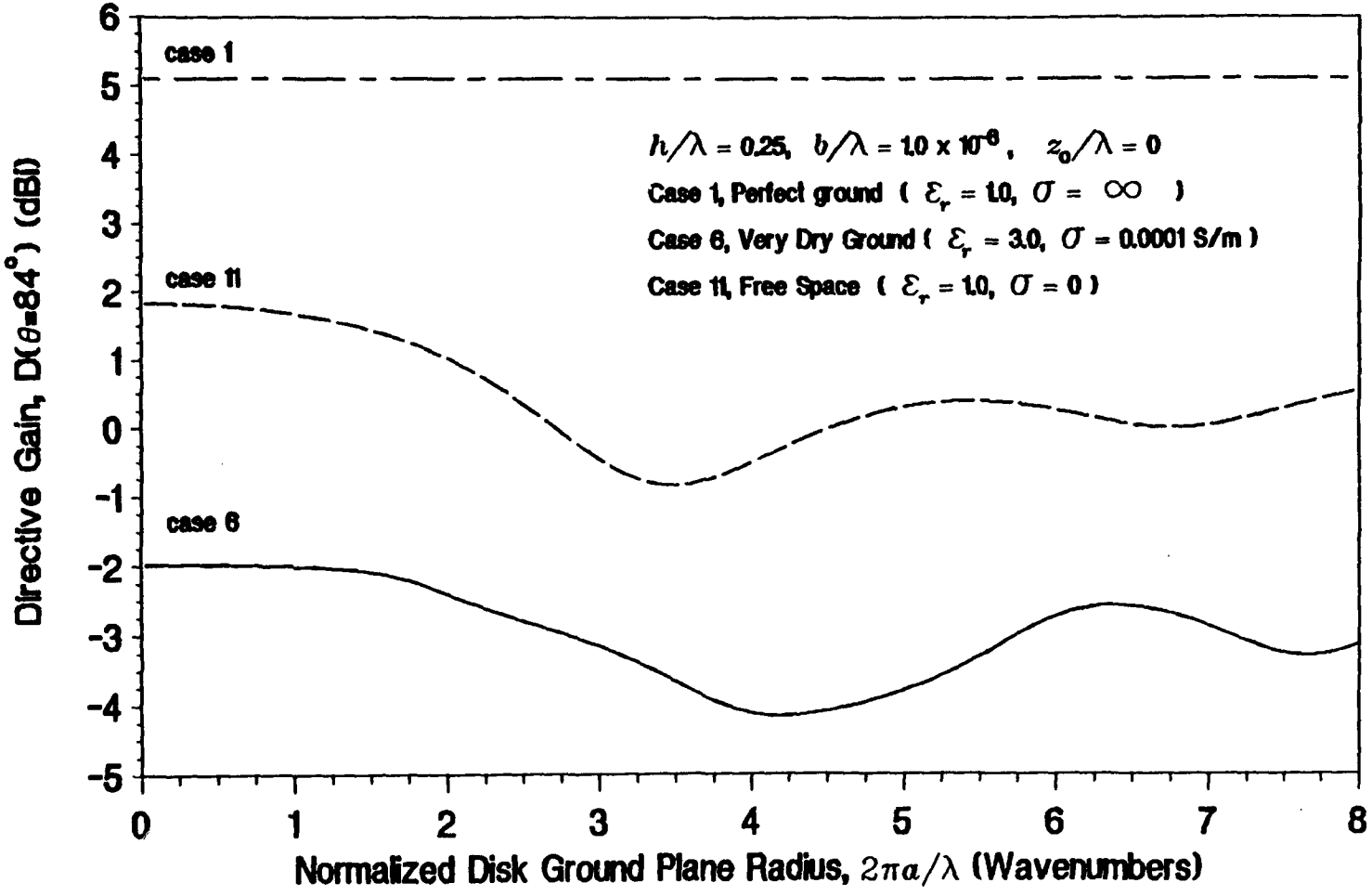

Figure 3-77. Directivity at 6 Degrees Above the Horizon, Very Dry Ground

DIRECTIVE GAIN AT 86 DEG ELEVATION

Case 6, Very Dry Ground at 15 MHz

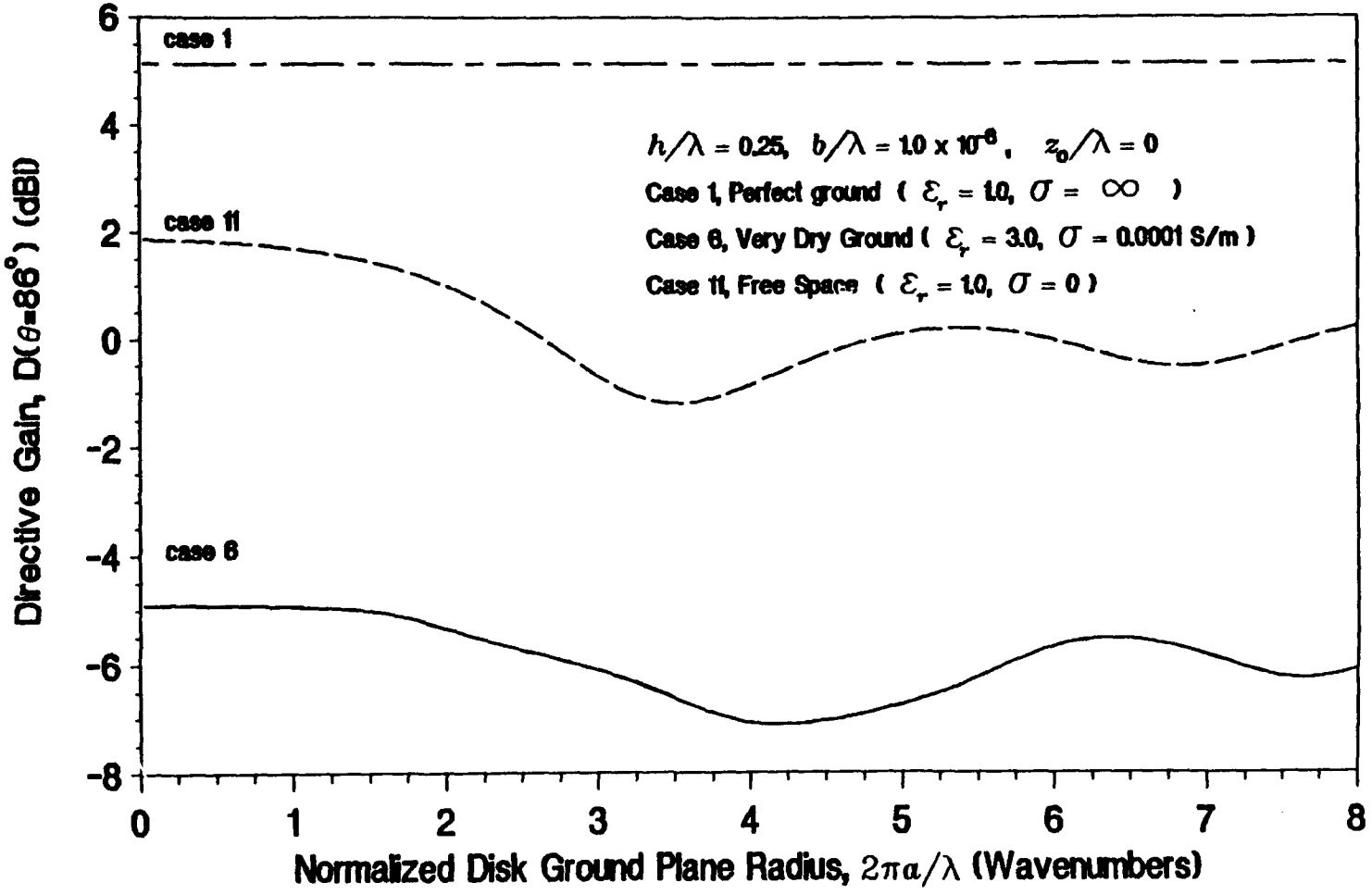

Figure 3-78. Directivity at 4 Degrees Above the Horizon, Very Dry Ground

DIRECTIVE GAIN AT 88 DEG ELEVATION

Case 6, Very Dry Ground at 15 MHz

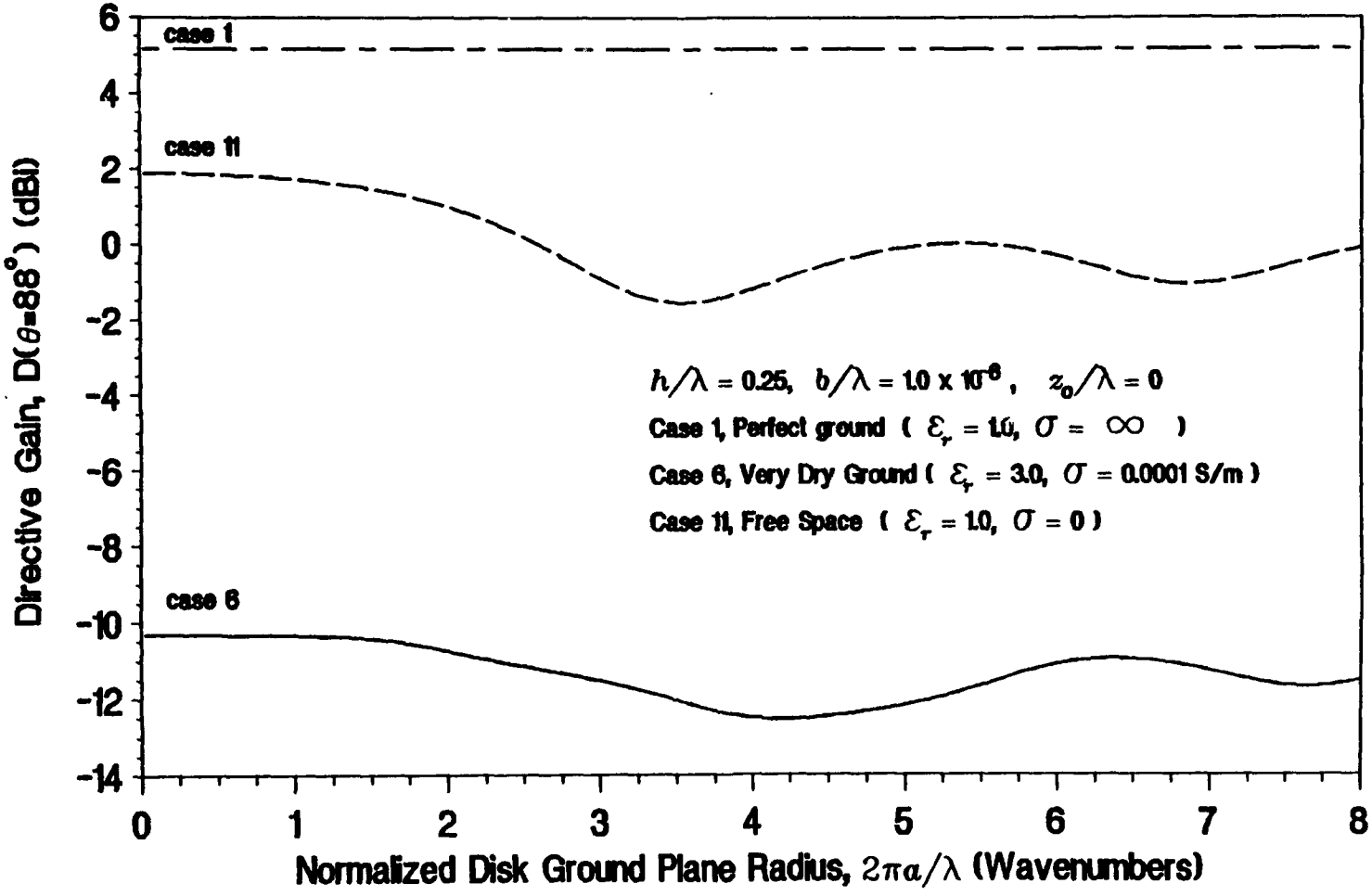

Figure 3-79. Directivity at 2 Degrees Above the Horizon, Very Dry Ground

DIRECTIVE GAIN ON THE HORIZON

Case 6, Very Dry Ground at 15 MHz

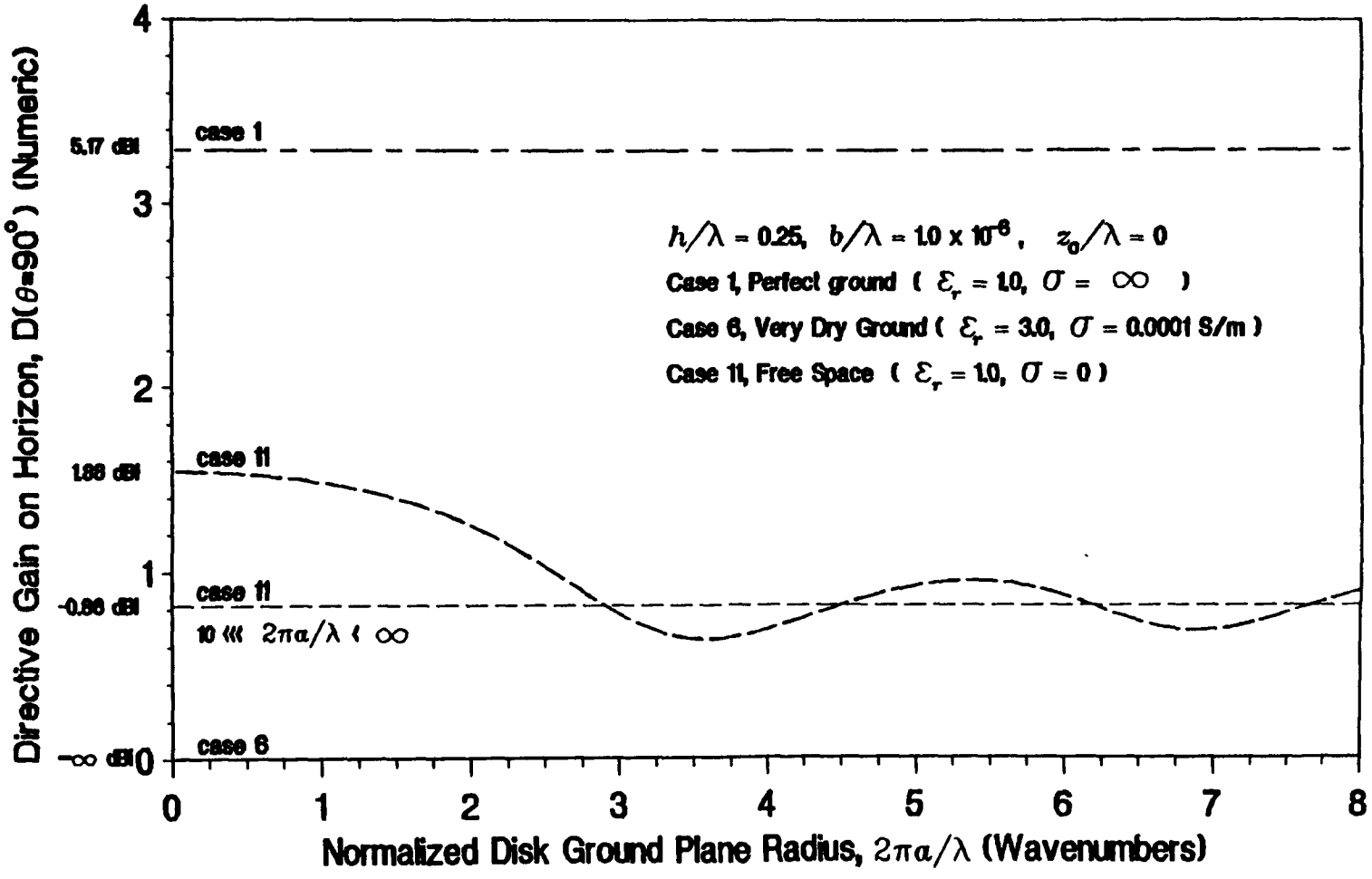

Figure 3-80. Directivity on the Horizon, Very Dry Ground

3.6 PURE WATER (20°C)

NUMERIC DIRECTIVE GAIN POLAR PLOT

Case 7, Pure Water (20 deg C) at 15 MHz

$2\pi a/\lambda = 0.025$ **(Wavenumbers)**

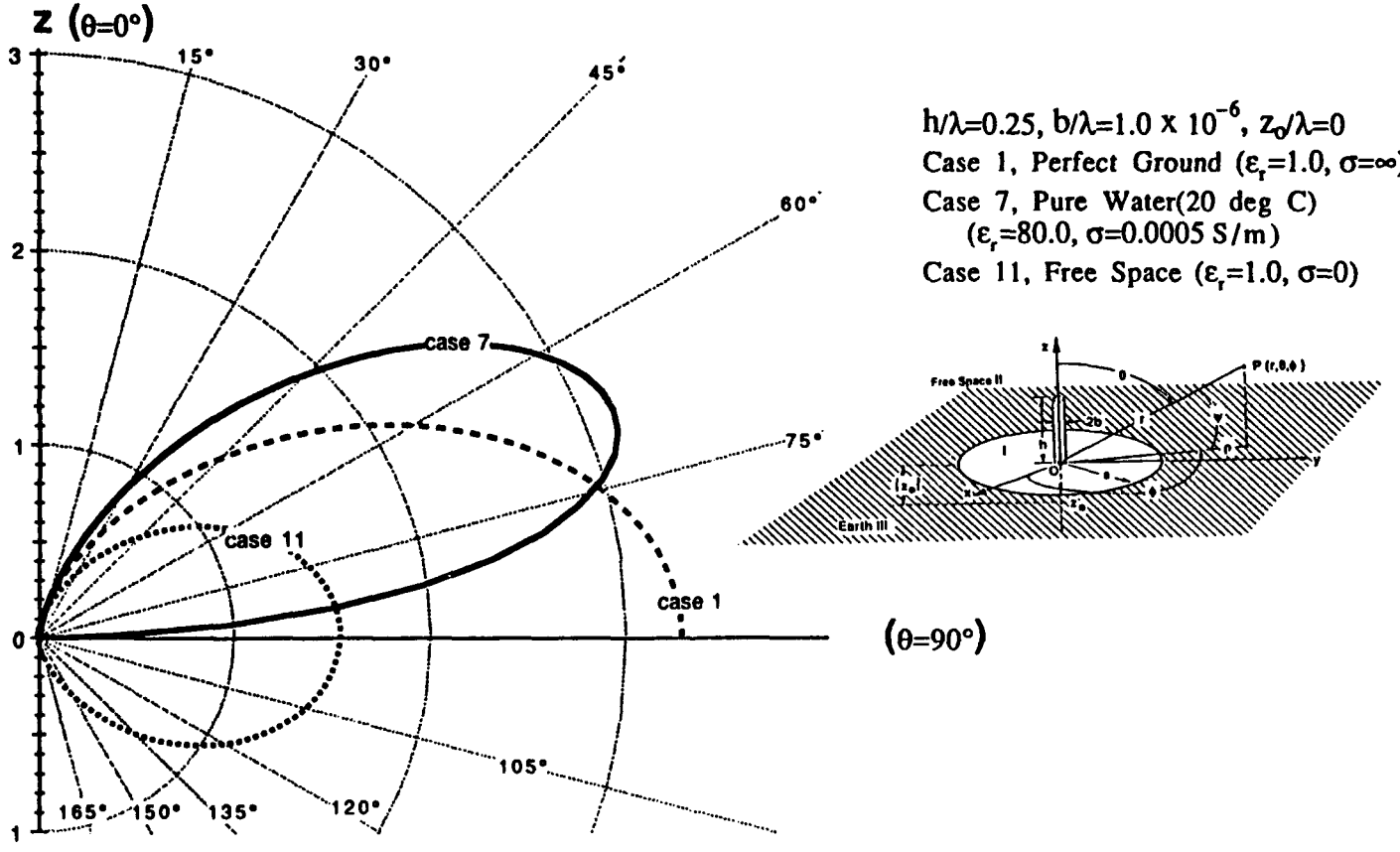

Figure 3-81. Directivity Pattern, $2\pi a/\lambda = 0.025$, Pure Water (20°C)

NUMERIC DIRECTIVE GAIN POLAR PLOT

Case 7, Pure Water (20 deg C) at 15 MHz

$2\pi a/\lambda =$ **3.0 (Wavenumbers)**

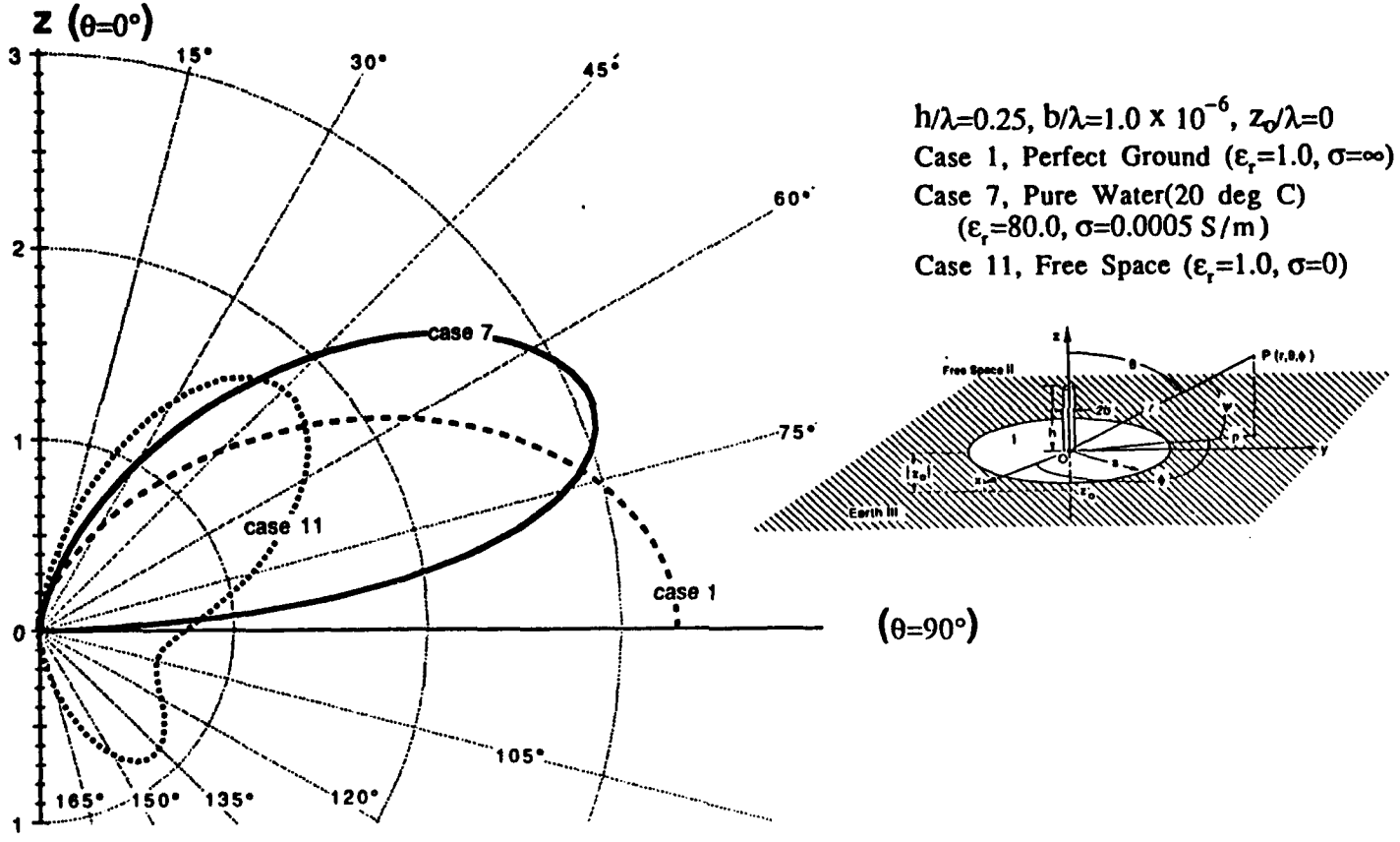

Figure 3-82. Directivity Pattern, $2\pi a/\lambda = 3.0$, Pure Water (20°C)

NUMERIC DIRECTIVE GAIN POLAR PLOT

Case 7, Pure Water (20 deg C) at 15 MHz

$2\pi a/\lambda =$ **4.0 (Wavenumbers)**

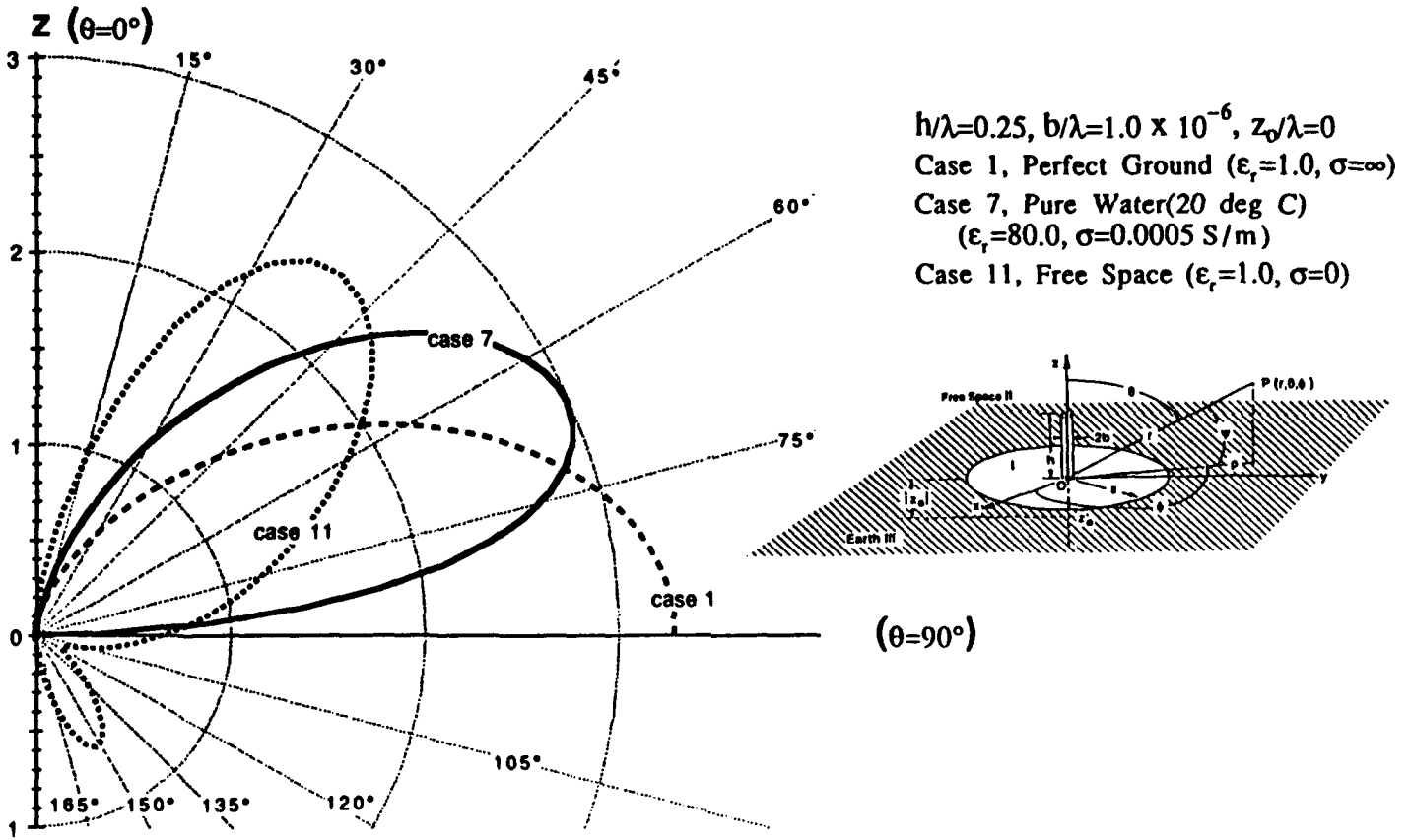

Figure 3-83. Directivity Pattern, $2\pi a/\lambda = 4.0$, Pure Water (20°C)

NUMERIC DIRECTIVE GAIN POLAR PLOT

Case 7, Pure Water (20 deg C) at 15 MHz

$2\pi a/\lambda =$ **5.0 (Wavenumbers)**

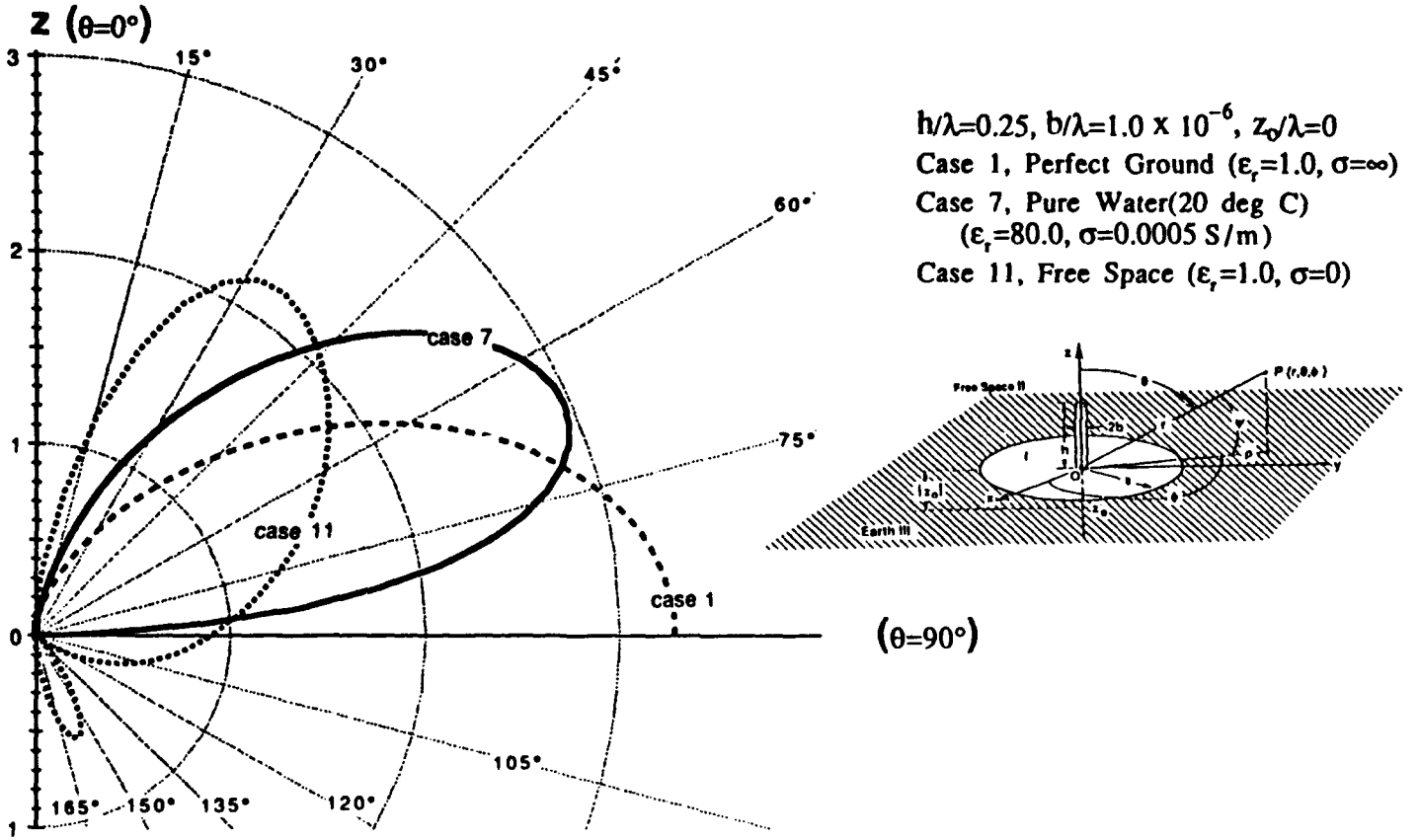

Figure 3-84. Directivity Pattern, $2\pi a/\lambda = 5.0$, Pure Water (20°C)

NUMERIC DIRECTIVE GAIN POLAR PLOT

Case 7, Pure Water (20 deg C) at 15 MHz

$2\pi a/\lambda =$ **6.5 (Wavenumbers)**

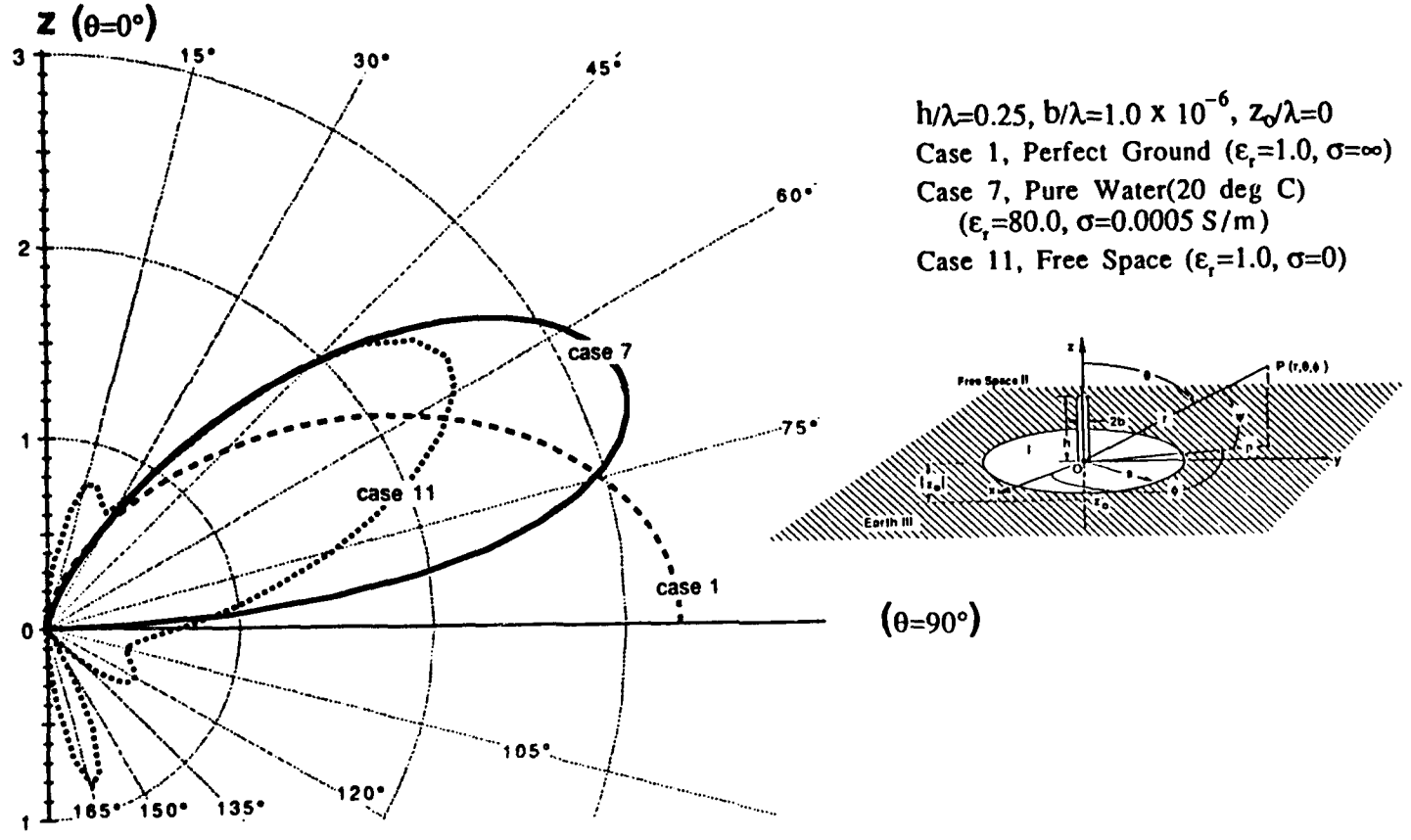

Figure 3-85. Directivity Pattern, $2\pi a/\lambda = 6.5$, Pure Water (20°C)

PEAK DIRECTIVITY

Case 7, Pure Water (20 deg C) at 15 MHz

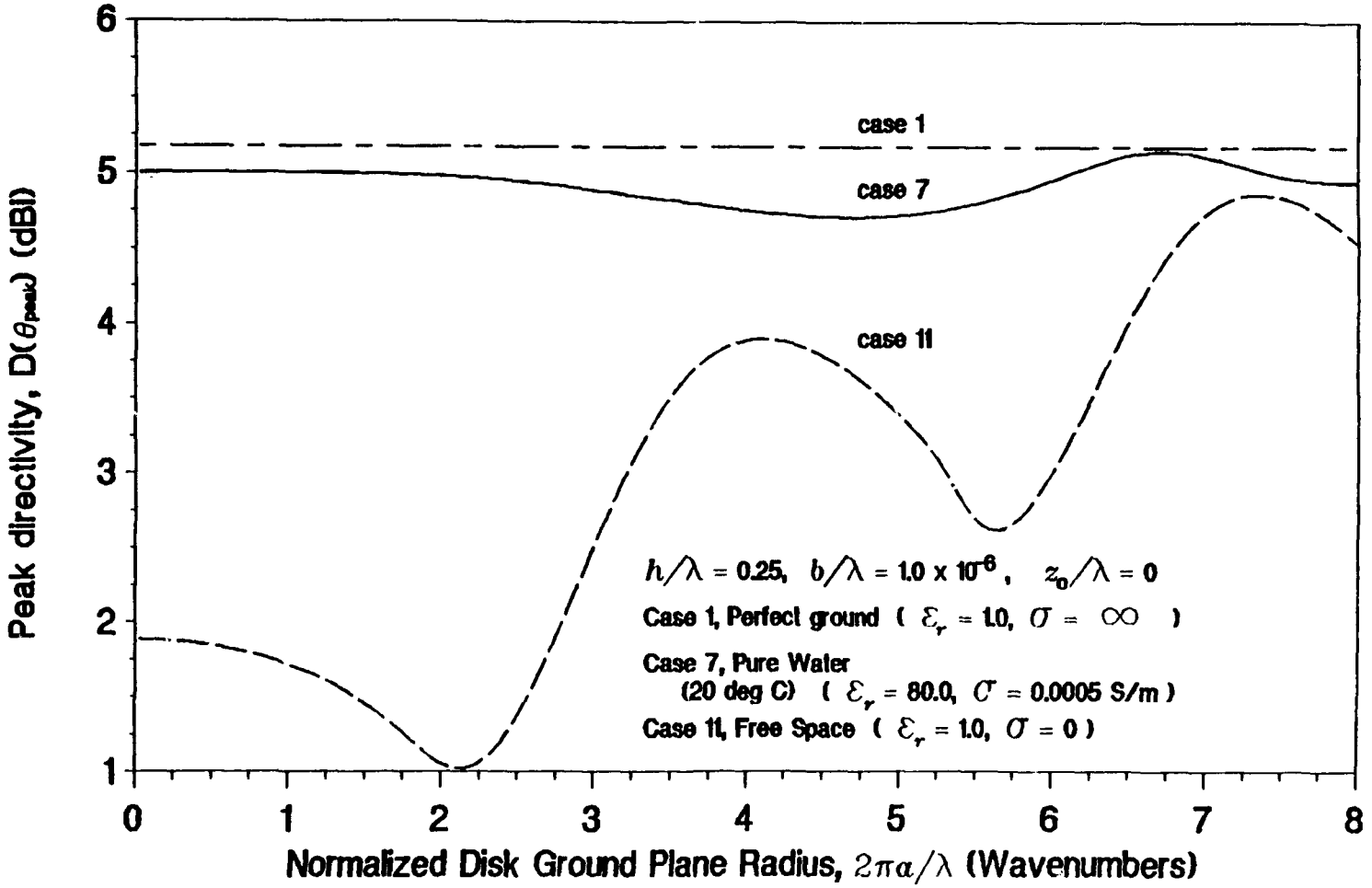

Figure 3-86. Peak Directivity, Pure Water (20°C)

ANGLE OF PEAK DIRECTIVITY

Case 7, Pure Water (20 deg C) at 15 MHz

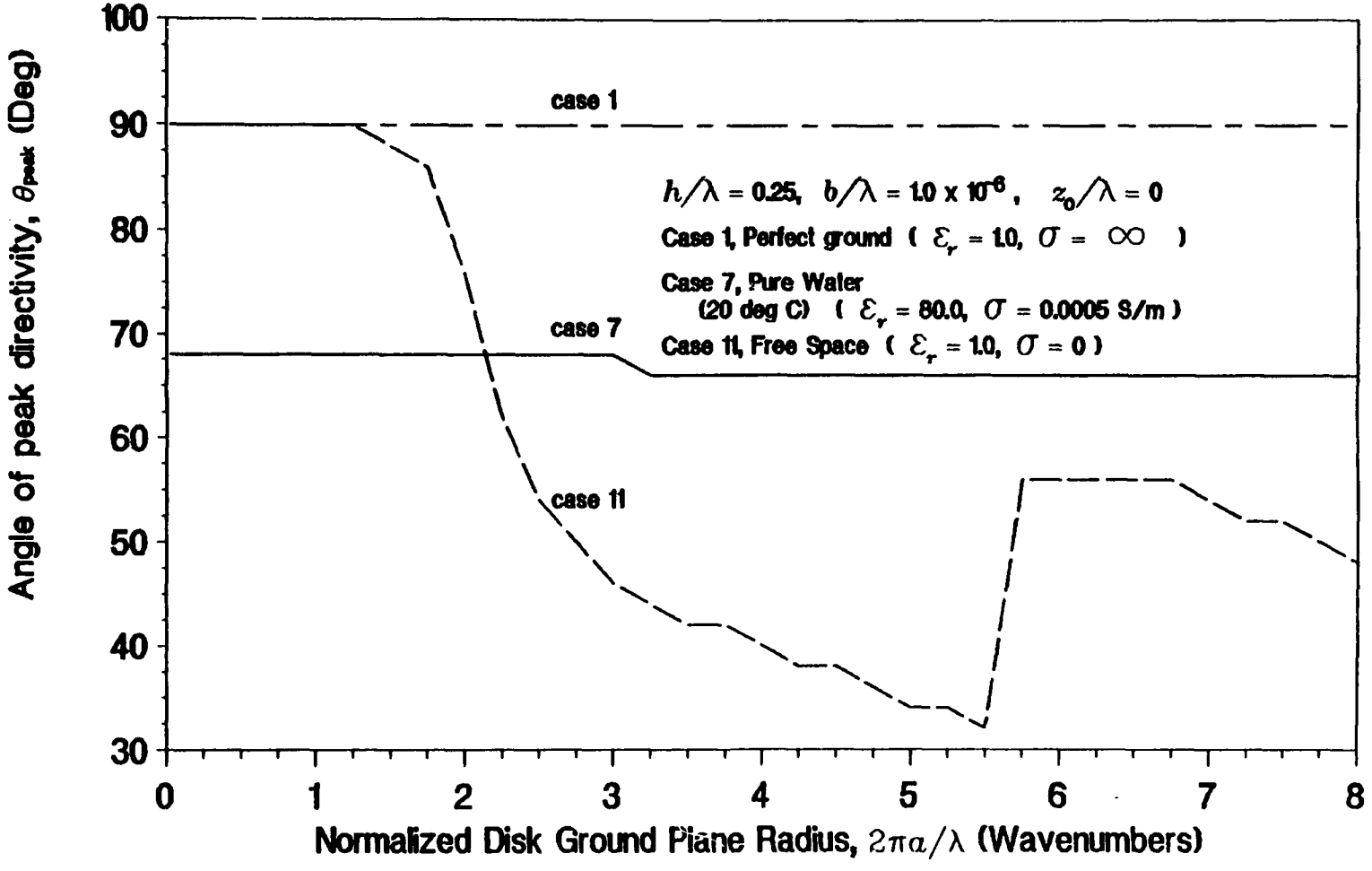

Figure 3-87. Angle of Incidence of Peak Directivity, Pure Water (20°C)

RADIATION EFFICIENCY

Case 7, Pure Water (20 deg C) at 15 MHz

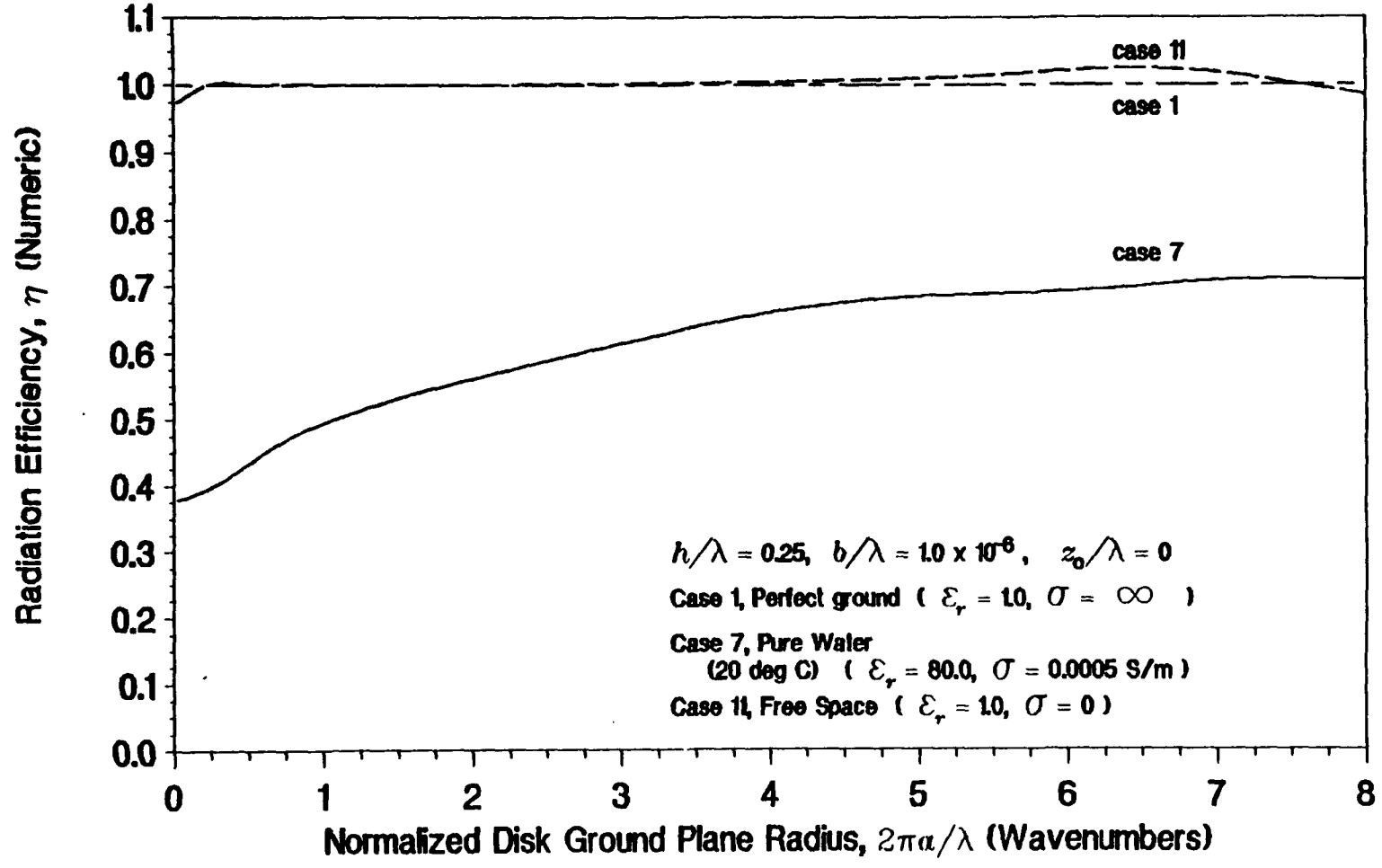

Figure 3-88. Radiation Efficiency, Pure Water (20°C)

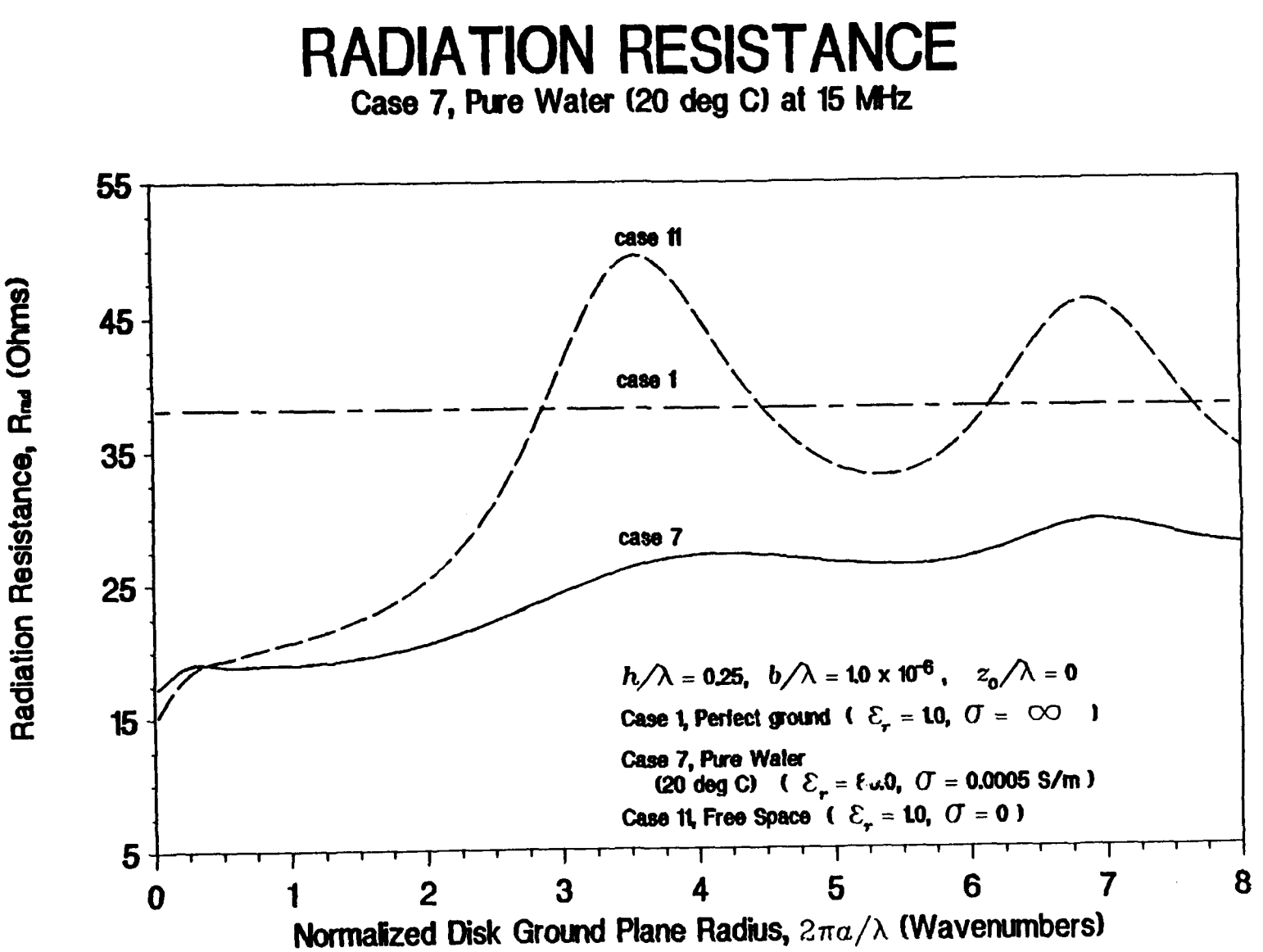

Figure 3-89. Radiation Resistance, Pure Water (20°C)

INPUT RESISTANCE

Case 7, Pure Water (20 deg C) at 15 MHz

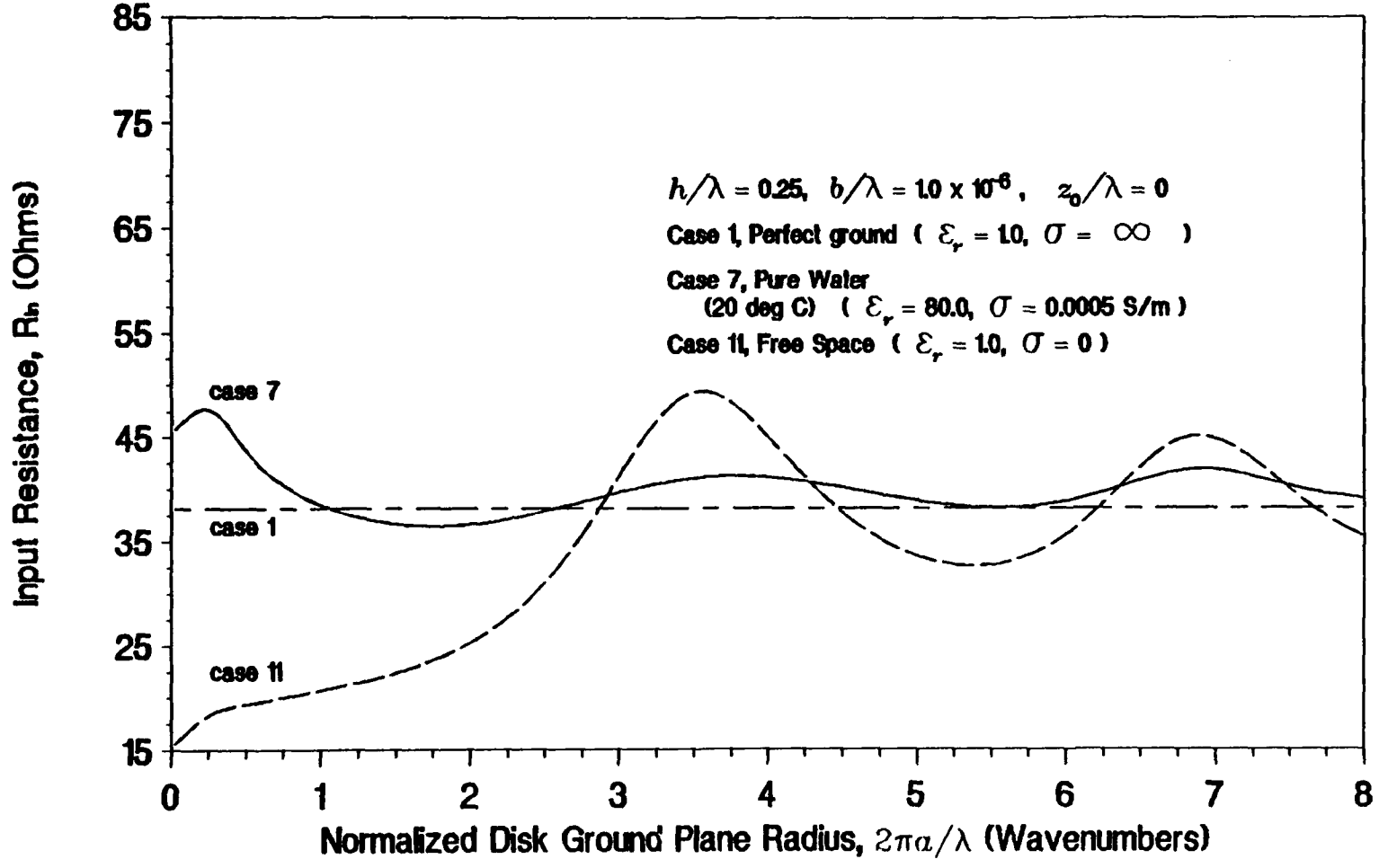

Figure 3-90. Input Resistance, Pure Water (20°C)

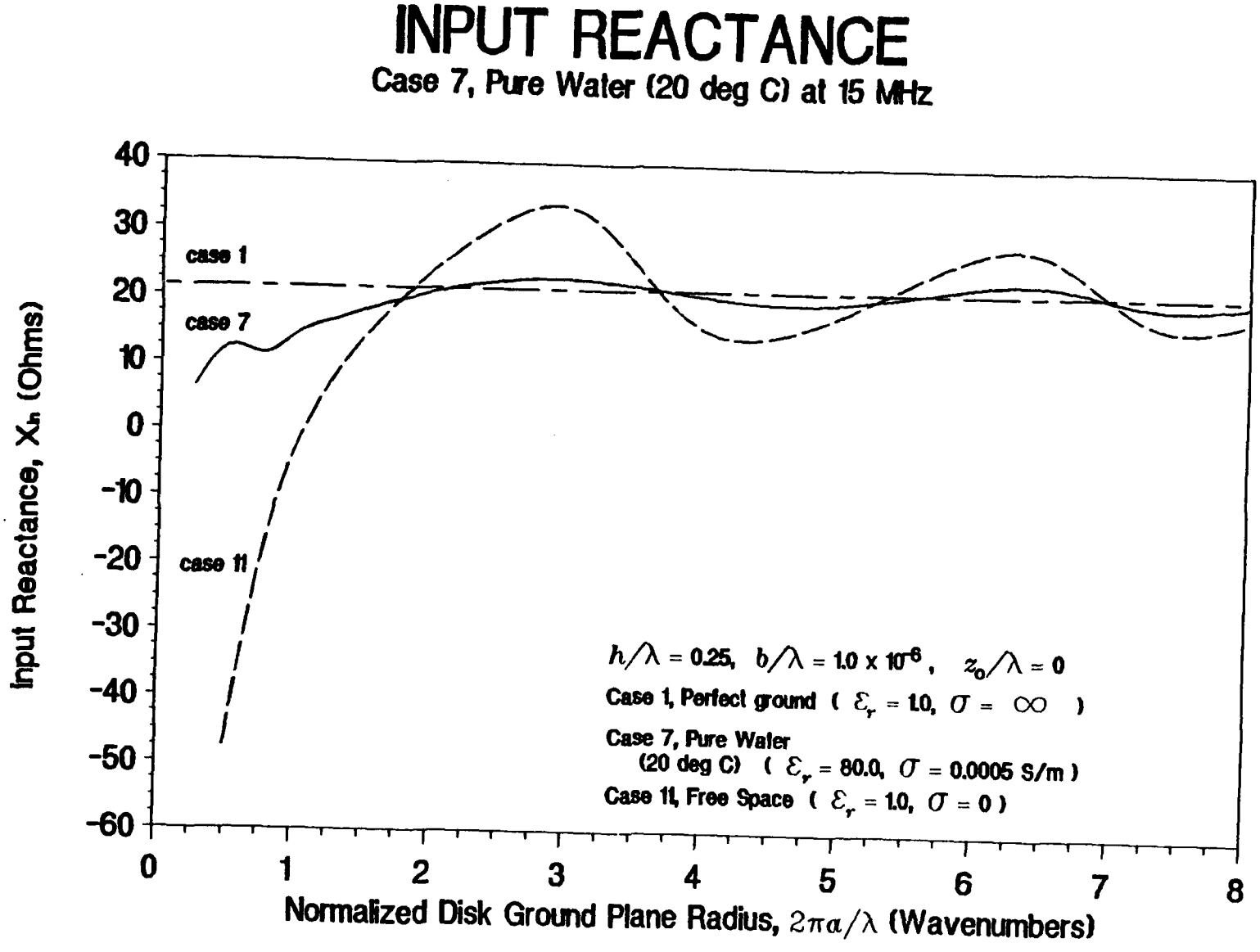

Figure 3-91. Input Reactance, Pure Water (20°C)

DIRECTIVE GAIN AT 82 DEG ELEVATION

Case 7, Pure Water (20 deg C) at 15 MHz

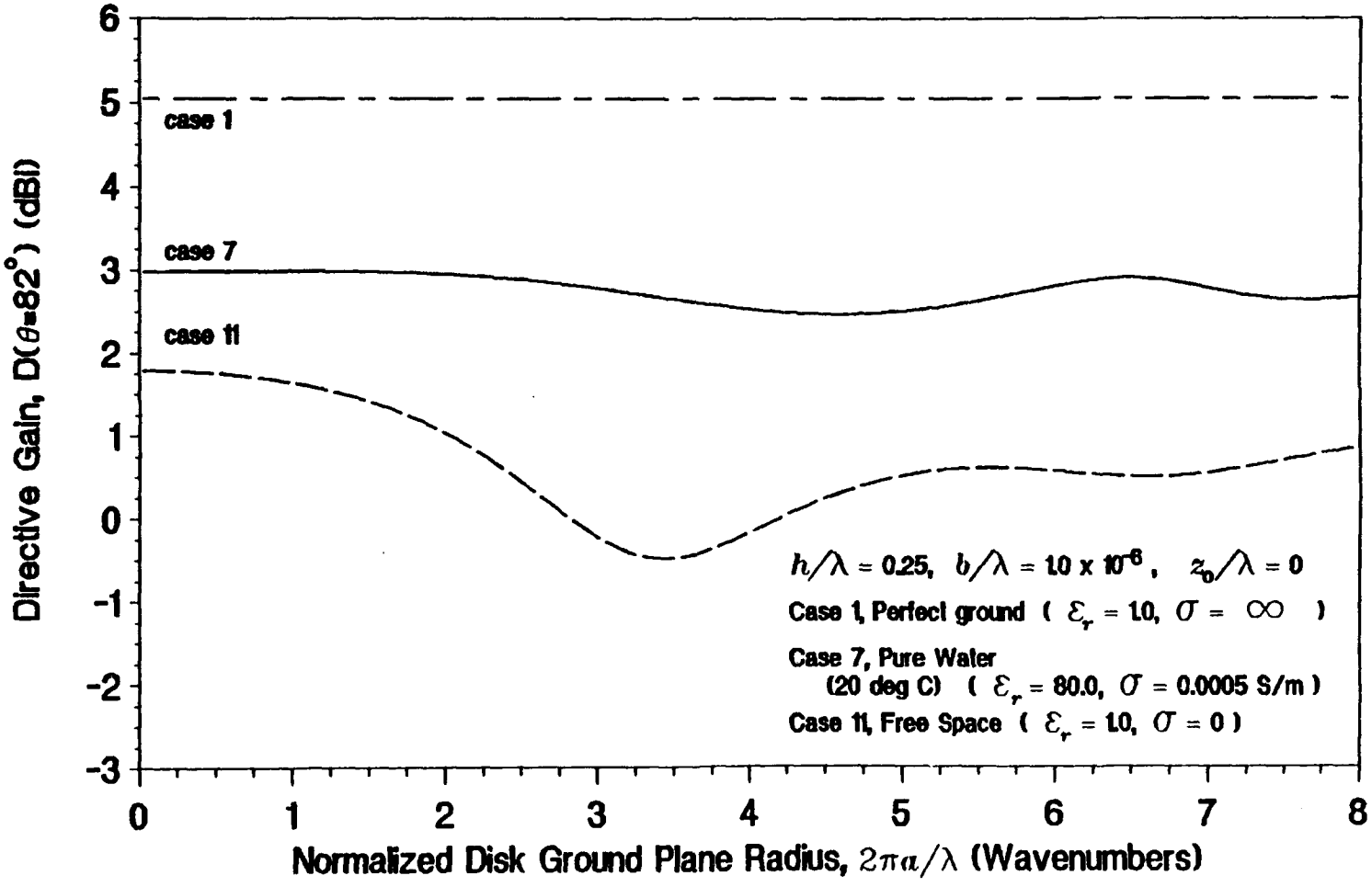

Figure 3-92. Directivity at 8 Degrees Above the Horizon, Pure Water (20°C)

DIRECTIVE GAIN AT 84 DEG ELEVATION

Case 7, Pure Water (20 deg C) at 15 MHz

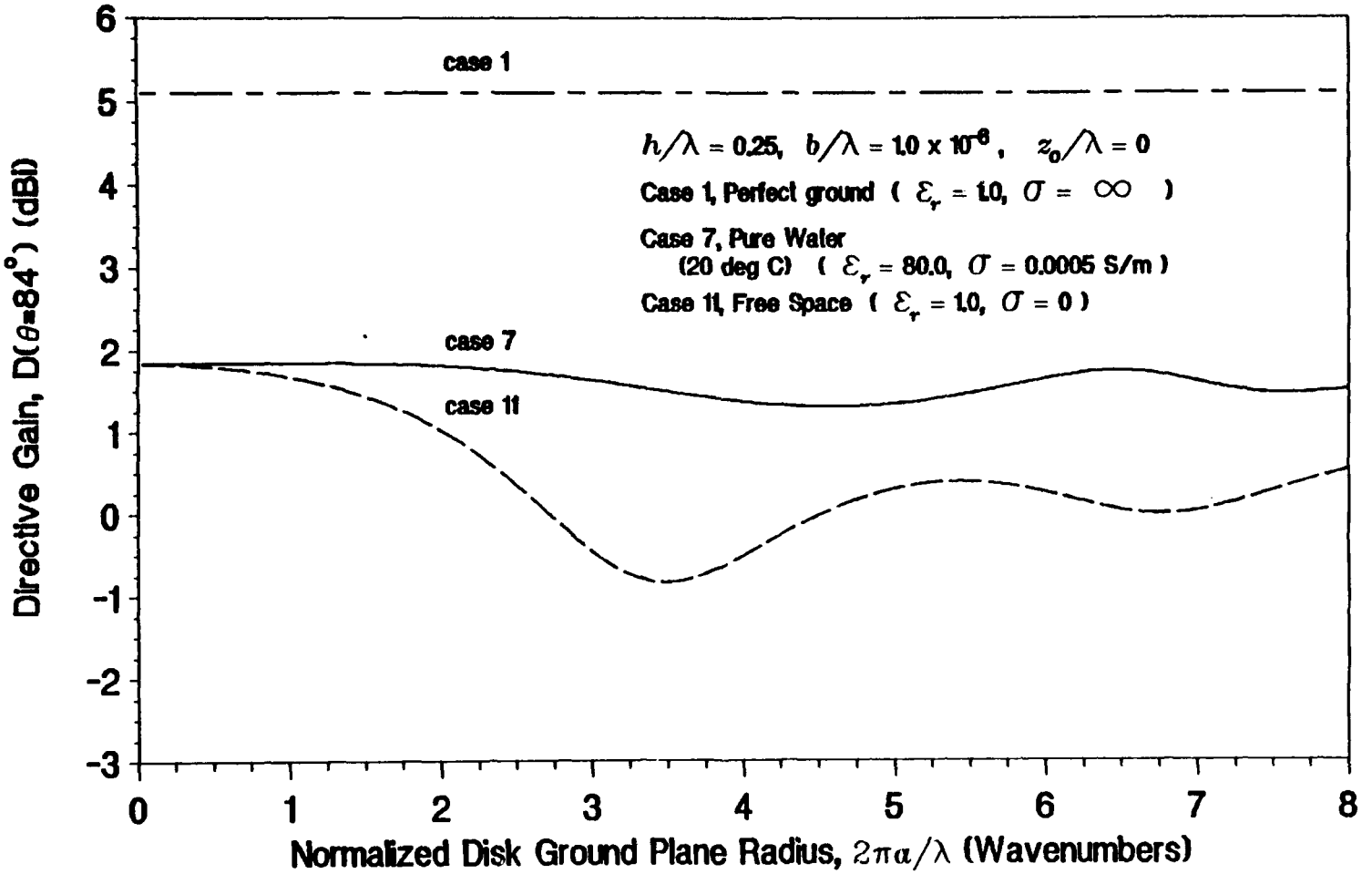

Figure 3-93. Directivity at 6 Degrees Above the Horizon, Pure Water (20°C)

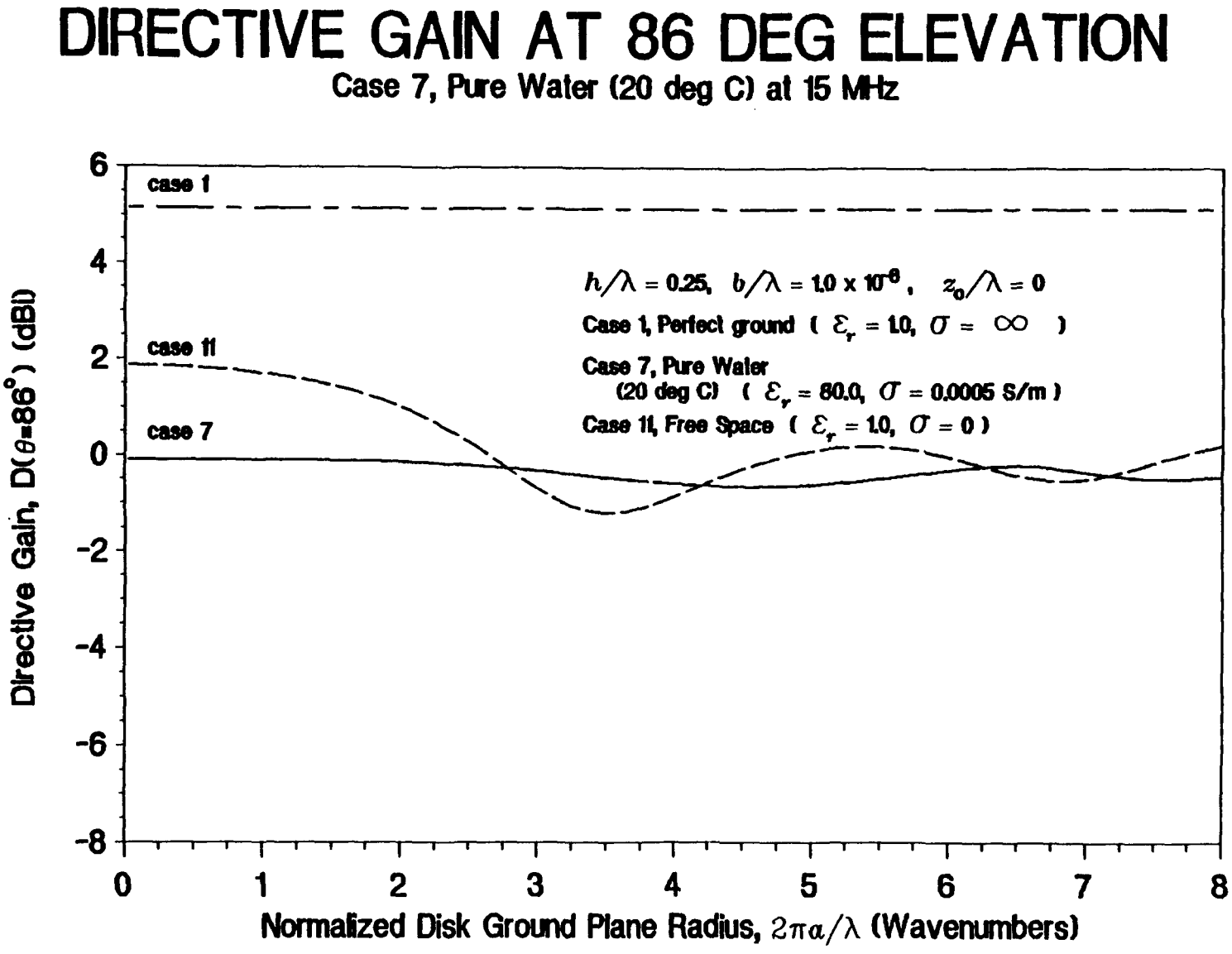

Figure 3-94. Directivity at 4 Degrees Above the Horizon, Pure Water (20°C)

DIRECTIVE GAIN AT 88 DEG ELEVATION

Case 7, Pure Water (20 deg C) at 15 MHz

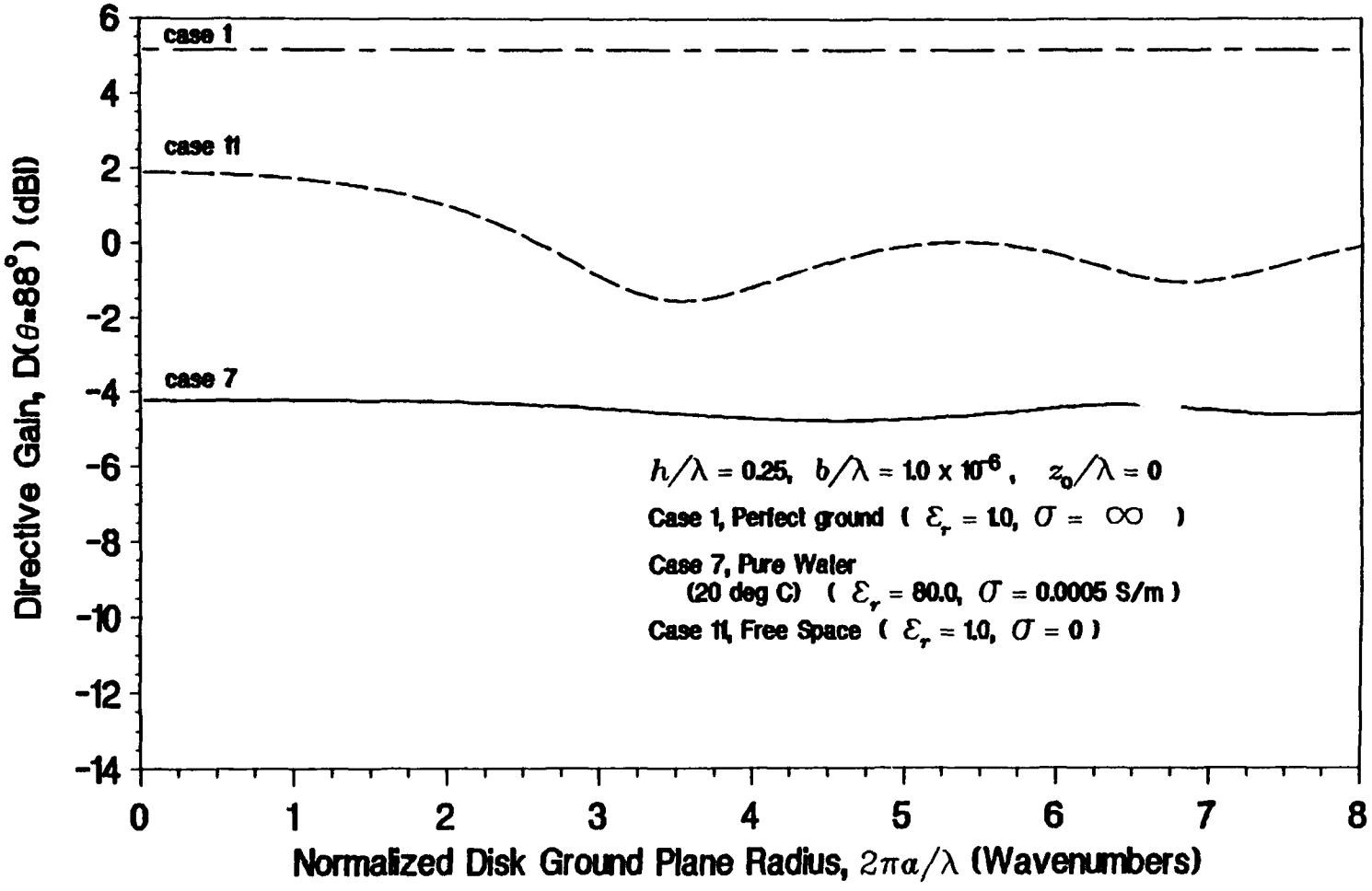

Figure 3-95. Directivity at 2 Degrees Above the Horizon, Pure Water (20°C)

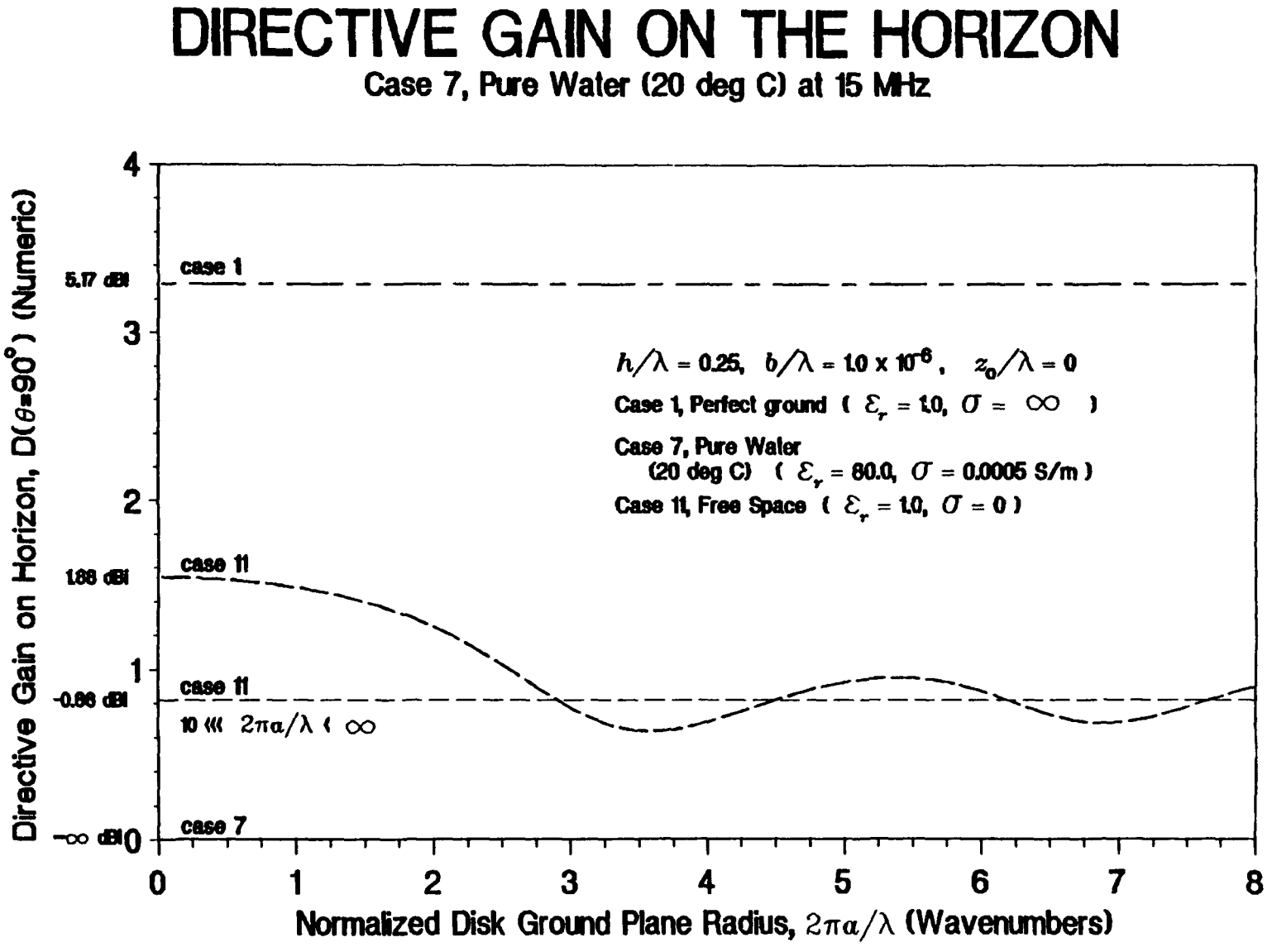

Figure 3-96. Directivity on the Horizon, Pure Water (20°C)

3.7 ICE (FRESH WATER, -1°C)

NUMERIC DIRECTIVE GAIN POLAR PLOT

Case 8, Ice (fresh water, -1 deg C) at 15 MHz

$2\pi a/\lambda = 0.025$ (Wavenumbers)

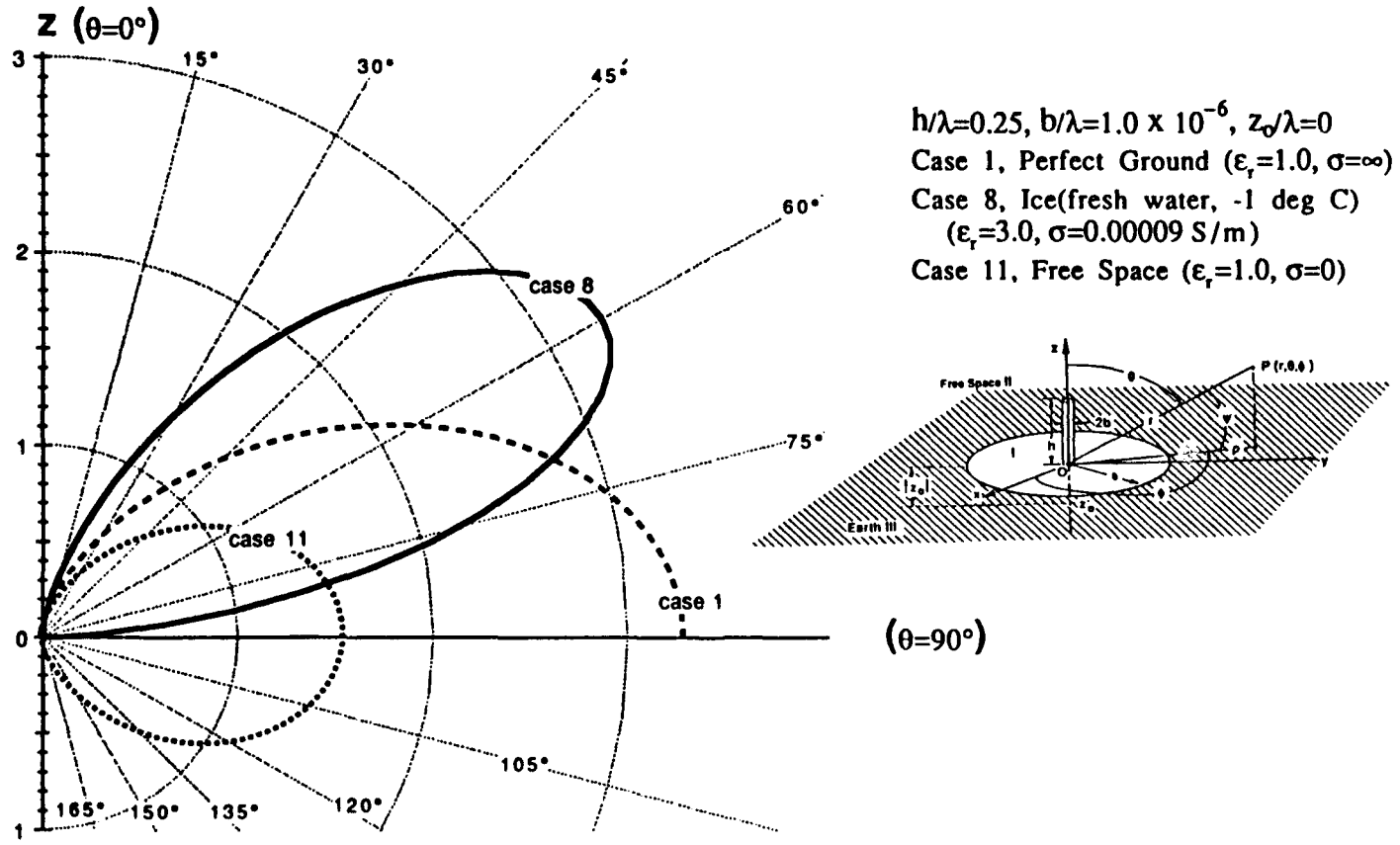

Figure 3-97. Directivity Pattern, $2\pi a/\lambda = 0.025$ Ice (Fresh Water, -1°C)

NUMERIC DIRECTIVE GAIN POLAR PLOT

Case 8, Ice (fresh water, -1 deg C) at 15 MHz

$2\pi a/\lambda =$ **3.0 (Wavenumbers)**

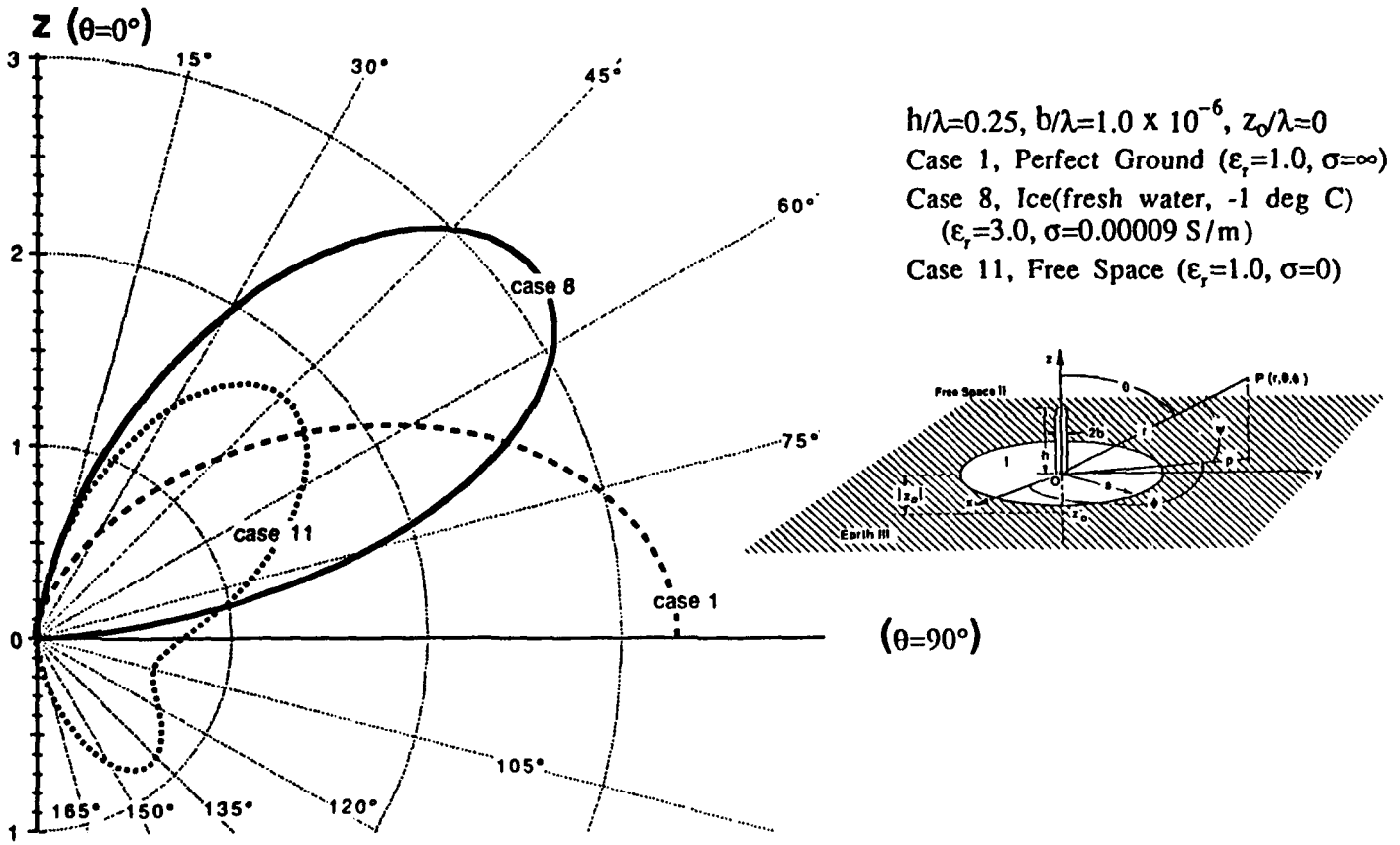

Figure 3-98. Directivity Pattern, $2\pi a/\lambda = 3.0$, Ice (Fresh Water, -1°C)

NUMERIC DIRECTIVE GAIN POLAR PLOT

Case 8, Ice (fresh water, -1 deg C) at 15 MHz

$2\pi a/\lambda =$ **4.0 (Wavenumbers)**

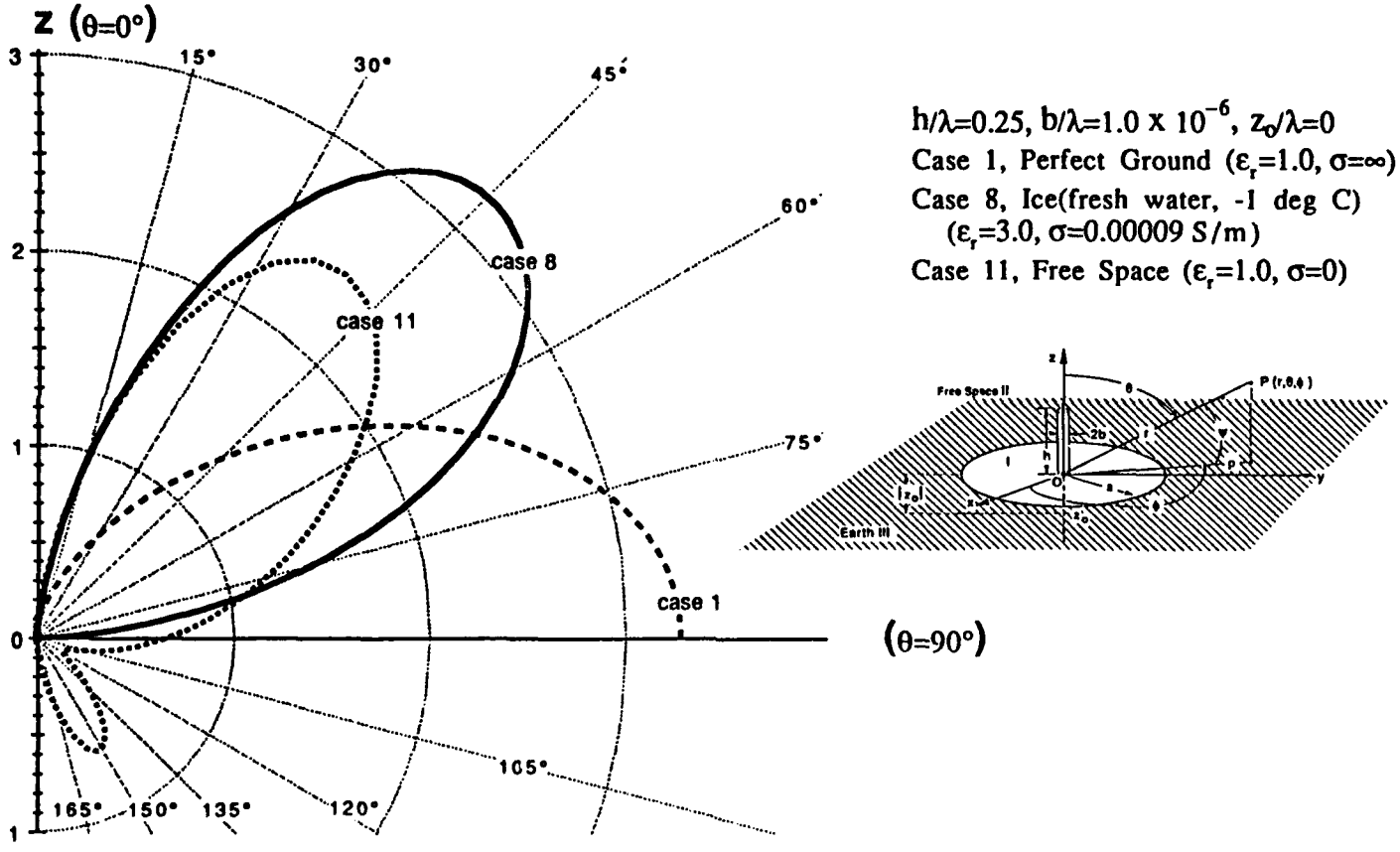

Figure 3-99. Directivity Pattern, $2\pi a/\lambda = 4.0$, Ice (Fresh Water, -1°C)

NUMERIC DIRECTIVE GAIN POLAR PLOT

Case 8, Ice (fresh water, -1 deg C) at 15 MHz

$2\pi a/\lambda =$ 5.0 (Wavenumbers)

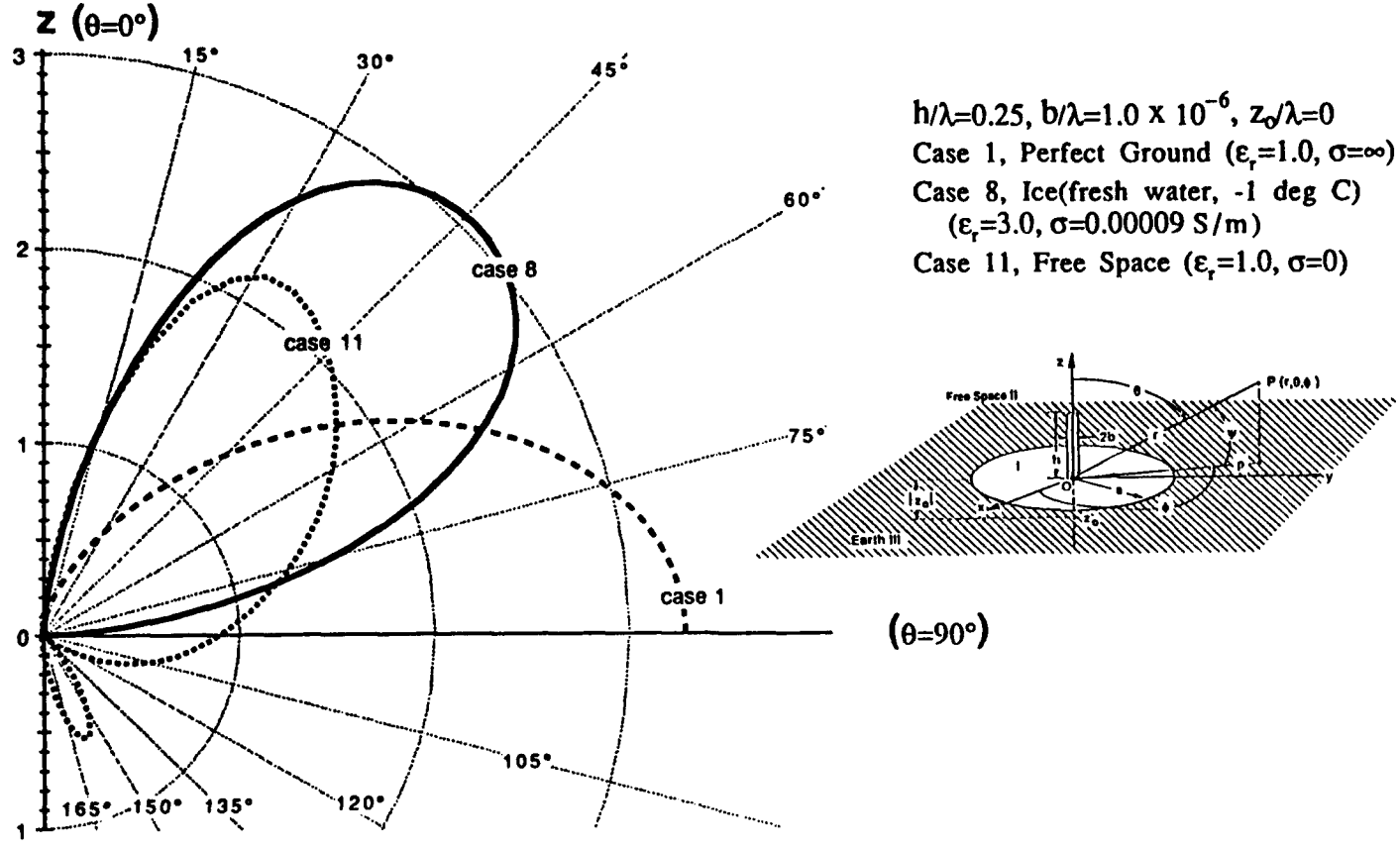

Figure 3-100. Directivity Pattern, $2\pi a/\lambda = 5.0$, Ice (Fresh Water, -1°C)

NUMERIC DIRECTIVE GAIN POLAR PLOT

Case 8, Ice (fresh water, -1 deg C) at 15 MHz

$2\pi a/\lambda =$ **6.5 (Wavenumbers)**

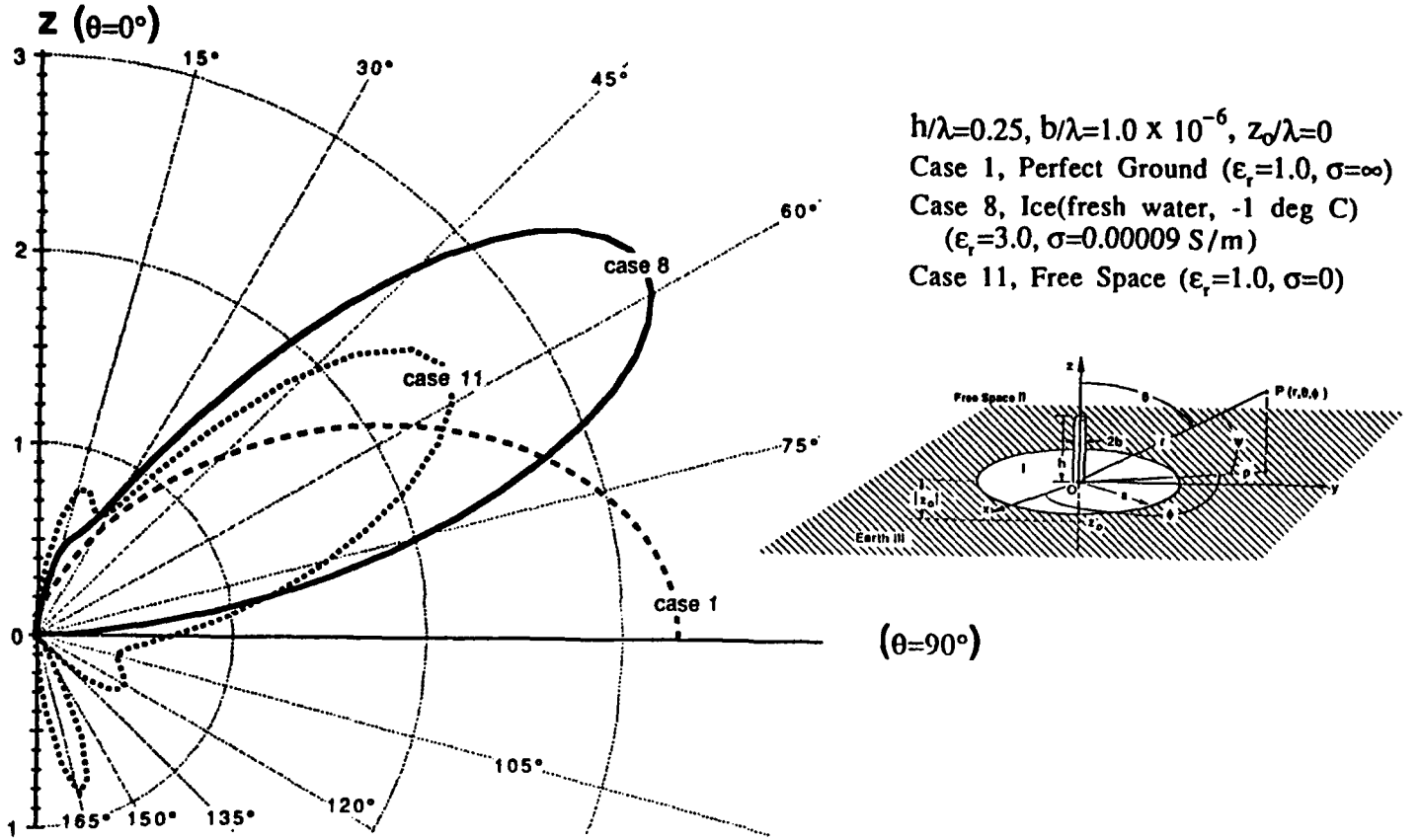

Figure 3-101. Directivity Pattern, $2\pi a/\lambda = 6.5$, Ice (Fresh Water, -1°C)

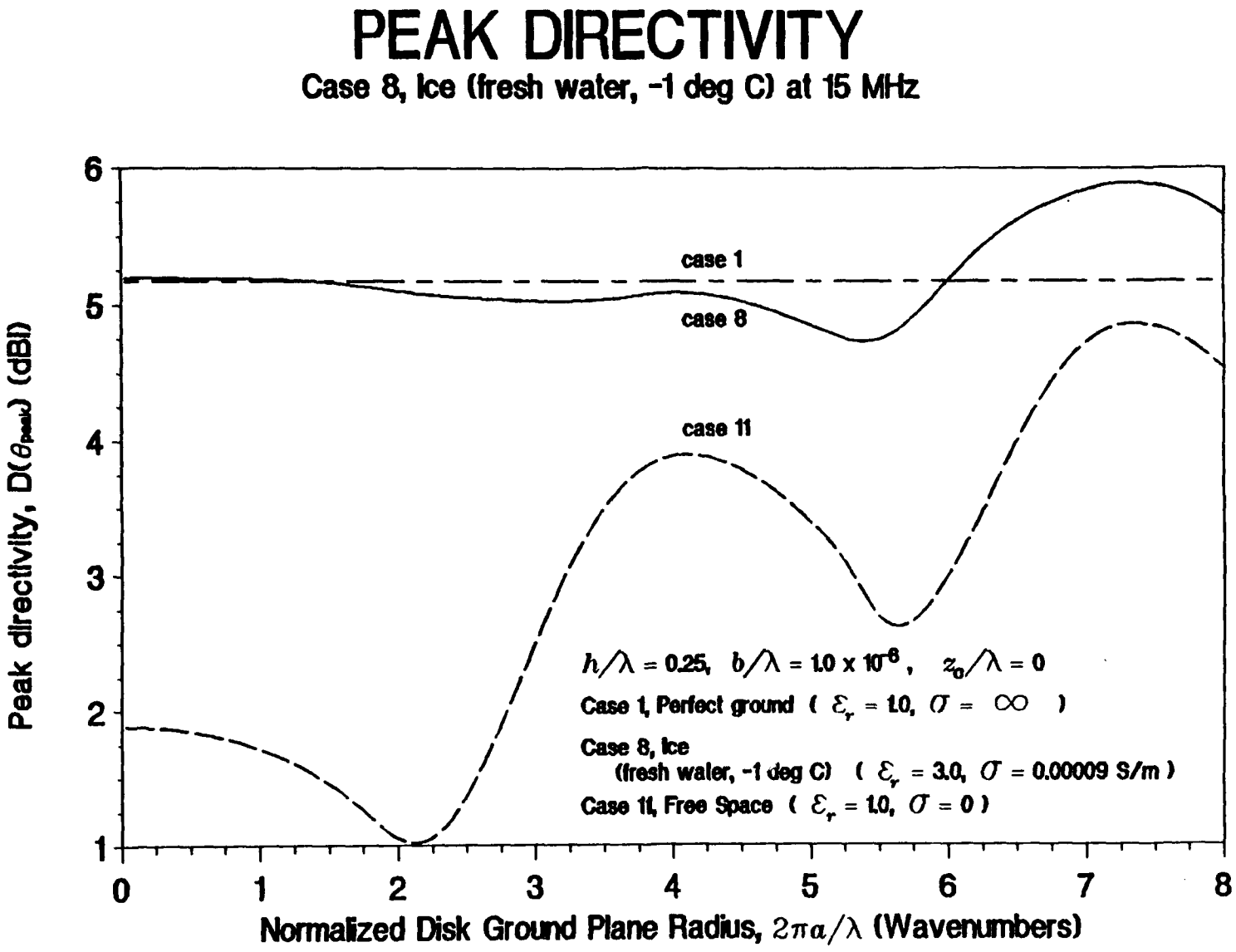

Figure 3-102. Peak Directivity, Ice (Fresh Water, -1°C)

ANGLE OF PEAK DIRECTIVITY

Case 8, Ice (fresh water, -1 deg C) at 15 MHz

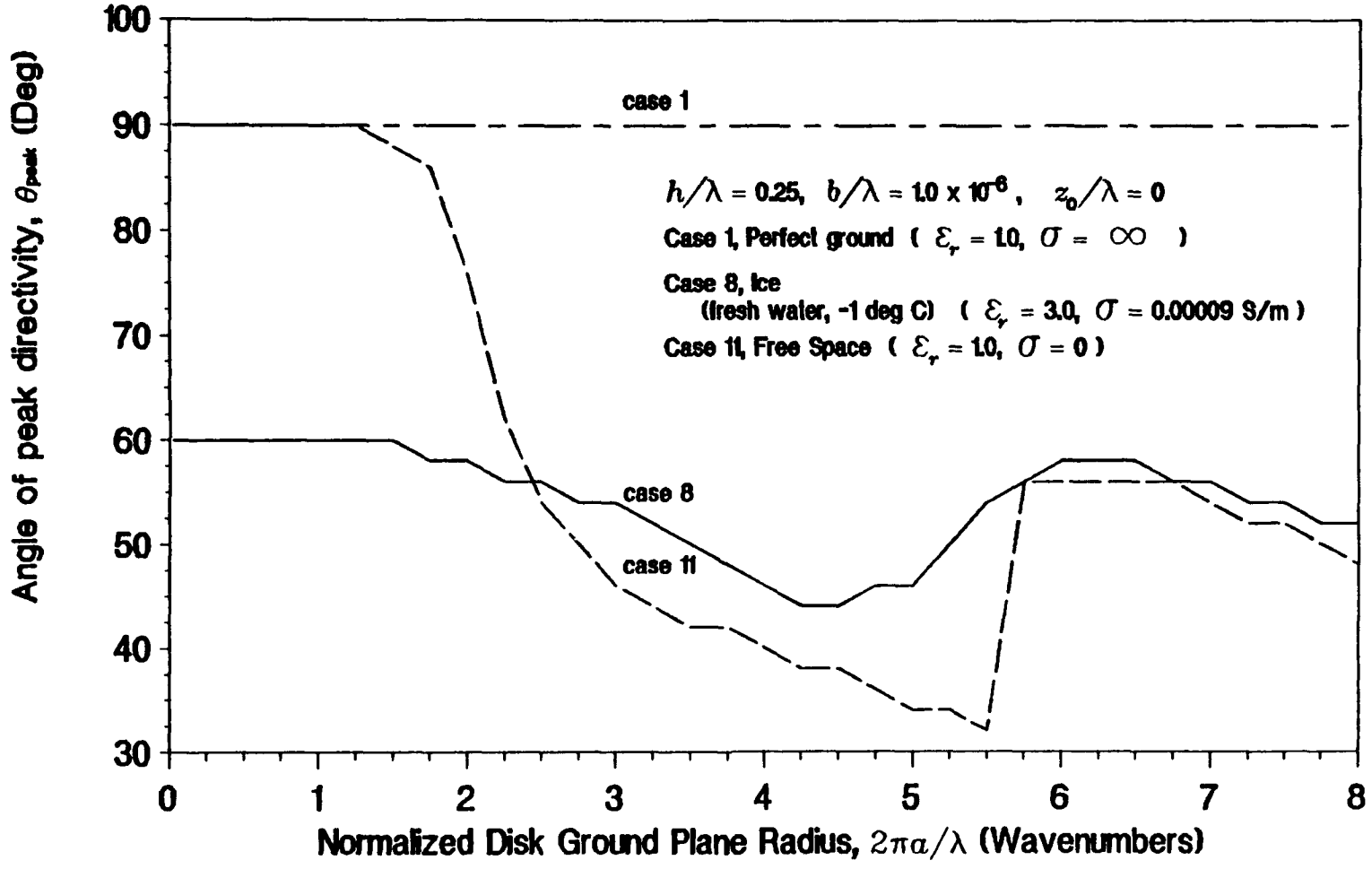

Figure 3-103. Angle of Incidence of Peak Directivity, Ice (Fresh Water, -1°C)

RADIATION EFFICIENCY

Case 8, Ice (fresh water, -1 deg C) at 15 MHz

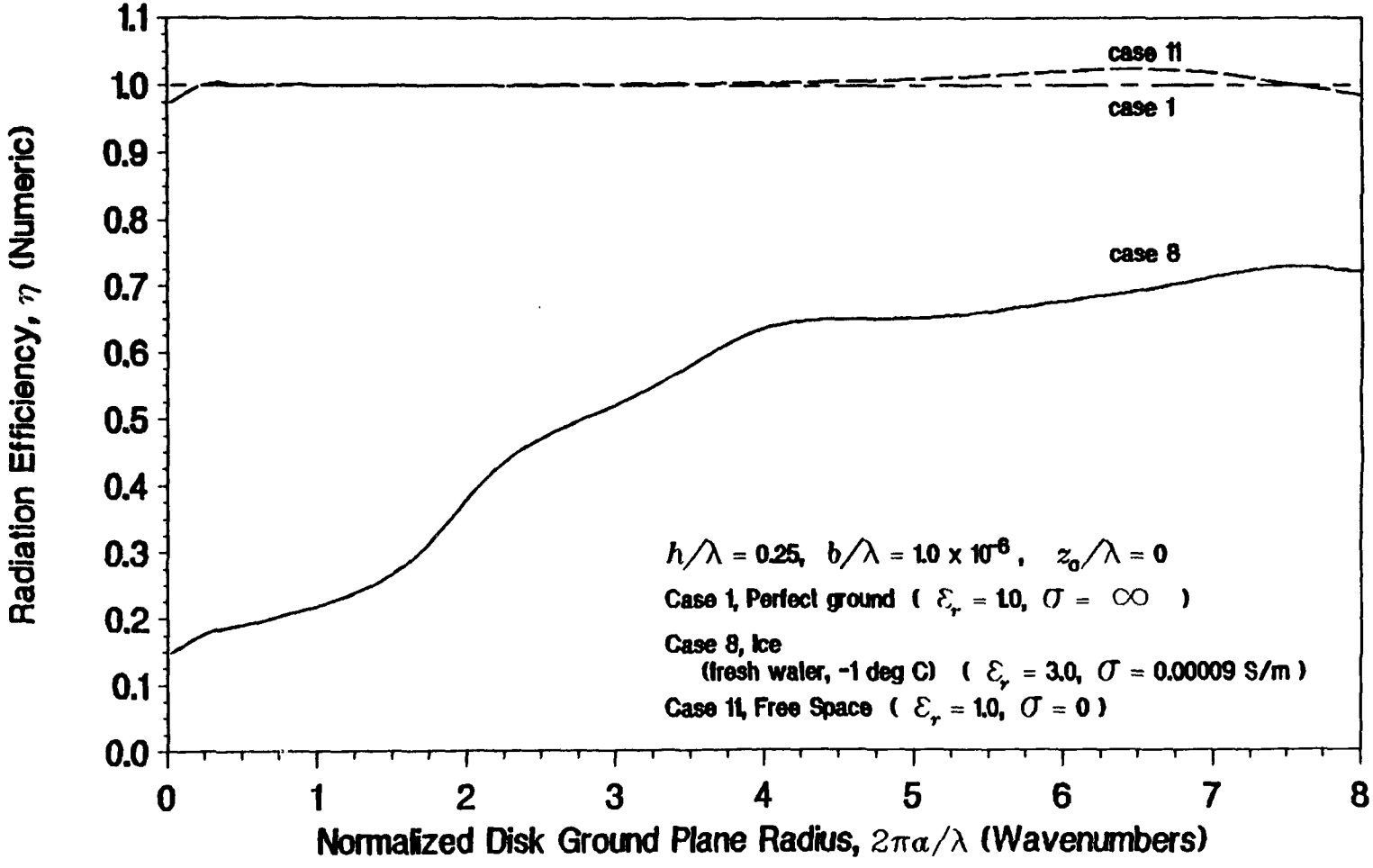

Figure 3-104. Radiation Efficiency, Ice (Fresh Water, -1°C)

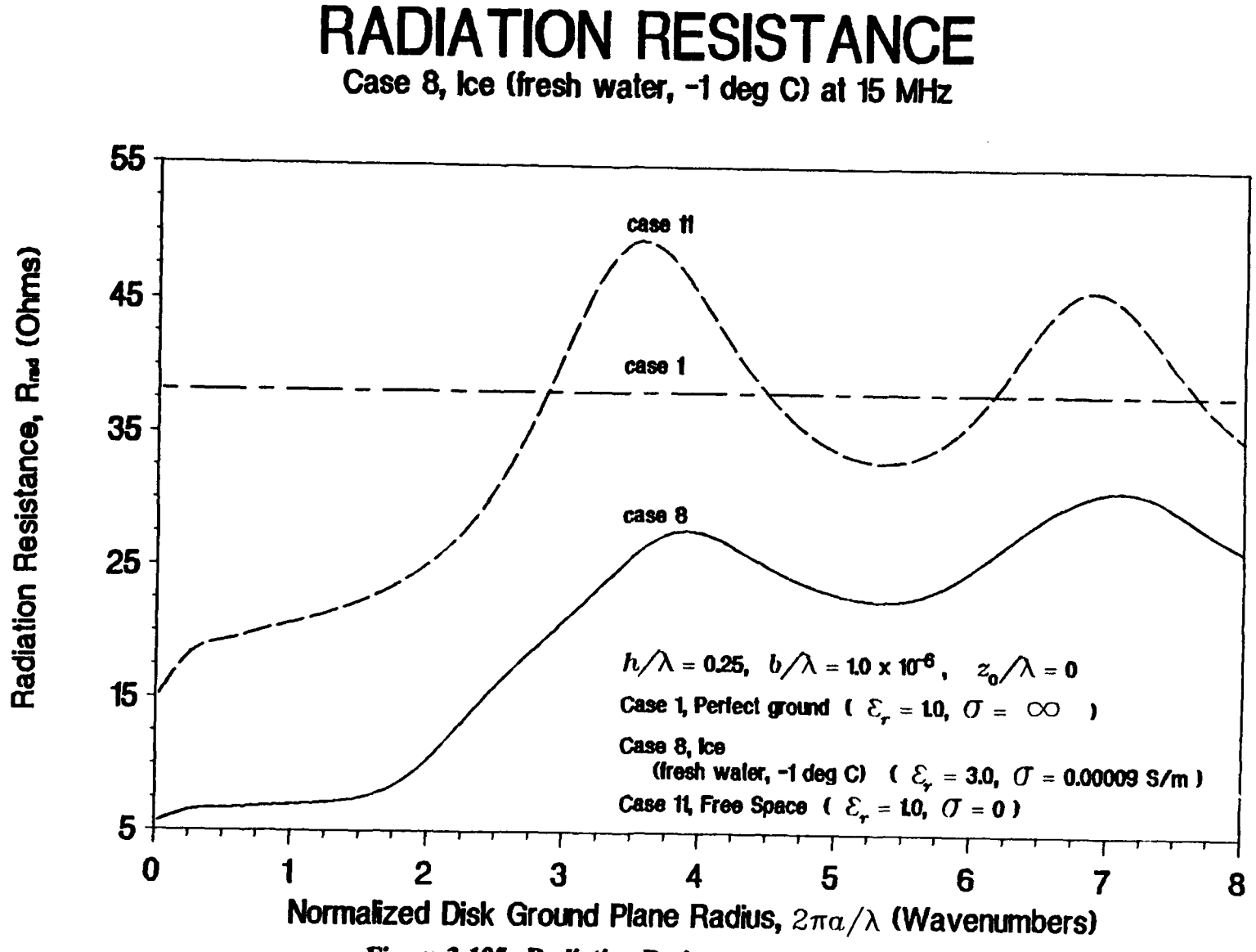

Figure 3-105. Radiation Resistance, Ice (Fresh Water, -1°C)

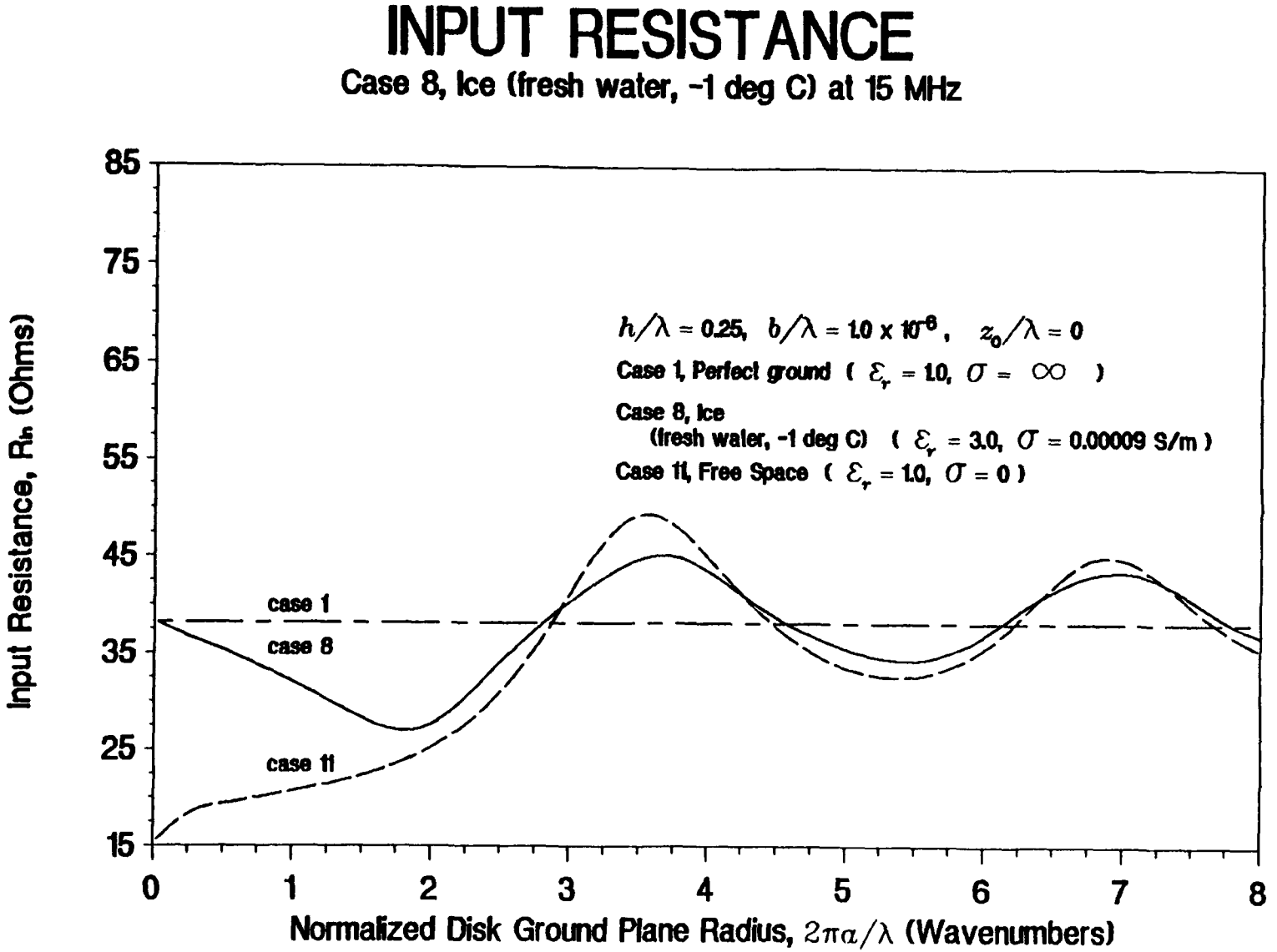

Figure 3-106. Input Resistance, Ice (Fresh Water, -1°C)

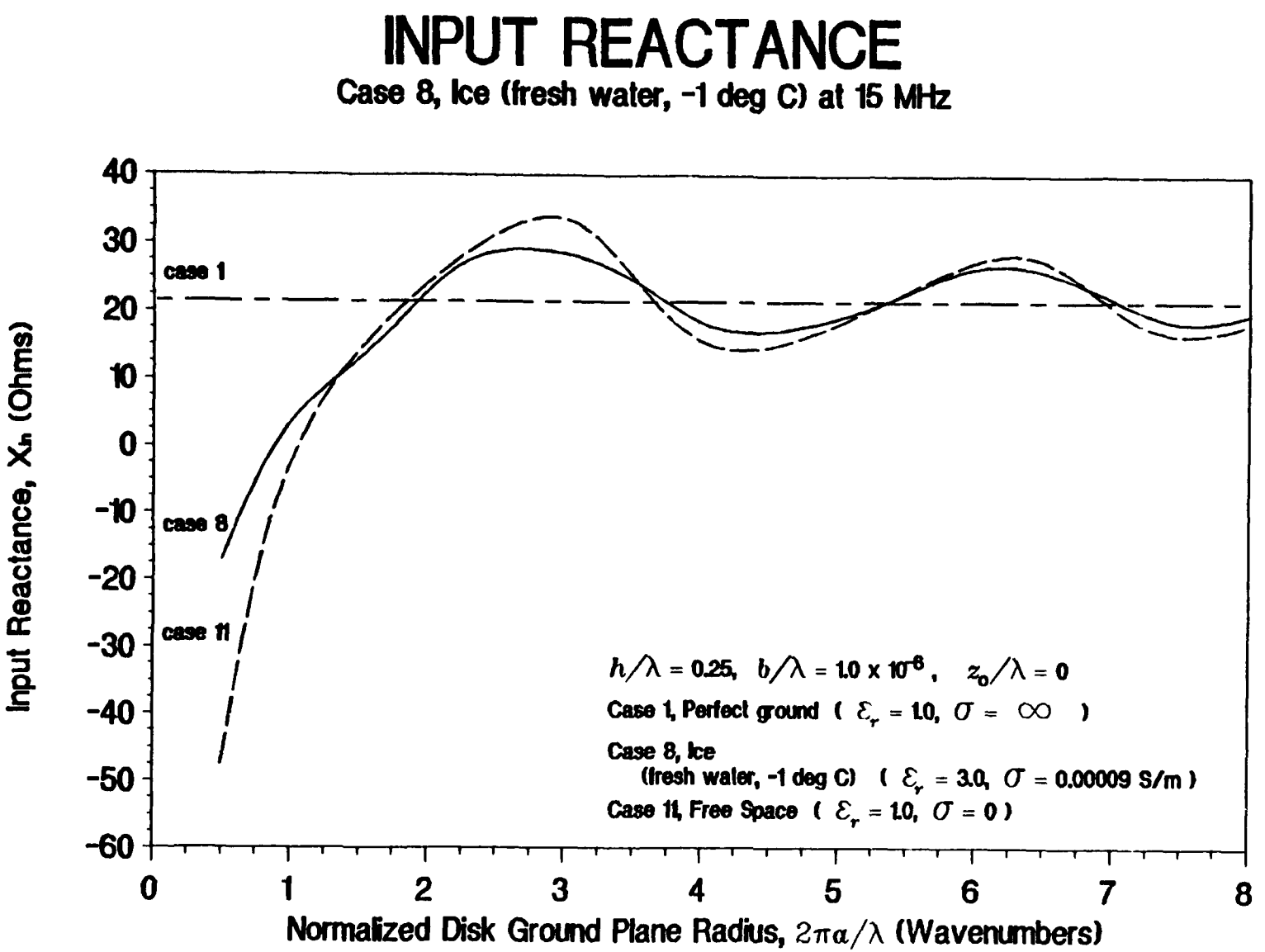

Figure 3-107. Input Reactance, Ice (Fresh Water, -1°C)

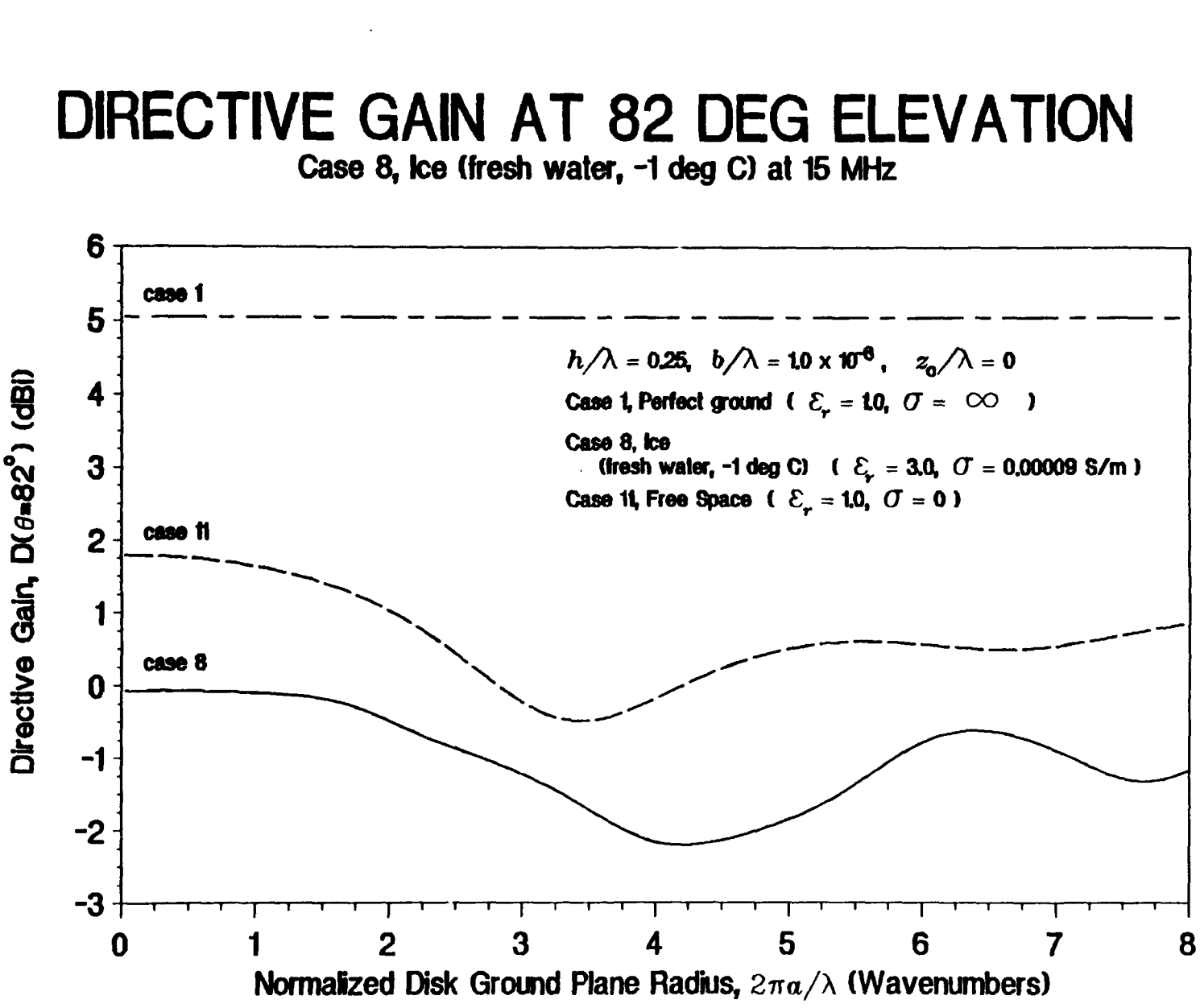

Figure 3-108. Directivity at 8 Degrees Above the Horizon, Ice (Fresh Water, -1°C)

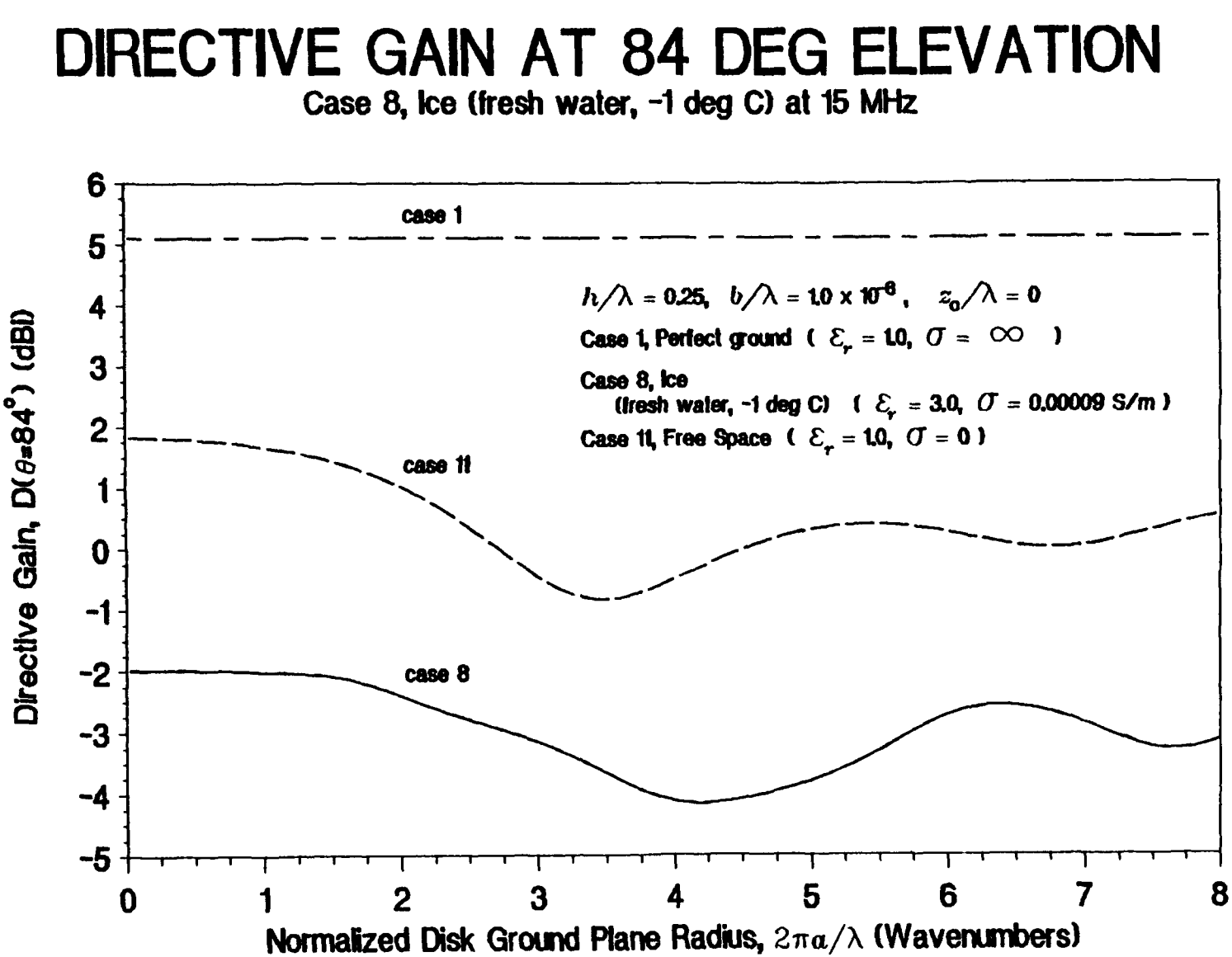

Figure 3-109. Directivity at 6 Degrees Above the Horizon, Ice (Fresh Water, -1°C)

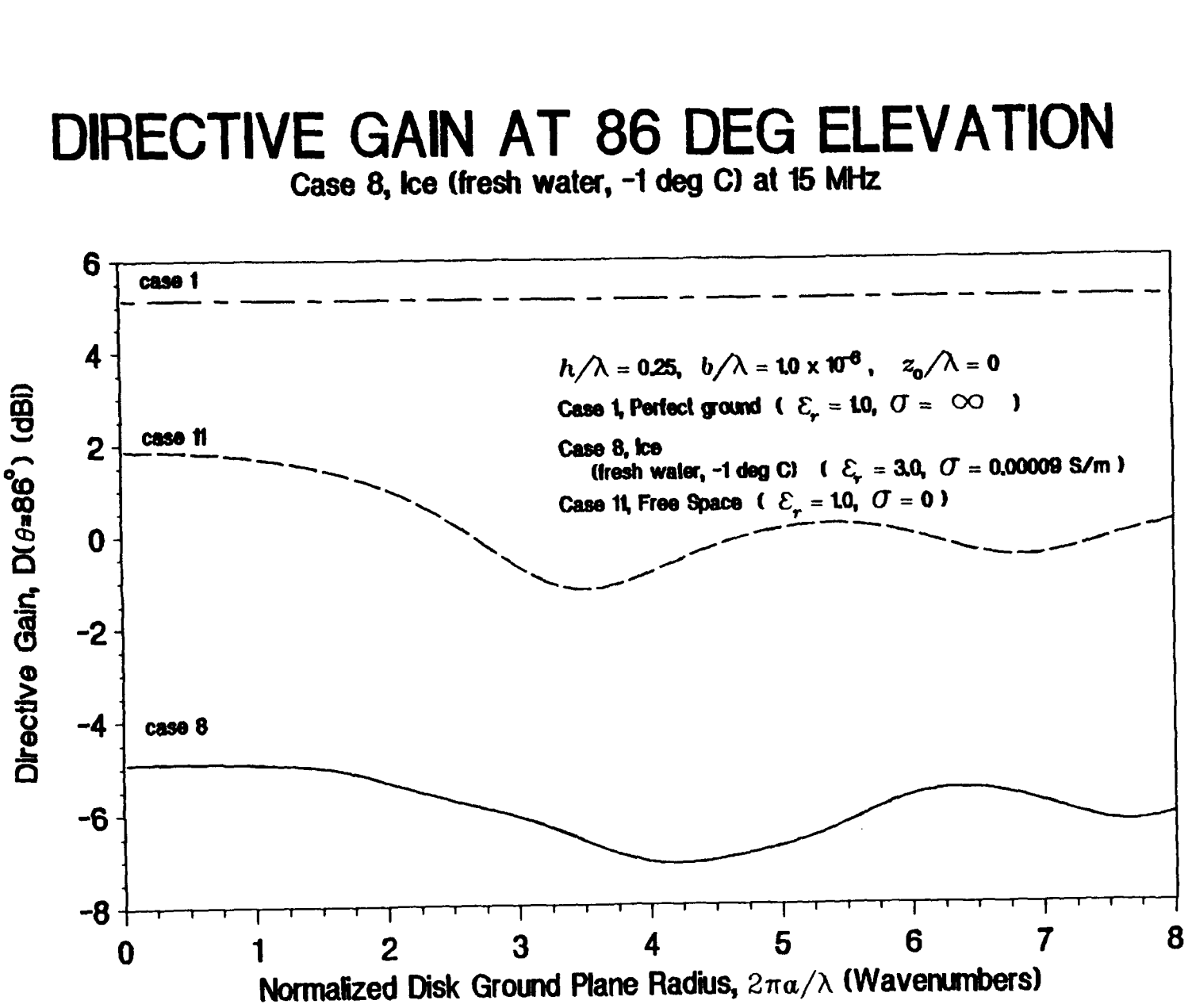

Figure 3-110. Directivity at 4 Degrees Above the Horizon, Ice (Fresh Water, -1°C)

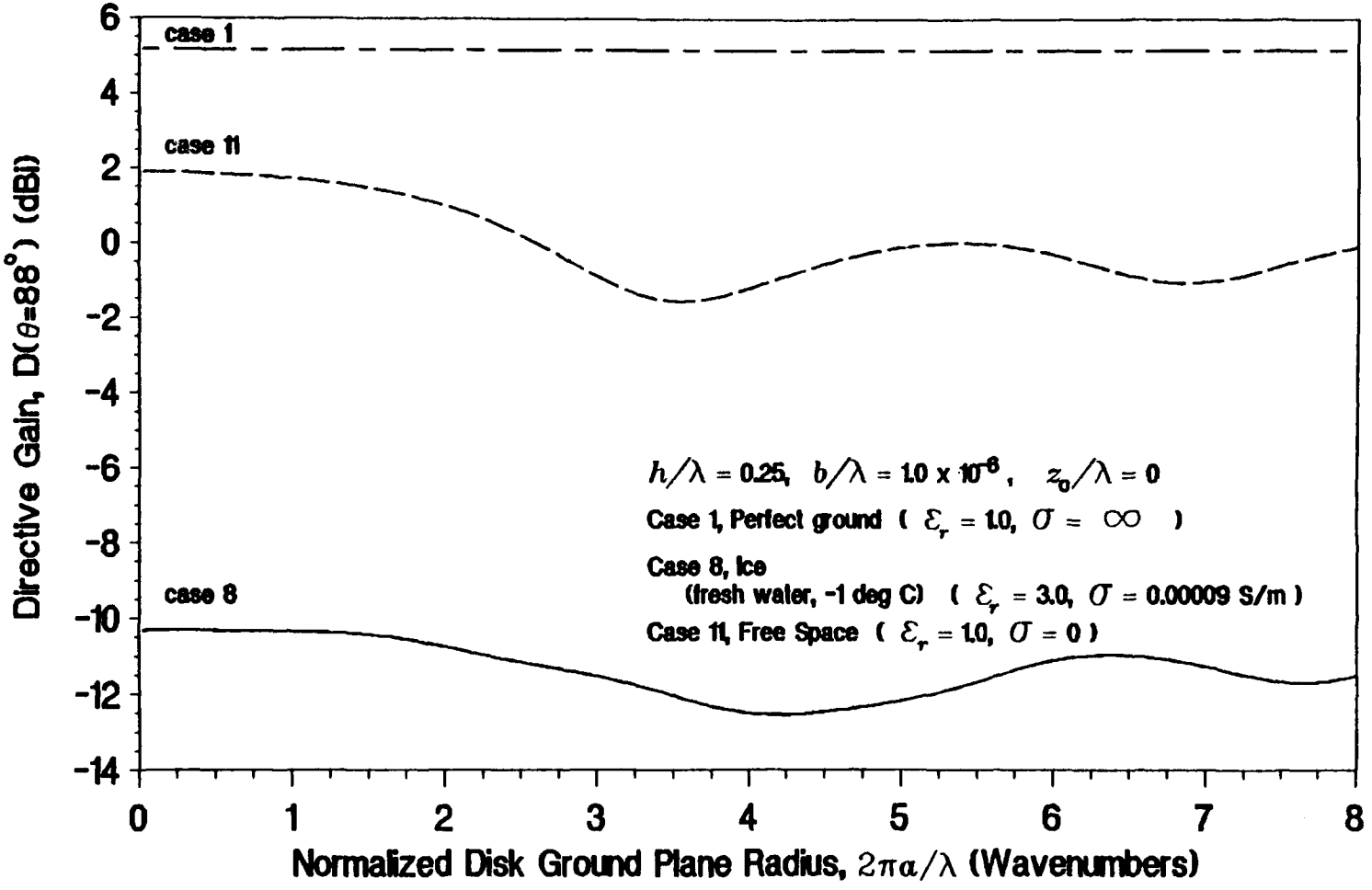

Figure 3-111. Directivity at 2 Degrees Above the Horizon, Ice (Fresh Water, -1°C)

DIRECTIVE GAIN ON THE HORIZON

Case 8, Ice (fresh water, -1 deg C) at 15 MHz

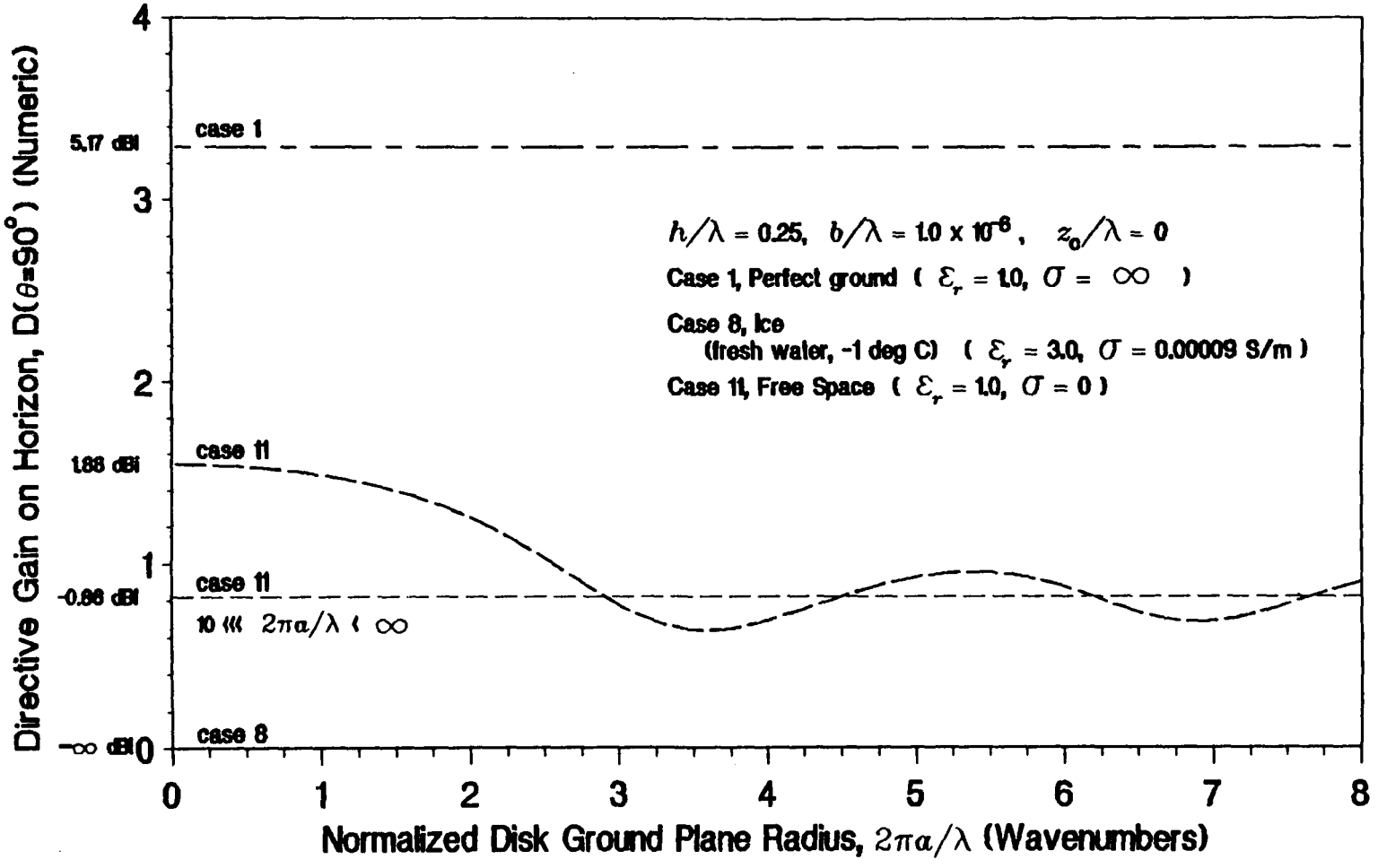

Figure 3-112. Directivity on the Horizon, Ice (Fresh Water, -1°C)

3.8 ICE (FRESH WATER, -10 °C)

NUMERIC DIRECTIVE GAIN POLAR PLOT

Case 9, Ice (fresh water, -10 deg C) at 15 MHz

$2\pi a/\lambda = 0.025$ **(Wavenumbers)**

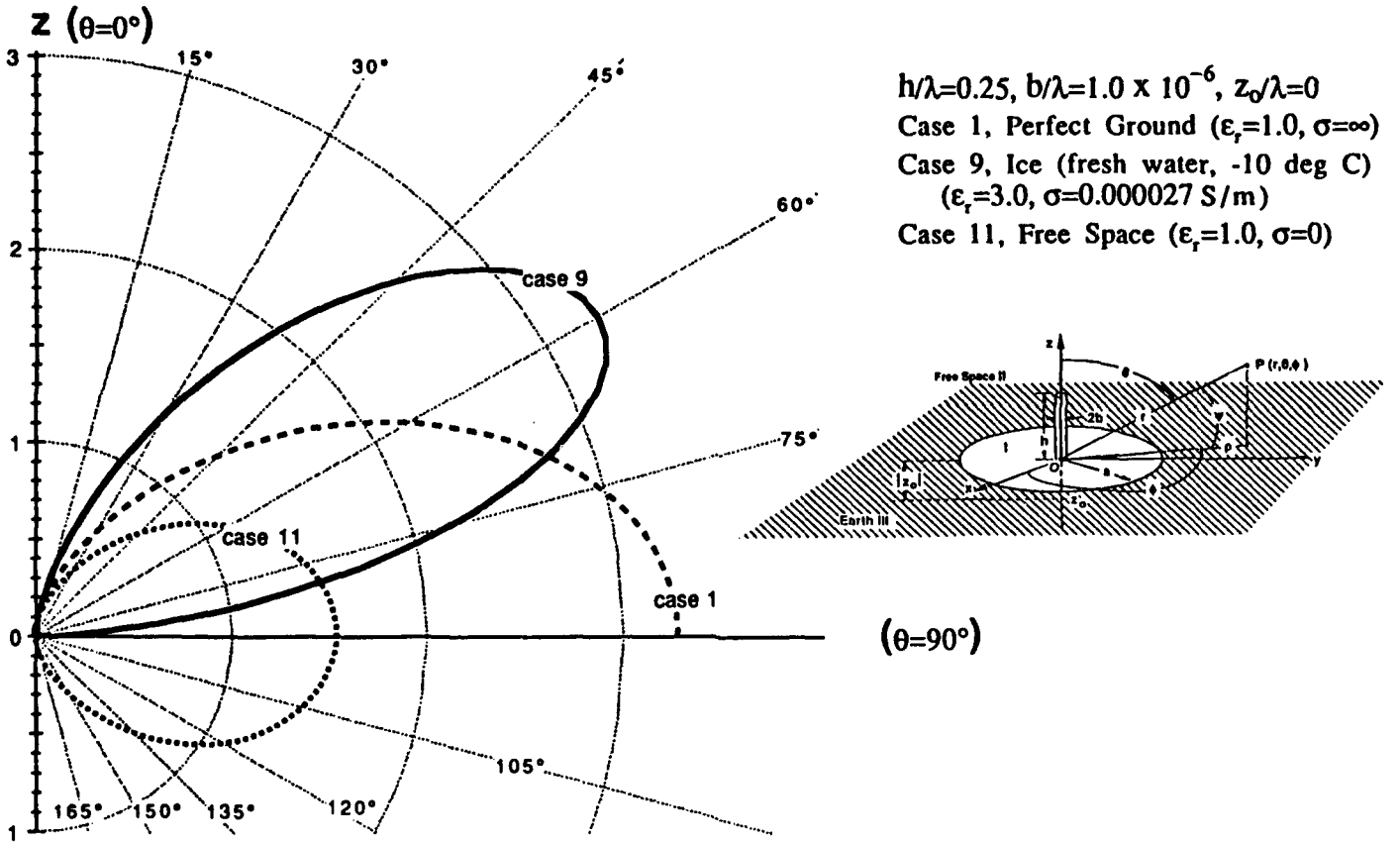

Figure 3-113. Directivity Pattern, $2\pi a/\lambda = 0.025$, Ice (Fresh Water, -10°C)

NUMERIC DIRECTIVE GAIN POLAR PLOT

Case 9, Ice (fresh water, -10 deg C) at 15 MHz

$2\pi a/\lambda =$ **3.0 (Wavenumbers)**

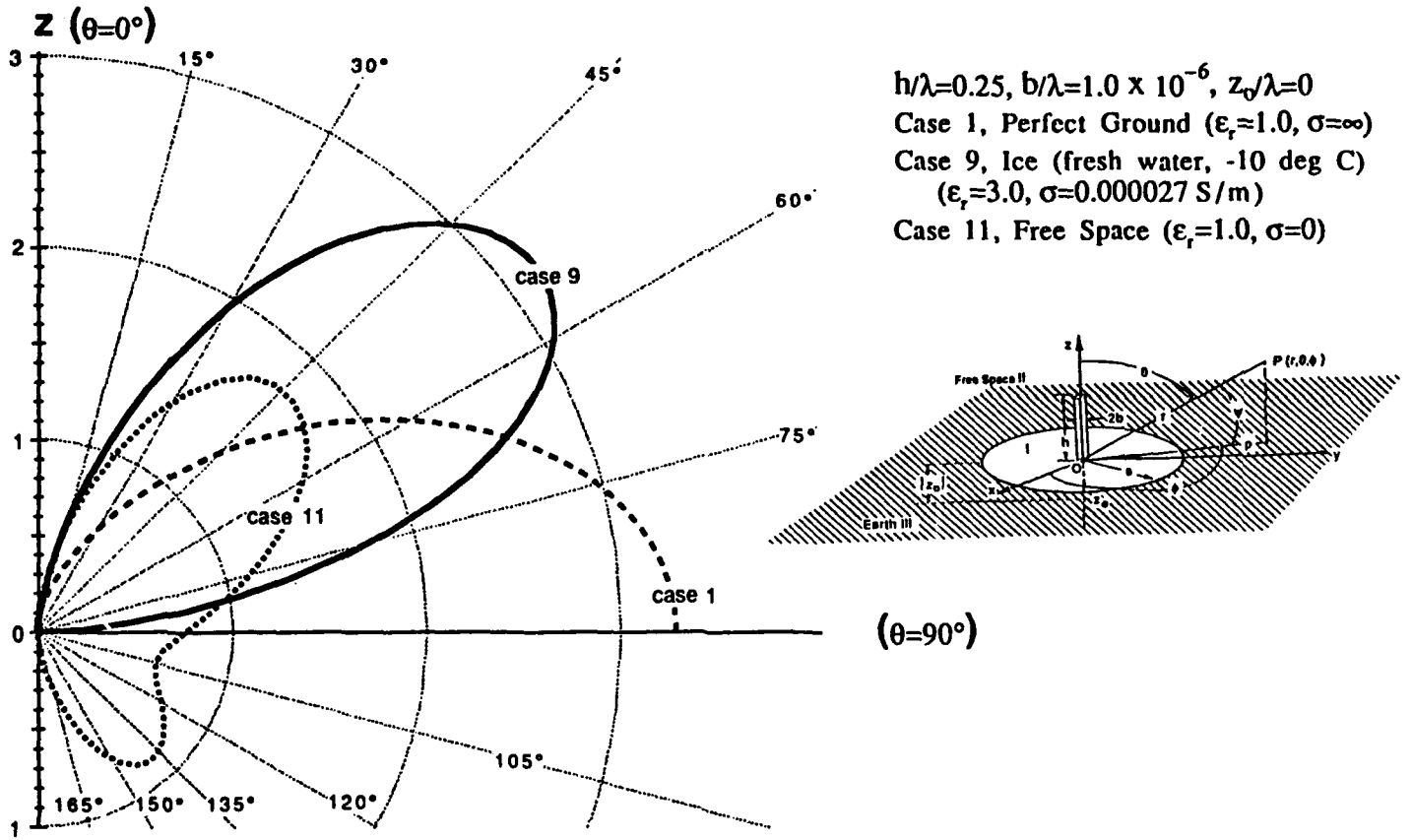

Figure 3-114. Directivity Pattern, $2\pi a/\lambda = 3.0$, Ice (Fresh Water, -10°C)

NUMERIC DIRECTIVE GAIN POLAR PLOT

Case 9, Ice (fresh water, -10 deg C) at 15 MHz

$2\pi a/\lambda =$ **4.0 (Wavenumbers)**

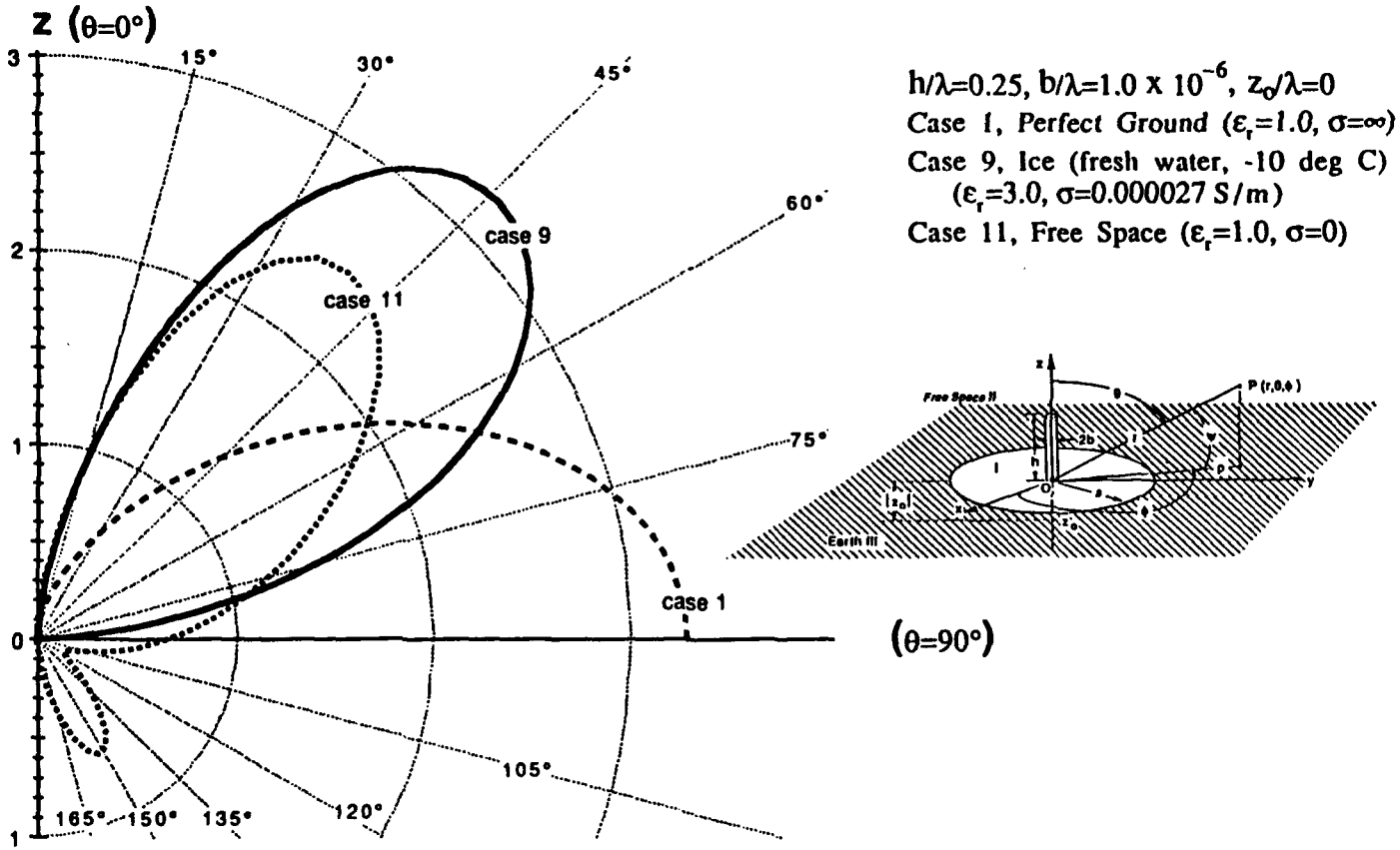

Figure 3-115. Directivity Pattern, $2\pi a/\lambda = 4.0$, Ice (Fresh Water, -10°C)

NUMERIC DIRECTIVE GAIN POLAR PLOT

Case 9, Ice (fresh water, -10 deg C) at 15 MHz

$2\pi a/\lambda =$ **5.0 (Wavenumbers)**

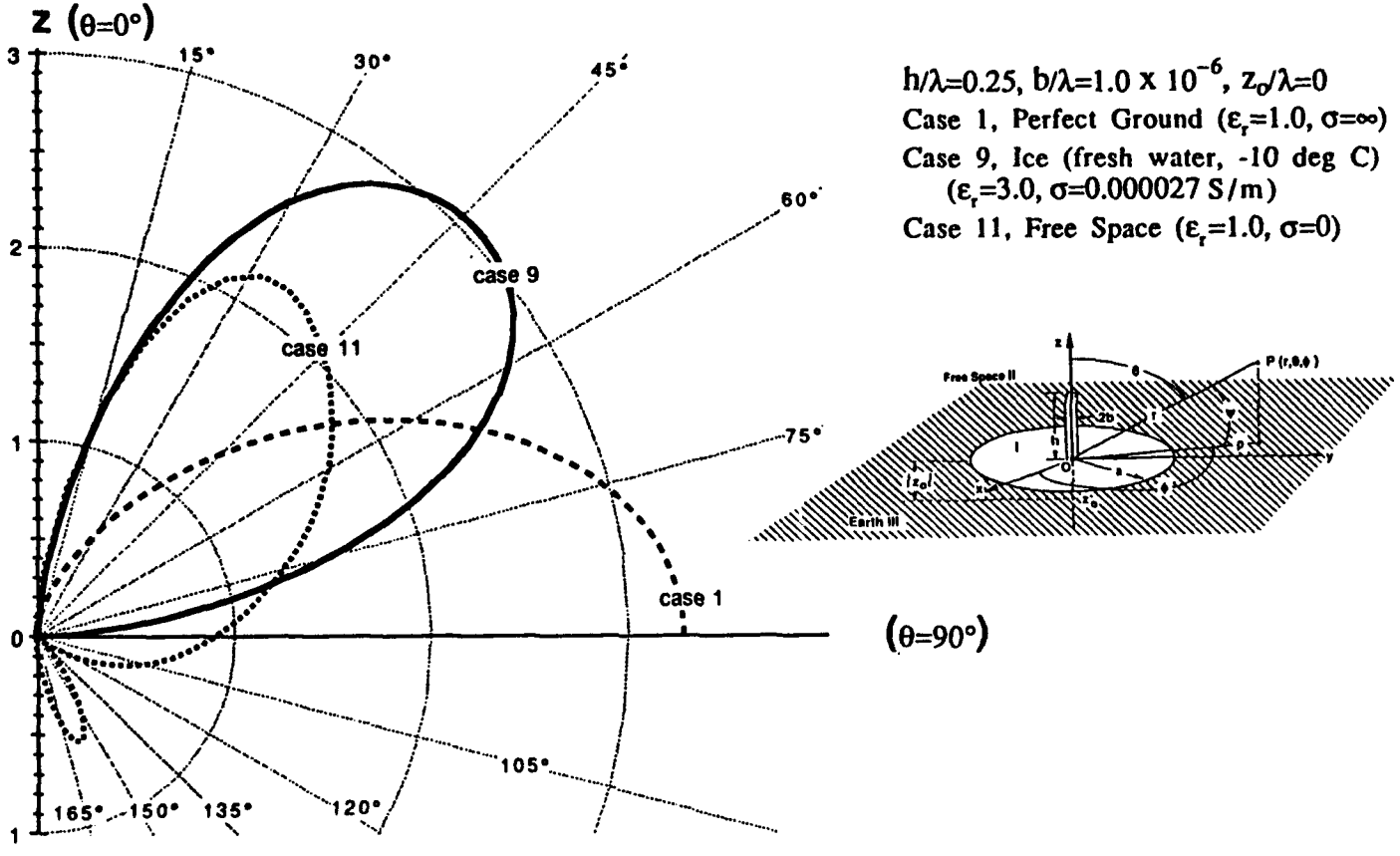

Figure 3-116. Directivity Pattern, $2\pi a/\lambda = 5.0$, Ice (Fresh Water, -10°C)

NUMERIC DIRECTIVE GAIN POLAR PLOT

Case 9, Ice (fresh water, -10 deg C) at 15 MHz

$2\pi a/\lambda =$ **6.5 (Wavenumbers)**

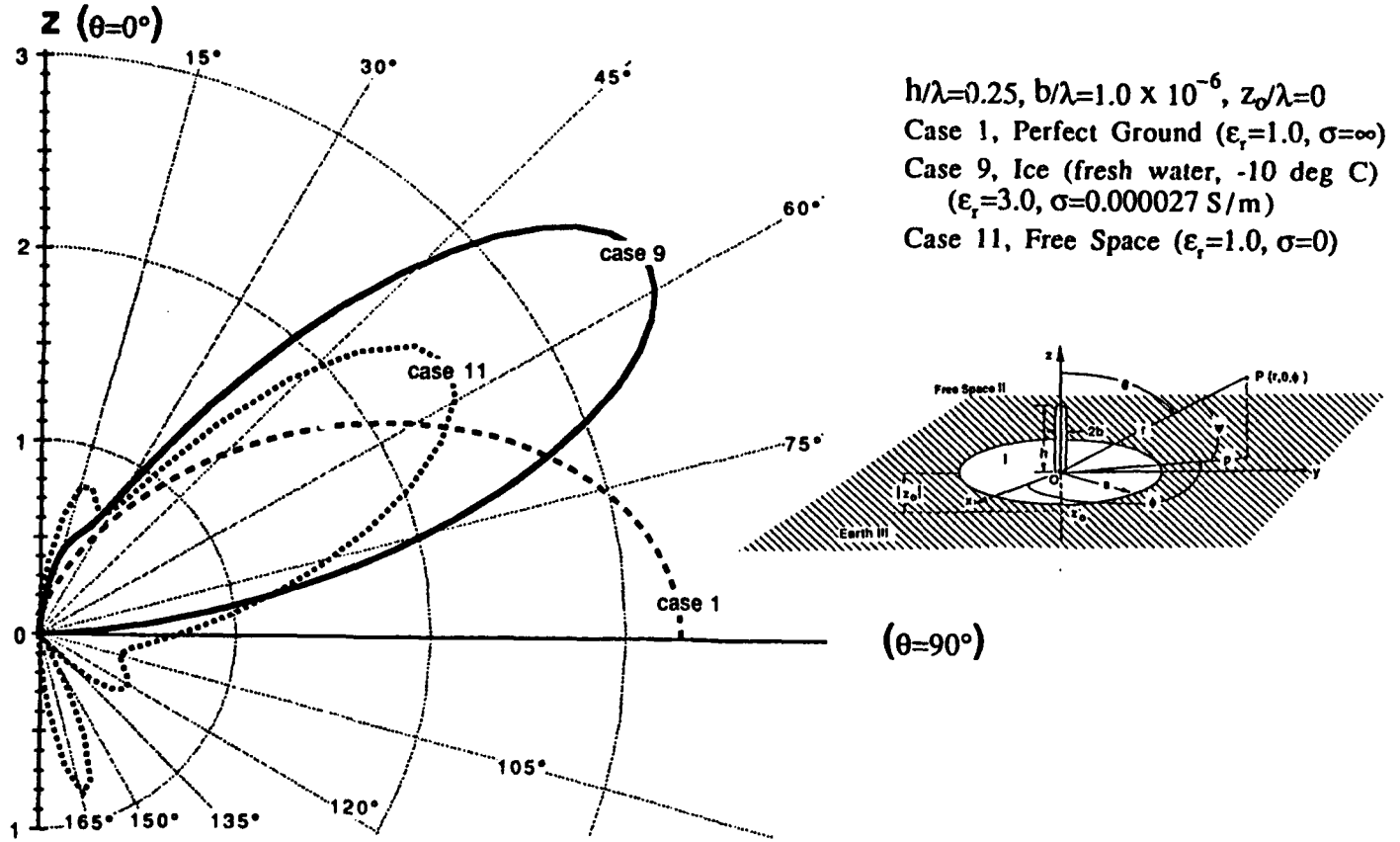

Figure 3-117. Directivity Pattern, $2\pi a/\lambda = 6.5$, Ice (Fresh Water, -10°C)

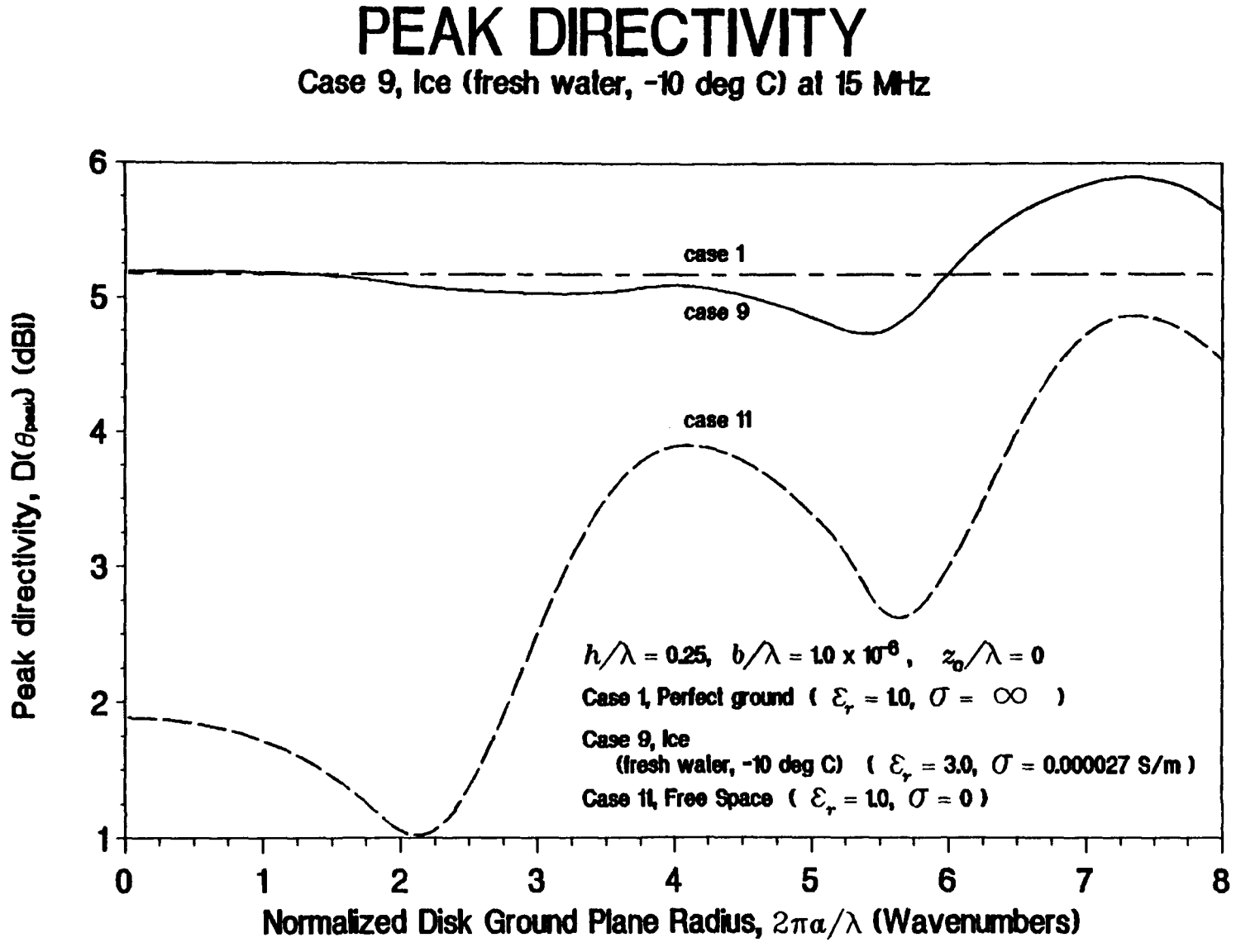

Figure 3-118. Peak Directivity, Ice (Fresh Water, -10°C)

ANGLE OF PEAK DIRECTIVITY

Case 9, Ice (fresh water, -10 deg C) at 15 MHz

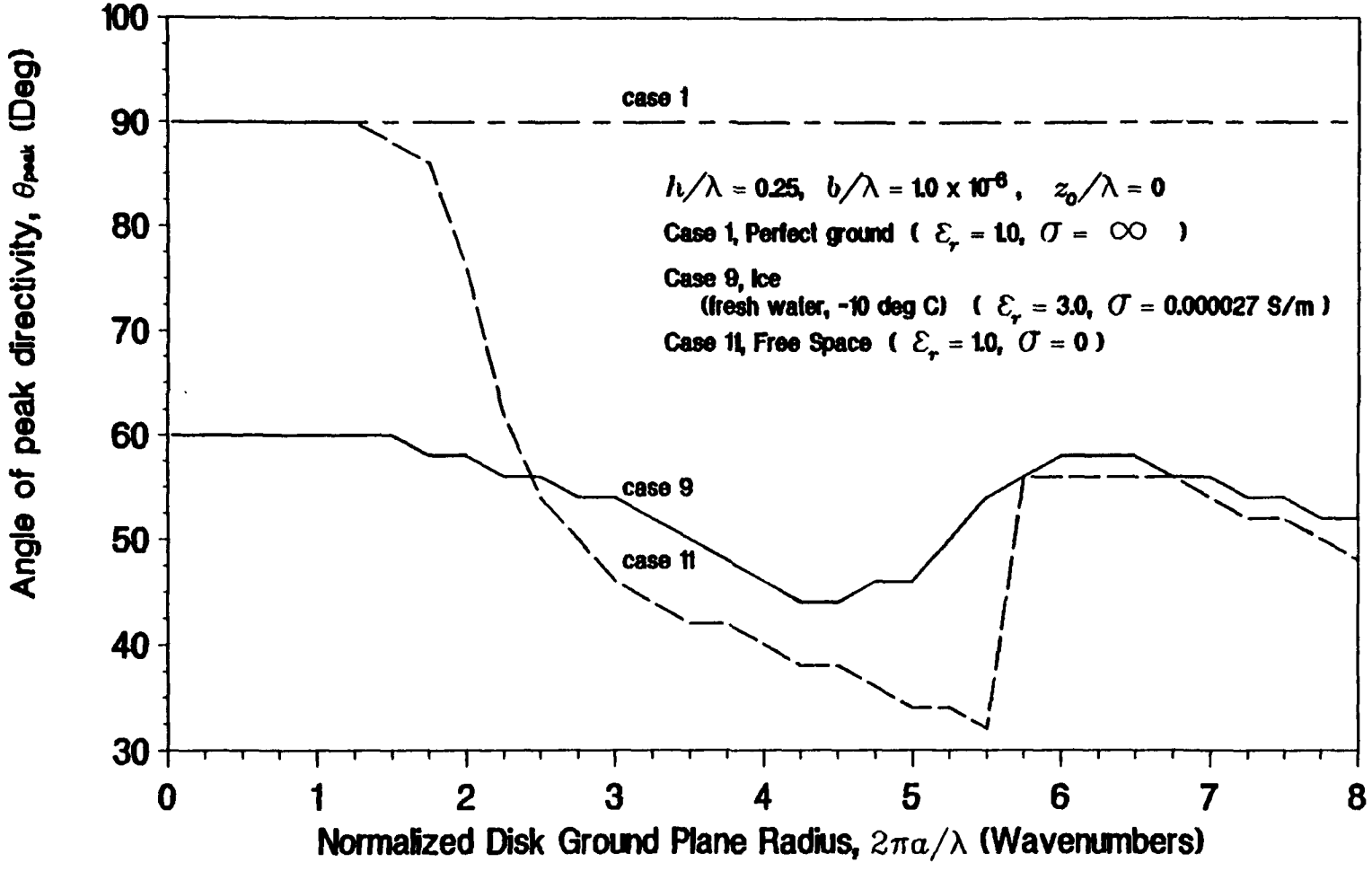

Figure 3-119. Angle of Incidence of Peak Directivity, Ice (Fresh Water, -10°C)

RADIATION EFFICIENCY

Case 9, Ice (fresh water, -10 deg C) at 15 MHz

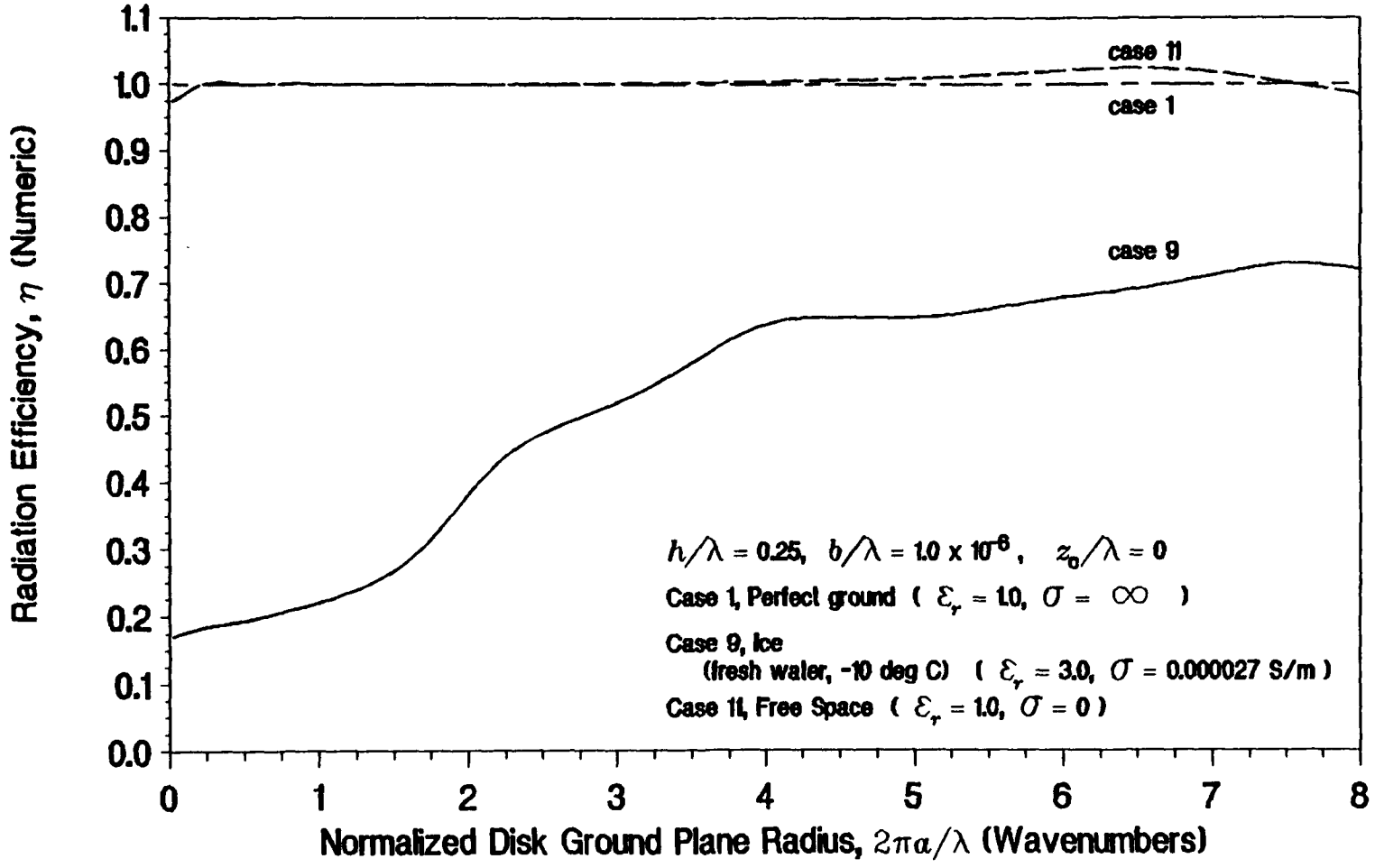

Figure 3-120. Radiation Efficiency, Ice (Fresh Water, -10°C)

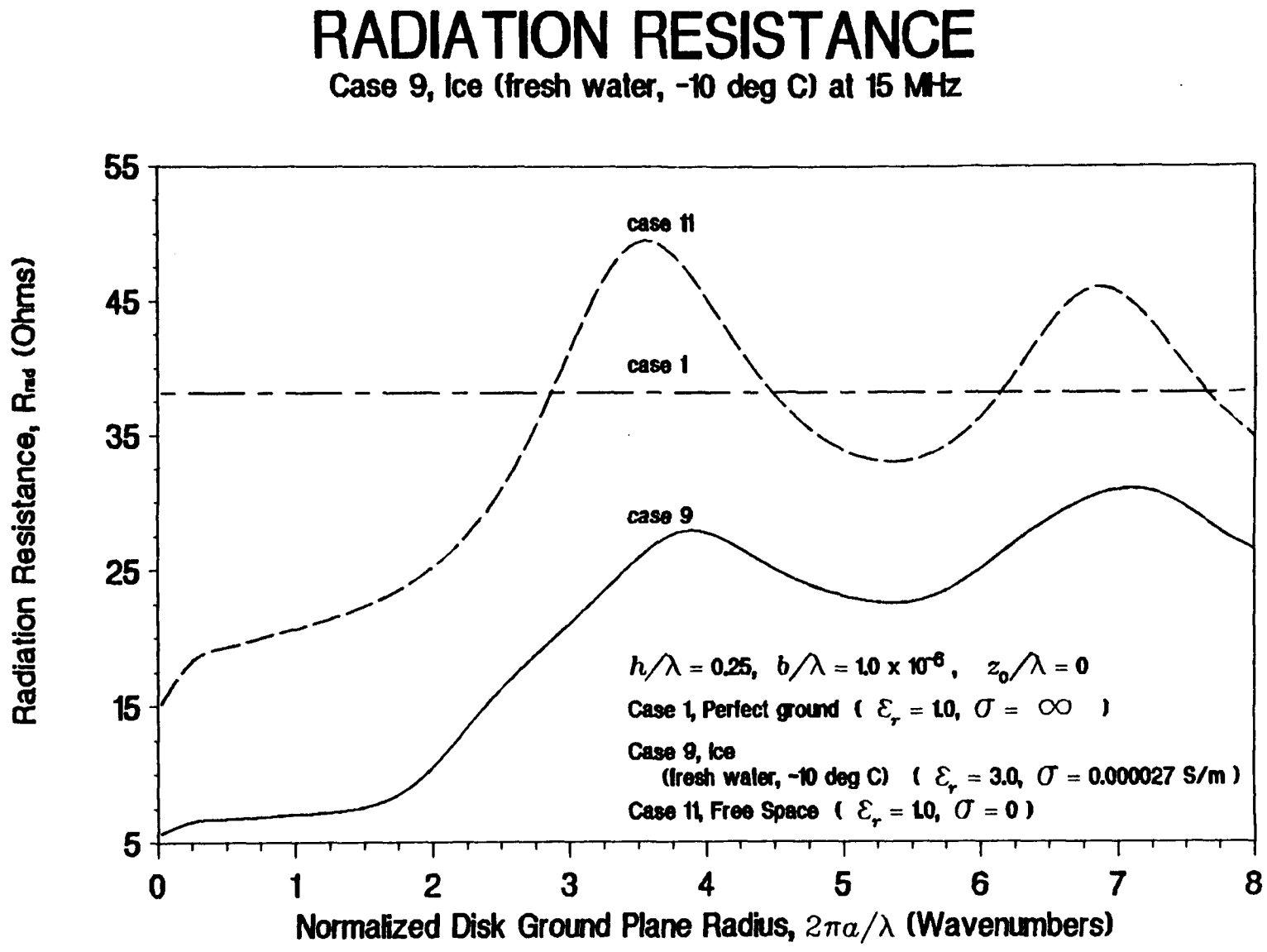

Figure 3-121. Radiation Resistance, Ice (Fresh Water, -10°C)

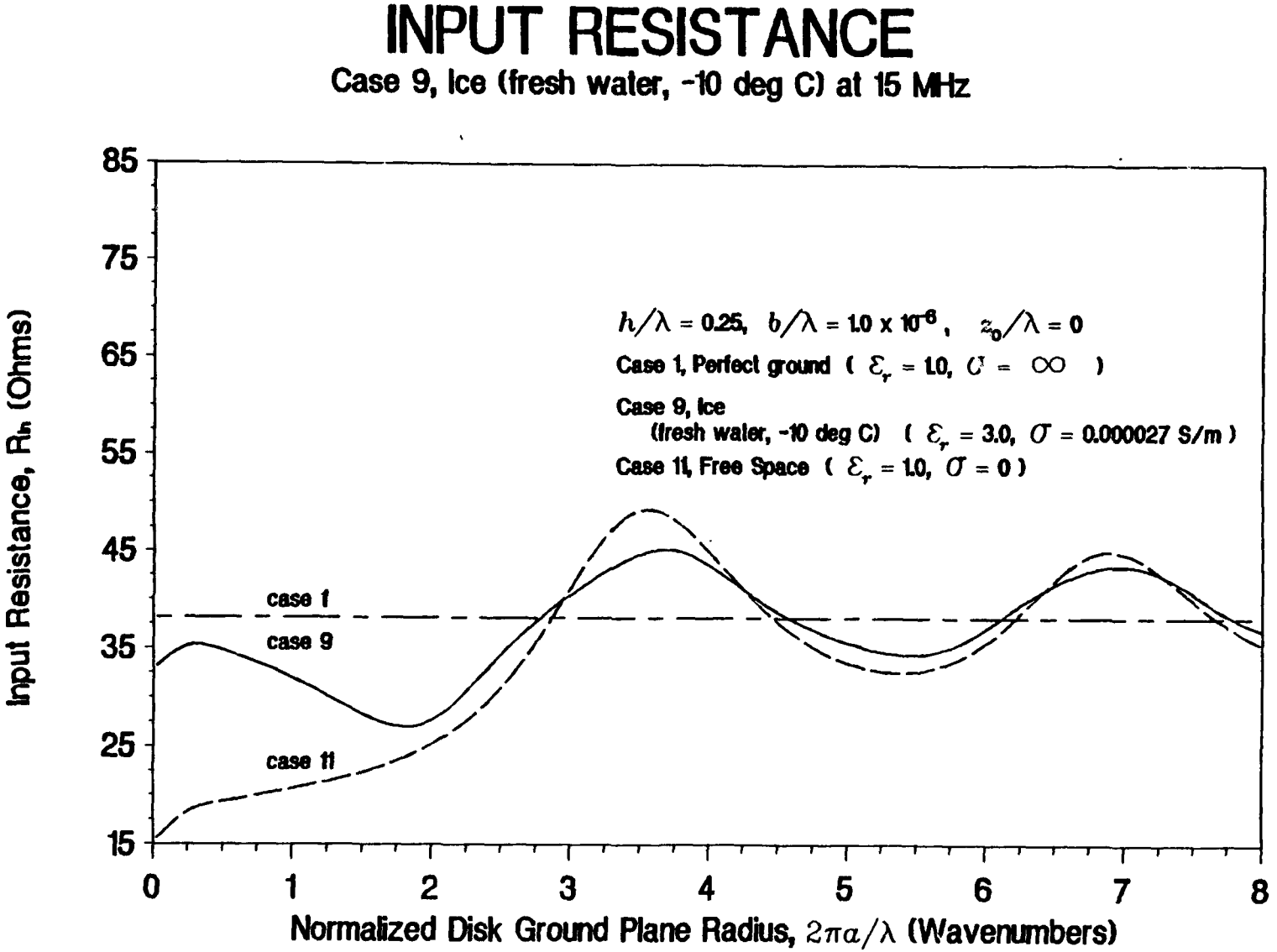

Figure 3-122. Input Resistance, Ice (Fresh Water, -10°C)

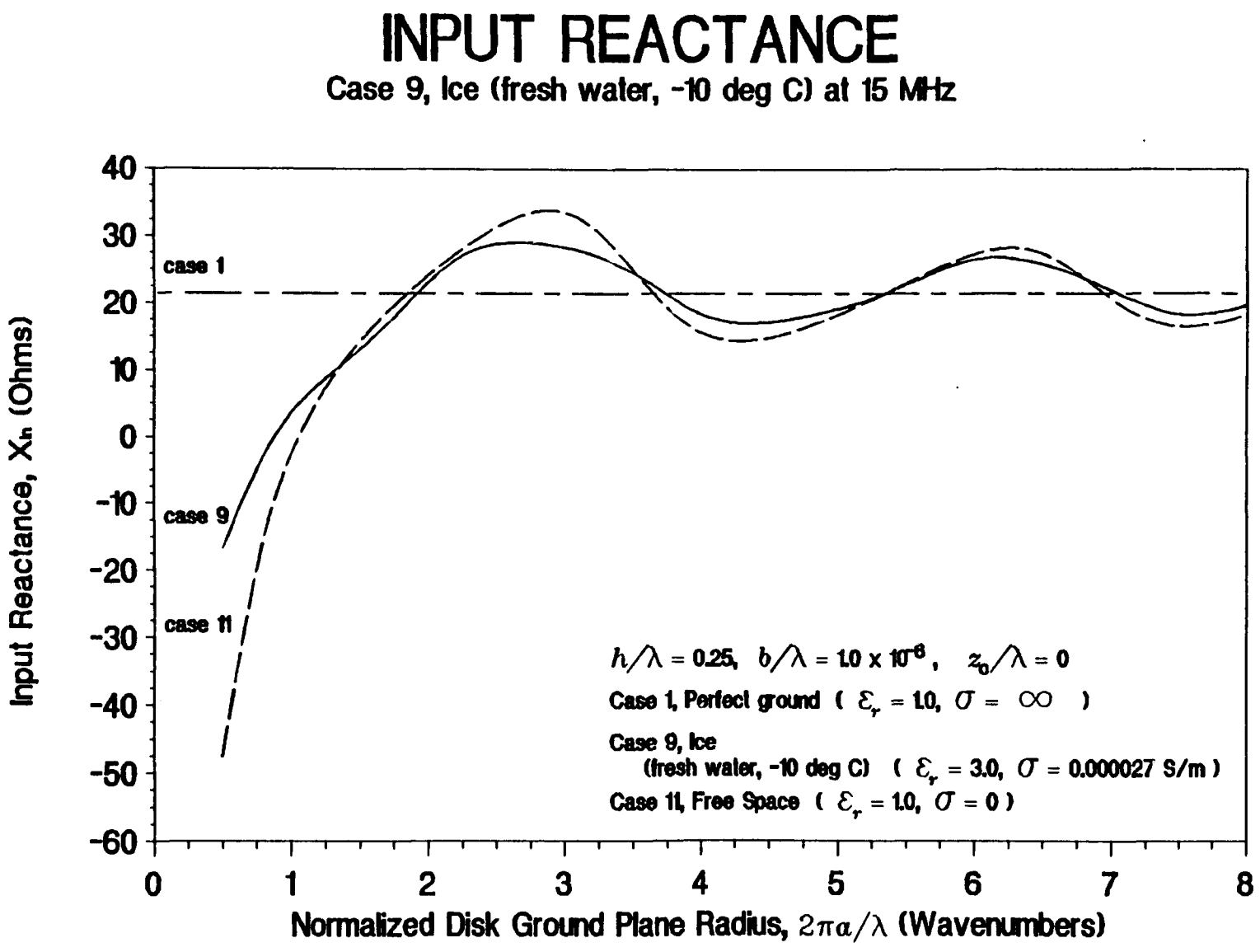

Figure 3-123. Input Reactance, Ice (Fresh Water, -10°C)

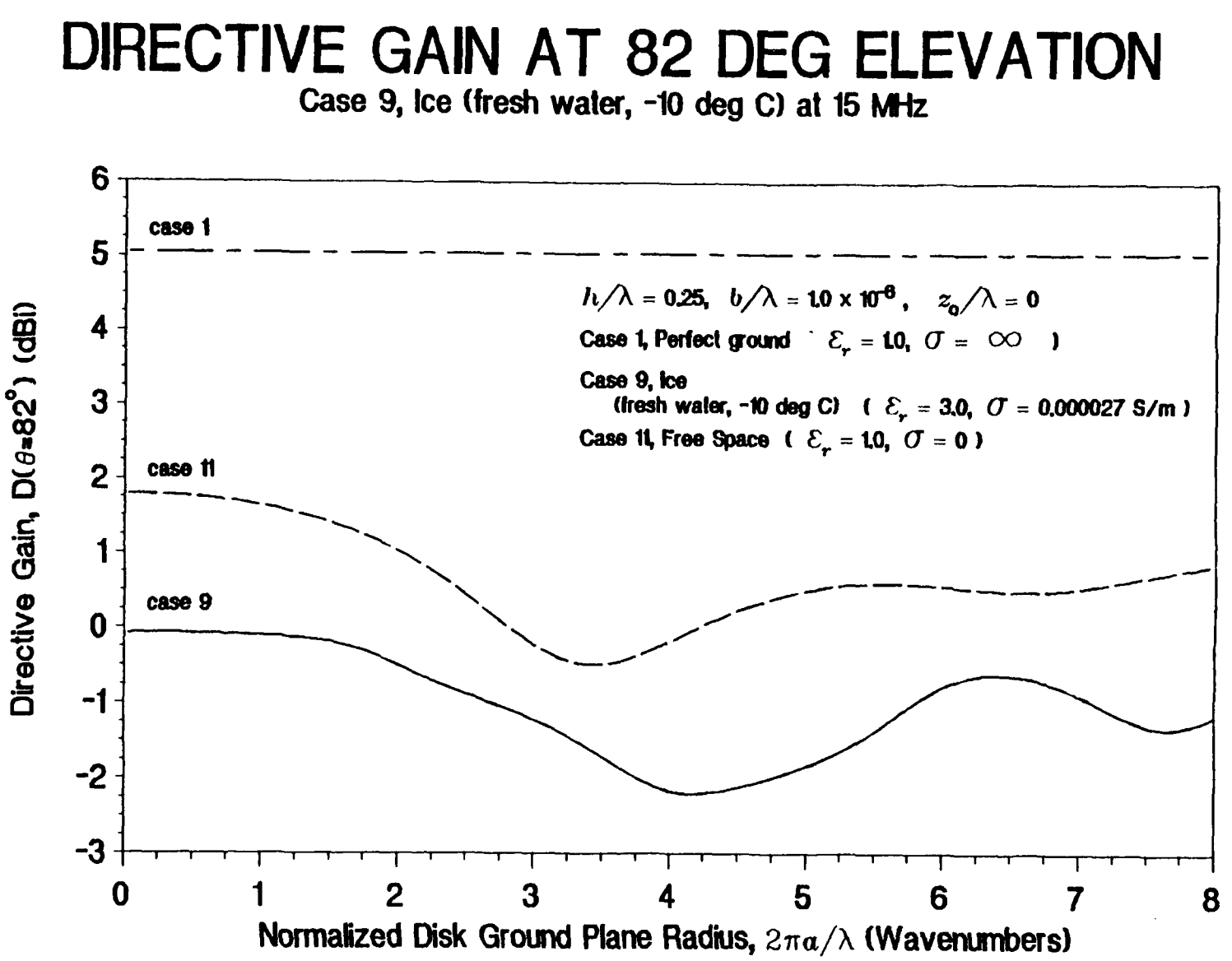

Figure 3-124. Directivity at 8 Degrees Above the Horizon, Ice (Fresh Water, -10°C)

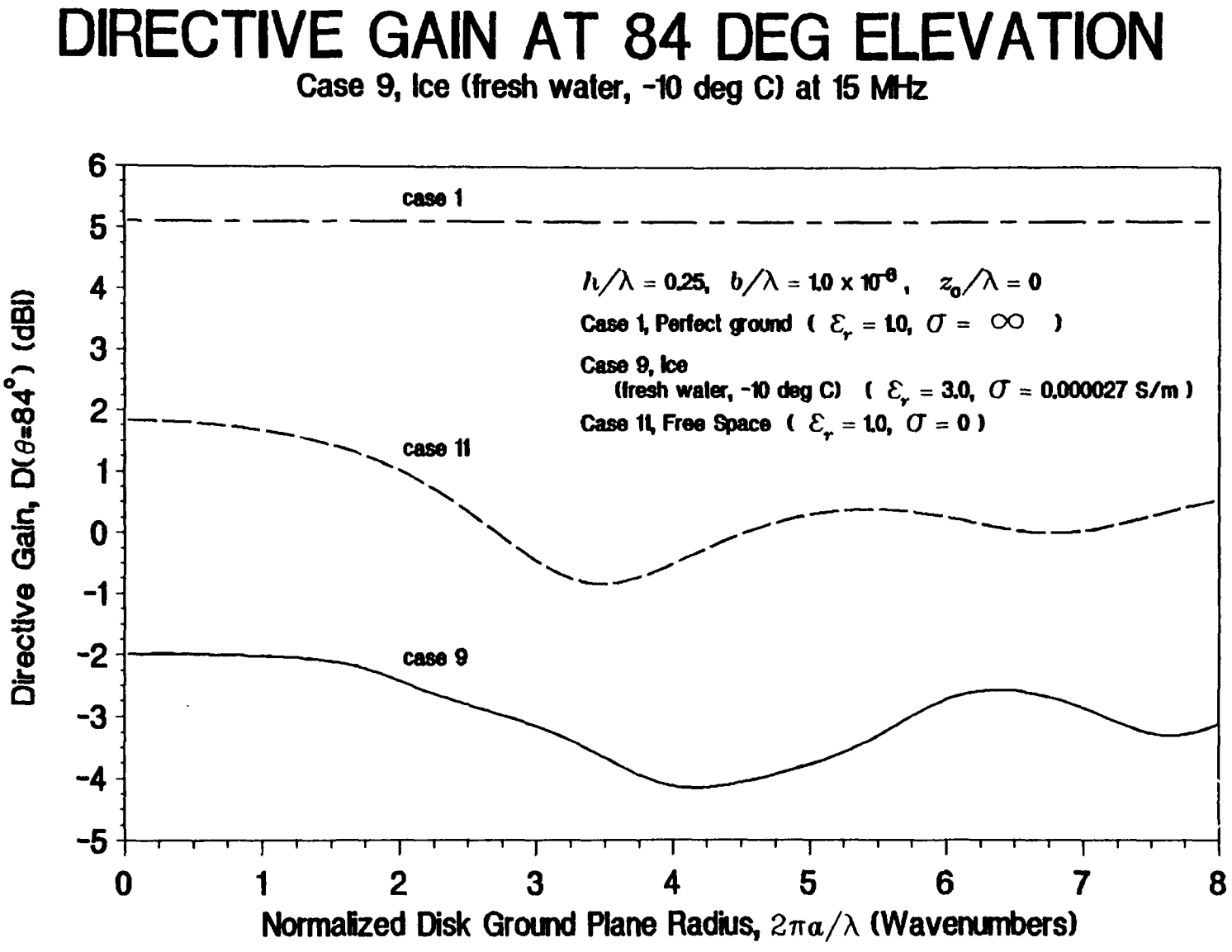

Figure 3-125. Directivity at 6 Degrees Above the Horizon, Ice (Fresh Water, -10°C)

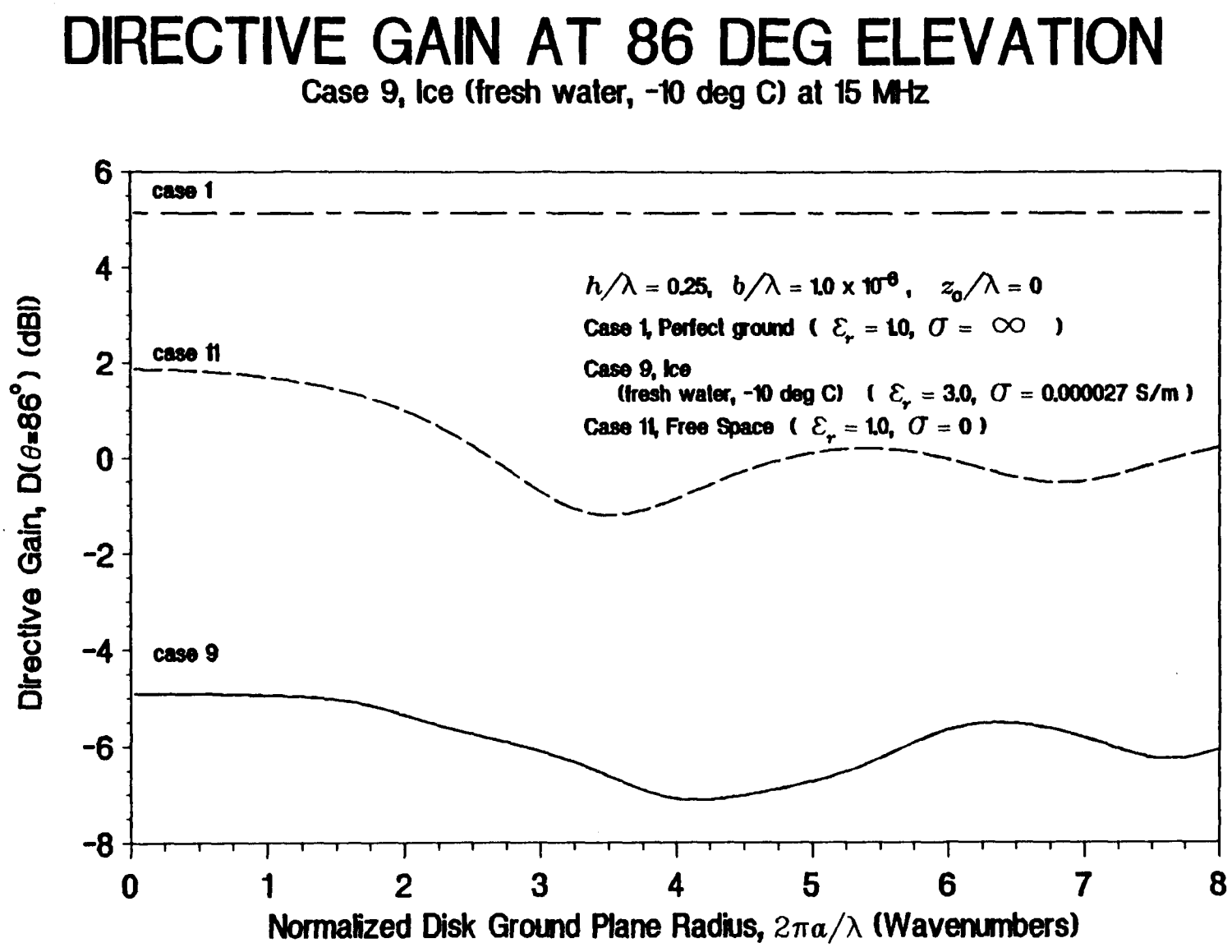

Figure 3-126. Directivity at 4 Degrees Above the Horizon, Ice (Fresh Water, -10°C)

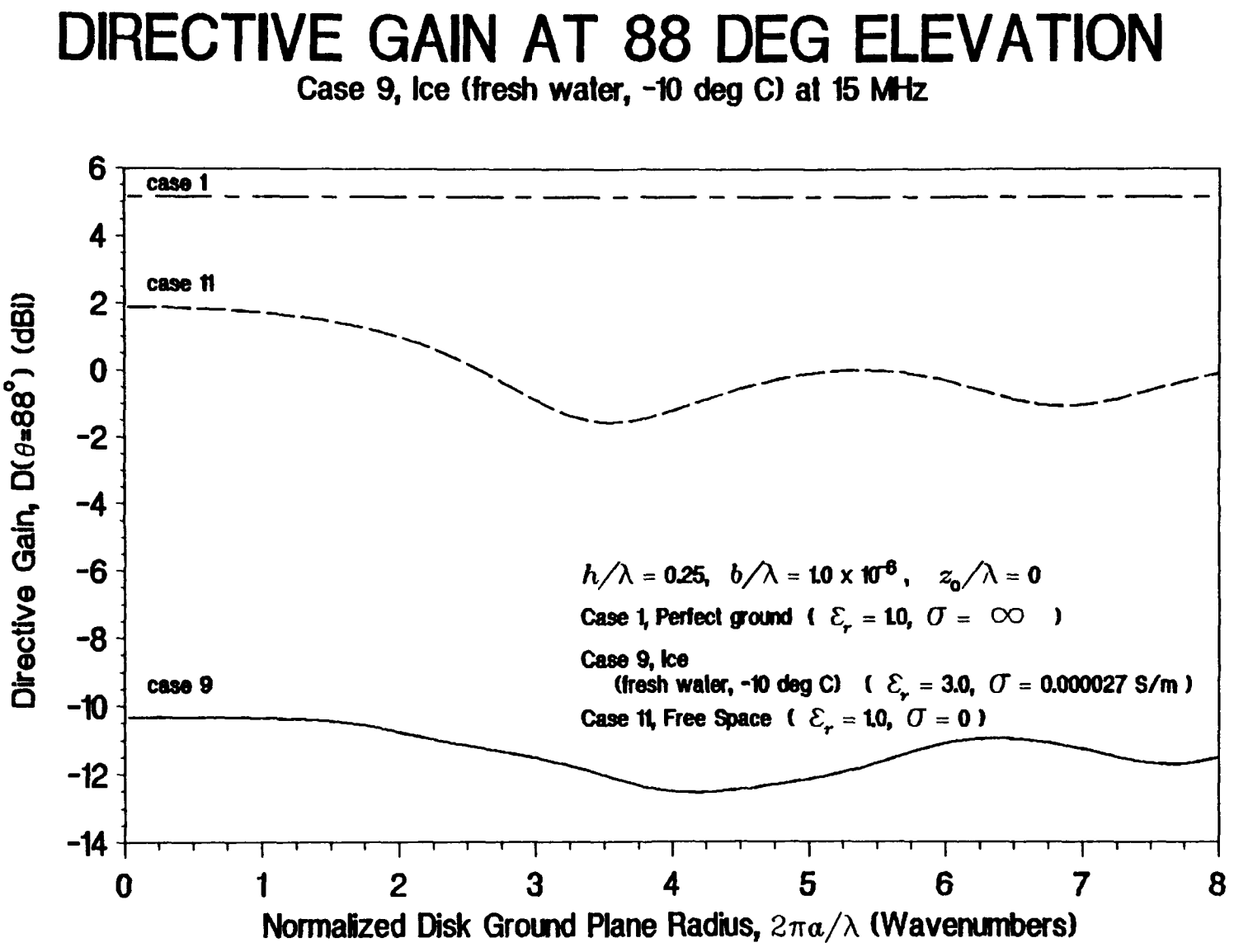

Figure 3-127. Directivity at 2 Degrees Above the Horizon, Ice (Fresh Water, -10°C)

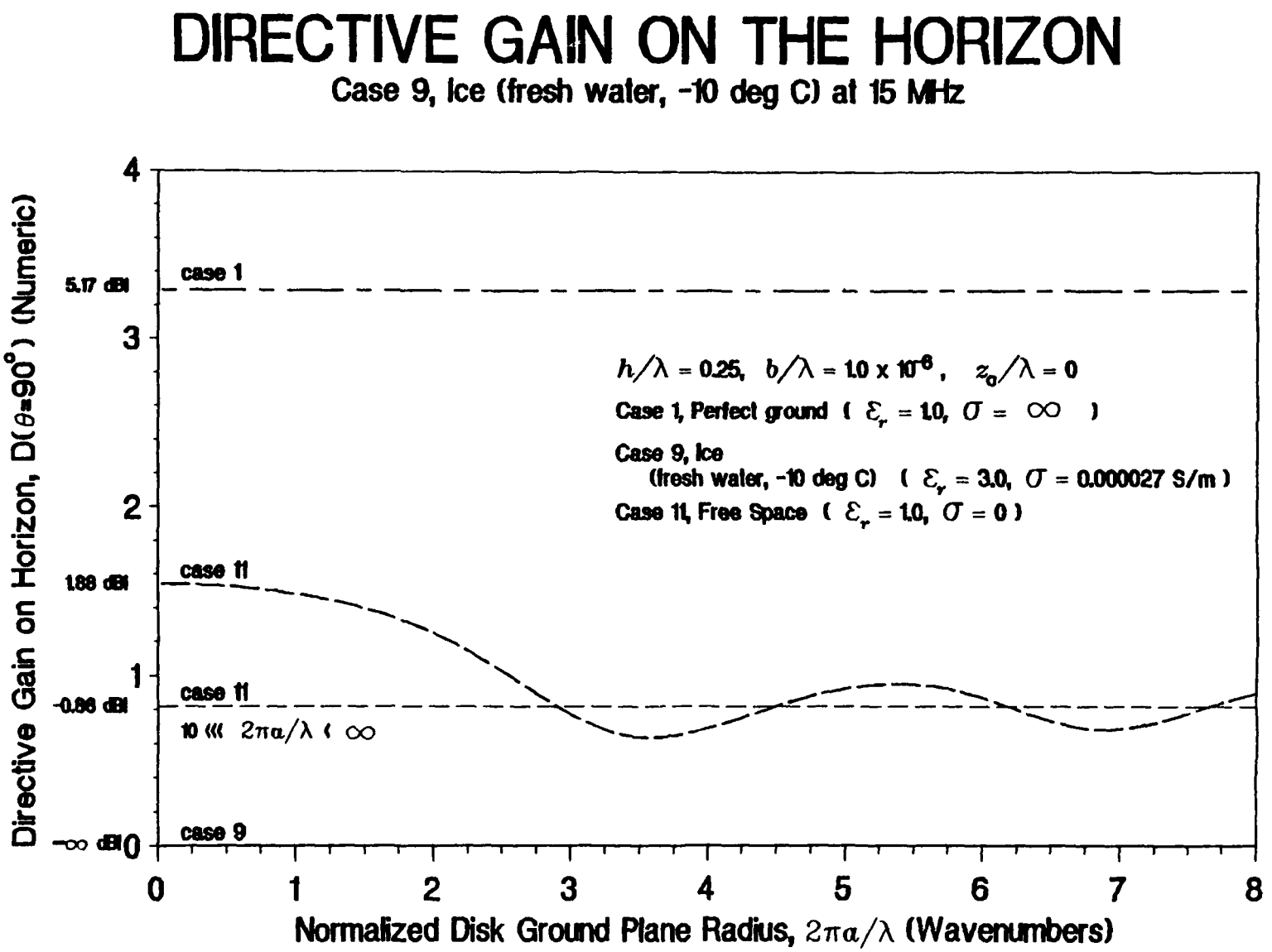

Figure 3-128. Directivity on the Horizon, Ice (Fresh Water, -10°C)

3.9 AVERAGE LAND

NUMERIC DIRECTIVE GAIN POLAR PLOT

Case10, Average Land at 15 MHz

$2\pi a/\lambda = 0.025$ **(Wavenumbers)**

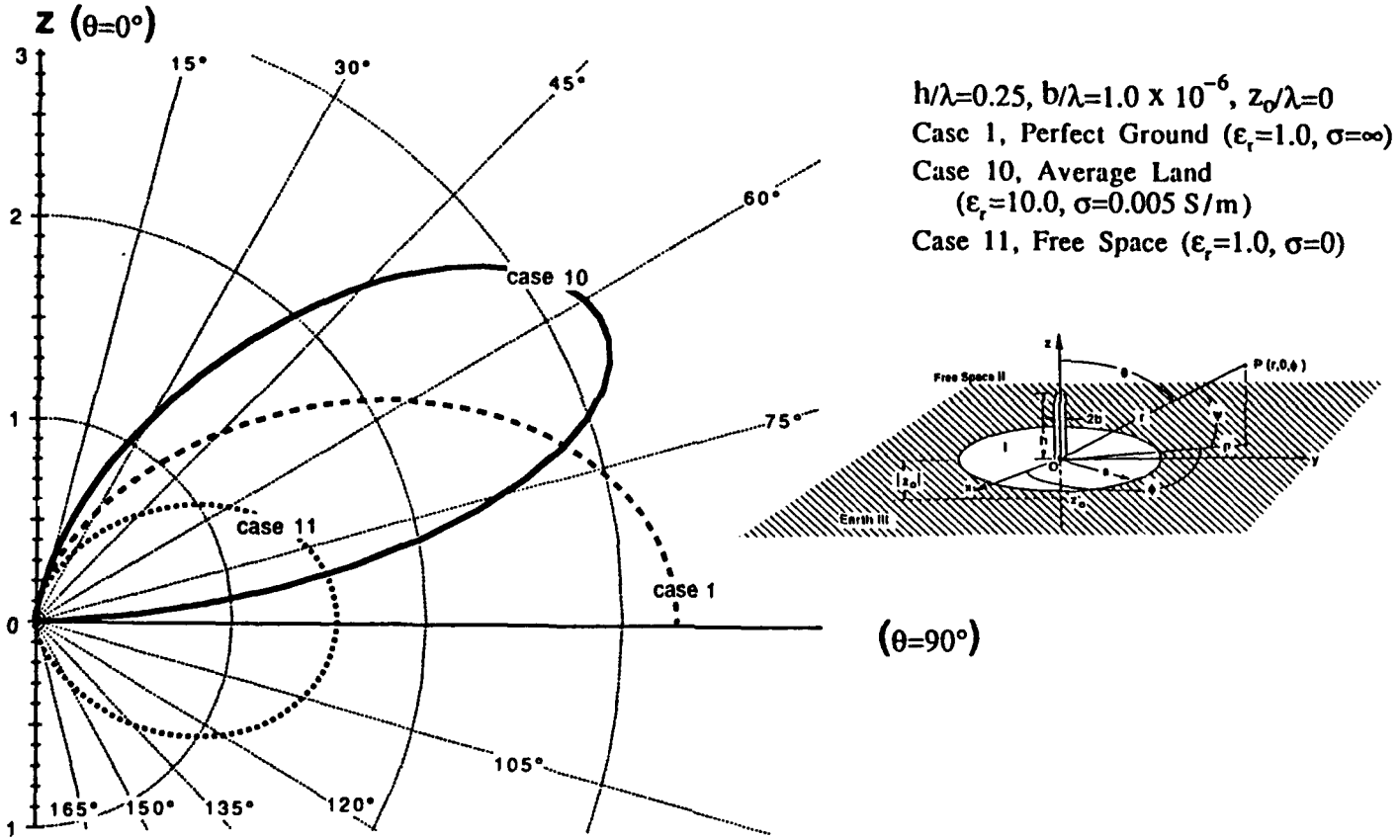

Figure 3-129. Directivity Pattern, $2\pi a/\lambda = 0.025$, Average Land

NUMERIC DIRECTIVE GAIN POLAR PLOT

Case10, Average Land at 15 MHz

$2\pi a/\lambda =$ **3.0 (Wavenumbers)**

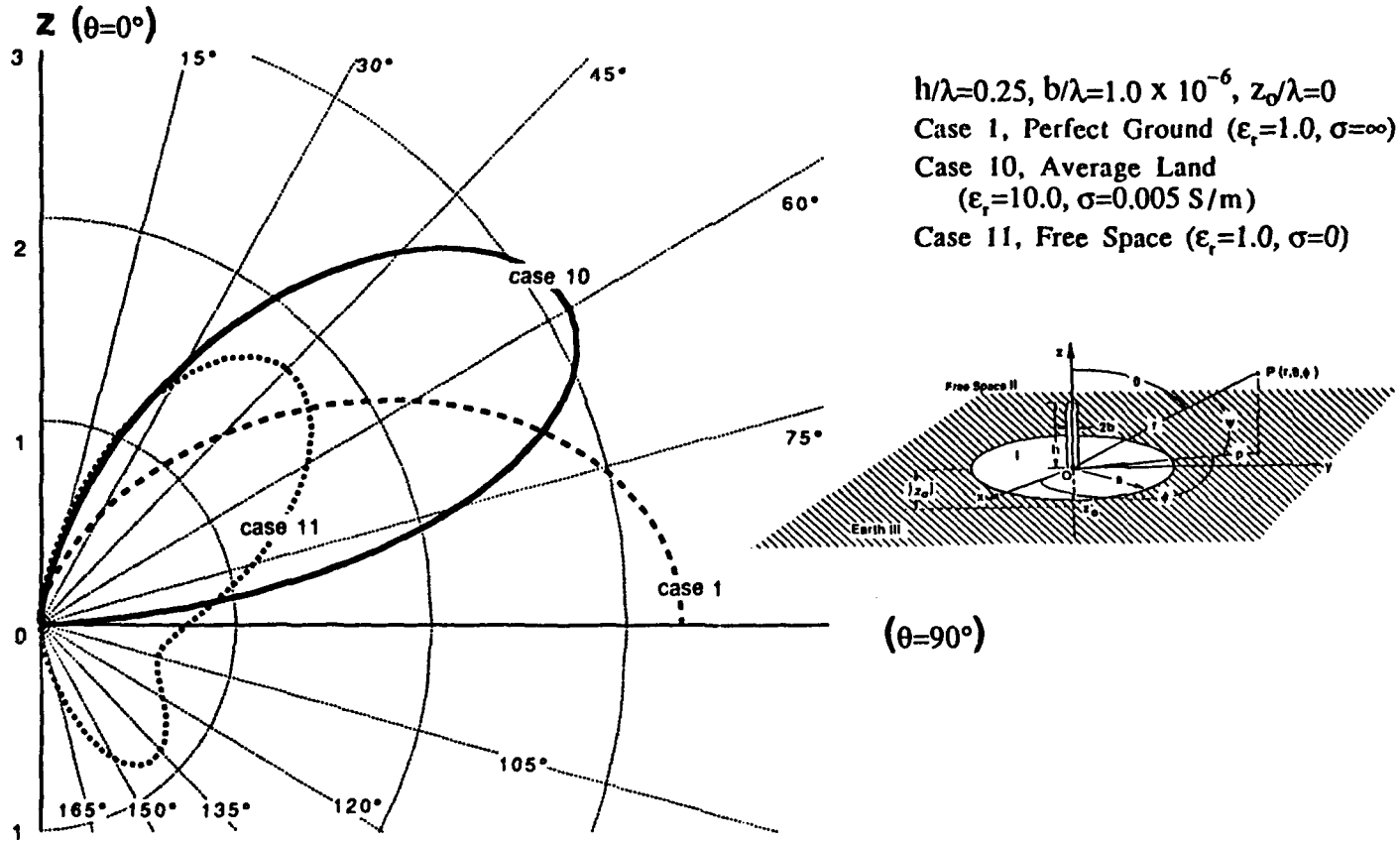

Figure 3-130. Directivity Pattern, $2\pi a/\lambda = 3.0$ Average Land

NUMERIC DIRECTIVE GAIN POLAR PLOT

Case10, Average Land at 15 MHz

$2\pi a/\lambda =$ **4.0 (Wavenumbers)**

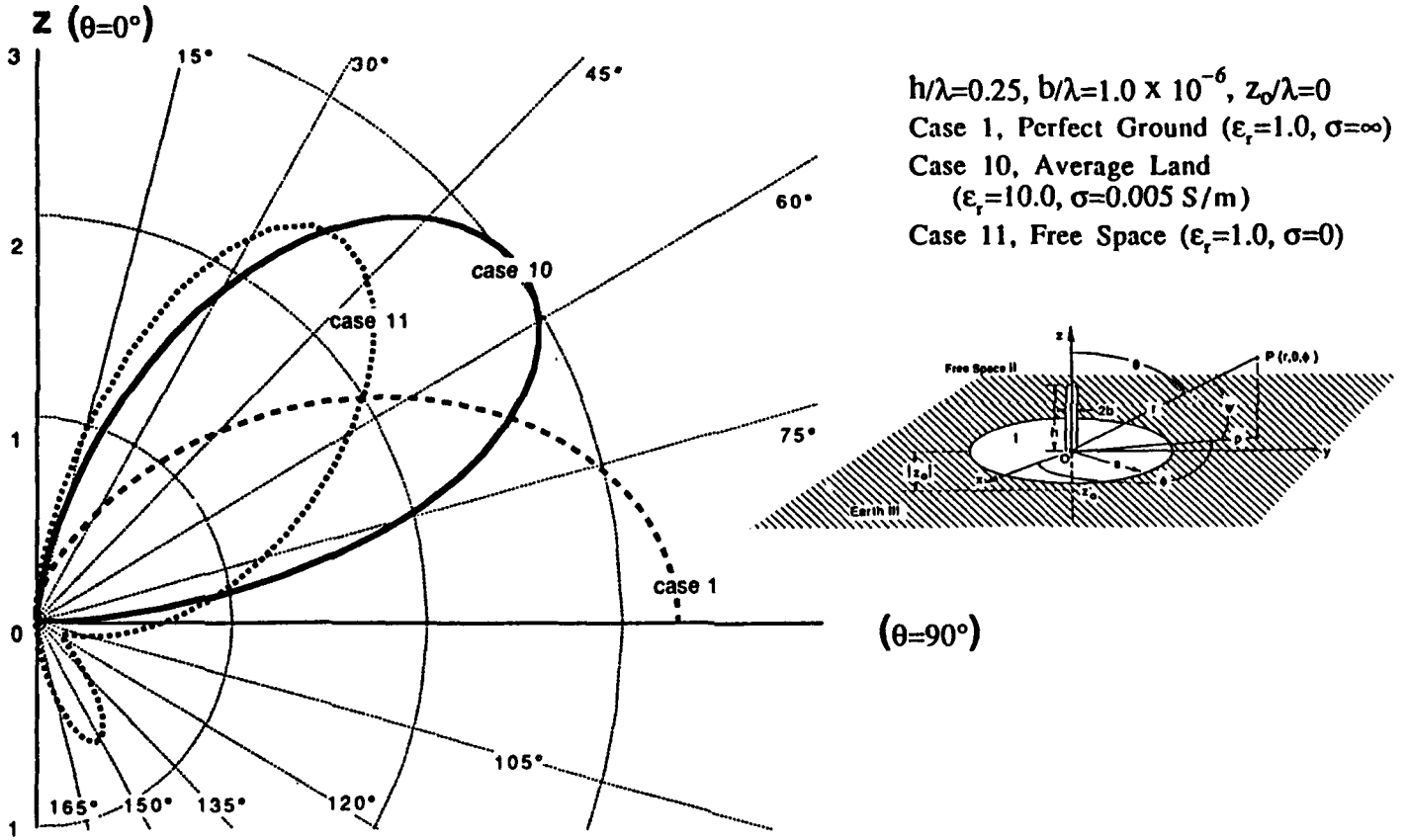

Figure 3-131. Directivity Pattern, $2\pi a/\lambda = 4.0$, Average Land

NUMERIC DIRECTIVE GAIN POLAR PLOT

Case10, Average Land at 15 MHz

$2\pi a/\lambda =$ **5.0 (Wavenumbers)**

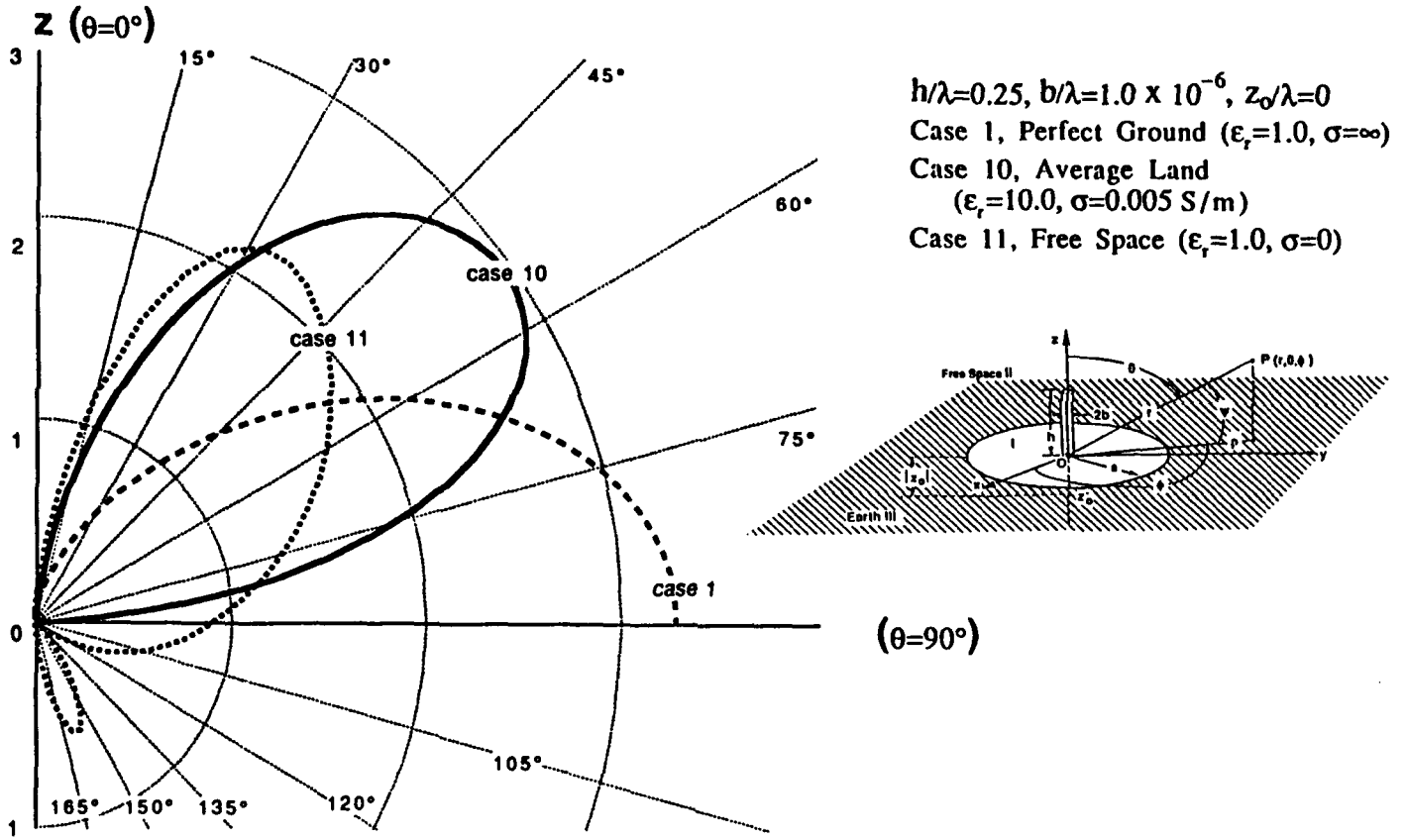

Figure 3-132. Directivity Pattern, $2\pi a/\lambda = 5.0$, Average Land

NUMERIC DIRECTIVE GAIN POLAR PLOT

Case10, Average Land at 15 MHz

$2\pi a/\lambda =$ **6.5 (Wavenumbers)**

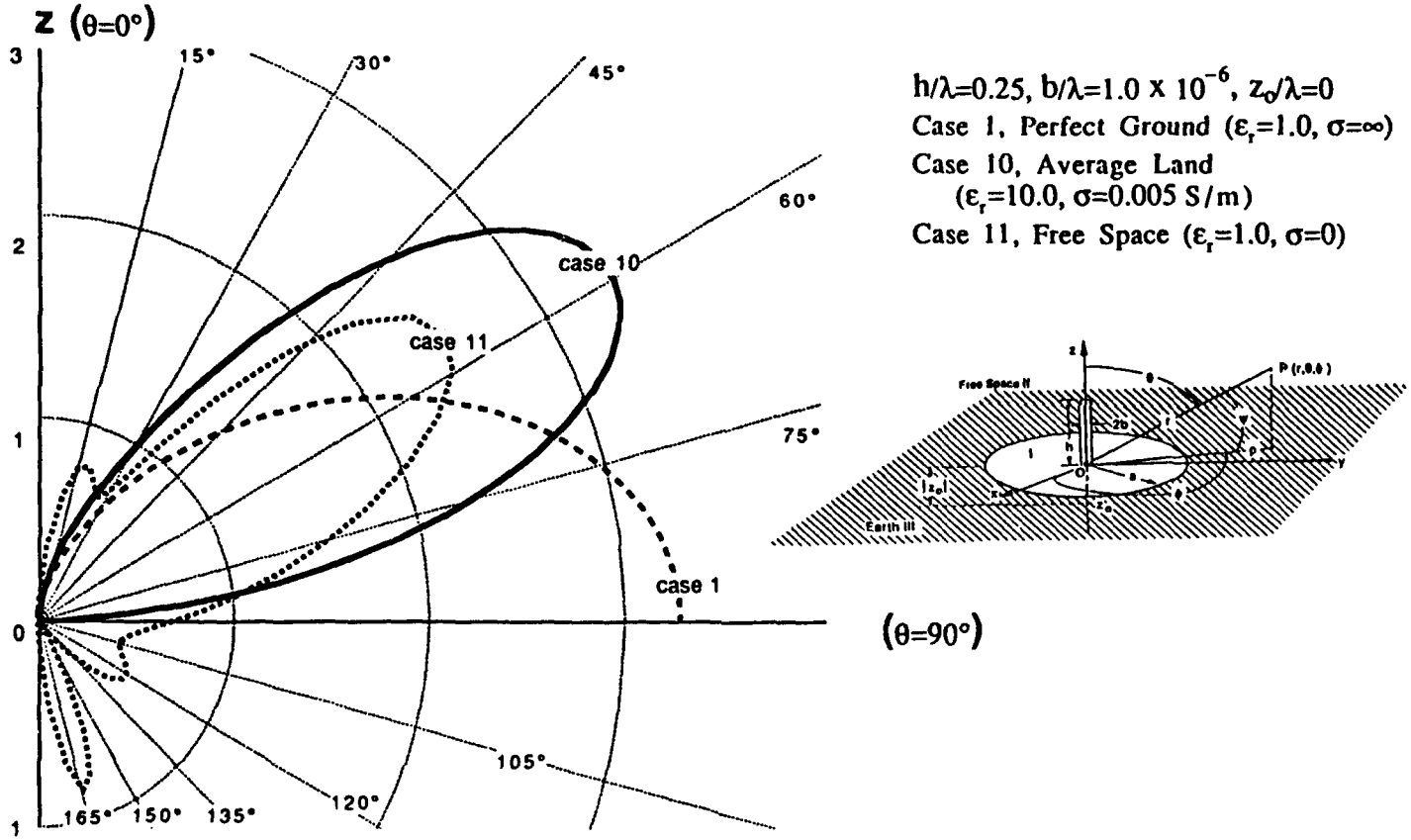

Figure 3-133. Directivity Pattern, $2\pi a/\lambda = 6.5$, Average Land

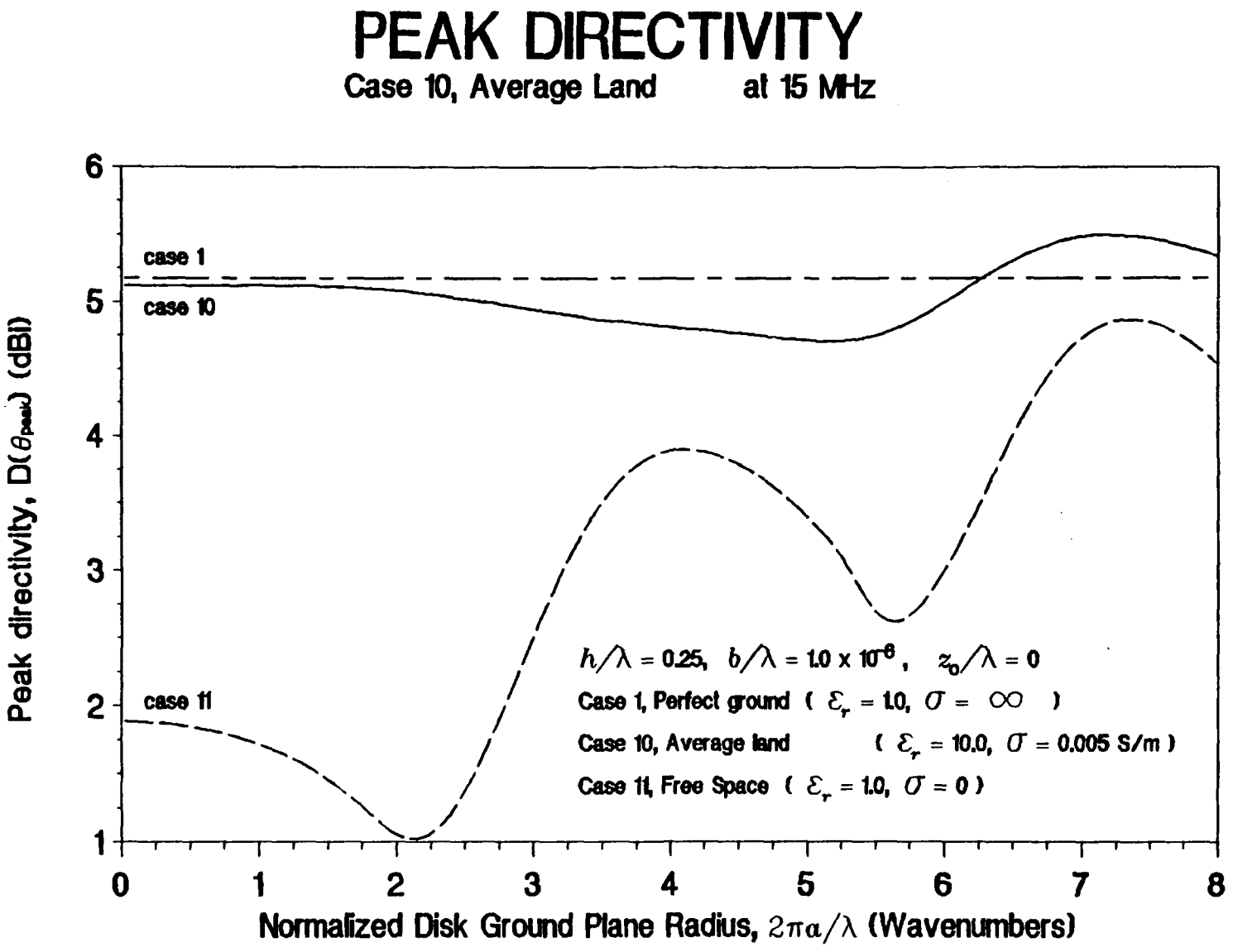

Figure 3-134. Peak Directivity, Average Land

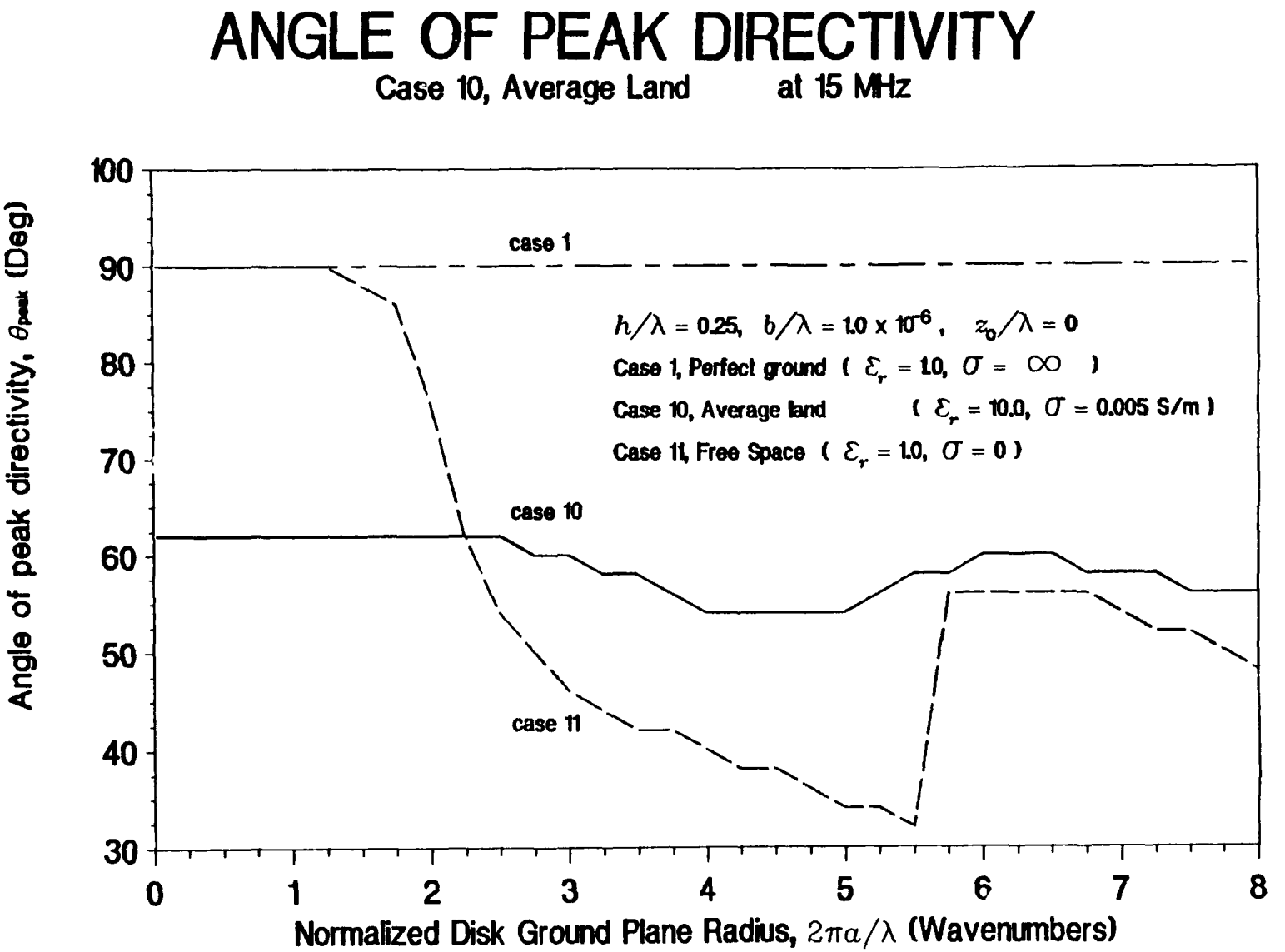

Figure 3-135. Angle of Incidence of Peak Directivity, Average Land

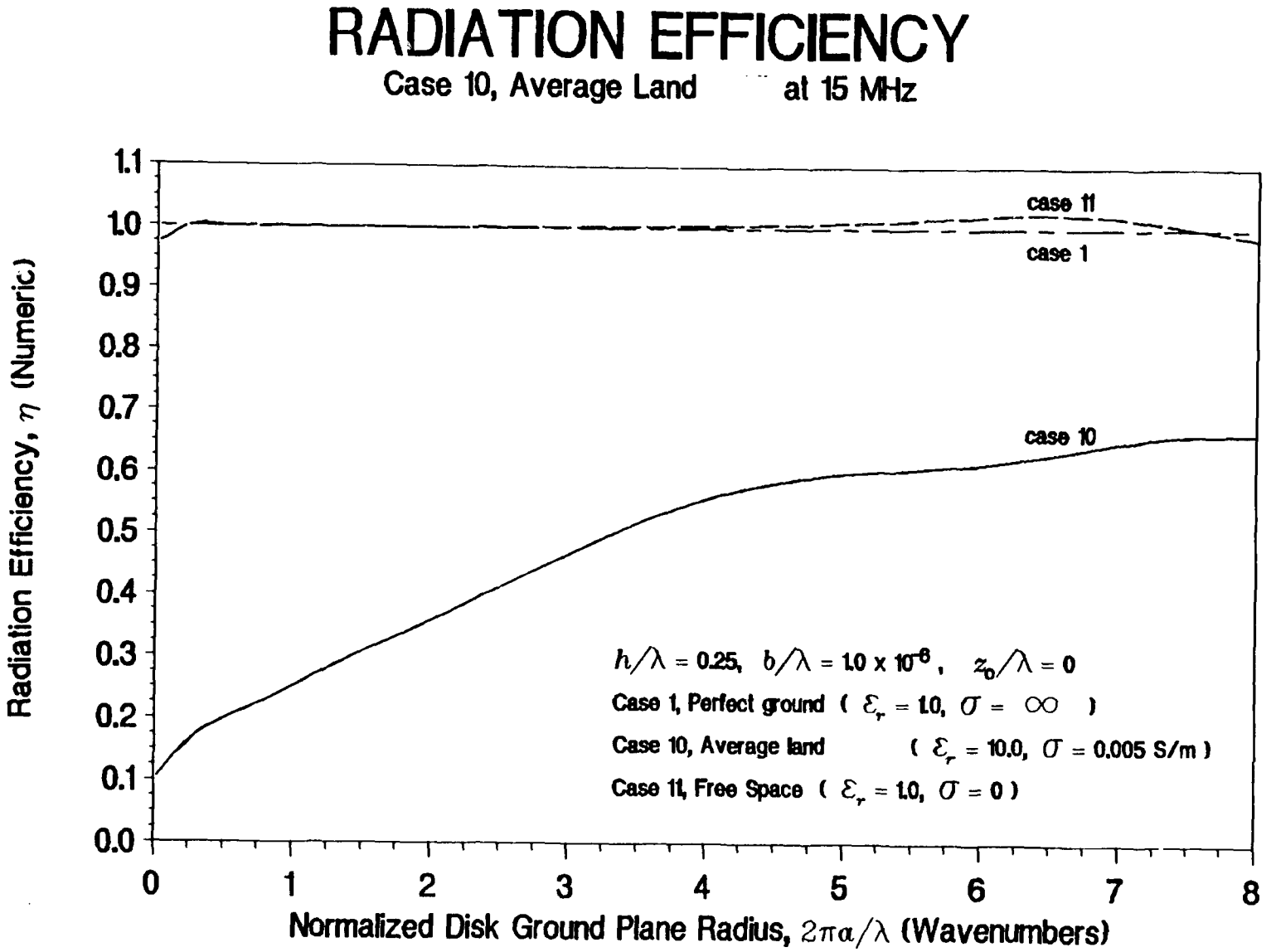

Figure 3-136. Radiation Efficiency, Average Land

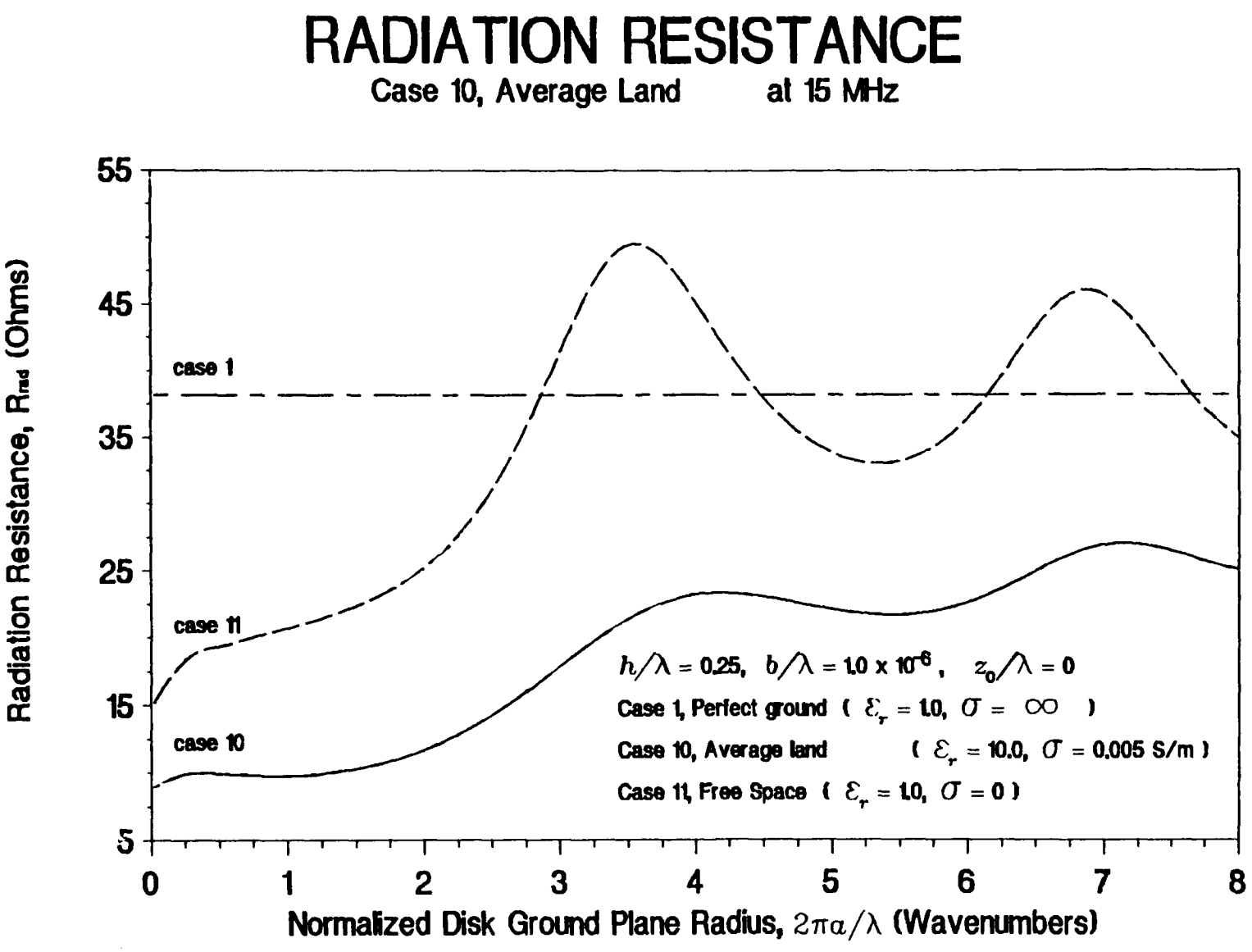

Figure 3-137. Radiation Resistance, Average Land

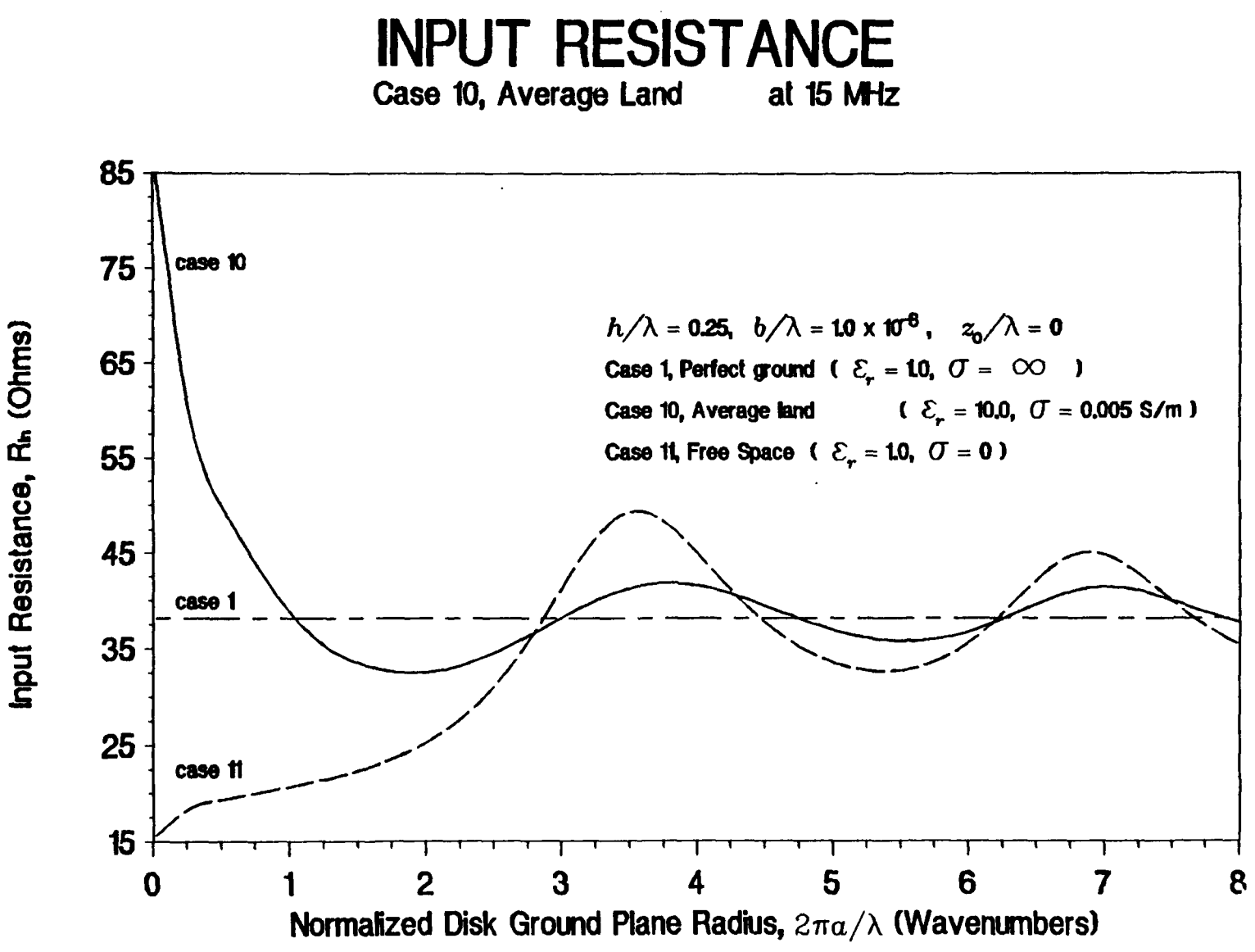

Figure 3-138. Input Resistance, Average Land

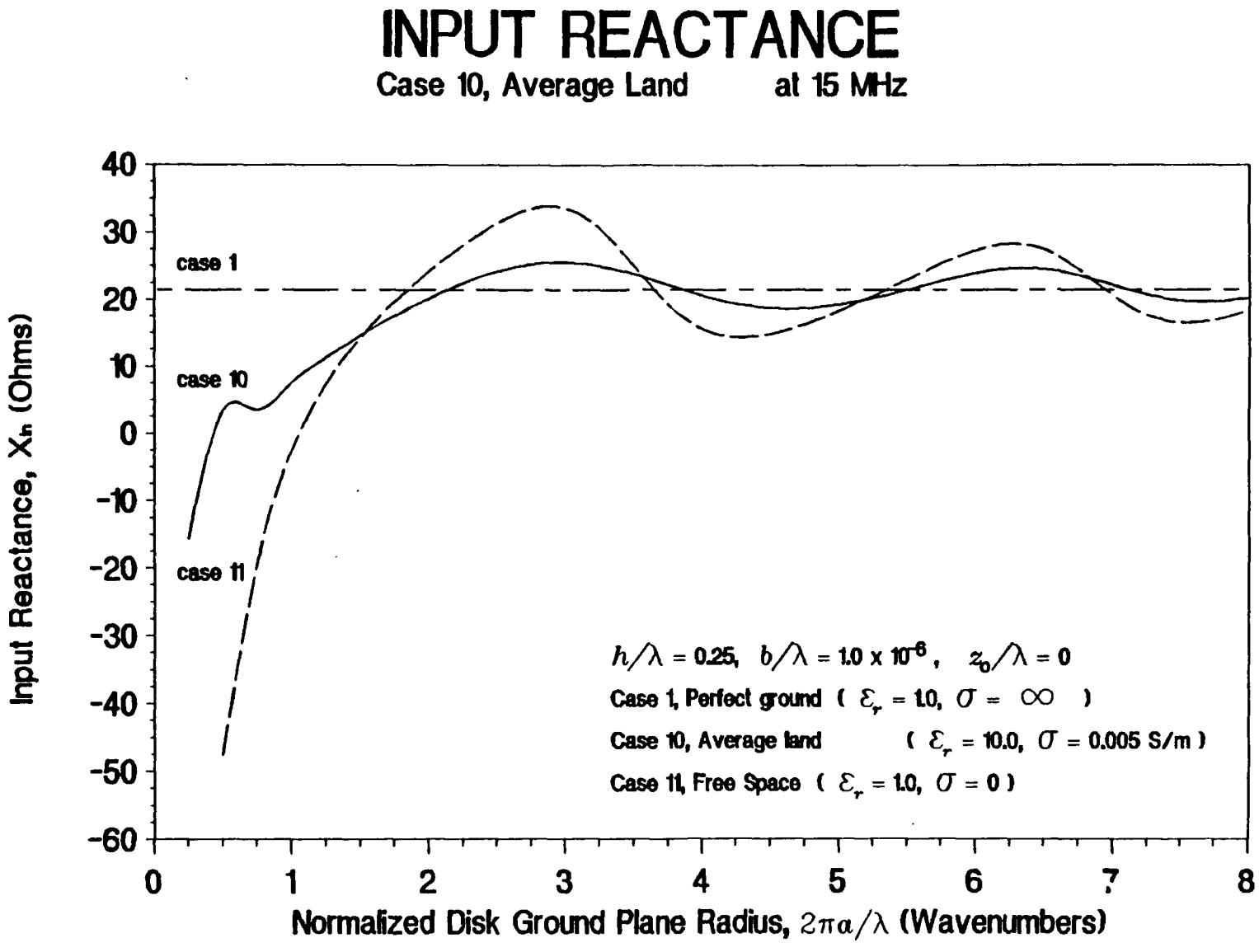

Figure 3-139. Input Reactance, Average Land

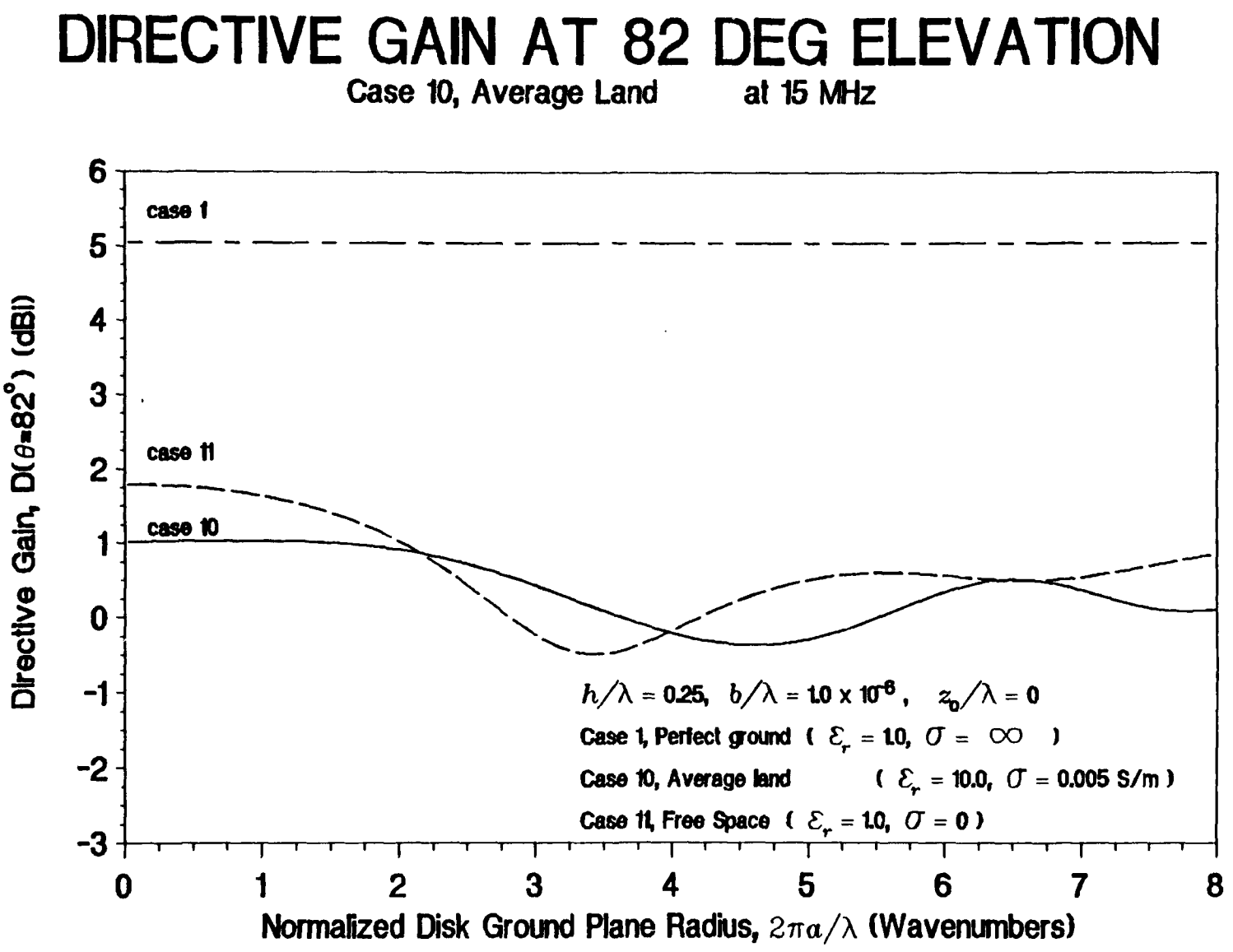

Figure 3-140. Directivity at 8 Degrees Above the Horizon, Average Land

DIRECTIVE GAIN AT 84 DEG ELEVATION

Case 10, Average Land at 15 MHz

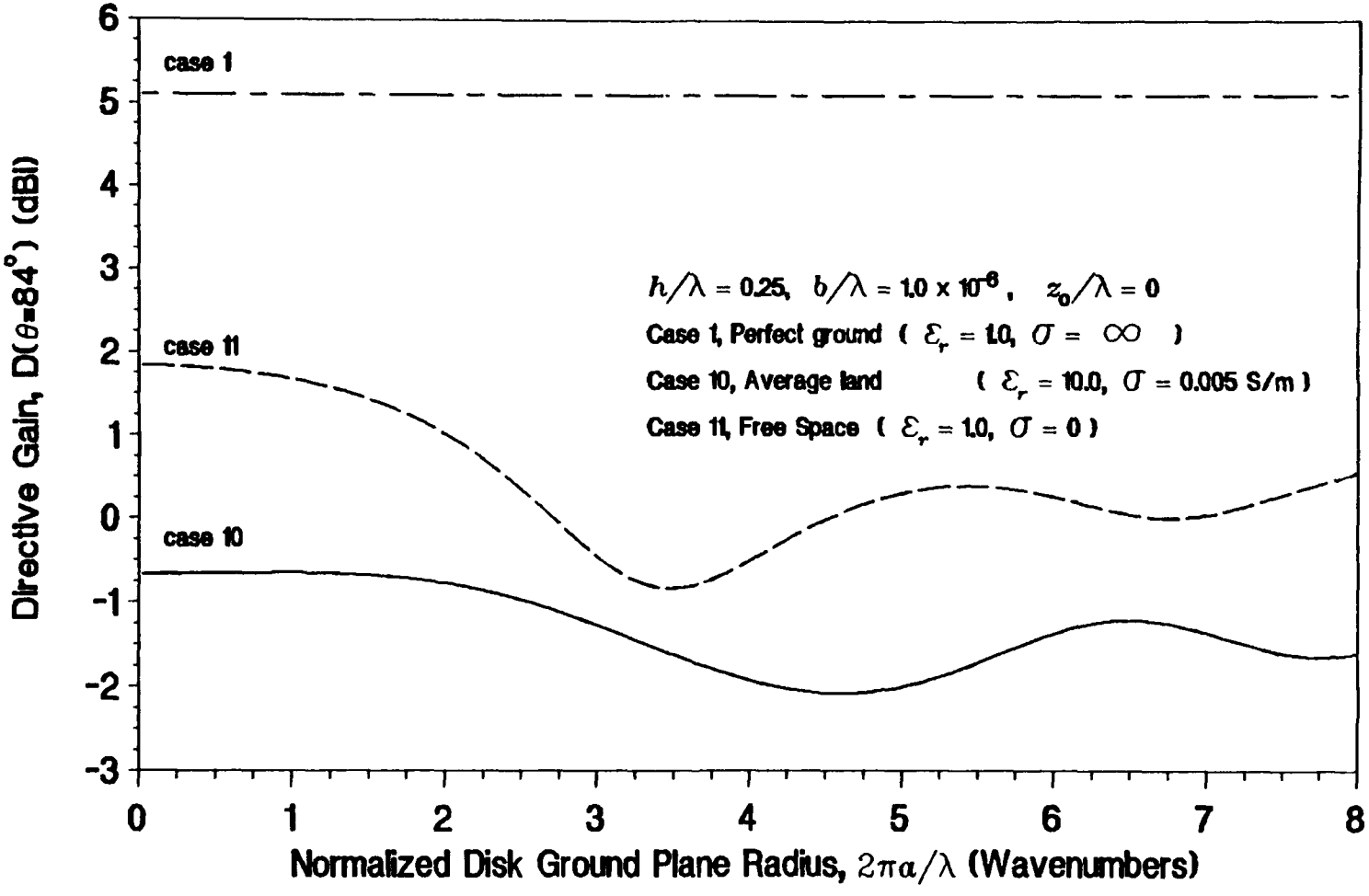

Figure 3-141. Directivity at 6 Degrees Above the Horizon, Average Land

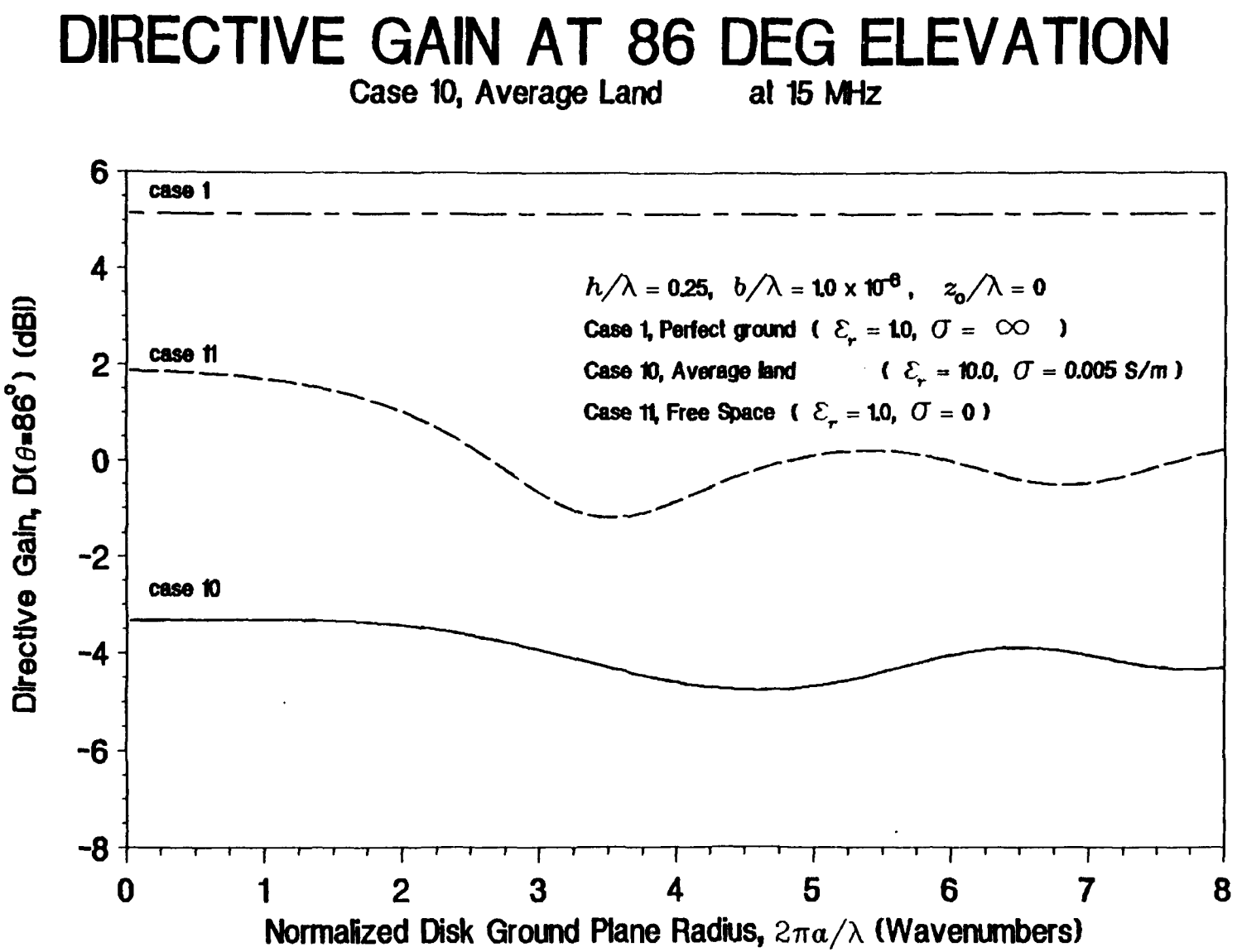

Figure 3-142. Directivity at 4 Degrees Above the Horizon, Average Land

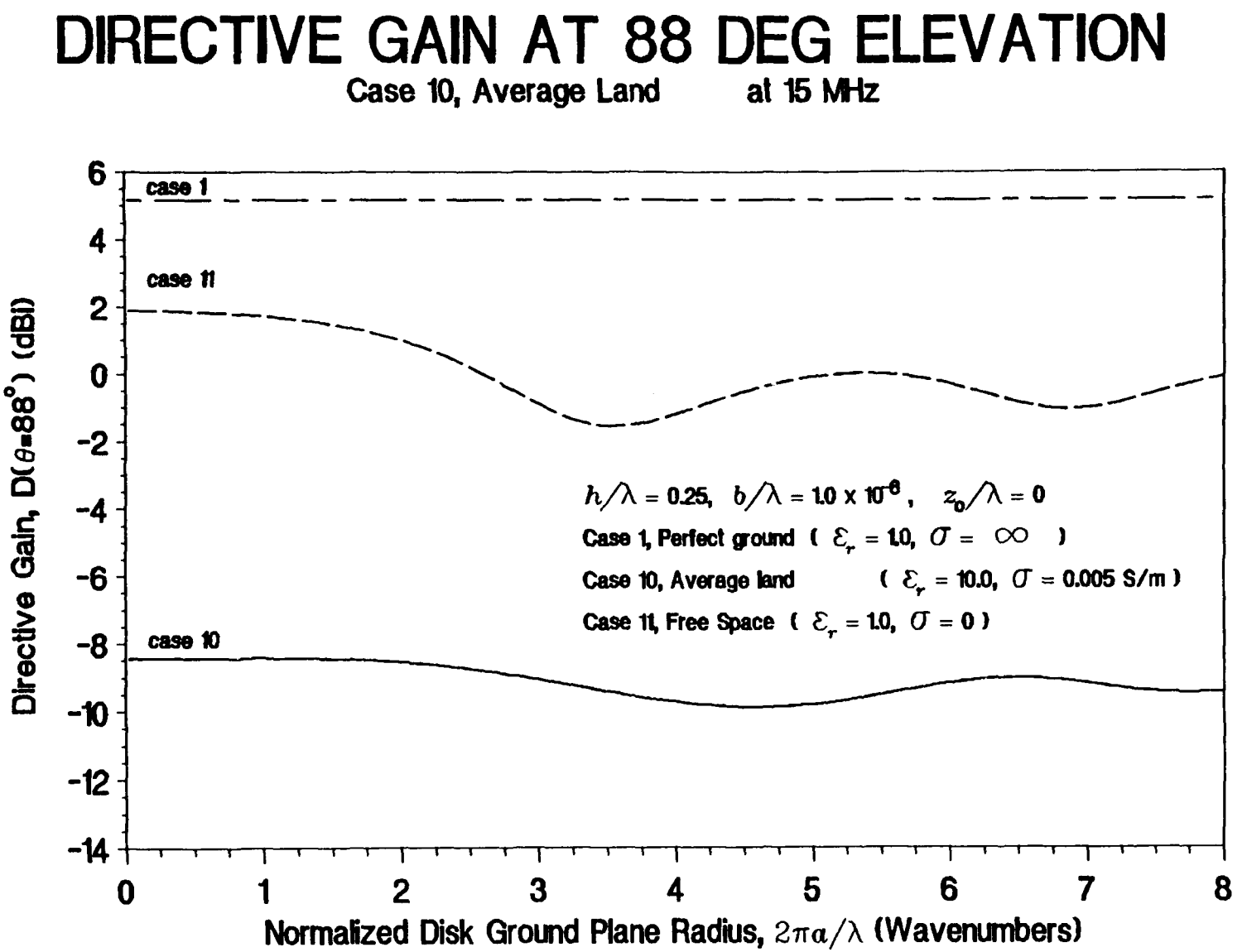

Figure 3-143. Directivity at 2 Degrees Above the Horizon, Average Land

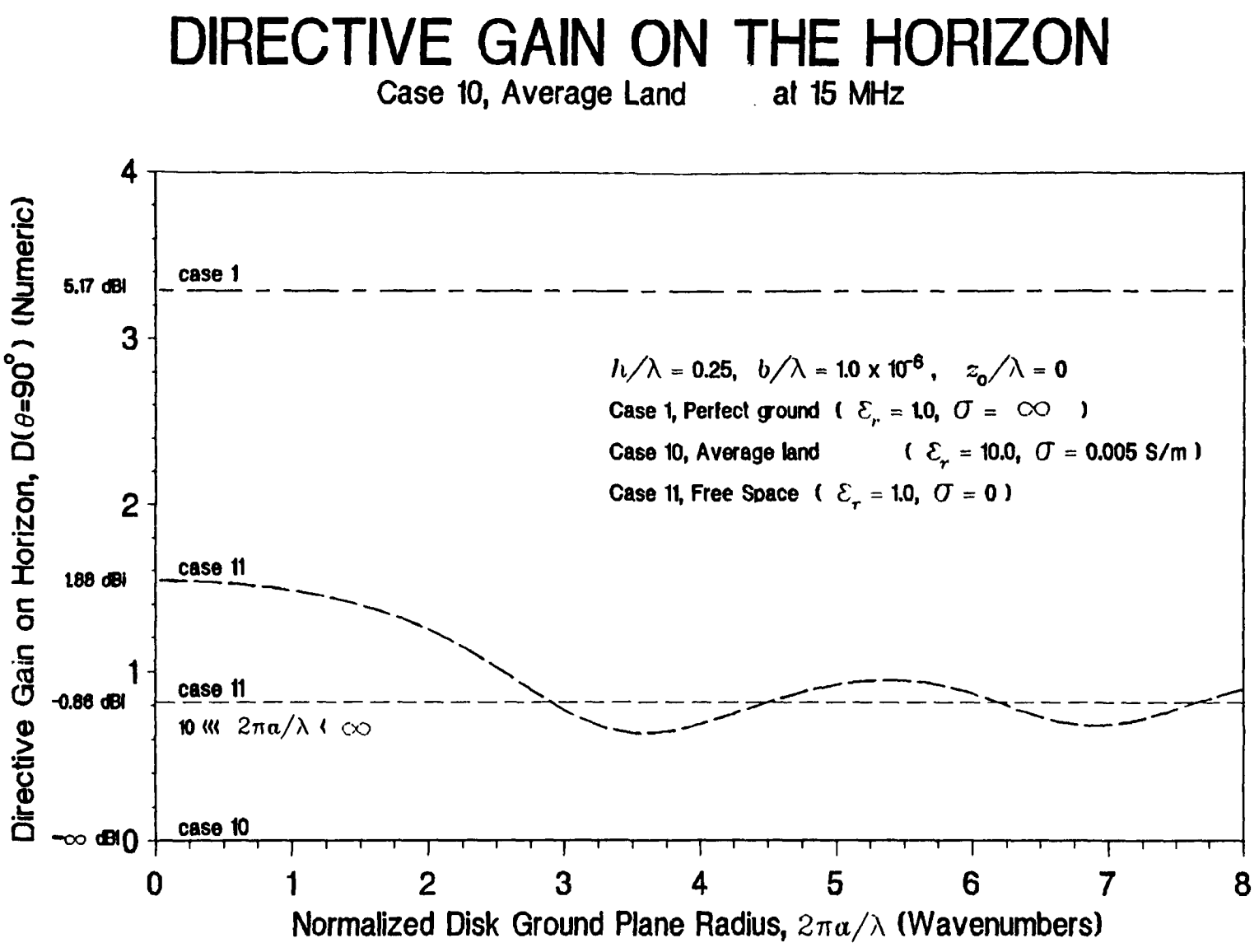

Figure 3-144. Directivity on the Horizon, Average Land

3.10 SEA WATER COMPARED WITH MEDIUM DRY GROUND

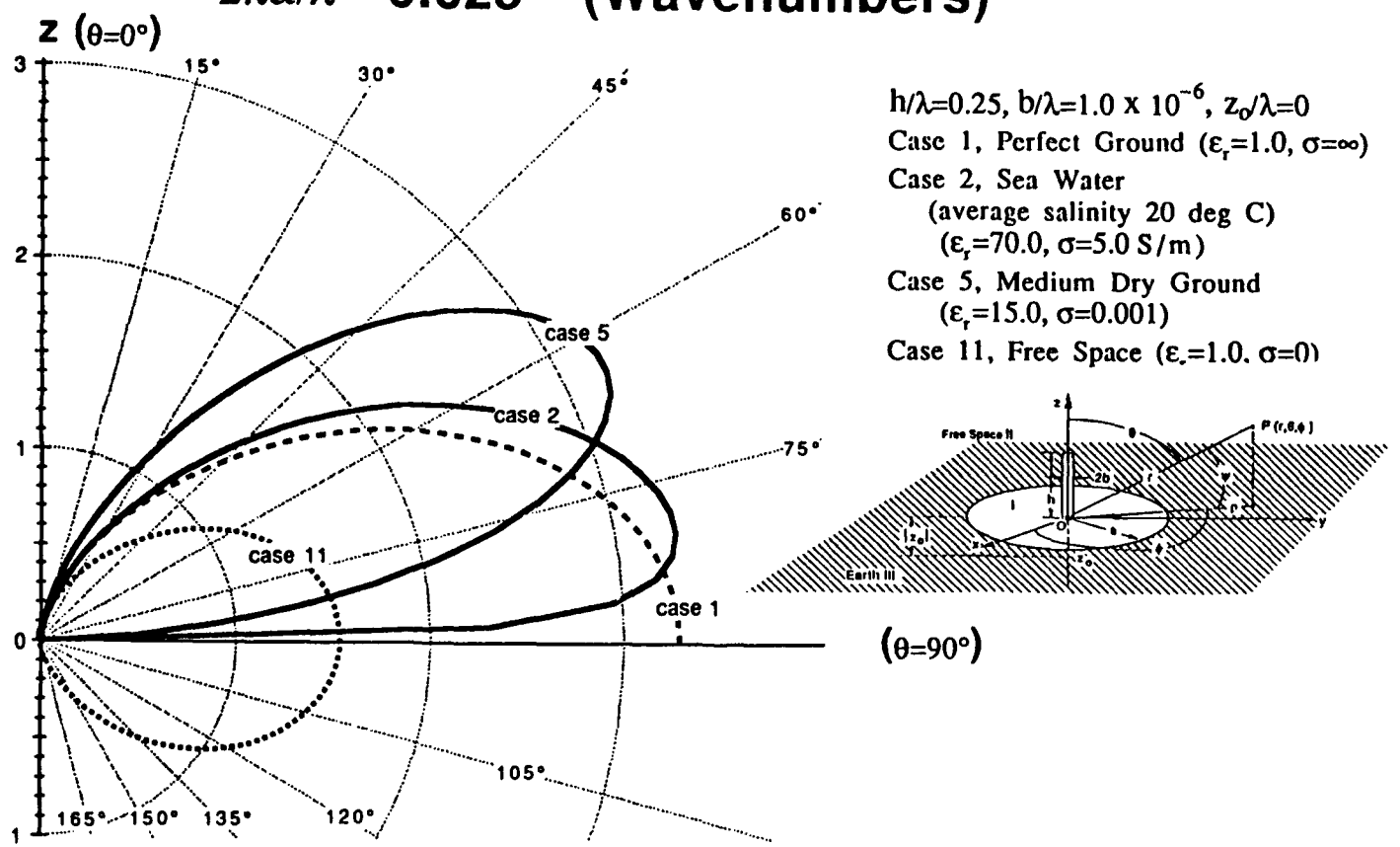

Figure 3-145. Directivity Pattern, $2\pi a/\lambda = 0.025$, Sea Water Compared with Medium Dry Ground

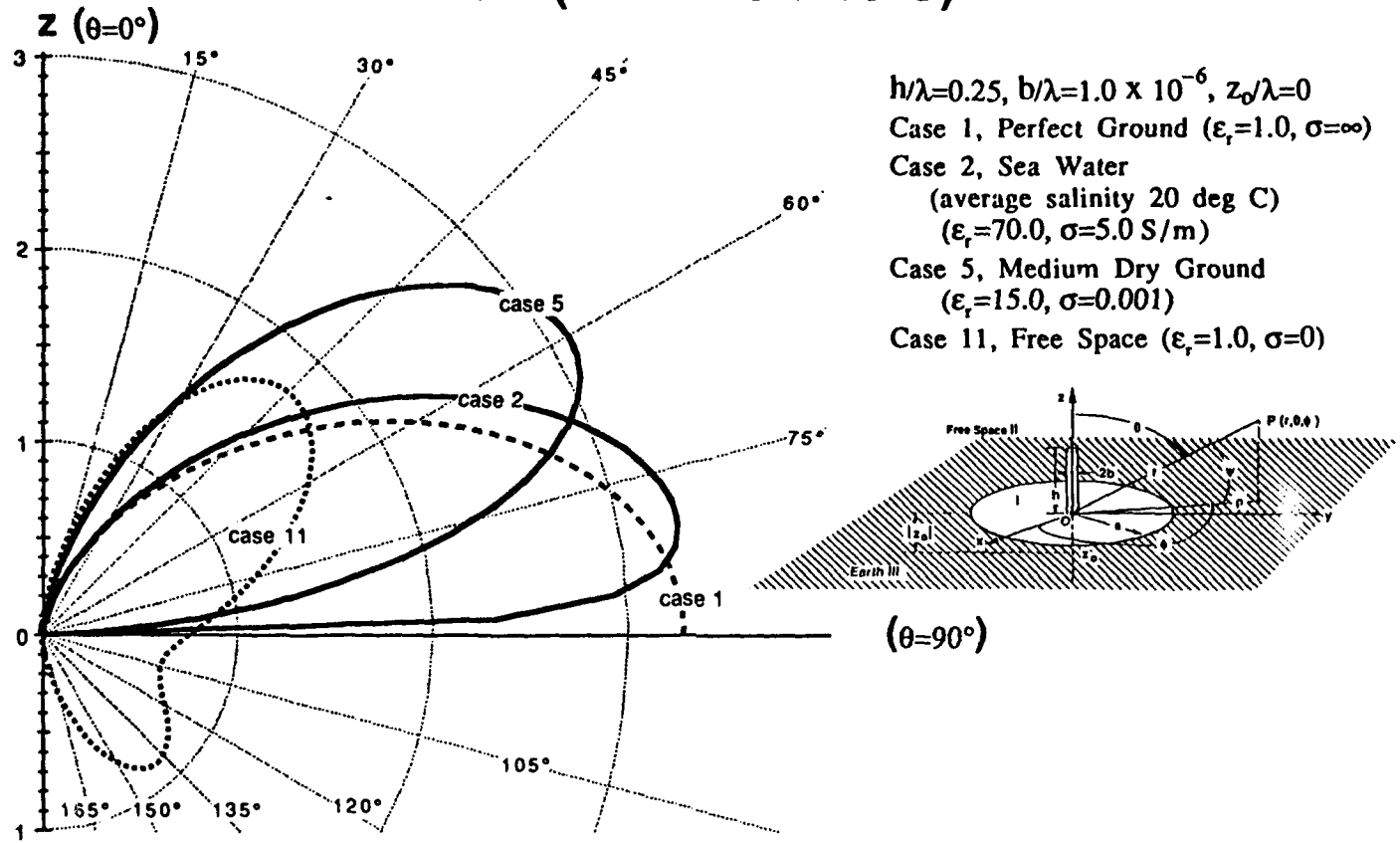

Figure 3-146. Directivity Pattern, $2\pi a/\lambda = 3.0$, Sea Water Compared with Medium Dry Ground

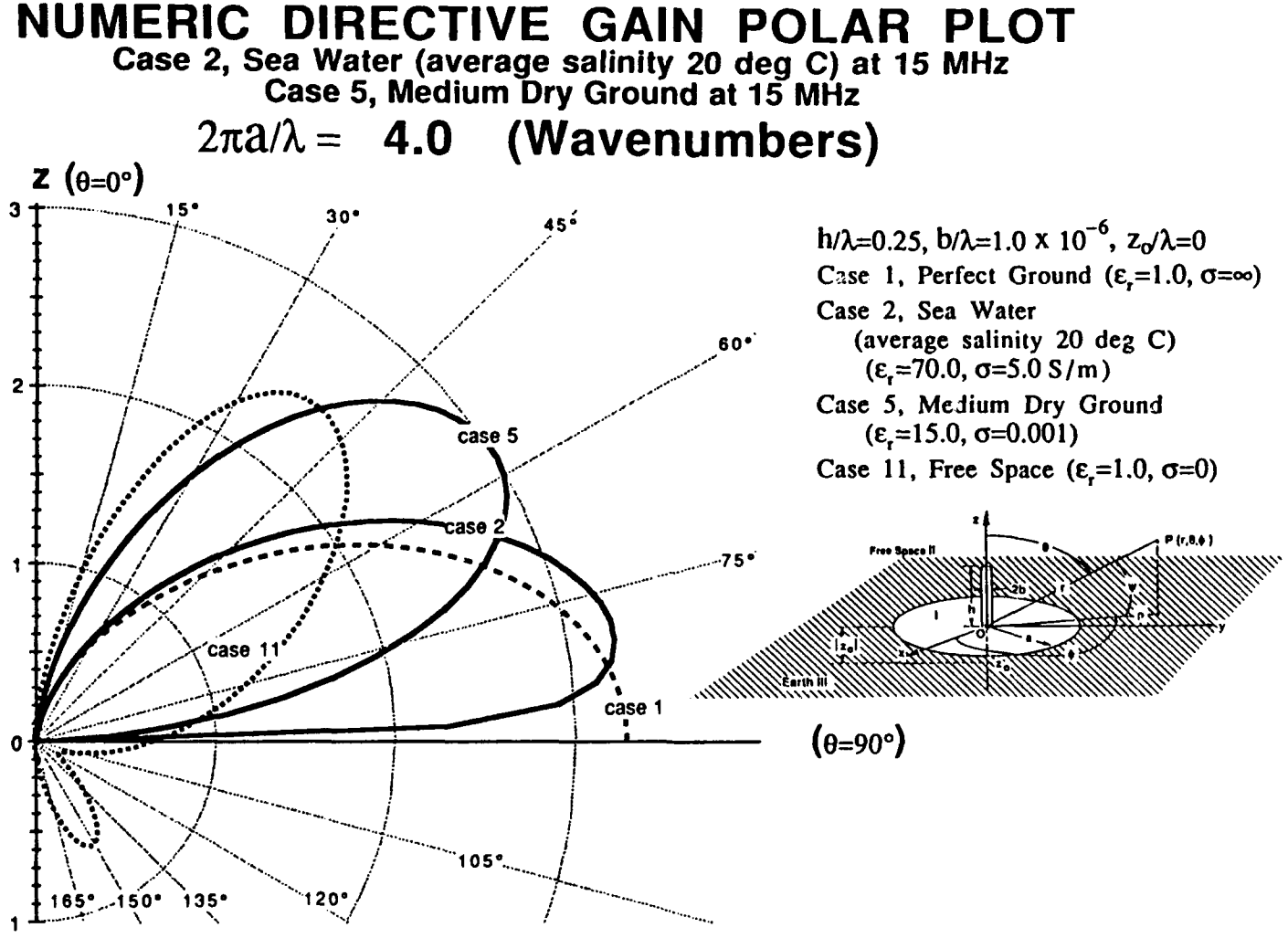

Figure 3-147. Directivity Pattern, $2\pi a/\lambda = 4.0$, Sea Water Compared with Medium Dry Ground

NUMERIC DIRECTIVE GAIN POLAR PLOT

Case 2, Sea Water (average salinity 20 deg C) at 15 MHz
Case 5, Medium Dry Ground at 15 MHz

$2\pi a/\lambda =$ **5.0 (Wavenumbers)**

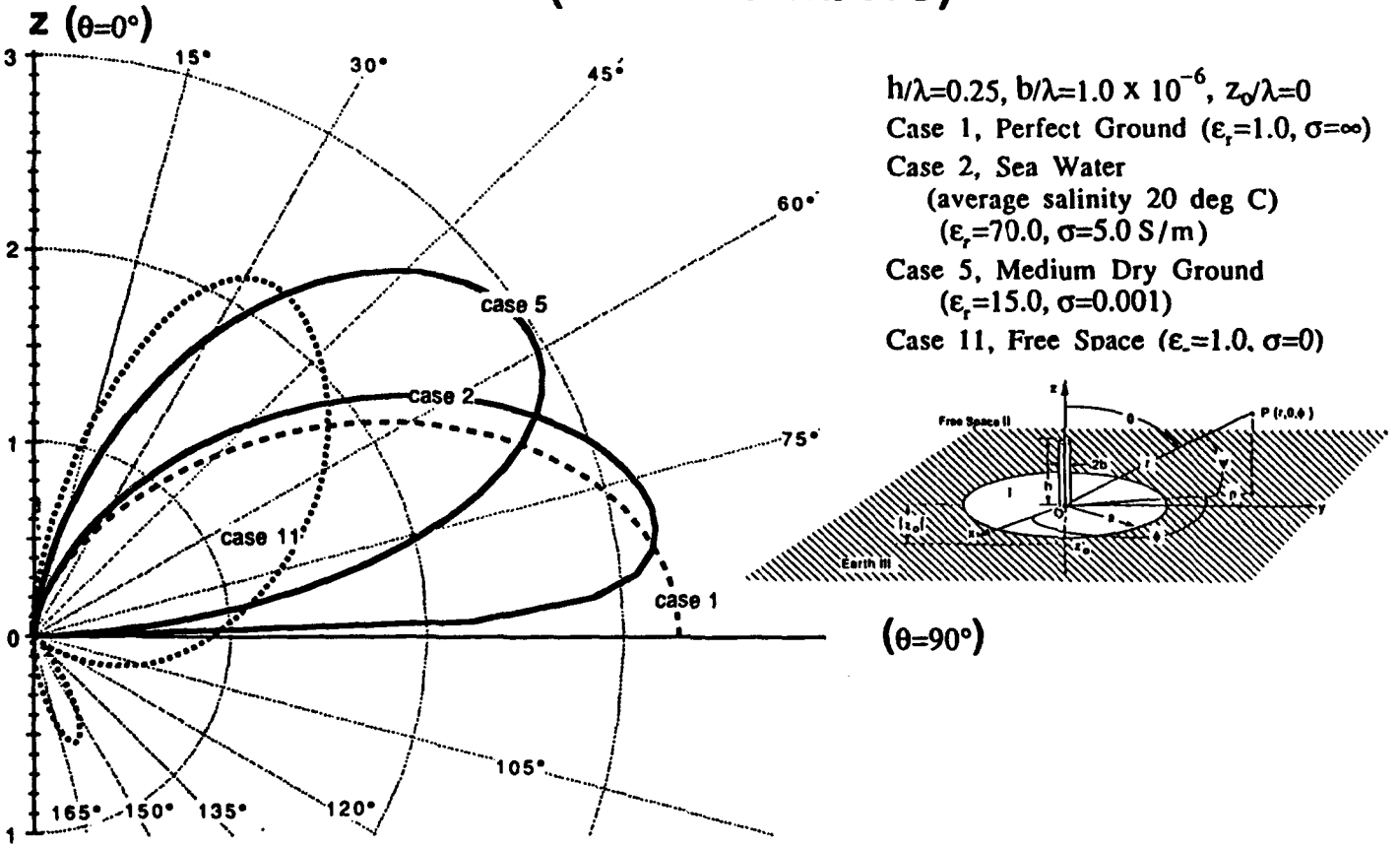

Figure 3-148. Directivity Pattern, $2\pi a/\lambda = 5.0$, Sea Water Compared with Medium Dry Ground

NUMERIC DIRECTIVE GAIN POLAR PLOT

Case 2, Sea Water (average salinity 20 deg C) at 15 MHz
Case 5, Medium Dry Ground at 15 MHz

$2\pi a/\lambda =$ **6.5 (Wavenumbers)**

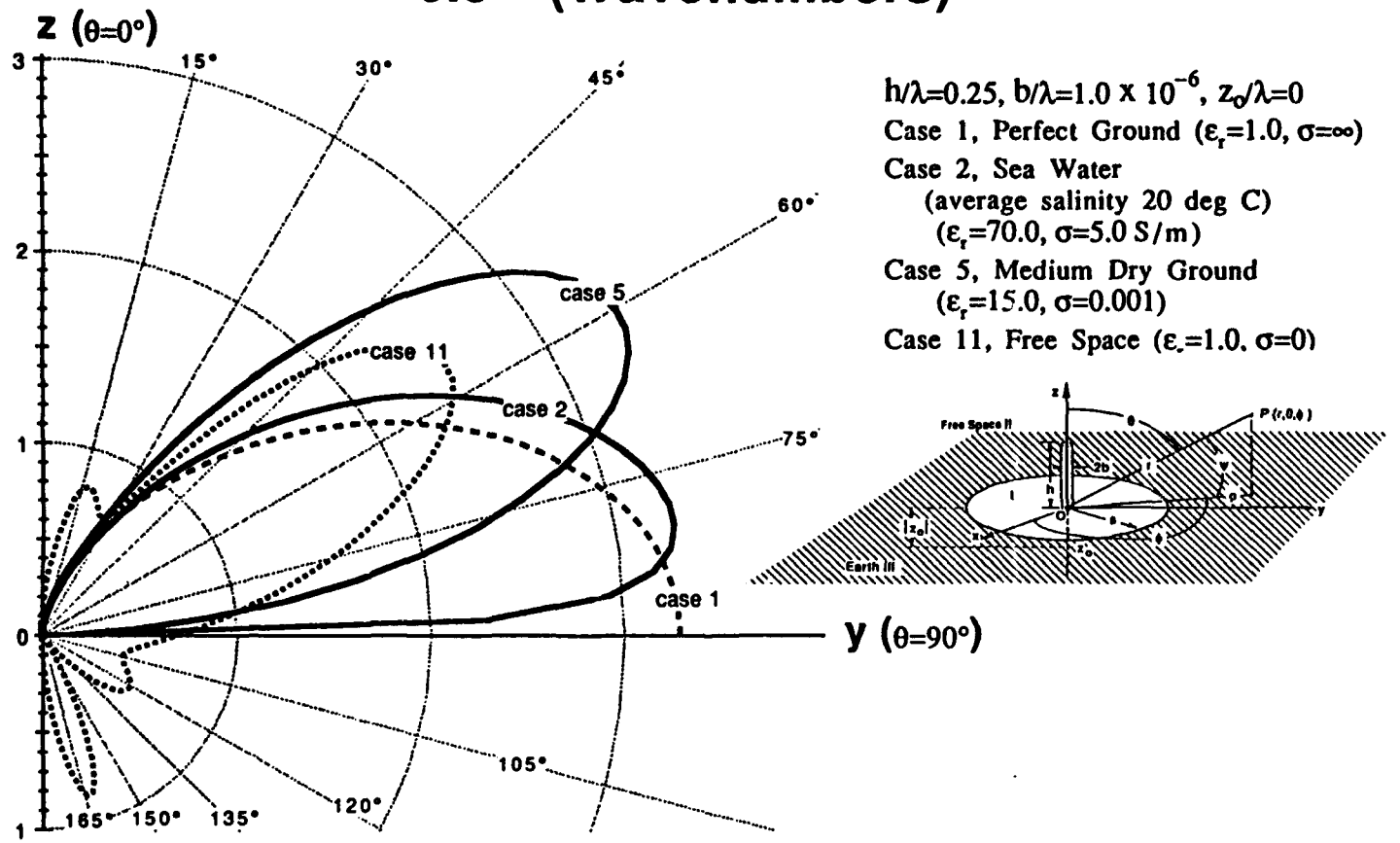

Figure 3-149. Directivity Pattern, $2\pi a/\lambda = 6.5$, Sea Water Compared with Medium Dry Ground

PEAK DIRECTIVITY

Case 2, Sea Water (average salinity 20 deg C) at 15 MHz
Case 5, Medium Dry Ground at 15 MHz

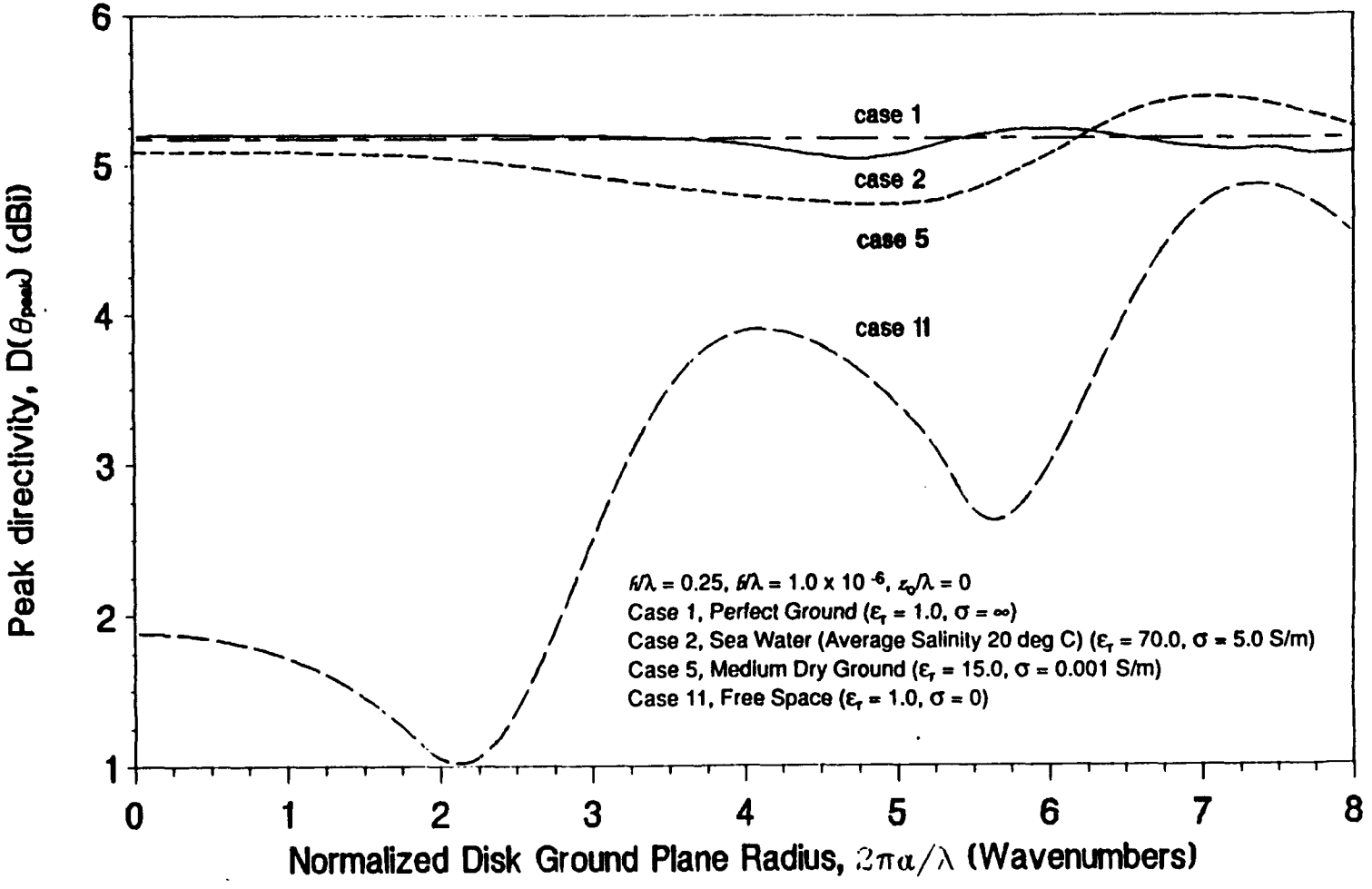

Figure 3-150. Peak Directivity, Sea Water Compared with Medium Dry Ground

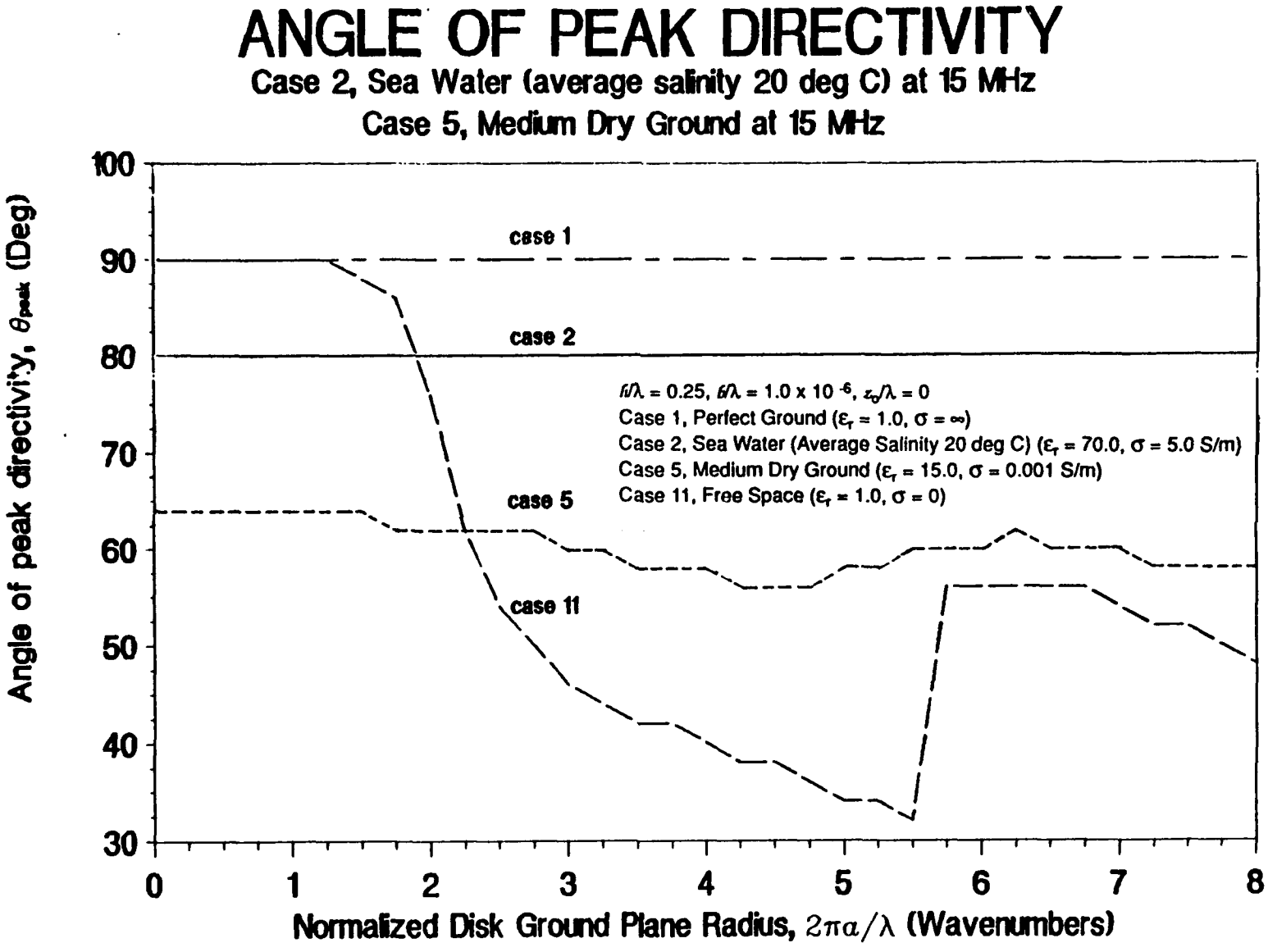

Figure 3-151. Angle of Incidence of Peak Directivity, Sea Water Compared with Medium Dry Ground

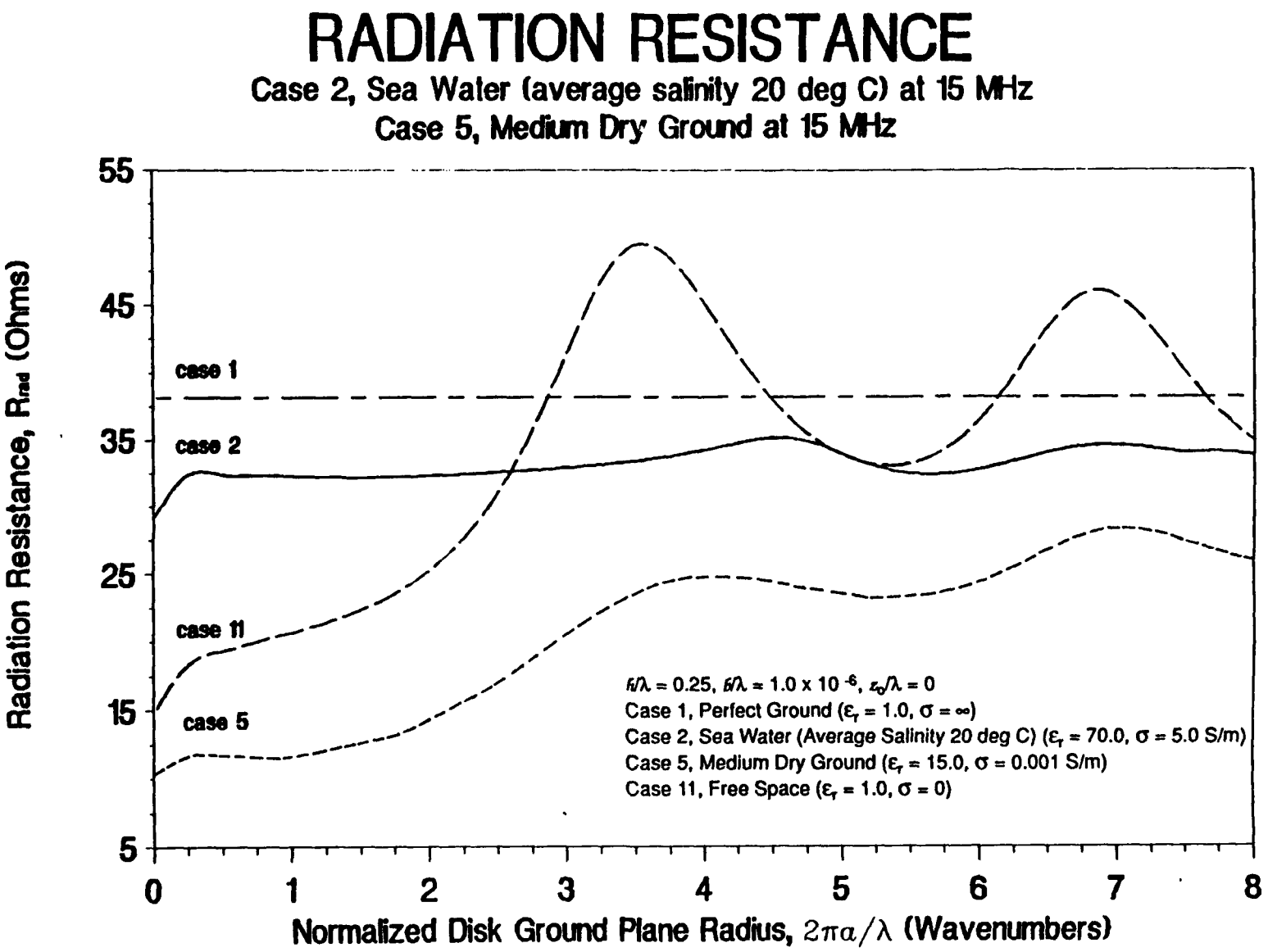

Figure 3-152. Radiation Efficiency, Sea Water Compared with Medium Dry Ground

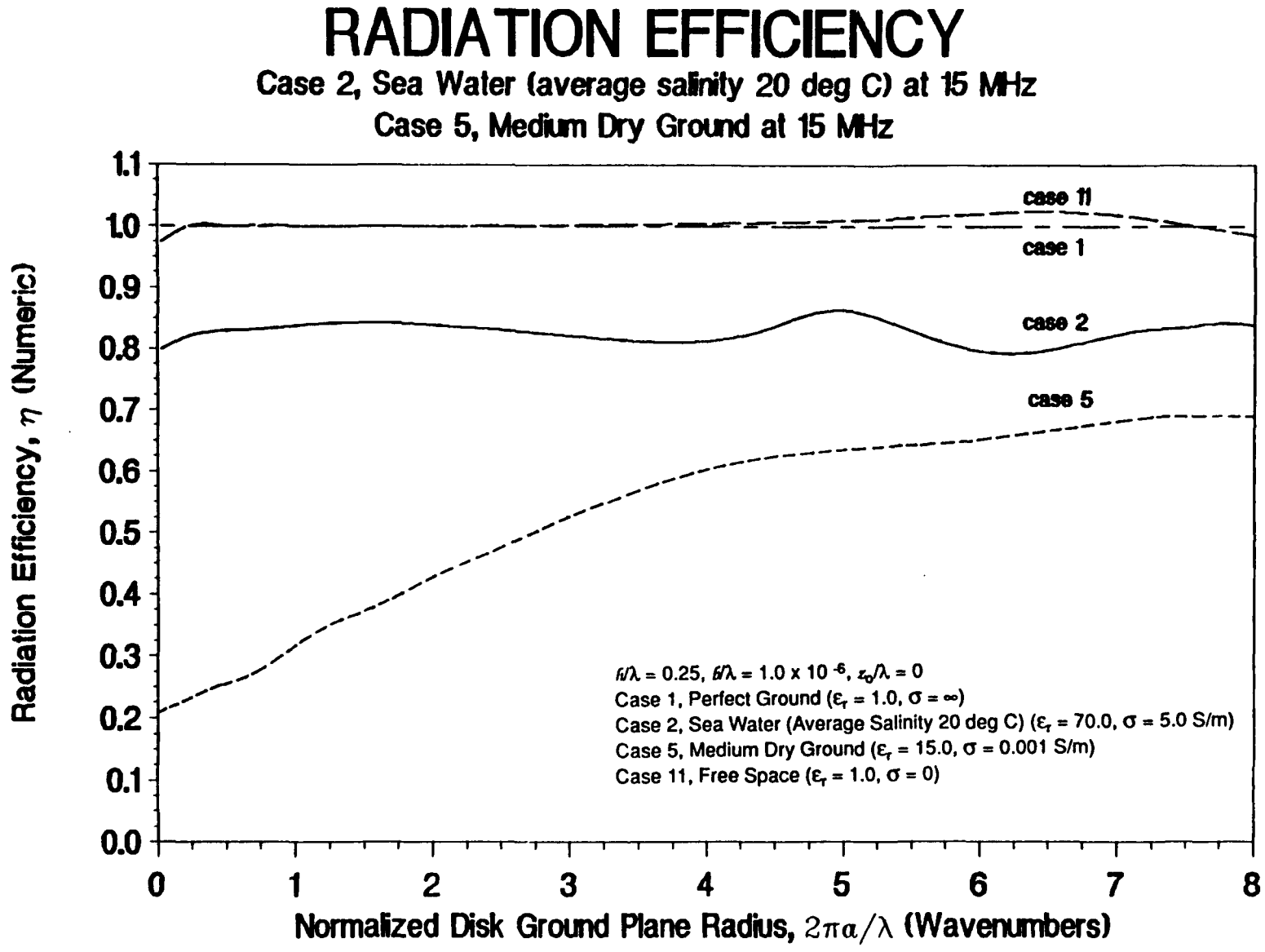

Figure 3-153. Radiation Resistance, Sea Water Compared with Medium Dry Ground

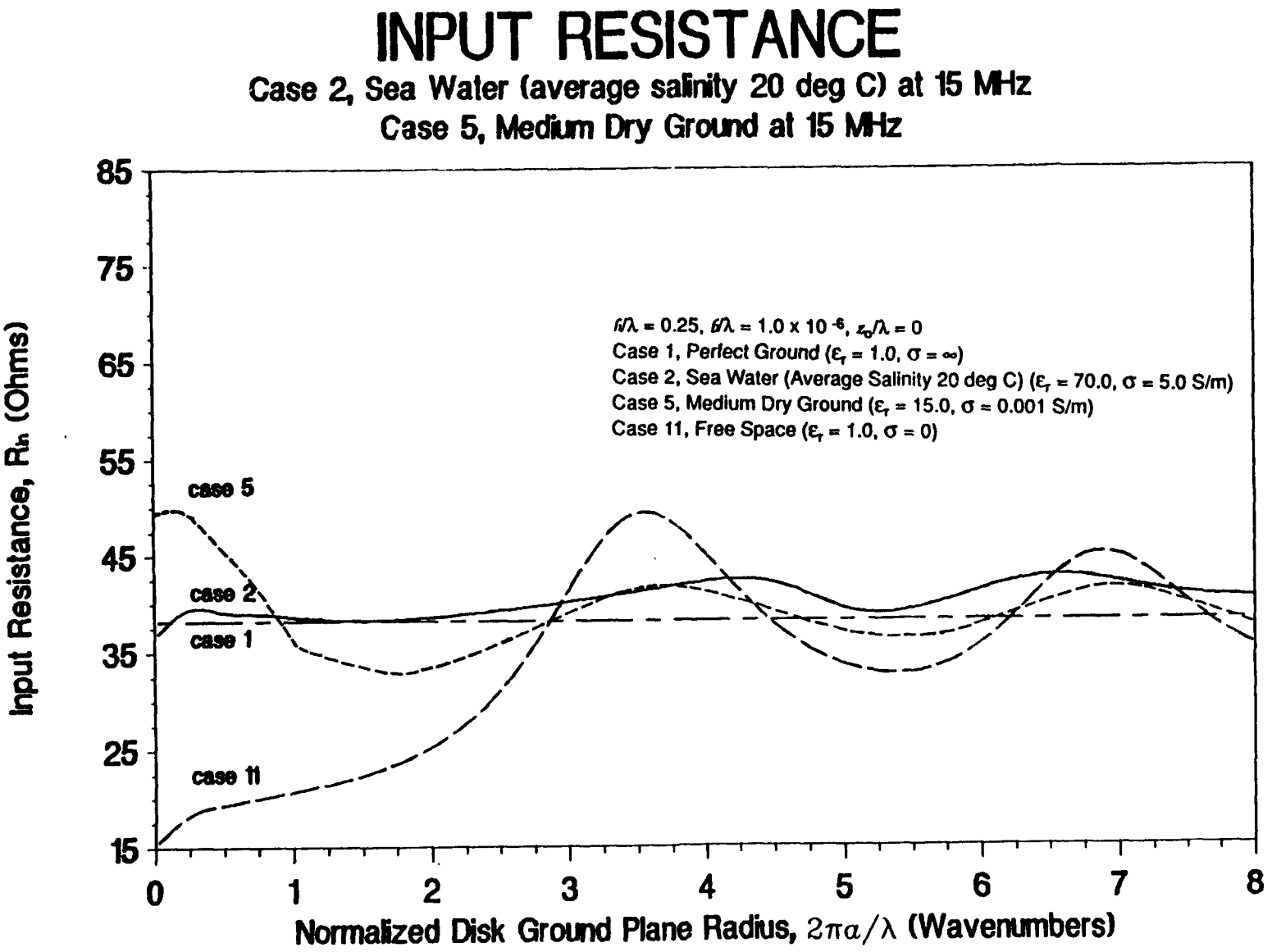

Figure 3-154. Input Resistance, Sea Water Compared with Medium Dry Ground

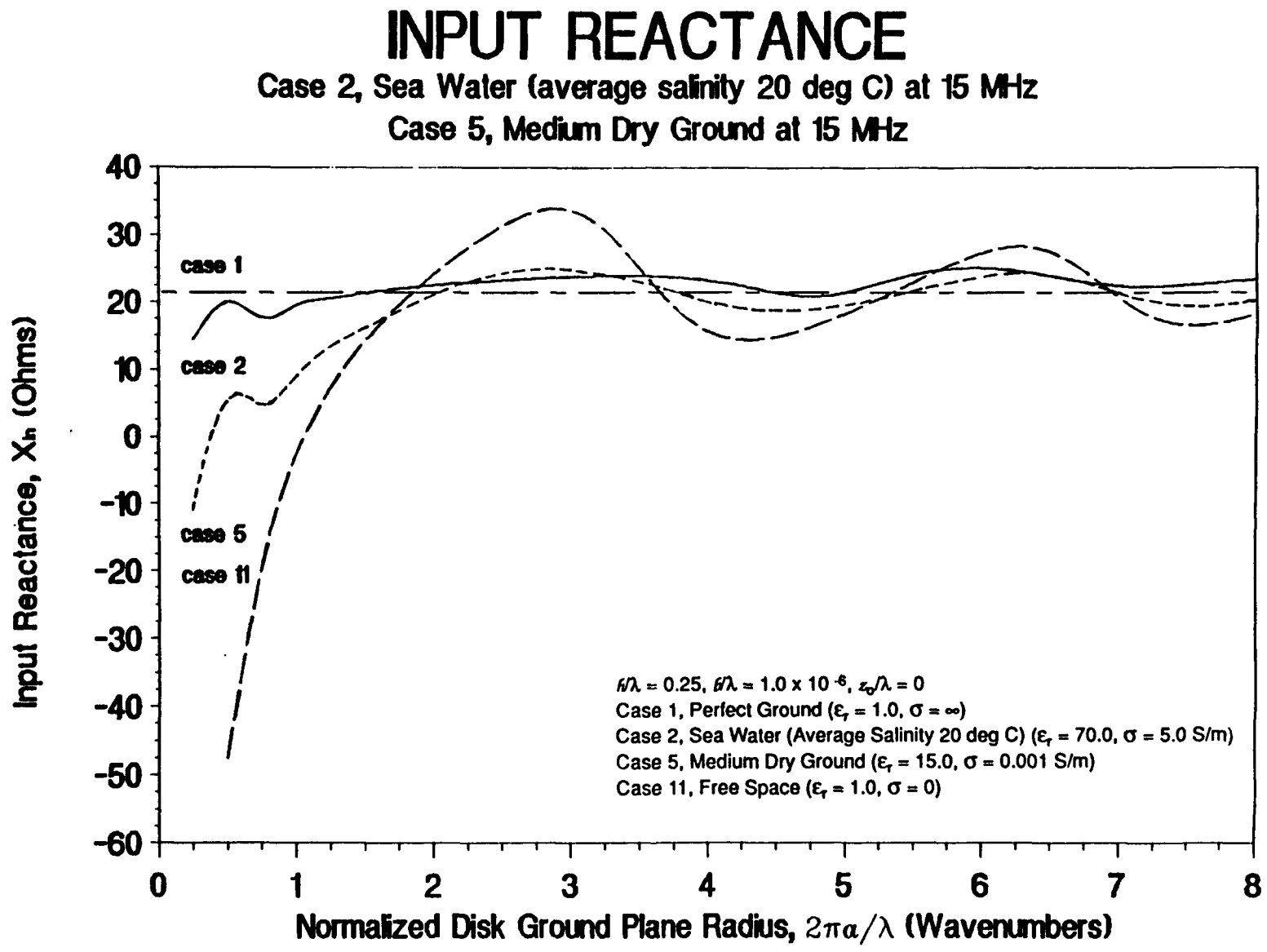

Figure 3-155. Input Reactance, Sea Water Compared with Medium Dry Ground

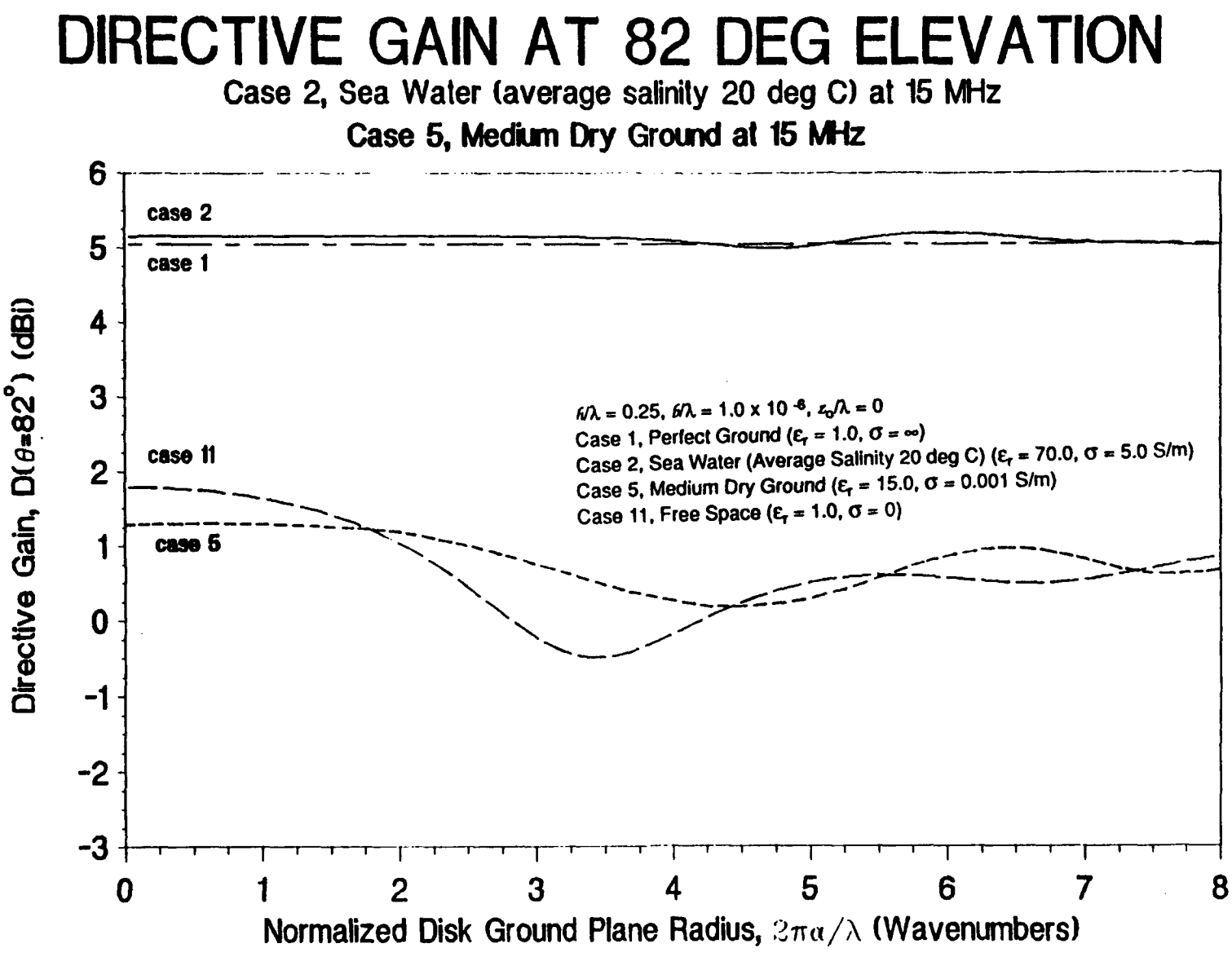

Figure 3-156. Directivity at 8 Degrees Above the Horizon, Sea Water Compared with Medium Dry Ground

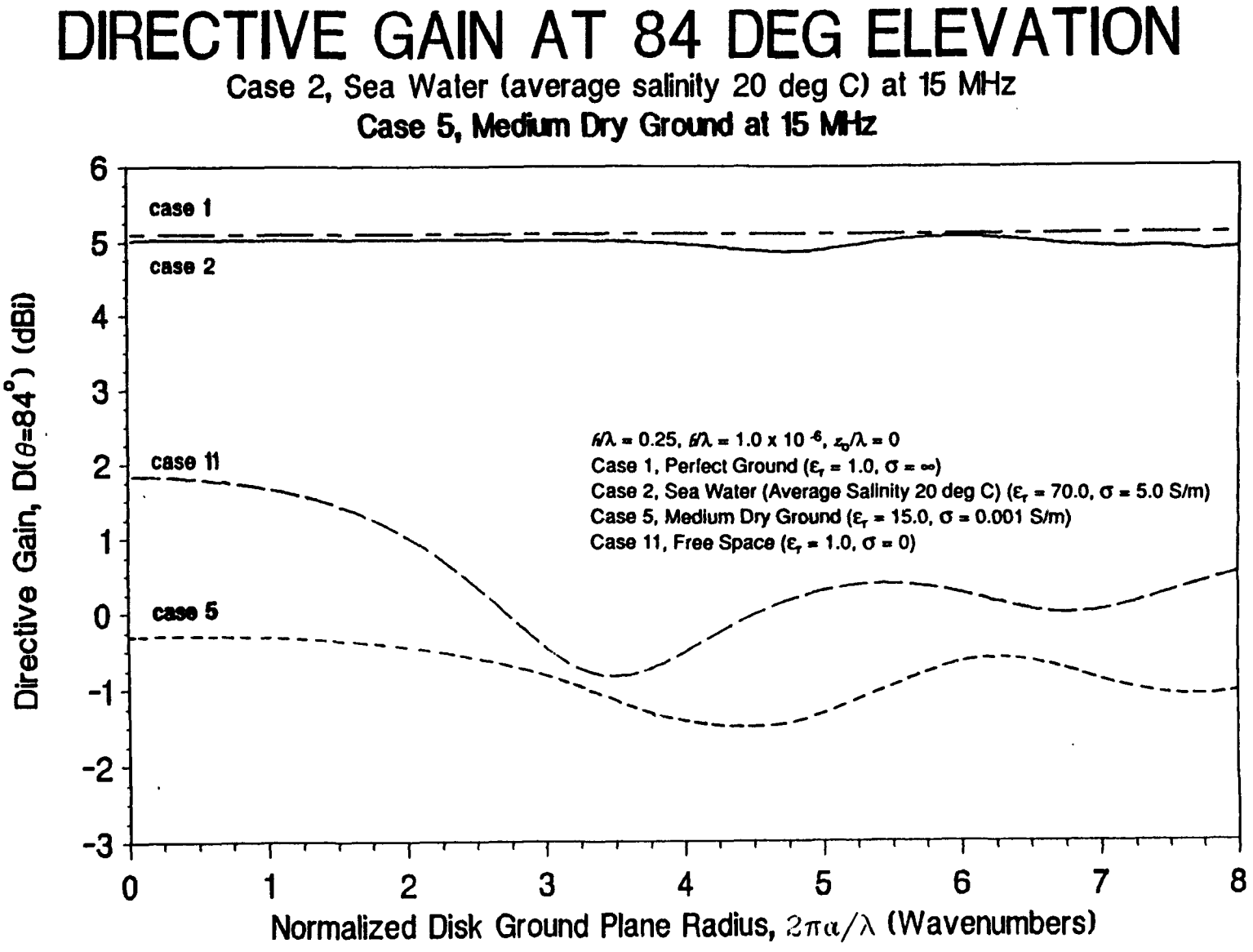

Figure 3-157. Directivity at 6 Degrees Above the Horizon, Sea Water Compared with Medium Dry Ground

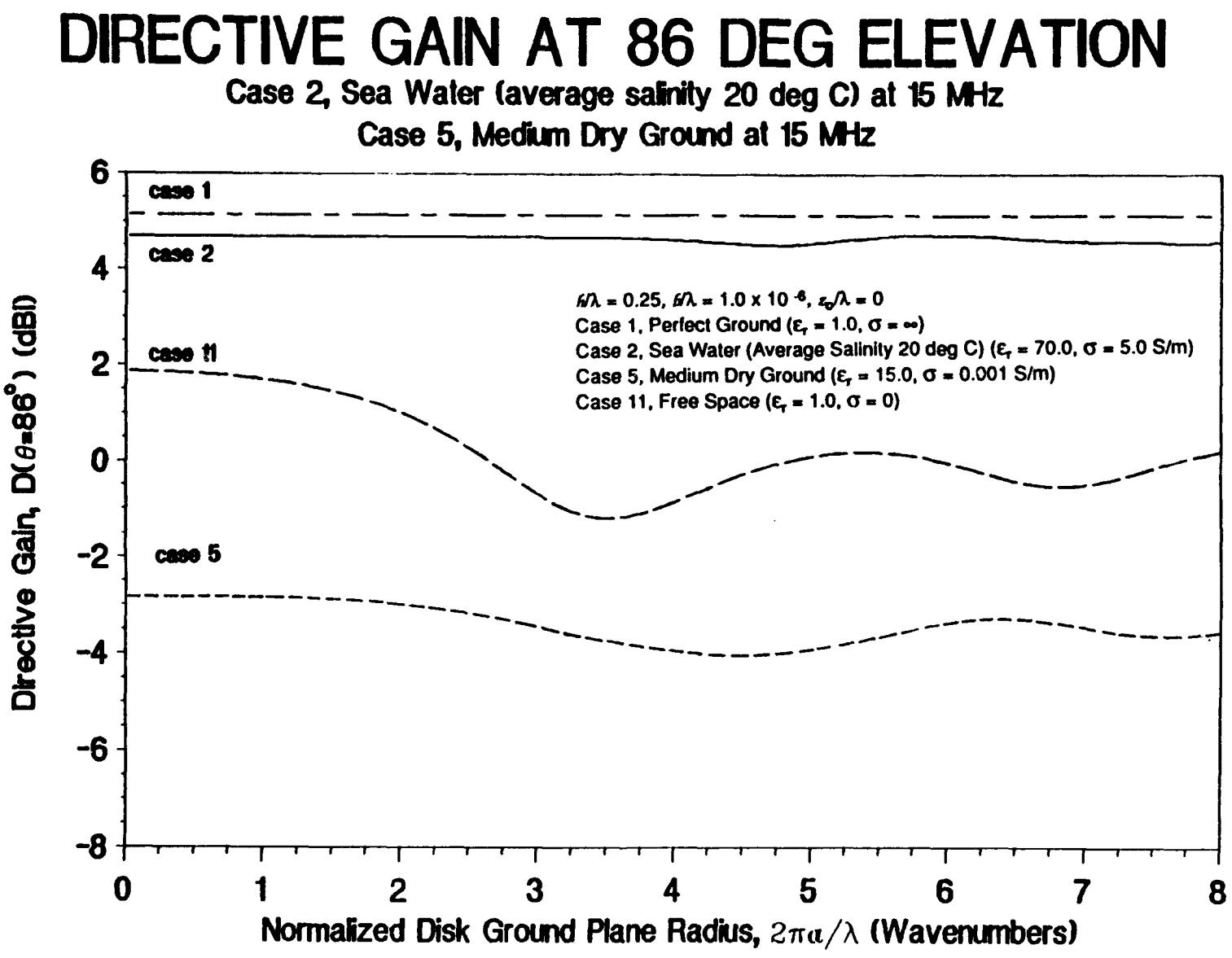

Figure 3-158. Directivity at 4 Degrees Above the Horizon, Sea Water Compared with Medium Dry Ground

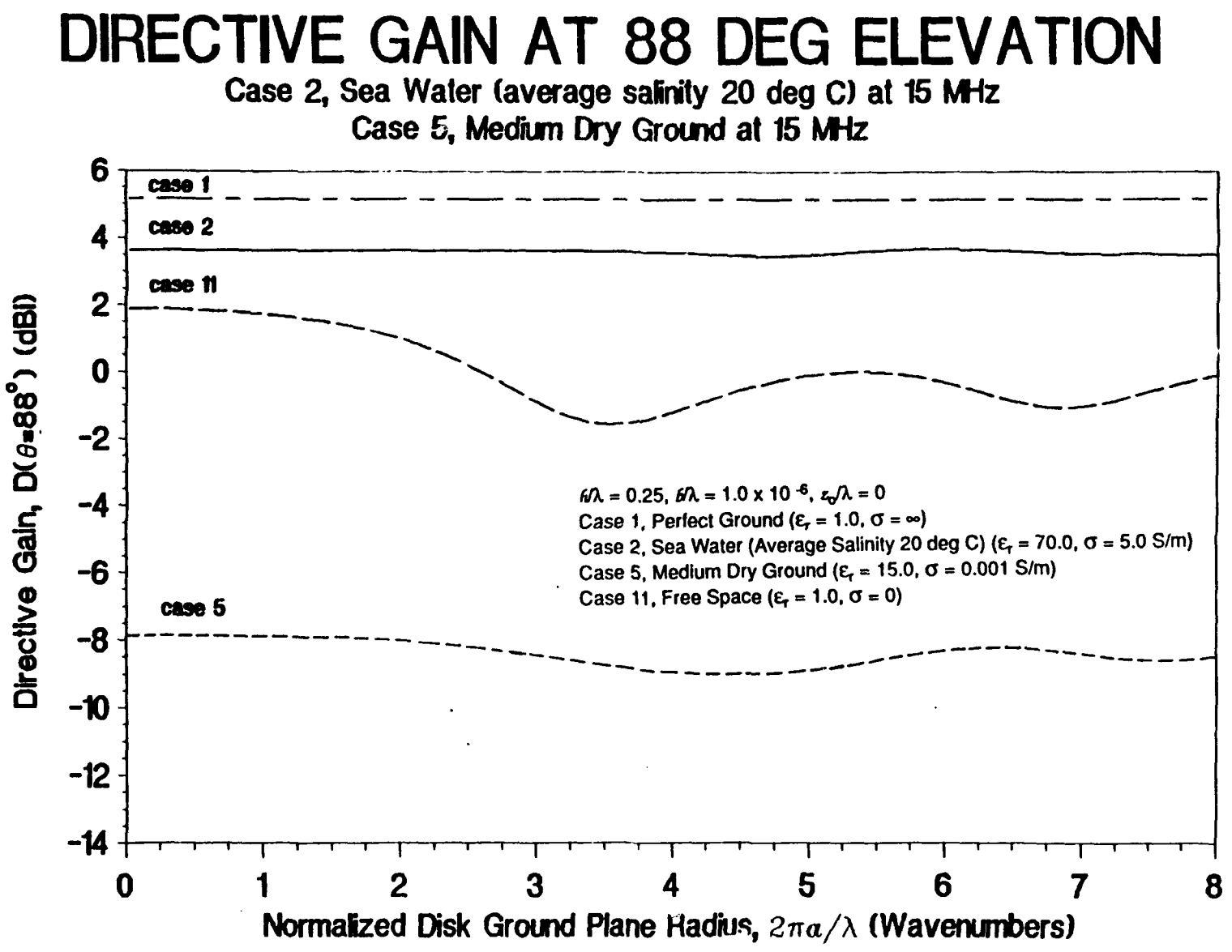

Figure 3-159. Directivity at 2 Degrees Above the Horizon, Sea Water Compared with Medium Dry Ground

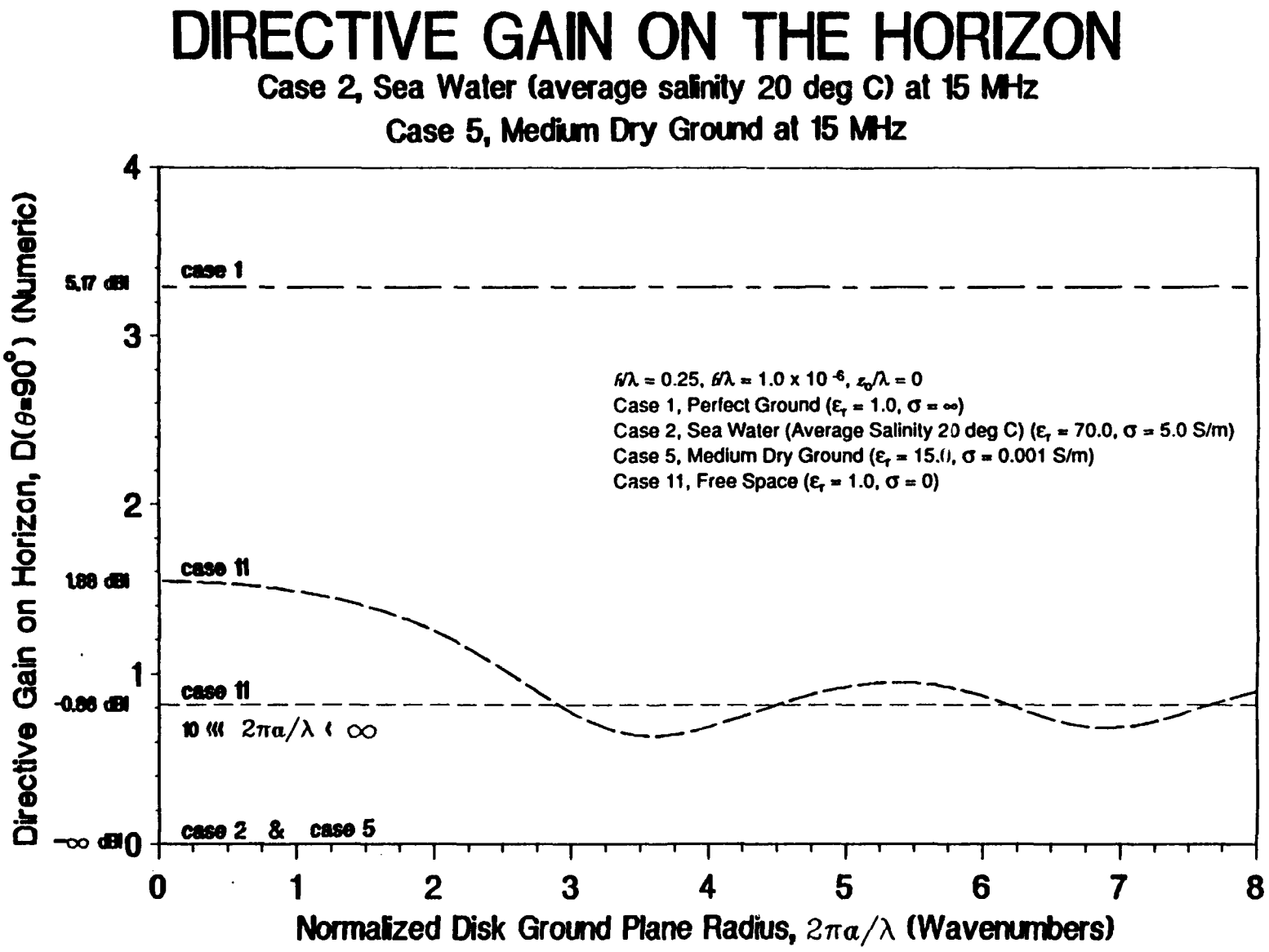

Figure 3-160. Directivity on the Horizon, Sea Water Compared with Medium Dry Ground

LIST OF REFERENCES

1. Richmond, J. H., December 1984, "Monopole Antenna on Circular Disk," *IEEE Trans. Antennas and Propagation*, Vol. AP-32, No. 12, pp. 1282-1287.

2. Richmond, J. H., June 1985, "Monopole Antenna on Circular Disk Over Flat Earth," *IEEE Trans. Antennas and Propagation*, Vol. AP-33, No. 6, pp. 633-637.

3. Burke, G. J., and A. G. Poggio, January 1981, "Numerical Electromagnetic Code (NEC) – Method of Moments," Lawrence Livermore National Laboratory, Report UCID-18834.

4. Burke, G. J., and E. K. Miller, 1984, "Modeling Antennas Near to and Penetrating a Lossy Interface," *IEEE Trans. Antennas and Propagation*, Vol. AP-32, pp. 1040-1049.

5. Burke, G. J., October 1983, "User's Guide Supplement for NEC-3 for Modeling Buried Wires," Lawrence Livermore National Laboratory, Report UCID-19918.

6. Rafuse, R. P., and J. Ruze, December 1975, "Low Angle Radiation from Vertically Polarized Antennas Over Radially Heterogeneous Flat Ground," *Radio Science*, Vol. 10, pp. 1101-1018.

7. Wait, J. R., and W. A. Pope, 1954, "The Characterization of a Vertical Antenna with a Radial Conductor Ground System," Applied Scientific Research, Vol. 4, Sec. B, pp. 177-195 (The Hague).

8. Wait, J. R., and W. J. Surtes, May 1954, "Impedance of a Top-Loaded Antenna of Arbitrary Length Over a Circular Grounded Screen," J. Applied Physics, Vol. 25, pp. 553-555.

9. Wait, J. R., and L. C. Walters, April 1963, "Influence of a Sector Ground Screen on the Field of a Vertical Antenna," U.S. National Bureau of Standards, Monograph 60, pp. 1-11.

10. Hill, D. A., and J. R. Wait, January 1973, "Calculated Pattern of a Vertical Antenna with a Finite Radial-Wire Ground System," *Radio Science*, Vol. 8, No. 1, pp. 81-86.

11. Weiner, M. M., May 1987, "Monopole Element at the Center of a Circular Ground Plane Whose Radius is Small or Comparable to a Wavelength," *IEEE Trans. Antennas and Propagation*, Vol. AP-35, No. 5, pp. 488-495.

12. Weiner, M. M., and S. P. Cruze, C. C. Li, and W. J. Wilson, 1987, Monopole Elements on Circular Ground Planes, Norwood, MA: Artech House.

13. Weiner, M. M., June 1992, "Far-Zone Field of a Monopole Element on a Disk Ground Plane Above Flat Earth," MITRE Technical Report MTR-B0000090, The MITRE Corporation, Bedford, MA.

LIST OF REFERENCES (CONCLUDED)

14. CCIR (1986), "Electrical Characteristics of the Surface of the Earth," Recommendation 527-1 (Based on CCIR Report 229, 1982), 16th Plenary Assembly, Dubrovik (1986), Int. Radio Consultative Committee (CCIR), Int. Telecommunication Union, Geneva, Switzerland, 1986.